Hydrodynamic Studies in a Slurry Bubble Column

by

Bimal C. Gandhi

Department of Chemical and Biochemical Engineering
Faculty of Engineering Science

Submitted in partial fulfillment
of the requirements for the degree of
Masters of Engineering Science

Faculty of Graduate Studies
The University of Western Ontario
London, Ontario
August 1997

Abstract

Hydrodynamics of a slurry bubble column have been investigated over a wide range of slurry concentrations (0% to 40vol%) and gas velocities (up to 0.25m/s). High slurry concentrations represent high catalyst loadings to increase reactor productivity while high gas velocities would be required to increase reactor throughputs. The solid particles used are 35μm glass beads representing a typical particle size for a catalytic slurry reactor. The two important hydrodynamic parameters investigated are gas holdup and solids concentration profiles. The average gas holdups decreased with increasing slurry concentration but the rate of decrease slowed down for higher slurry concentrations. The axial gas holdup profiles analyses indicated that decrease in gas holdup due to solids addition could be attributed to decrease in bubble breakup rates. The experimental gas holdups were compared with literature correlations and new correlations based on a drift flux model were developed. Axial distribution of slurry concentration followed the classical sedimentation-dispersion model. Effects of gas velocity on axial distribution were found to be minimal over the range of gas velocities investigated.

Plugs of solids were observed to form and move up the column during the startup operation as the solids concentration in the column increased. The plugs posed serious problems to column internals. Moreover, inspection of the column base plate after a series of experiments showed pitting marks due to impinging gas jets. In order to minimize these practical problems, a procedure to select sparger location was developed based on experiments conducted by varying the sparger height in the column.

Acknowledgments

The author wishes to express his sincere gratitude Dr. Anand Prakash for his constructive suggestions and guidance during this work. I am also thankful to Dr. Maurice Bergougnou for being a constant source of encouragement.

Special thanks are also due to Mr. Souheil Afara for his valuable help in various aspects of the study. Thanks are due to fellow graduate students in the department, who provided tremendous support.

The professors and staff of the Department of Chemical and Biochemical Engineering, the staff of the University Machine Shop and Library personnel are also thanked for their assistance.

Finally, I would like to thank Esther Lee and Richard Saunders for their continued support and encouragement during tough times.

Table of Contents

List of Tables

List of Figures

Nomenclature

A_1	coefficient in Eq. 2.9
A_c	column cross sectional area (m^2)
A_d	effective area through which the solids de-entrainment flux crosses (m^2)
A_e	effective area through which the solids entrainment flux crosses (m^2)
b_1, b_2	coefficients in Eq. 2.28 and Eq. 4.7
B_1-B_4	coefficients in Eq. 2.17
c	coefficient in Eq. 2.7
c_1, c_2	coefficients in Eq. 2.29
C_1-C_4	coefficients in Eq. 2.21
$C_{(P_v)}$	pressure corresponding to the midpoint of the dispersion in the column
C_s	average solids concentration in slurry (kg/m^3)
$C_{s(z)}$	slurry concentration at height z in the column (kg/m^3)
C_{so}	solids concentration at bottom of column (kg/m^3)
d_o	diameter of sparger orifice (m)
d_p	particle diameter (m)
D_c	column diameter (m)
$E_{pot,p}$	potential energy of the particles in suspension (J)
E_s	axial solids dispersion coefficient (m^2/s)
f_1	coefficient in Eq. 2.10
F_1, F_2	coefficients in Eq. 4.23
Fr_g	gas Froude number
g	acceleration due to gravity (m/s^2)
H_c	height of column (m)
H_d	expanded bed height (with gas present) (m)
H_s	static bed height (without gas) (m)
k	ratio of wake region volume fraction to total gas holdup

k_1 coefficient in Eq. 2.18

l_e length of energy containing eddy (m)

L critical length (m)

L_{jet} length of jets from sparger orifice (m)

m_s mass of solids in slurry sample (kg)

m_{sl} mass of slurry sample (kg)

n Richardson-Zaki constant

n_d flux of solids particles due to dispersion (kg/m^2s)

N_b total number of bubbles

$P_{in,g}$ incoming power with the gas phase (W)

P_o pressure at atmospheric conditions (Pa)

Pe_p particle Peclet number

P/V specific power input (W/m^3)

$\Delta P/\Delta z$ pressure gradient along the column wall (Pa/m)

ΔP_{bed} pressure drop across the bed (Pa)

ΔP_f frictional pressure drop (Pa)

Q_g volumetric flowrate of gas (m^3/s)

$Q_{o,g}$ volumetric flowrate of gas at atmospheric conditions (m^3/s)

Q_l volumetric flowrate of liquid (m^3/s)

r radial distance from center of column (m)

R radius of column (m)

Re_g gas Reynold's number

Re_p particle Reynold's number

Re_{sl} slurry Reynold's number

t time (s)

T temperature (K)

u' turbulent fluctuation velocity (m/s)

U_b bubble rise velocity (m/s)

$U_{b\infty}$ terminal rise velocity for a swarm of bubbles (m/s)

U_{lmf} liquid minimum fluidization velocity (m/s)

$U_{l.b.}$ large bubble rise velocity (m/s)

$U_{s.b.}$ small bubble rise velocity (m/s)

U_{st} generalized term for solids settling velocity (m/s)

U_p hindered settling velocity of solids particles in slurry (m/s)

U_t terminal settling velocity of a single particle (m/s)

U_{trans} transition gas superficial velocity (m/s)

V_d average solids deentrainment velocity relative to bubble rise velocity (m/s)

V_e average solids entrainment velocity relative to bubble rise velocity (m/s)

V_g gas superficial velocity (m/s)

V_{gl} drift flux velocity (m/s)

V_l liquid superficial velocity (m/s)

V_{lf} average liquid velocity in particulate fluidization phase (m/s)

V_o velocity of gas through sparger orifice (m/s)

V_p average solids convective velocity in particulate fluidization phase (m/s)

V_{refill} volume of refill water (m^3)

V_R reactor volume (m^3)

V_s slip velocity between gas bubbles and liquid (slurry) flow (m/s)

V_{sl} volume averaged slurry superficial velocity (m/s)

V_{slurry} sample slurry volume (m^3)

V_T volume averaged dispersion velocity (m/s)

W_s mass of solids in bed (kg)

x ratio of solids holdup in the wake phase to the solids fraction in the particulate fluidization phase

Δy difference in U-tube manometer readings (m)

z axial distance along the column (m)

Z normalized axial distance along the column (m)

Δz a small increment in vertical distance (m)

Greek symbols

α angle of internal friction (°)

β virtual coefficient for liquid displacement in Eq. 2.43

ε bed voidage

ε_f overall volume fraction of particulate fluidization phase

ε_g gas holdup

ε_{kin} specific kinetic energy conversion rate (W/kg)

ε_l liquid holdup

ε_{lf} axial volume fraction of liquid in the particulate fluidization phase

ε_{lw} axial volume fraction of liquid in the bubble engagement phase

ε_s solids holdup

ε_s^f volume fraction of solids in the feed

ε_{sf} axial volume fraction of solids in the particulate fluidization phase

ε_{sl} slurry holdup

ε_{sw} axial volume fraction of solids in the bubble engagement phase

ε_w overall volume fraction of bubble engagement phase

γ electrical conductivity of the bed

γ_l electrical conductivity of the liquid alone

η_f dynamic fluid viscosity (kg/m s)

μ_g gas viscosity (kg/m s)

μ_l liquid viscosity (kg/m s)

μ_{sl} slurry viscosity (kg/m s)

ν_l kinematic liquid viscosity (m^2/s)

ν_{sl} effective kinematic slurry viscosity (m^2/s)

$\nu_{eff,rad}$ radial momentum transfer coefficient (m^2/s)

θ poured angle of repose (°)

ρ_d dispersion density (kg/m^3)

ρ_f density of manometer fluid (kg/m^3)

ρ_g gas density (kg/m^3)

ρ_l liquid density (kg/m^3)

ρ_s solids density (kg/m^3)

ρ_{sl} slurry density (kg/m^3)

ρ_w density of water (kg/m^3)

σ liquid surface tension (kg/s^2)

τ_p particle response time (s)

τ_t characteristic fluctuation time (s)

ψ_l liquid fraction in non-fluidized slurry (vol%)

ψ_s solids fraction in non-fluidized slurry (vol%)

Subscripts

g gas

l liquid

o atmospheric conditions

p particle

s solid

sl slurry

1.0 Introduction

Multiphase reactors are commonly used in chemical, biochemical, petrochemical, and waste water treatment industries. The three main broad categories of these reactors are the trickle bed reactor (fixed or packed bed), the gas-liquid-solid fluidized bed reactor and the bubble (slurry) column reactor. Bubble column and slurry bubble column reactors have recently emerged to be very promising technologies for multiphase operation. Biological waste water treatment, flue gas desulphurization, coal liquefaction, Fischer-Tropsch synthesis, methanol synthesis, dimethyl ether production, chlorination (production of aliphatic and aromatic chlorinated compounds), polymerization (production of polyolefins), oxidation (adiponitrile synthesis), hydrogenation (saturation of fatty acids), fermentation (production of ethanol and mammalian cells), and hydrotreating and conversion of heavy petroleum residues are such processes that are now conducted in bubble and slurry bubble columns (Fan, 1989; Dudukovic and Devanathan, 1992; Lewnard et al., 1990).

One particular area of current interest for slurry bubble columns is the fuel processing industry. This is true for Fischer-Tropsch and oxygenates processes. Zhou et al. (1992) reported the slurry bubble column technology application for these processes to be a high priority research activity area for the indirect coal liquefaction program of the US Department of Energy Pittsburgh Energy Technology Center (DOE-PETC). Fischer-Tropsch slurry phase synthesis is considered to be an economical way of converting coal derived synthesis gas into liquid fuels due to its improved thermal efficiency and ability to process CO-rich synthesis gas. The slurry process presents substantial

potential advantages over conventional fixed bed and entrained bed vapor phase processes (Bukur and Daly, 1987; Bukur et al., 1987).

Methanol synthesis is another promising alternative for slurry bubble column reactor technology (Sherwin and Frank, 1976; Weimer et al., 1987; Roberts et al., 1990). It is particularly important knowing that methanol as an alternative fuel, fuel additive, fuel intermediate, and gas turbine fuel for power generation is becoming increasingly important. With slurry reactors, the water gas shift, methanol synthesis and methanol dehydration reactions can proceed concurrently in a single three phase reactor.

Bubble column reactors offer many advantages over other types of multiphase reactors (Deckwer and Schumpe, 1993) :

- High liquid (slurry) phase content for the reaction to take place.
- Reasonable interphase mass transfer rates at low energy input.
- High selectivity and conversion per pass.
- Excellent heat transfer properties and easy temperature control (isothermal operation).
- Online catalyst addition and withdrawal.
- Washing effect of the liquid on the catalyst.
- Solids can be handled without serious erosion or plugging problems.
- Little maintenance is required due to simple construction and no problems with sealing due to absence of any moving parts.
- Bubble column reactors are relatively cheap.

However, there are several disadvantages which must also to be considered. These include:

- Considerable backmixing in both the continuous liquid (slurry) phase and the dispersed gas phase.
- Low volumetric catalyst loading
- Bubble coalescence.
- Difficult to scale up.

Industry has also identified some problems of practical importance. For example, the catalyst deactivation rate can increase with increasing slurry concentration. Separation of the fine catalyst particles from liquid products can also be difficult. Foaming can also become a problem in certain applications. For continuous systems, the solids can produce erosion in the impeller and pump housings. Abrasion in the slurry reactor also interferes with the flow of product (Kurten and Zehner, 1979).

Although relatively simple in construction, slurry bubble columns are difficult to scale-up due to lack of information on hydrodynamics and mass transfer over a wide range of operating conditions of commercial interest. Only more recently has research been carried out to try to improve the slurry reactor knowledge base. This study investigates hydrodynamics of slurry bubble columns over a wide range of slurry concentration (up to 40vol% solids) and gas velocities. There is currently a lack of information on the hydrodynamic behavior of slurry bubble columns at high slurry concentrations. It is important to identify practical operational limits and the design implications of increasing slurry concentrations in the column. For example, gas distributor design and configuration and column startup procedure could be influenced by high slurry concentrations. The two important hydrodynamic parameters investigated are gas holdup

profiles and solids dispersion profiles. Attempts have been made to gain insight into the behavior of concentrated slurries based on measured data.

2.0 Bubble Columns and Slurry Bubble Columns

Bubble columns are multiphase contactors of relatively simple construction. In these reactors, gas is usually the discontinuous phase rising in the form of bubbles through a continuous liquid or slurry phase. The column can be operated in a batch or continuous mode with cocurrent or countercurrent flow, though vertically sparged bubble columns with cocurrent flow are most common in industry. Fig. 2.1 shows a schematic of a typical bubble column reactor. Gas enters the bottom of the reactor through a sparger or perforated plate. Liquid/slurry enters at the bottom of the reactor and exits from the side. A heat exchanger may also be also be necessary to control temperature. The main focus of this study is the slurry bubble column reactor. This type of reactor has a suspension of relatively fine solid particles (d_p < 500μm) in the liquid phase. A number of hydrodynamic and transport characteristics of slurry bubble columns are similar to solids-free bubble columns and/or three phase fluidized beds. For low solids loadings (usually < 5vol%), the behavior of the slurry bubble column is often close to that of a solids-free bubble column (Sada et al., 1986b; Sauer and Hempel, 1987; Wolff et al., 1990). As pointed out by Fan et al. (1987), slurry bubble column systems and three phase fluidized beds have common operating ranges for particle terminal velocities in the range of 0.03m/s to 0.07m/s. A comprehensive review on bubble columns has been provided by Shah et al. (1982). Reviews for three phase fluidized beds are also available (Ostergaard, 1968 and 1971; Epstein, 1981; Wild et al., 1984; Muroyama and Fan, 1985; Fan et al., 1987).

Fig. 2.1 Slurry Bubble Column Reactor

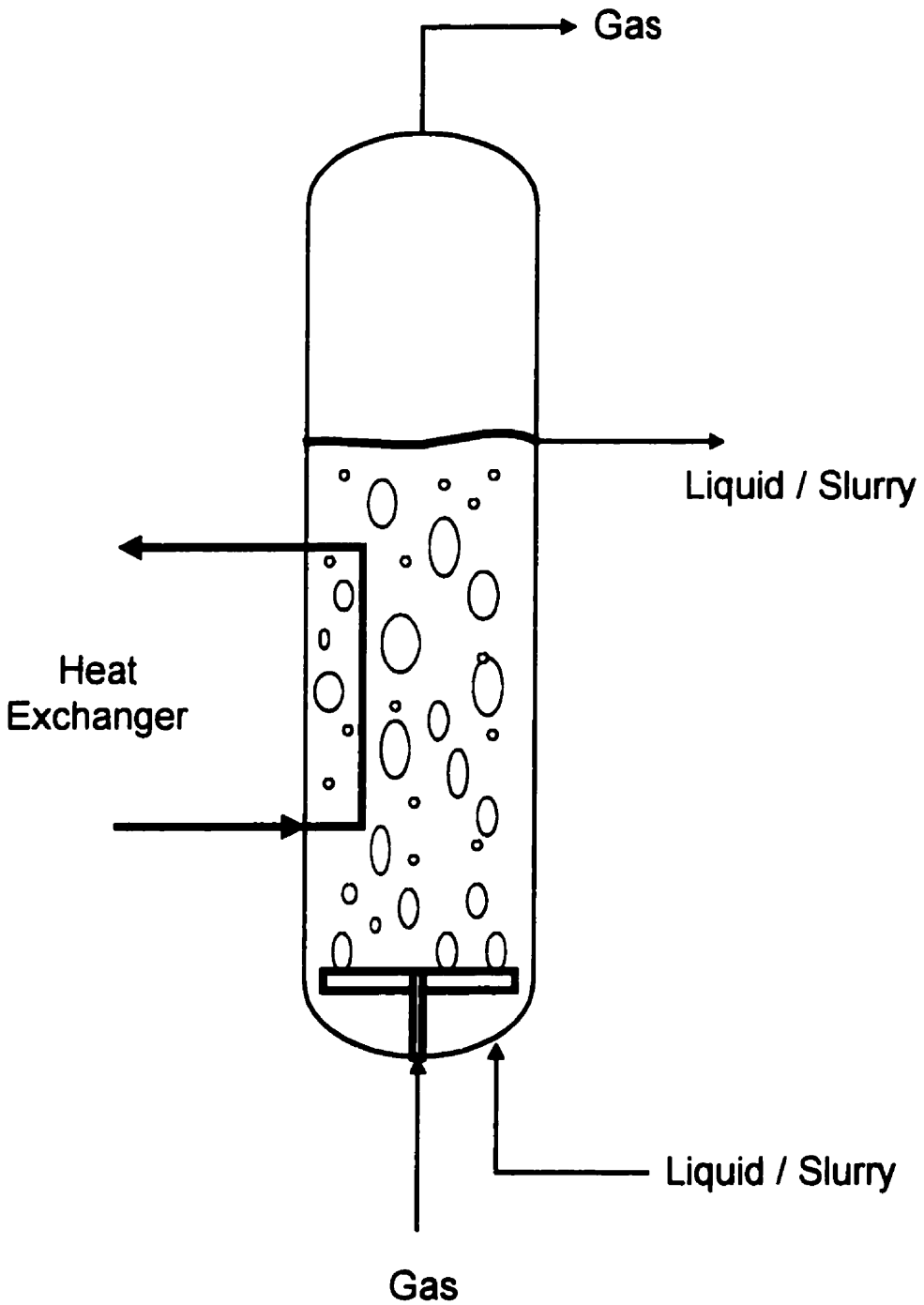

2.1 Classification and Flow Regimes

Classification of three phase systems can readily be extended from that of gas-liquid, gas-solid or liquid-solids systems; however, it is more convenient (and practical) to classify them according to the state of particle motion. Particle motion can be subdivided into three basic operating regimes: the fixed bed regime, the expanded (fluidized) bed regime and the transport regime. An example of an operating regime map for an air-water-solid system with cocurrent upward flow of gas and liquid is shown in Figure 2.2 (Fan et. al., 1987). The fixed bed regime exists when the drag force on the particles induced by the flow of a gas-liquid mixture is smaller than the effective weight of the particles in the system. With an increase in gas and/or liquid velocity, the drag force counterbalances the effect of particle weight in the system. This point is known as the minimum fluidization velocity (U_{lmf}) as the bed is in a state of minimum fluidization. The mode of operation is now known as the expanded bed regime as the gas and/or liquid velocity is further increased. This regime continues until the gas and/or liquid velocity reaches the terminal velocity of the particle (U_t) beyond which the transport regime begins.

Typical operating ranges for three phase fluidized beds and slurry bubble columns for an air-water-solid system are shown in Figure 2.3 (Fan et al., 1987). Three phase fluidized beds operate in the expanded bed regime covering U_t from 3 to 50 cm/s. Slurry bubble columns may operate in both the expanded and transport regimes covering U_t from 0.03 to 7 cm/s.

Bubble columns normally operate with a height to diameter ratio of greater than five and with a superficial gas velocity at least an order of magnitude greater than the superficial liquid velocity. Typical ranges of superficial velocities for

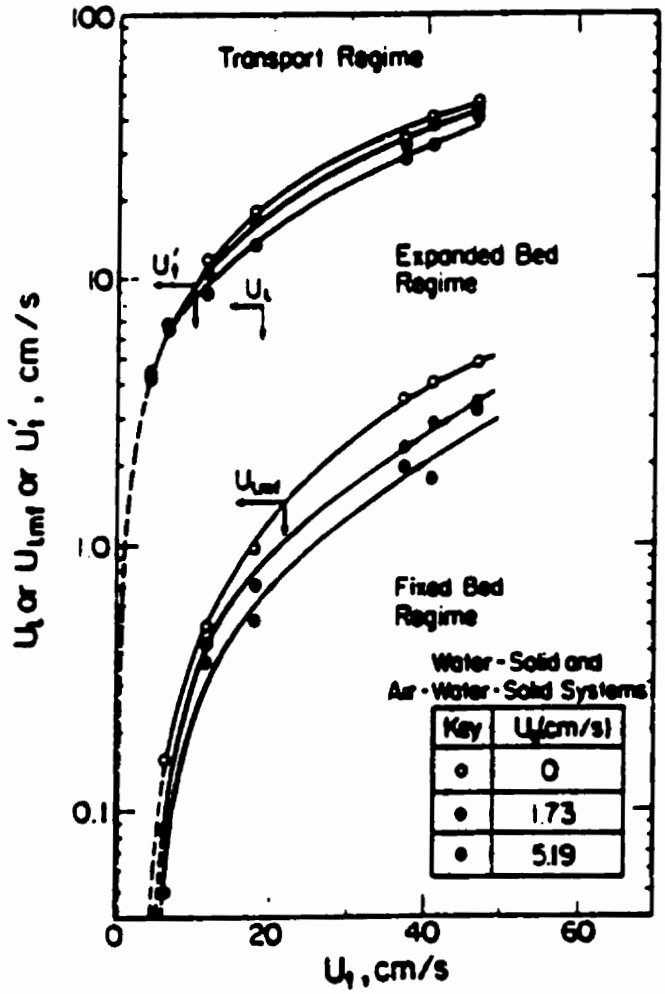

Fig. 2.2 Operating regimes for cocurrent upward gas-liquid-solid systems with liquid as the continuous phase (from Fan et al., 1987)

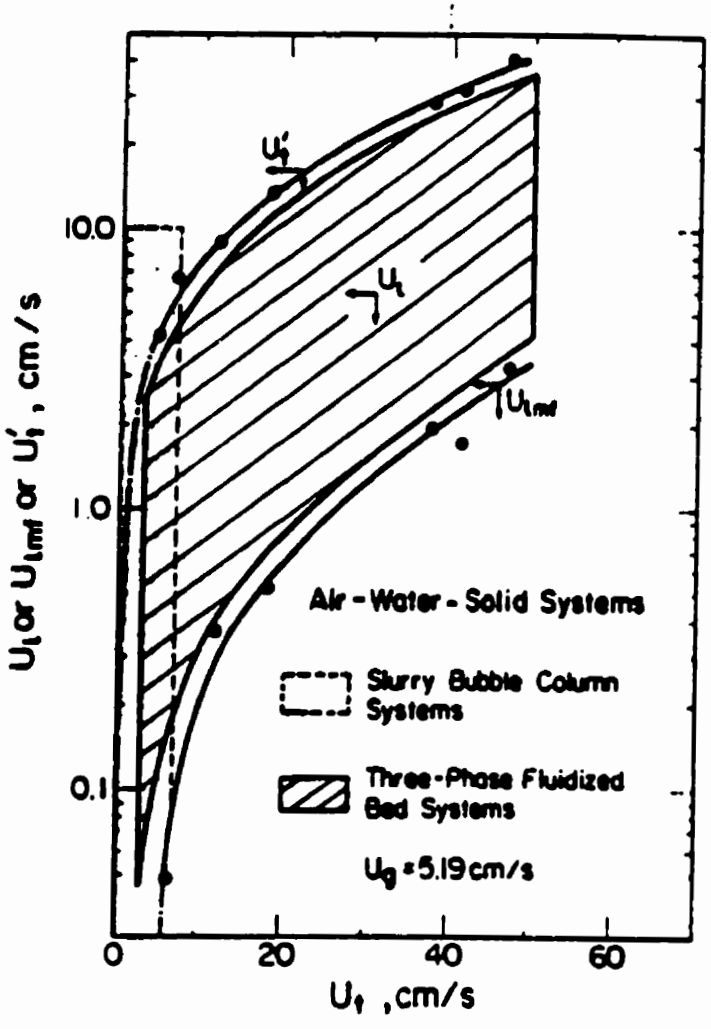

Fig. 2.3 Common operating ranges for three-phase fluidized bed and slurry bubble column systems (from Fan et al., 1987)

bubble column operation are 1 to 30 cm/s for the gas phase and 0 to 2 cm/s for the liquid phase (Dudukovic and Devanathan, 1992). Coils and other internals may be present to promote heat transfer. The column may also be sectionalized using baffles or perforated plates to inhibit liquid phase backmixing or bubble coalescence.

2.1.1 Flow Regimes

Several researchers have studied and outlined criteria to differentiate the flow regimes (Wallis, 1969; Michelsen and Ostergaard, 1970; Rigby et al., 1970; Kim et al., 1972; Darton and Harrsion, 1975; Hills, 1976; Kawagoe et al., 1976; Matsuura and Fan, 1984). Often, these flow regimes (and their boundaries) are determined visually. As with three phase fluidized beds, three distinct flow regimes have been observed in slurry bubble columns. They include the dispersed bubble regime, the coalesced bubble regime and the slugging regime. For bubble columns, the terminology used for the corresponding regimes is slightly different but still consistent. Here, the dispersed bubble regime is referred to as the homogeneous or bubble flow regime and the coalesced bubble regime as heterogeneous or churn turbulent regime.

2.1.1.1 Dispersed Bubble Flow Regime

Within this regime, relatively small bubbles are distributed over the entire cross sectional area of the column. Most bubbles are of uniform size with bubble diameter less than 6 mm. The regime has been reported to exist at low and intermediate gas velocities (< 5 cm/s) and at high liquid velocities in continuous bubble columns (Hills, 1974; Fan, 1989). In this regime, as the superficial gas velocity increases, gas holdup increases very rapidly. In fact, gas holdup has

been found to be proportional to the superficial gas velocity for this regime (Kawagoe et al., 1976).

2.1.1.2 Coalesced Bubble Flow Regime

This regime is characterized by rapid coalescence and break up, resulting in a wide bubble size and velocity distribution. With higher gas velocities, the pseudo homogeneous gas/liquid dispersion can no longer be maintained and an unsteady flow pattern results. Coalesced bubbles tend to rise near the center of the column with high velocity. This results in highly turbulent motion stirring the bed violently. This flow regime will exist at superficial gas velocities higher than 0.05 m/s in batch columns (Hills, 1976). Matsuura and Fan (1984) reported that the coalesced bubble regime consisted of a mixture of large and small bubbles with diameters ranging from a few millimeters to a few centimeters.

2.1.1.3 Slug Flow Regime

This regime has been observed mostly in small diameter columns, usually with high gas flow rates. Here, gas bubbles can easily grow to the size of the column diameter creating "slugs" which occupy nearly the entire cross section. These slugs have been observed in columns with diameters up to 0.15 m (Hills, 1976; Miller, 1980). For highly viscous fluids, slug flow is observed even at relatively low gas velocities (Fan, 1989). Matsuura and Fan (1984) also detected smaller bubbles intermixed with larger bubbles in the slugging regime. In columns of larger diameters, however, slugging may not occur.

2.1.2 Flow Regime Charts

Several flow regime charts have been presented in literature to identify the boundaries of the various flow regimes (Shah et al., 1982; Fan et al., 1985; Muroyama and Fan, 1985). The transition from one regime to another is usually identified by visual observations which make the precise determination of the boundaries rather difficult and subjective. Deckwer et al. (1980) proposed the typical flow regime map given in Figure 2.4 for both bubble and slurry bubble columns with a batch liquid phase. The specific operating conditions for the transitions between the three regimes depend on particle size and density, gas and liquid flowrates, column diameter and liquid properties (Kim et al., 1972; Darton and Harrison, 1975; Kara et al., 1982; Fan et al., 1985, Fan et al., 1986a; Bukur and Daly, 1987; Wilkinson and Dierendonck, 1990; Krishna et al., 1991; Wilkinson et al., 1992) . Bukur and Daly (1987) observed the coalesced bubble regime for gas superficial velocities between 2 cm/s and 15 cm/s under conditions simulating the slurry Fischer-Tropsch process. Krishna et al. (1991) noted that the transition from dispersed to coalesced bubble regime was accompanied by the formation of large fast rising bubbles. Consequently, any factor influencing the formation of large bubbles can also influence the transition between flow regimes. For example, Wilkinson et al. (1992) reported that higher liquid viscosity promotes bubble coalescence which consequently favors transition to the coalesced bubble regime at lower superficial gas velocities. They also reported that lower surface tension liquids encourage bubble breakup and thus transition to the coalesced bubble regime would occur at higher superficial gas velocities. Higher gas densities (as a result of higher pressures) have also been found to promote bubble breakup and extend the dispersed bubble flow regime to higher superficial gas velocities (Clark, 1990; Wilkinson and Dierendonck, 1990; Krishna et al., 1991). The addition of fine solids to the liquid phase also promotes rapid bubble coalescence which can result in the column completely operating in the coalesced bubble regime. Kara et al. (1982)

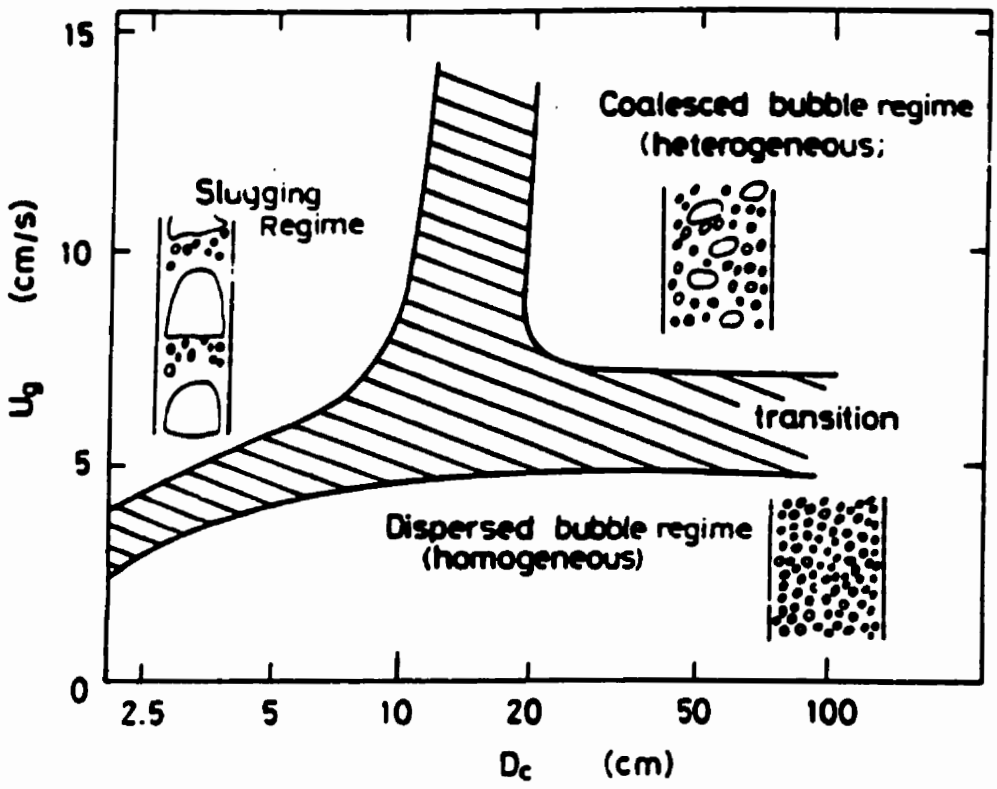

Fig. 2.4 Flow regime map for a liquid-batch bubble column or a slurry-batch bubble column containing a low viscosity liquid phase (from Deckwer et al., 1980)

observed that an increase in solids concentration, particle size and slurry velocity resulted in very early transition to coalesced regime from the dispersed regime.

2.2 Phase Holdups

The gas phase dynamics play a very important role in the design and operation of a bubble column reactor and in determining the chemical conversion achieved. The design of a gas sparger determines the uniformity of gas release across the bubble column reactor and the initial bubble size. The properties of the liquid and solid phases control the bubble growth and equilibrium bubble size in the column. If internals are present, the bubble size is also controlled by their geometrical spacing and configuration. The bubble velocity and hence the residence time of the gas phase depends on bubble size among other factors. The interfacial gas-liquid area which influences mass transfer and product yield also depends on the bubble diameter. From these general considerations, it is evident that a proper understanding of bubble dynamics in a slurry reactor is crucial and fundamental to the operation of such a reactor. For the remainder of this study, we shall concentrate on batch and continuous slurry bubble columns with cocurrent upward gas and liquid flows (with liquid as the continuous phase).

The phase holdup in a multiphase system is defined as the volume fraction occupied by the considered phase in the system. For slurry bubble columns, the solids holdup are almost uniformly distributed along the column height. The following expression represents this relationship between individual holdups:

$$\varepsilon_g + \varepsilon_s + \varepsilon_l = 1 \qquad (2.1)$$

The average solids holdup can be calculated using:.

$$\varepsilon_s = W_s / (\rho_s A_c H_d) \qquad (2.2)$$

where

A_c is the cross-sectional area of the column,

H_d is the height of dispersion

W_s is the mass of solids in the column

The static pressure gradient, neglecting frictional pressure drop (ΔP_f), is represented by the following equation:

$$(\Delta P/\Delta z) = g (\varepsilon_g \rho_g + \varepsilon_s \rho_s + \varepsilon_l \rho_l) \qquad (2.3)$$

Equations 2.1 through 2.3 can be used to calculate individual holdups knowing W_s, H_d and the static pressure gradient.

2.2.1 Phase Holdup Measurement Techniques

To completely understand hydrodynamic characteristics of bubble and slurry bubble columns, we require reliable and precise measurement techniques. The following section reviews various techniques that have been used to measure phase holdups in bubble column and slurry bubble column systems. They will be grouped into two sections: overall (average) and local phase holdup measurement techniques. Reviews of phase holdup measurement techniques are presented in the Ph.D Thesis of Dr. Anand Prakash (1991) and Cheryl Hudson (1996). For this study, the techniques have been updated.

2.2.1.1 Overall Phase Holdup Measurement Techniques

Various techniques have been used to measure the average phase holdup in multiphase systems. They include:

2.2.1.1.1 Phase holdups from the pressure profile

2.2.1.1.2 Simultaneous closure of gas and liquid flows

2.2.1.1.3 Gas disengagement technique

2.2.1.1.4 Gamma ray attenuation

2.2.1.1.5 Shutter plate technique

2.2.1.1.1 Phase Holdup Measurements Based on Pressure Profile

The most widely used technique in the determination of phase holdups is the pressure profile method (Hikita et al., 1980; Miller, 1980; Fan et al., 1985; Reilly et al., 1986; Wachi et al., 1987; Del Pozo, 1992). Pressure profile along the column height can be obtained by measuring the static pressure at two or more points along the column. This can be accomplished by using manometers. The pressure profile, when plotted as a function of the pressure tap heights will give two straight lines, the intercept of which corresponds to the bed height. This technique can also be extended to three phase fluidized beds to determine both fluidized and total bed heights. The phase holdups can be obtained using Eqs. 2.1 through 2.3. Dhanuka and Stepanek (1978) and Begovich and Watson (1978) have shown that phase holdups obtained by the pressure profile technique are within 5% of the values obtained through electroconductivity methods.

This technique has proven to be very accurate at low gas flowrates. The fluctuations in the manometer levels are small and accurate readings of the static pressure can be obtained at low gas flowrates. However, as the gas velocity is increased, large liquid level fluctuations in the manometers occur reducing accuracy. To solve this problem, Catros (1986) took photographs of his manometer lines to monitor and record the liquid level. He then projected these photographs on a screen to determine the holdups. Unfortunately his technique was not error free. He did not take enough pictures to get an accurate reading. He also failed to take into account the fact that every manometer had a different response time, and that each one contained a different mass of liquid, thus measurement errors were found. Prakash (1991) inserted capillaries in the manometer lines in order to dampen the liquid level fluctuations. The use of capillaries proved to be an excellent idea since they not only minimized the large fluctuations of the liquid levels in the manometer lines but they did not interfere with the pressure readings.

With slurry systems, another common problem will arise. Because small particles are present in the system, they may enter the manometer lines and introduce measurement errors. One possible solution is to place filters (porous) at the column wall which prevent the solids particles from entering the manometer line. This issue shall be discussed in more detail in the experimental section of this thesis.

2.2.1.1.2 Simultaneous Closure of Gas and Liquid Flows

The average gas holdup can be determined over the column height by simultaneously stopping the gas and liquid flows and subsequently measuring the bed (liquid or slurry) height after gas escape. This technique is based on the

knowledge of the gas-liquid (slurry) dispersion height (H_d) and bed height (H_s) after turning off the gas and liquid flows. The volume of the gas present is equal to the difference between the initial dispersion height and the recorded bed level:

$$H_d A_c \varepsilon_g = (H_d - H_s) A_c \qquad (2.4)$$

and

$$\varepsilon_g = \frac{(H_d - H_s)}{H_d} \qquad (2.5)$$

The liquid and solids holdups can then be calculated using Eqs. 2.1 and 2.2. In continuous bubble columns, the dispersion height is usually assumed to correspond to the column height (H_c), while in batch bubble columns the dispersion height varies with the initial bed height. A number of researchers have used this technique to measure phase holdups in two phase and three phase systems (Akita and Yoshida, 1973; Pal et al., 1980; Grover et al., 1986; Hatate et al., 1986; Ozturk et al., 1987, Trudell, 1995).

This technique is relatively simple, and able to provide a wide range of information about bubble column hydrodynamics. However, these are several errors which can significantly reduce the accuracy of the results. Some errors associated with this technique are described below:

- In batch systems, it is difficult to determine an accurate gas-liquid dispersion height when there are large fluctuations at the interface due to liquid splashing or when foam is formed at the liquid surface. In continuous bubble columns, it is also inaccurate to assume a dispersion height equal to the column height because of weir effects (Prakash, 1991).
- The design of the gas and liquid spargers plays a vital role in limiting the magnitude of the errors. Some gas is capable of flowing into the column after the gas has been turned off due to the higher pressure found inside the

distributor when the gas is flowing compared to the pressure inside the column. The gas velocity gradually reduces to zero as the pressure equilibrates. Also, liquid (or slurry) may also drain into the gas sparger and into the gas line (Schumpe and Grund, 1986).

- In continuous bubble columns, shutting off the gas promotes surface waves due to the escaping gas bubbles, thus, potentially resulting in the some liquid entrainment out of the column (Prakash, 1991).
- It is often difficult to simultaneously shut off liquid and gas flows to the column. The problem was corrected by Trudeil (1995) who combined the liquid and gas lines prior to column entrance. The two streams were mixed and then passed through a valve before entering the column. The installation of the valve did allow for simultaneous closure of both streams.
- Some gas bubbles may remain trapped between defluidized solid particles. By recirculating the remaining liquid and thereby refluidizing the bed should eliminate these bubbles (Prakash, 1991).

Wenge et al. (1995) extended this procedure to also measure solids holdup. The method depends on measurements of hydrostatic pressure in the three phase dispersion followed by interruption of gas flow, complete gas disengagement, and a second pressure measurement in the resulting two phase (solid-liquid) slurry over a short period of time. This technique was found to give accurate measurements of both solids and gas holdups.

2.2.1.1.3 Gas Disengagement Technique

The dynamic gas disengagement technique can be used to estimate the holdup structure and the bubble rise velocities. The size distribution of bubbles affects the gas holdup, the interfacial area for mass transfer, and the residence time

distribution of the gas and liquid circulation patterns in the column (Prakash, 1991). The gas disengagement technique is used to study the hydrodynamics in bubble columns since knowledge of the gas holdups and bubble sizes is essential in evaluation of performance (Patel et al., 1989).

The technique was first performed by Sriram and Mann (1977). It required an accurate measurement of the rate at which the level of the gas-liquid dispersion dropped once the gas flow to the bubble column was closed. The change in gas-liquid dispersion height was originally determined by filming the drop after turning off the gas. The rate at which the height dropped depended on the concentration and the velocity of the gas bubbles in the dispersion (Prakash, 1991). The measured disengagement profile was then used to estimate the holdup structure that existed in the dispersion prior to flow interruption. The rate of this change also provided information on the bubble size distribution since the bubble rise velocity depends on bubble size (Schumpe and Grund, 1986).

This technique requires that the holdup structure remain undisturbed by bubble interactions (i.e., coalescence and breakup) after shutting off the gas (Schumpe and Grund, 1986). It is possible to separate the contribution of small and large bubbles to the gas holdup (Sriram and Mann, 1977). Large bubbles disengage first when the gas flow is initially shut off, thus the transient gas holdup is due to small bubbles (Guy et al., 1986).

The main advantages of this technique include its simplicity and its ability to provide a wide range of hydrodynamic information. It is possible to obtain from the disengagement profile the holdup structure, bubble size and Sauter mean bubble diameter.

Gas Disengagement Technique using a Simple Digital Sensor

One major problem of dynamic disengagement technique is the poor measurement accuracy. Lee et al. (1985) modified this technique to improve its accuracy. A level measuring procedure was automated using a novel digital sensor, which was readily interfaced with a computer to record the real time, dynamic gas disengagement profile. The sensor consisted of a buoy, an encoded rod, and a light emitter-detector pair. The sensor required no calibration, no column modifications and was found to measure the dynamic gas holdup profile rapidly with high accuracy and reproducibility (Lee et al., 1985). Also, by acquiring the data with an inexpensive microcomputer, the measurements could be performed continuously (Lee et al., 1985). At higher gas velocities (> 3 cm/s), the fluctuations in the buoy became significant, thus a heavier buoy and the averaging of repeat runs were essential. The rates of change of gas holdup and bubble size distribution with time were found easily with this modified gas disengagement technique. The sensor used in the above work was extremely effective in dampening out radial and temporal fluctuations in the gas/liquid level. This technique is excellent for bubble columns, however, it would be ineffective with slurry systems because of the opaqueness of the slurry.

Gas Disengagement Technique using Pressure Transducer Signals

Daly et al. (1992) used pressure transducer signals to measure the rate of the liquid level drop. Pressure transducers permit the use of the gas disengagement technique in opaque systems, and they reduce the uncertainty involved in estimating the rate at which the liquid level dropped during large bubble disengagement (Daly et al., 1992). Five pressure transducers were placed at various heights above the distributor along the column wall in order to measure the steady state, axial gas holdup profiles and the change in output voltage during the bubble disengagement (i.e., after shutting off the gas flow to the

column using a solenoid valve). The determination of the Sauter mean bubble diameters in both a stainless steel and a glass bubble column, at similar gas holdups, showed excellent agreement using the gas disengagement technique (Daly et al. 1992).

2.2.1.1.4 Gamma-ray Attenuation

The Gamma-ray attenuation method is a non-intrusive technique based on the principle that the attenuation of the radiation in a mixture results from the absorption of the radiation by the liquid. Lockett and Kirkpatrick (1975) used the γ-ray attenuation technique to obtain the mean gas holdup in gas-liquid dispersions. To verify the results, they also obtained the mean gas holdup by shutting off the gas and liquid flows. The results were in good agreement. Vasalos et al. (1982) used the γ-ray technique to measure holdups in slurry fluidized beds. From the theoretical profile of the γ-ray absorption, they were able to estimate the bed height, and the liquid and gas holdups were easily obtained using Eqs. 2.1 and 2.3. One disadvantage with this process is that it requires elaborate handling arrangements and precautions with respect to radiation. Also, the application of this technique is limited to the accurate determination of bed height. It should be used in conjunction with other techniques (i.e. pressure profile measurements) to obtain the phase holdups. More recently, Bukur et al. (1987) have used the technique to estimate holdups for Fischer-Tropsch waxes in bubble columns. Hewitt (1978) has reviewed the γ-ray attenuation technique in more detail.

2.2.1.1.5 Shutter Plate Technique

Kato et al. (1985) used a shutter plate technique to obtain the phase holdups in a slurry system. The mean holdup of each phase was obtained by measuring the volume of trapped gas and solid particles between two shutter plates. The accuracy of this technique is greatly limited by the requirement of simultaneous and quick closure of the shutter plates.

2.2.1.2 Local Phase Holdup Measurement Techniques

This section includes the local (axial and/or radial) phase holdup measurement techniques. Some of the following techniques have a dual function in that they can be also used in measuring the cross-sectional average phase holdups. The techniques include the following:

2.2.1.2.1 Electroconductivity technique

2.2.1.2.2 Resistance or capacitance probe technique

2.2.1.2.3 Average residence time (using a gas or liquid tracer)

2.2.1.2.4 Ultrasonic technique

2.2.1.2.5 Laser holography

2.2.1.2.6 Optical probes

2.2.1.2.7 Particle image velocimetry

2.2.1.2.8 Real Time Neutron Radiography

2.2.1.2.1 Electroconductivity Technique

The electroconductivity method is based on the measurement of the electrical conductivity of the bed. The major requirement when using electrical probes in multiphase flow is that the phases have significantly different electrical conductivities. In general, the liquid phase is conductive and the gas phase is relatively non-conductive. Maxwell (1881) appears to be the first person to attempt to relate the properties of a mixture to those of its constituents (Turner, 1976). He found that the effective conductivity of a dispersion was related to the volume fraction of a dispersed non-conductive phase. The dispersed phase had an electrical conductivity different from that of the continuous phase. Consequently, variations in conductance permit the measurement of the local void fractions (local gas holdups). In fact, electroconductivity probes have been extensively used to obtain local gas porosities, bubble frequencies, as well as averages and distribution of bubble sizes and rising bubble velocities. The probes have been used in two phase systems (Hills, 1974; Soria-Lopez, 1991), in three phase fluidized beds (Fan et al., 1987; Kim and Kim, 1983; Soria-Lopez, 1991) and in slurry bubble columns (Smith et al., 1984; Yasunishi et al., 1986) using electroconductivity properties of the liquid.

Begovich and Watson (1978) applied the theory to three phase fluidized beds and reported the liquid holdup to be equal to the ratio of the conductivity of the bed to the conductivity of the liquid alone:

$$\varepsilon_l = \gamma/\gamma_l \qquad (2.6)$$

The above relationship assumes that the tortuosity factor remains approximately constant over the length of the bed (i.e. it is not substantially affected by the amount of gas in the system). Kato et al. (1981) introduced a correction factor to Eq. 2.6 after calibrating the electrodes with known liquid holdups:

$$\varepsilon_l^c = \gamma/\gamma_l \qquad (2.7)$$

where c has a value of 1.2

Marchese et al. (1992) measured phase holdups in a three phase cocurrent downflow system using both electrical conductivity and pressure based techniques. They found results to be very comparable. Uribe-Salas et al. (1994) developed a technique for measuring holdup in two phase and three phase systems under conditions relevant to column flotation. The technique relies on measurement of the effective conductivity of the dispersion and the continuous phases alone. A conductivity cell consisting of two grid electrodes covering the cross sectional area of the column and separated by a fixed distance was used to perform the measurements. Results in the three phase system showed that holdup estimates were in good agreement with those obtained by direct measurements. The empirical correlation proposed by Achwal and Stepanek (1975) also fitted the data, however, the models of Begovich and Watson (1978) and Kato et al. (1981) did not fit the data because they used facing plate electrodes.

There are several limitations to this technique. The technique suffers from its limited application to conducting liquids. The addition of salt can make the liquid conductive, however, it inhibits bubble coalescence and thus changes the coalescing properties. Also, poor distribution of the liquid can lead to erroneous results. The probes can also fail to detect very small bubbles and very large bubbles that avoid the probe entirely. Finally, the conductive solution may lead to probe corrosion.

2.2.1.2.2 Resistance or Capacitance Probe Technique

The determination of the gas holdup from electrical impedance measurements has been widely used by several researchers (Rigby et al., 1970; Hardy and Hylton, 1984; Morooka et al., 1986; Hu et al., 1986; Wolff et al., 1990). This technique is also based on the different conductivity responses given by the gas and liquid phases (i.e. different values are obtained depending on whether the tip of the probe is in the liquid or the gas phase). The basic technique has been reviewed by Hewitt (1978, 1982). Depending upon the system, the impedance will be governed by the conductance or capacitance or both. However, it is recommended to operate at conditions to assure domination of capacitance since liquid conductivity can be easily affected by the presence of dissolved salts and/or temperature variations and the dielectric constant varies less (Hewitt, 1982). Razumov et al. (1973) used a capacitance probe to measure the solid and liquid holdups in a three phase fluidized bed. Local changes in phase holdup could be detected from the changes in dielectric permeability.

The impedance method provides a very rapid response but the accuracy of this technique is somewhat doubtful due to uncertainties in the data interpretation (Prakash, 1991). The main disadvantage is its potential sensitivity to flow patterns. Gas bubbles may tend to swerve to avoid the probes and, depending on the flow configuration, a wide range of impedance values might be expected for a given void fraction (Prakash, 1991). Problems with noise may become predominant when cables are long. Probe calibration also strongly depends on bed material as well as reactor temperature and pressure.

2.2.1.2.3 Average Residence Time (using a gas or liquid tracer)

This technique is based on the determination of the real gas or liquid velocity (interstitial velocity) from the mean time of passage of a tracer between two points separated by a known vertical distance. The phase holdup can be obtained by dividing the phase superficial velocity by its phase interstitial velocity (Wild et al., 1984). The tracer selected must be easily detectable at small concentrations so that only a small quantity needs to be injected into the system, thus minimizing disturbances in the established flow pattern (Shah et al., 1978). The selected tracer should not change the properties of the phase whose holdup is being measured (i.e., the tracer used should not affect the coalescing behavior of the liquid and it should have physical properties similar to the phase of interest). The tracer should be non-reacting and the tracer detection device should cause the least amount of disturbance in the system. Sensitivity and a quick response time are required to detect the tracer in a fast moving system.

2.2.1.2.4 Ultrasonic Technique

The ultrasonic technique is a relatively new technique that can be used to simultaneously measure phase holdups in three phase systems (Maezawa et al., 1993). The technique requires a transmitter to emit an ultrasonic wave that travels through a three phase system and is received by an ultrasonic receiver located at the other end. The technique uses the change in acoustic velocity and attenuation of the sound wave to determine phase holdups. The acoustic velocity of the wave is higher in solids than in liquids which in turn is higher than in gases, therefore from the change in acoustic velocity, one can determine the makeup of the mixture. Since only a portion of the wave is transmitted through

the medium (some are reflected back and others are scattered by particles and bubbles), the amplitude of the wave will also be reduced. The change in amplitude (or attenuation) and acoustic velocity of a mixture depend on the particle size and applied frequency. Warsito et al. (1995) applied the ultrasonic technique to gas-liquid and liquid-solid systems. Since a simple system was being used, only the transmission time (or acoustic velocity) needed to be measured. Soong et al. (1995a, 1995b) applied the ultrasonic technique to three phase slurry systems to measure solids concentration.

2.2.1.2.5 Laser Holography

The laser holography technique is capable of providing the diameter, shape, and position of every gas bubble at a given time without hampering the bubble motion (Peterson, 1984). When compared with the pressure gradient measurements it provides reasonably accurate estimates of phase holdups over a range of gas flow rates. This technique does have some drawbacks in that it is expensive, hard to set up, and difficult to use at higher gas velocities and in large column diameters. This technique also requires that the liquid and solids have the same refractive index.

2.2.1.2.6 Optical Probes

Optical probes detect the change in the index of refraction in the medium to provide local values of phase holdup. Several researchers have used this technique to measure phase holdup in three phase fluidized beds. Ishida and Tanaka (1982) used a single quartz fiber probe with the dual function of projecting light and receiving its reflection. This probe could distinguish between gas bubbles, liquid and solid particles from the reflected light characteristics in a

three phase fluidized bed. De Lasa et al. (1984) and Lee et al. (1984, 1986, 1987) used a silica optical fiber probe, with a U-shaped tip sensor whose operation is based on the difference of refraction indices between the gas and the liquid. The gas holdup was then obtained from the summation of all the gas bubbles contact time with the probe. Lee (1986) noted that the base line of the probe signals increased with increasing solid holdup in liquid fluidized beds. Hu (1985) and Hu et al. (1986) used special calibration techniques to obtain solids holdup using optical fiber probes.

The main advantage of such probes is that they can be used in non-conducting liquids and at high temperatures (Lee, 1986). The limitation of the probes are high equipment costs and interference of the probes with the motion of small bubbles and possible breakup of larger bubbles. Although suitable for bubble columns and three phase fluidized beds, this technique may not be suitable for slurry bubble columns due to the opacity of the slurry.

2.2.1.2.7 Particle Image Velocimetry

More recently, non-intrusive digital analysis techniques have been developed for the measurement of bubble velocities, angles of bubble rise and phase holdups (Kim and Agarwal, 1992). The motion of bubbles are observed through a charge-coupled device video camera, which snaps image frames at random. The captured image is then digitized by a frame grabber and stored on a computer. The digitized image is analyzed on the computer using specialized software. This system is capable of measuring the time-averaged bubble characteristics.

The Particle Image Velocimetry (PIV) system is capable of providing instantaneous, quantitative results on a flow plane including instantaneous

velocity distribution of different phases, accelerations, gas and solid holdups, bubble sizes and their distributions and other statistical flow information (Chen et al., 1994). The system can be used to measure local flow properties in 2-dimensional, 3-dimensional bubble columns and fluidized beds (Chen and Fan, 1992; Chen et al. 1994; Lin et al, 1996). The PIV system consists of schemes which identify the particle images, discriminate the particle images between phases, and compute the displacement between the particle images from successive frames.

Since a detailed visual representation of the system can be examined using this technique, accurate information on the hydrodynamic conditions at a particular location in the column should be obtained. The main advantage of this technique over probe type systems is its ability to operate without affecting the flow characteristics in the column. However, the technique may be more difficult to adapt to an industrial application as compared to electroconductivity probes. Because images are to be analyzed, this system is not suitable for slurry systems because of opacity of the system.

2.2.1.2.8 Real Time Neutron Radiography

This technique is similar to the Gamma-ray attenuation method. The Real-Time Neutron Radiography (RTNR) technique can be used in a gas-liquid bubble column to determine the cross-sectional average void fraction at different axial locations and interfacial areas (Chang and Harvel, 1992). The determination of the void fraction is based on neutron attenuation. The technique operates in real time and uses thermal neutrons to penetrate the pipe wall. Thermal neutrons do not disturb the fluid flow because they have low energy contact with the fluid in the pipe. Previous research in this area has indicated that the RTNR

technique can visualize two-phase flow through aluminum and steel pipes to determine the flow regime, void fraction and interfacial area (Harvel and Chang, 1992). The volume averaged void fraction determined by neutron attenuation agrees quite well with the void fraction by the liquid level method. The instantaneous void fraction profile can be obtained in a relatively large section of the pipe and it can provide relevant information regarding the location and shape of interfaces (Chang and Harvel, 1992). This method also can be used to determine bubble shape and size, and the interfacial area. The cost and the availability of equipment limit the use of this technique. This system has not been tested on three phase systems, however, it should theoretically operate.

2.2.2 Effects of Operating Parameters on Phase Holdups

Studies on slurry bubble columns have shown that the effect of solids on gas holdup depends on a number of factors. The gas holdup can be affected by parameters including: gas and liquid velocities, physical properties of the liquid, gas density and pressure, column diameter, gas distributor design and solids concentration, size, density and wettability (Bukur et al., 1990). The gas holdup is also significantly affected by the operating flow regime in the column.

2.2.2.1 Effects of Gas Velocity

Gas holdup in bubble columns depends mainly on superficial gas velocity (Shah et al., 1982). For bubble columns and slurry bubble columns, gas holdup has been found to increase with increasing superficial gas velocity (Michelsen and Ostergaard, 1970; Kim et al., 1972; Koide et al., 1984; Fan et al., 1986b; Saxena et al., 1989). In the dispersed bubble flow regime, this increase has been found to be proportional (Bach and Pilhofer, 1978; Deckwer et al., 1980). For

coalesced bubble regime, the effect of V_g on ε_g is less pronounced (Akita and Yoshida, 1973; Kara et al., 1982; Koide et al., 1984). The extent of increase of gas holdup with superficial gas velocity (when comparing two and three phase systems) becomes more significant with a decrease in gas velocity. Ying et al. (1990) found that with low gas velocities (V_g < 0.03 m/s), the existence of solids did not change the gas holdup. However, Sauer and Hempel (1987) observed that the presence of small light particles (density < 1300 kg/m^3) at low superficial gas velocities (V_g < 0.04 m/s) resulted in optimum interaction between the particles and liquid turbulence, thus producing smaller bubbles and consequently higher gas holdup values. This was also noted by Wolff et al. (1990) who reported higher gas holdup (than the two phase system) at low gas flowrates and low solids concentrations. Sauer and Hempel (1987) also noted that high superficial gas velocities, higher solid concentrations and particle densities resulted in larger bubbles and consequently lower gas holdups. Again, this was concluded by Wolff et al. (1990).

The shape of radial gas holdup profiles are also influenced by gas flowrate. At low gas velocities the gas holdup is almost independent of the radius, with only a slight decrease near the wall (Nottenkaemper et al., 1983). Hills (1974) also observed that the radial profile of the gas holdup was relatively flat for gas velocities below 0.03 m/s. With increasing gas flowrates, however, the profile of the local gas holdups in a vertical bubble column shows a characteristic parabolic shape, with a sharp maximum at the center. The results fit the intuitive concept of bubbles rising in the center and, thus inducing a circular liquid flow. At the top of the column, the majority of bubbles leave the liquid medium and then the liquid streams downward close to the column wall (Fisher et al., 1994). Wachi et al. (1987) observed the gas holdup to be 10% to 20% lower at the column wall than at the center. Lin et al. (1996) also reached the same conclusions using the particle image velocimetry technique.

2.2.2.2 Effects of Liquid Velocity

Bukur et al. (1989, 1990) studied the effect of the operating mode on the gas holdup. They used two types of solids (iron oxide and silica) in two size ranges (0 to 5 μm and 20 to 44 μm), with solids concentrations of 0 to 30wt%. The experiments were conducted in a 0.05 m inside diameter, 3 m high column equipped with a single hole 2 mm orifice plate distributor. Both batch and circulating modes were studied for the slurry. Nitrogen was used as the gas phase and the superficial gas velocity was varied between 0.02 and 0.12 m/s. The operating conditions were generally selected to closely simulate slurry bubble column reactors for Fischer-Tropsch synthesis applications. Hydrotreated reactor wax (FT-300 paraffin) and SASOL wax were employed as the liquid medium. They observed that even a small upward liquid flow (0.005 m/s) lowers the gas holdup significantly; however, a further increase in the liquid flow had only a marginal effect on the average gas holdups. It appears that the significant differences in gas holdups between the batch and continuous modes of operation are due to changes in the foaming characteristics of the medium. For the batch case, the foam accumulates at the top of the dispersion and increases the gas holdup, whereas in the continuous mode of operation the foam is removed from the column by the recirculating slurry. These results were confirmed by Pino et al. (1990a, 1990b) who found that the operating mode strongly affects the gas holdup of foaming systems. In the semi-batch mode, the gas holdup is higher than in the continuous mode. These observations were explained by the effect of foam degradation owing to the drag forces at the column exit in the continuous mode, which are absent at the free surface in the semi-batch mode. This effect was so important that, in some cases, foaming occurred only in the semi-batch mode. They found that an increase in the superficial liquid velocity (0 to 3.21 cm/s) in foaming systems results in a

decrease in gas holdup at first and then, as the liquid velocity is increased, the gas holdup goes through a minimum and then begins to increase again. This was primarily due to the higher turbulence of the liquid. They did not observe any influence of the liquid superficial velocity on the gas holdup for non-foaming systems.

Results obtained in the continuous mode of operation by other researchers indicate that liquid velocity either has no effect on the average gas holdup (Shah et al., 1982; Kelkar et al., 1984; Ying et al., 1990) or decreases the gas holdup slightly (Kara et al., 1982; Kelkar et al., 1984). This was also more recently confirmed by Wilkinson et al. (1992). According to Kelkar et al. (1984), the effect of the slurry velocity on the gas holdup was more pronounced at lower gas velocities where the bubbly flow regime prevailed, being negligible in the case of a 10wt% oil shale particle and water slurries for gas velocities greater than 6 cm/s. However, it should be noted that most previous studies were conducted with liquids that do not have the tendency to foam. In the case of foaming systems, the method used to measure the gas holdup is very important. Local measurements of the gas holdup which have the ability to discriminate between the foaming regime and other regimes are to be preferred.

2.2.2.3 Effects of Liquid Physical Properties

Liquid properties affect the gas holdup behavior through effects on bubble formation and/or bubble coalescing tendencies. An increase in liquid viscosity will decrease gas holdup; the increase in viscosity leads to larger stable bubbles and thus higher bubble rise velocities. Gas holdup data obtained for slurry bubble columns containing various organic solvents are available from Hammer (1979).

Liquid interfacial properties also play an important role in gas holdup. Adding a small amount of a surface acting material (surfactant) to water, such as a short chain alcohol, produced significantly higher gas holdup (Kelkar et al., 1983).

The presence of electrolyte or impurities can also lead to a higher gas holdup (Hikita et al., 1980; Kelkar et al., 1984; Morooka et al., 1986; Sada et al., 1986a). Sada et al. (1986a) also noted that the presence of suspended solids particles has a much smaller influence on gas holdup in electrolyte solutions than in non-electrolyte solutions.

2.2.2.4 Effects of Gas Density and Pressure

Studies have shown that gas holdup in bubble columns generally increases with increasing operating pressure, and hence gas density (Idogawa et al., 1987; Clark, 1990; Kojima et al., 1991). The influence of pressure has been found to depend on pressure level, distributor type, gas velocity and solids concentration. Results show that a correlation for gas holdup should account for the effects of operating pressure (and gas density), however, most literature correlations are based on data obtained at atmospheric pressure and as a result they do not account for influence of gas density. In solids-free bubble columns, several equations have been developed based on high pressure operation (Idogawa et al., 1986, 1987) or experiments using various gases (Reilly et al., 1986). The limited gas holdup values that have been reported are in general relatively high (Brown, 1984; Clark, 1990).

Kojima et al. (1991) studied the effects of pressure on gas holdup in slurry bubble columns. They found that the gas holdup decreased as the pressure and

solids concentration was increased. However, at 30wt% solids concentration, no effect of pressure was observed. This reduced effect of pressure on gas holdup was attributed to the coalescence of bubbles enhanced by the presence of solids particles. Clark (1990) also concluded that the addition of fine solids to the liquid phase promoted rapid bubble coalescence and a significant decrease in overall gas holdup when under high pressure.

2.2.2.5 Effects of Column Diameter

The gas holdups have been found to decrease with increasing column diameter (Begovich and Watson, 1978; Tsungting et al., 1985). Begovich and Watson (1978) also found no significant effect of column diameter on liquid and solid holdups. Hu et al. (1986) found that the gas holdup in their large diameter column was significantly lower than in the smaller diameter column used by Ostergaard (1971). Tsungting et al. (1985), however, did not account for the effect of gas distribution which could explain most of the difference observed by these authors. Saxena et al. (1990a) concluded that the gas holdup is not highly dependent on column diameter when the diameter is larger than 0.10 m, however, the holdup is dependent on the nature of internals present in the column. The gas holdup increases if the internals in the column prevent bubble coalescence and thereby limit the size of the coalesced bubbles.

Pino et al. (1992) also studied the effects of column dimensions on gas holdup in slurry bubble columns using a foaming liquid (kerosene). They found that both column height and column diameter do not affect the gas holdup values in three phase systems at high gas velocities when foaming occurs.

2.2.2.6 Effects of Gas Distributor Design

Very few researchers have investigated the effects of gas and liquid distribution on bed hydrodynamics and phase holdups. Gas holdup has been found to be strongly affected by type of gas distributor, especially for gas velocities below 0.06m/s (Yamashita and Inoue, 1975; Oels et al., 1978). Yamashita and Inoue (1975) found a maximum in gas holdup as a function of hole size when using different hole sizes. They also found that when holes of less than 1.0mm were used, two distinct types of regimes could be observed. At low velocities (below 0.06m/s), the gas holdup increased linearly with gas velocity, corresponding to the dispersed bubble flow regime. At higher velocities, there was significant deviation in linearity. They found that the gas holdup depended on the fraction of the column base which was aerated and on the number, pitch and diameter of orifice holes. For orifice diameters of greater than 1.0mm, the effect of orifice diameter on gas holdup became insignificant (Yamashita and Inoue, 1975). Koide et al. (1984) also tested various perforated plate distributors with differing hole diameters in a slurry bubble column. They concluded that the distributor affected gas holdup in the transition regime as well as the onset conditions for the transition regime. For columns with a perforated plate distributor having an orifice diameter smaller than 2.0mm or having a pitch greater than 25mm, the gas holdup was found to increase linearly with the gas velocity up to a maximum value in the dispersed bubble regime. The gas holdup then decreased in the transition regime and increased again in the coalesced bubble regime. They also found that the gas holdup decreased with increasing solids concentration but this effect of concentration on gas holdup was less pronounced as hole diameter was increased. Kojima et al. (1986) also observed that an increase in solids holdup (solids concentration in feed of 3.1 to 62 kg/m^3, glass beads with diameter 105 to 125 μm) decreased the gas holdup when a porous plate (with mean pore size of 185 μm) was used as the gas distributor. When a perforated plate (31 x 1.05 mm; 7 x 1.05 mm) or a single nozzle (3 mm ID x 10 mm OD) was

used as gas distributor, an increase in solids concentration did not result in lower gas holdups.

Thus gas holdup depends on the number, pitch and diameter of orifice holes. With small holes (<1.0mm), gas holdup increases linearly with gas velocity in the dispersed bubble regime. This linearity disappears for higher gas velocities (coalesced bubble regime). Also, an increase in solids concentration decreases gas holdup when porous plates are used but has no effect when a single nozzle distributor is used.

2.2.2.7 Effects of Particle Size and Slurry Concentration

The gas holdup in slurry bubble columns has been found to be affected by solids concentration, particle size and density and solids wettability.

Particle Size

A number of researchers have investigated the effects of particle size and concentration on gas holdup (Kato et al., 1973; Kara et al., 1982; Sada et al., 1986a; Morooka et al., 1986). The influence of particle size has been found to depend on a number of factors including flow regime, gas velocity, liquid properties and slurry concentration. Khare and Joshi (1990) found gas holdups to increase with particle sizes up to 70μm at low solids loadings (<10vol%). The fractional increase (above gas-liquid systems) depended on sparger type, liquid properties and gas velocity. The increase in gas holdup was more significant for spargers generating fine bubbles at low gas velocities. The influence of particles decreased with increasing liquid viscosity. For larger particles (>70μm), Khare and Joshi (1990) observed gas holdup to be lower than gas-liquid systems. The results of Khare and Joshi (1990) can be compared with

those of Sada et al. (1986a) who also observed an increase in gas holdup with 3μm alumina particles using low solids loadings (0.1wt%) and a porous plate distributor. However, no increase of gas holdup was observed when a perforated plate was used for gas distribution. Pandit and Joshi (1984) observed an increase in gas holdup for fine particles (<50μm), followed by a decrease for medium sized particles (50-350μm) followed by another increase for larger sized particles (>350μm) when using a slurry concentration of 1vol%. Saxena et al. (1990a) also reported an increase in gas holdup for particles sizes up to 100μm followed by a decrease. Saxena et al. (1992a) also concluded that the effect of particle size is more pronounced for low concentration slurry systems. These results indicate that fine particles at low concentrations can enhance gas holdup mainly by hindering bubble coalescence. This influence has been found to disappear with increasing slurry concentrations when larger bubbles would be formed at the distributor.

Kara et al. (1982) did not observe significant differences in gas holdup between gas-liquid and gas-liquid-solid systems when 10 μm size particles were used because their slurry concentrations were higher at 9-18vol%. They observed, however, that an increase in the solids particle size (up to 70μm) for slurry concentrations of about 10vol% decreased the gas holdup. Kato et al. (1973) also observed this using higher solids concentrations and particle sizes from 60-175 μm, as did Morooka et al. (1986). But in the presence of water containing a surfactant, Morooka et al. (1986) also observed an increase in the gas holdup upon solids addition (44 μm and 113 μm).

Kelkar et al. (1984) tested solids wettability and found that wettability played an important factor in enhancing the coalescence tendencies in the liquid phase, thereby reducing the gas holdup.

Slurry Concentration

Most studies have been conducted in the slurry concentration ranges up to 20vol% solids. Several researchers concluded that an increase in solids concentration generally reduces the gas holdup (Kato et al., 1973; Deckwer et al., 1980; Kara et al., 1982; Koide et al., 1984; Pandit and Joshi, 1984; Sada et al., 1986b; Yasunishi et al., 1986; Nigam and Schumpe, 1987; Sauer and Hempel, 1987; and Ying et al., 1990). For low solids loadings (<5vol%), the behavior of the slurry bubble column is often close to that of a solids-free bubble column (Sada et al., 1986a; Sauer and Hempel, 1987; Wolff et al., 1990). Saxena et al. (1990b) reported only a slight decrease of the gas holdup upon solids addition and solids loading up to 30wt%. However, Kato et al. (1973) found that this effect becomes significant at high gas velocities (V_g > 0.10-0.20m/s).

2.2.3 Gas Holdup Correlations

A large number of correlations for the prediction of gas holdup in bubble columns have been reported in the literature, as reviewed by Shah et al. (1982). These correlations cover a wide range of variables such as liquid properties, gas density, gas velocity, etc.. However, a number of authors reported major discrepancies in using existing correlations to predict gas holdup. For example, Quicker and Deckwer (1981) noted that existing literature correlations did not describe their measurements on xylene, decaline, C_{10}-C_{14} paraffins or Vestowax. Even for the most studied system (air/water) fairly large differences in predicting gas holdups were encountered. The large scatter observed is partly due to the lack of knowledge about the nature of the flow patterns (Reilly et al., 1986; Tsuchiya and Nakanishi, 1992) and to the extreme sensitivity of the gas holdup

on the system medium, in particular, the effect of trace impurities. Furthermore, the easily available liquid physical properties such as density, viscosity and surface tension are not necessarily sufficient to explain the observed scatter. Most correlations developed in predicting the gas holdup show a pronounced difference in the dependence of the gas holdup on the superficial gas velocity. It is well known that the gas holdup is proportional to the superficial gas velocity, the dependence varying with the flow regime. Consequently, a correlation developed with a fixed dependence of the gas holdup on the superficial gas velocity would be hardly applicable to different flow regimes. Moreover, the potential influence of the equipment design was usually ignored in most correlations. It appears, that in order to be able to moderate the influence of these factors, the bubble formed at the distributor should have a size close to the equilibrium bubble size or the medium must be coalescence promoting, and the bubble column must have a liquid height such that the stable bubble size is reached in a small fraction of the total liquid height (Chabot, 1993). Table 2.1 lists several gas holdup correlations suitable for bubble columns and slurry bubble columns.

2.2.3.1 Bubble Columns

Hughmark (1967) used wide range of operating parameters ($0.025<D_c<1.1$m, $0.004<V_g<0.45$m/s, and $780<\rho_l<1700$kg/m^3) to develop the following correlation for average gas holdup in a bubble column:

$$\varepsilon_g = \frac{V_g}{\left(2V_g + 0.35\left(\sigma\rho_l/72\right)^{1/3}\right)} \qquad (2.8)$$

Although this correlation does account for liquid physical properties, the effects of gas physical properties and column diameter have been neglected.

Table 2.1 Correlations for Gas Holdup in Bubble Columns and Slurry Bubble Columns

Investigator	Correlation for Gas Holdup (SI Units)	System	Range of Variables
Hughmark (1967)	$\varepsilon_g = \left(\frac{V_g}{\left(2V_g + 0.35(\rho_l \sigma/72)^{1/3}\right)} \right)$	gas: air liquid: water, kerosene, light oil, glycerol aqueous solution, Na_2SO_3 aqueous solution, $ZnCl_2$ aqueous solution	$0.025 < D_c < 1.1$ m $0.004 < V_g < 0.45$ m/s $780 < \rho_l < 1700$ kg/m^3 $0.0009 < \mu_l < 0.152$ kg/m s $0.025 < \sigma < 0.076$ kg/s^2 (multi orifice sparger)
Akita and Yoshida (1973)	$\frac{\varepsilon_g}{(1-\varepsilon_g)^4} = A_1 \left(\frac{D_c^2 \rho_l g}{\sigma} \right)^{1/8} \left(\frac{D_c^3 \rho_l^2 g}{\mu_l^2} \right)^{1/12} \left(\frac{V_g}{\sqrt{g D_c}} \right)$	gas: air, He, O_2, CO_2 liquid: water, glycol, methanol, glycol aqueous solution, methanol aqueous solution	$0.152 < D_c < 0.6$ m $0.006 < V_g < 0.42$ m/s $790 < \rho_l < 1590$ kg/m^3 $0.00058 < \mu_l < 0.021$ kg/m s $0.0223 < \sigma < 0.074$ kg/s^2 (single nozzle sparger)
Hikita et al. (1980)	$\varepsilon_g = 0.672 \left(\frac{V_g \mu_l}{\sigma} \right)^{0.578} \left(\frac{\mu_l^4 g}{\rho_l \sigma^2} \right)^{0.131} \left(\frac{\rho_g}{\rho_l} \right)^{0.062} \left(\frac{\mu_g}{\mu_l} \right)^{0.107}$	gas: air, H_2 liquid: water, methanol, n-butanol, 30%-50% sucrose solution	$D_c = 0.1$ m $0.0042 < V_g < 0.38$ m/s $790 < \rho_l < 1170$ kg/m^3 $0.0009 < \mu_l < 0.0178$ kg/m s $0.0229 < \sigma < 0.0759$ kg/s^2 (single nozzle sparger)

Table 2.1 (cont.) Correlations for Gas Holdup in Bubble Columns and Slurry Bubble Columns

Investigator	Correlation for Gas Holdup (SI Units)	System	Range of Variables
Kara et al. (1982)	$\varepsilon_g = \dfrac{\mathrm{Re}_g}{\left(B_1 + B_2\,\mathrm{Re}_g + B_3\,\mathrm{Re}_{sl} + B_4\left(\varepsilon_s / (\varepsilon_s + \varepsilon_l)\right)\right)}$	gas: air liquid: water solids: coal, dried mineral (d_p = 10, 30, 70 μm)	D_c = 0.152 m 0.03 < V_g < 0.30 m/s 0 < V_{sl} < 0.10 m/s ρ_s = 1300 kg/m^3 0% < ψ_s < 30vol%
Koide et al. (1984)	$\dfrac{\varepsilon_g}{(1-\varepsilon_g)^4} = \dfrac{k_1\left(V_g\mu_l/\sigma\right)^{0.918}\left(g\mu_l^4/(\rho_l\sigma^3)\right)^{-0.232}}{1+4.35\left(\psi_s\right)^{0.748}\left[(\rho_s-\rho_l)/\rho_l\right]^{0.88}\left(D_c V_g/\rho_l\right)^{-0.148}}$	gas: air liquid: water, ethylene glycol aqueous solution, glycerol aqueous solution solids: glass and bronze spheres (47.5 < d_p < 192 μm)	0.14 < D_c < 0.30 m 0.01 < V_g < 0.18 m/s V_{sl} = 0 m/s 997 < ρ_l < 1178 kg/m^3 ρ_s = 2500, 8770 kg/m^3 (perforated plate)
Smith et al. (1984)	$\varepsilon_g = \left(\dfrac{V_g}{\left(2.25V_g + 0.339\left(\rho_{sl}\sigma/72\right)^{0.31}\mu_{sl}^{0.016}\right)}\right)$	gas: N_2 liquid: water, silicone oil, ethylene glycol, aqueous ethanol solids: glass beads (48.5 < d_p < 194 μm).	D_c = 0.108 m 0.03 < V_g < 0.20 m/s 820 < ρ_l < 1100 kg/m^3 ρ_s = 2500, 8770 kg/m^3 (multi orifice sparger)

Table 2.1 (cont.) Correlations for Gas Holdup in Bubble Columns and Slurry Bubble Columns

Investigator	Correlation for Gas Holdup (SI Units)	System	Range of Variables
Sada et al. (1986b)	$\frac{\varepsilon_g}{(1-\varepsilon_g)^3} = 0.019 U_t^{1.16} \psi_s^{-(0.125 U_t^{0.16})} V_g$	gas: O_2, N_2 liquid: water, sucrose solution, Na_2SO_4, NaCl and KCl solutions solids: $Ca(OH)_2$, glass beads, nylon ($7 < d_p < 96$ μm) (d_p for nylon = 2000 μm)	$D_c = 0.078$ m $0.02 < V_g < 0.20$ m/s $848 < \rho_l < 1296$ kg/m^3 $\rho_s = 240, 1140, 2480$ kg/m^3 $0\% < \psi_s < 10$vol% (perforated plate)
Sauer & Hempel (1987)	$\frac{\varepsilon_g}{(1-\varepsilon_g)} = 0.0277 \left(\frac{V_g}{(\nu_{sl} g)^{1/4}}\right)^{0.844} \left(\frac{\nu_{sl}}{\nu_{eff,rad}}\right)^{-0.136} \left(\frac{C_s}{C_\infty}\right)^{0.0392}$	gas: air liquid: water solids: sand, various plastics (110 μm $< d_p < 2.9$ mm)	$D_c = 0.14$ m $0.01 < V_g < 0.08$ m/s $1020 < \rho_s < 2780$ kg/m^3 $0\% < \psi_s < 20$vol% (perforated plate)
Wilkinson et al. (1992)	$\varepsilon_g = \frac{U_{trans}}{U_{s,b}} + \frac{(V_g - U_{trans})}{U_{l,b}}$	gas: N_2 liquid: water, n-heptane, mono ethylene glycol	$D_c = 0.158, 0.23$ m $0.25 < V_g < 0.28$ m/s $683 < \rho_l < 2960$ kg/m^3 $0.0004 < \mu_l < 0.055$ kg/m s $0.02 < \sigma < 0.073$ kg/s^2 (ring sparger)

Akita and Yoshida (1973) also used a wide range of conditions ($0.152<D_c<0.6$m, $0.006<V_g<0.42$m/s, and $790<\rho_l<1590$kg/m^3) to propose the following dimensionless empirical equation for predicting the average gas holdup in bubble columns:

$$\frac{\varepsilon_g}{(1-\varepsilon_g)^4} = A_1\left(\frac{gD_c^{\,2}\rho_l}{\sigma_l}\right)^{1/8}\left(\frac{gD_c^{\,3}}{\nu_l^{\,2}}\right)^{1/12}\left(\frac{V_g}{\sqrt{gD_c}}\right) \qquad (2.9)$$

Several different gases and liquids were used in their study. The value of A_1 was determined to be 0.2 for pure liquids and non-electrolyte solutions and 0.25 for electrolyte solutions. This correlation is known to provide for reliable and conservative estimates for low viscosity and coalescing liquids (μ_l < 0.02 Pa s). However, it is not recommended for hydrocarbon fluids, non-Newtonian fluids or non-coalescing liquids.

Hikita et al. (1980) recorded gas holdup measurements in a 0.10 m diameter column using various gases and liquids ($0.004<V_g<0.38$m/s and $790<\rho_l<1170$kg/m^3). These authors proposed the following relation:

$$\varepsilon_g = 0.672 f_1\left(\frac{V_g\mu_l}{\sigma}\right)^{0.578}\left(\frac{\mu_l^{\,4}g}{\rho_l\sigma^2}\right)^{-0.131}\left(\frac{\rho_g}{\rho_l}\right)^{0.062}\left(\frac{\mu_g}{\mu_l}\right)^{0.107} \qquad (2.10)$$

Here, f_1 is a function of the ionic strength and has a value of 1 for non-electrolyte solutions and salt solutions. Hikita et al. (1980) were one of the first researchers to consider physical properties of the gas phase. The influence of the gas density is limited for normal conditions but becomes significant for systems operating under high pressure. Again, this correlation may not be reliable for complex mixtures of fluids, non-Newtonian fluids, non-coalescing fluids and hydrocarbon liquids.

Krishna et al. (1991) proposed a gas holdup model based on the two-bubble class theory. They proposed that for superficial gas velocities below the transition gas superficial velocity (U_{trans}), the gas holdup increases proportionally to the superficial gas velocity, whereas, for higher gas superficial velocities (churn turbulent regime) it was assumed that the gas velocity in excess of the transition (V_g-U_{trans}) flows through the bubble column in the form of large bubbles. This theory was further developed by Wilkinson et al. (1992) and generalized to incorporate the effects of both the gas and liquid physical properties. Nitrogen was used as the gas phase along with several different liquids. For the transition and heterogeneous regimes, the gas holdup can be expressed as follows:

$$\varepsilon_g = \frac{U_{trans}}{U_{sb}} + \frac{V_g - U_{trans}}{U_{lb}} \tag{2.11}$$

where $U_{s.b.}$ is the bubble rise velocity of the small bubbles, and $U_{l.b.}$ is the rise velocity of the large bubbles. Furthermore, $U_{s.b.}$, $U_{l.b.}$, and U_{trans} can be obtained using:

$$\frac{U_{sb}\mu_l}{\sigma} = 2.25\left(\frac{\sigma^3\rho_l}{g\mu_l^4}\right)^{-0.273}\left(\frac{\rho_l}{\rho_g}\right)^{0.03} \tag{2.12}$$

$$\frac{U_{lb}\mu_l}{\sigma} = \frac{U_{sb}\mu_l}{\sigma} + 2.4\left(\frac{\mu_l(V_g - U_{trans})}{\sigma}\right)^{0.757}\left(\frac{\sigma^3\rho_l}{g\mu_l^4}\right)^{-0.077}\left(\frac{\rho_l}{\rho_g}\right)^{0.077} \tag{2.13}$$

$$\frac{U_{trans}}{U_{s.b.}} = 0.5\exp\left(-193\rho_g^{-0.61}\mu_l^{0.5}\sigma^{0.11}\right) \tag{2.14}$$

These equations were found to give an excellent description of the experimental data for gas-liquid systems. The average error reported by the authors was only 10% and experimental gas holdup data up to 50% were successfully described by this model. However, only a narrow range of gas velocities were used to develop this correlation ($0.25<V_g<0.28$m/s).

2.2.3.2 Slurry Bubble Columns

For systems with low solids concentrations (<10vol% solids), Smith et al. (1984) confirmed that the correlation of Hughmark (1967) could be applied by replacing the liquid density, ρ_l, with a slurry density, ρ_{sl} and adding a viscosity term, μ_{sl}:

$$\varepsilon_g = \left(\frac{V_g}{\left(2.25 V_g + 0.339 \left(\rho_{sl}\sigma/72\right)^{0.31} \mu_{sl}^{\,0.016}\right)} \right) \qquad (2.15)$$

where

$$\mu_{sl} = \mu_l \exp\left(\frac{(5/3)\psi_s}{1-\psi_s} \right) \qquad (2.16)$$

The correlation is based on the assumption that a slurry of fine particles behaves as a homogeneous liquid of higher viscosity and density. Experiments were carried out in a 0.108m diameter column with varying gas velocities and liquid densities ($0.03<V_g<0.20$m/s and $820<\rho_l<1100$kg/m^3). The correlation does not, however, take into account the effects of particle size and column diameter.

Kara et al. (1982) proposed the following correlation based on cocurrent upflow of gas and slurry:

$$\varepsilon_g = \frac{\mathrm{Re}_g}{\left(B_1 + B_2 \mathrm{Re}_g + B_3 \mathrm{Re}_{sl} + B_4 \left(\varepsilon_s / (\varepsilon_s + \varepsilon_l) \right) \right)} \qquad (2.17)$$

where B_1 through B_4 are adjustable parameters for specified particles (i.e. for coal and dried minerals ranging in particle diameter from 10μm to 70μm). A wide range of gas flowrates ($0.03<V_g<0.30$m/s), slurry flowrates ($0<V_{sl}<0.10$m/s)

and slurry concentrations (0%<ψ_s< 30vol%) were also studied. The values of B_1 through B_4 must be determined experimentally for each particle type and size.

Koide et al. (1984) worked with a system of air, various aqueous liquid solutions and glass and bronze spheres to develop the following correlation:

$$\frac{\varepsilon_g}{\left(1-\varepsilon_g\right)^4} = \frac{k_1\left(V_g\mu_l/\sigma\right)^{0.918}\left(g\mu_l^4/(\rho_l\sigma^3)\right)^{-0.252}}{1+4.35\left(\psi_s\right)^{0.748}\left[\left(\rho_s-\rho_l\right)/\rho_l\right]^{0.88}\left(D_cV_g/\rho_l\right)^{-0.168}} \qquad (2.18)$$

where k_1 has a value of 0.227 for water and aqueous solutions of glycerol and glycol and a value of 0.364 for aqueous solutions of inorganic electrolytes. Fine concentrations of solids (0%<ψ_s<12vol%) were used with particle sizes ranging from 48μm to 200 μm and gas velocities from 0.01 to 0.18m/s. The correlation, however, does not take into account the effect of particle size or gas physical properties on gas holdup.

Sada et al. (1986b) proposed the following correlation for fine solids suspensions:

$$\frac{\varepsilon_g}{\left(1-\varepsilon_g\right)^3} = 0.019U_t^{1/16}\psi_s^{-\left(0.125U_t^{-0.16}\right)}V_g \qquad (2.19)$$

where U_t is the particle terminal velocity, and both U_t and V_g are in cm/s. The terminal velocity can be correlated with the following:

$$U_t = \frac{g\left(\rho_s-\rho_l\right)d_p^{\,2}}{18\mu_l} \qquad (2.20)$$

Varying solids, liquids and gases (0.02<V_g<0.20m/s) were used to develop this correlation, however, only a narrow range of solids concentrations (0%<ψ_s<10vol%) were studied. Furthermore, measurements were carried out in a very small diameter column (D_c=0.078m).

Sauer and Hempel (1987) proposed the following correlation:

$$\frac{\varepsilon_g}{\left(1-\varepsilon_g\right)} = C_1\left(\frac{V_g}{\left(\nu_{sl} g V_g\right)^{0.25}}\right)^{C_2}\left(\frac{\nu_{sl}}{\nu_{eff,rad}}\right)^{C_3}\left(\frac{C_s}{C_{so}}\right)^{C_4} \qquad (2.21)$$

where C_1, C_2, C_3, and C_4 are empirical constants based on distributor type, and ν_{sl} is the effective kinematic slurry viscosity, and $\nu_{eff,rad}$ is the effective radial momentum transfer coefficient. Both ν_{sl} and $\nu_{eff,rad}$ can be correlated using:

$$\nu_{sl} = \frac{\mu_l\left(1+2.5\varepsilon_s+10.05\varepsilon_s^{\,2}+0.00273\exp\left(16.6\varepsilon_s\right)\right)}{\varepsilon_s\rho_s+(1-\varepsilon_s)\rho_l} \qquad (2.22)$$

$$\nu_{eff,rad} = 0.011 D_c\sqrt{gD_c}\left(V_g^{\,3}/\nu_l g\right)^{0.125} \qquad (2.23)$$

Even though a wide range of variables were studied ($0\%<\psi_s<20$vol%, $110<d_p<2900\mu$m, and $1020<\rho_s<2780$kg/m^3), the correlation of Sauer and Hempel (1987) does not take into account the effects of particle size on gas holdup.

2.2.4 Gas Holdup Correlations Based on Drift Flux

The interaction between two phases in a gas-liquid system is usually assumed to depend upon the relative motion between the phases rather than the absolute velocity of each phase. Two approaches have been used to describe this phase interaction: one correlates the relative (slip) velocity as a unique function of the phase holdup (e.g. Richardson and Zaki, 1954) and the other correlates the drift velocity or drift flux as a function of phase holdups (Wallis, 1969). Both concepts are very similar however there is one major difference - relative

velocity refers to the slower moving phase velocity and the drift velocity refers to a volumetric mean velocity of all phases (Fan, 1989).

The drift flux can generally be defined as the volumetric flux of the gas relative to a surface moving with the average velocity of the dispersion. The concept of drift flux for two and three phase systems have been reviewed by several researchers (Nicklin, 1962; Zuber and Findlay, 1965; Wallis, 1969; Darton and Harrison, 1975; Nacef et al., 1988; Fan, 1989; Saxena and Chen, 1994). It is useful in that a plot of the drift flux velocity versus gas holdup (V_{gl} vs. ε_g) can show at which gas velocity the bubble flow regime switches to the churn turbulent regime, since at that point the drift flux increases sharply (Kelkar et al., 1983).

For a two phase (gas-liquid) systems, if the volume averaged velocity (V_T) of the dispersion is

$$V_T = V_g + V_l \tag{2.24}$$

then the drift flux velocity (V_{gl}) is defined as

$$\frac{V_{gl}}{\varepsilon_g} = \frac{V_g}{\varepsilon_g} - V_T \tag{2.25}$$

Similarly, for a three phase (gas-liquid-solid) slurry systems, the drift flux is defined as

$$\frac{V_{gl}}{\varepsilon_g} = \frac{V_g}{\varepsilon_g} - \frac{V_T}{\varepsilon_g + \varepsilon_l} \tag{2.26}$$

where

$$V_T = V_g + V_{sl} \tag{2.27}$$

Nacef et al. (1988) found that the drift flux velocity in three phase fluidized beds can be predicted by a correlation of the form

$$V_{gl} = b_1(V_g)^{b_2} \tag{2.28}$$

The value of the constants b_1 and b_2 can vary depending on distributor type and column diameter. The applicability of this correlation does however need to be tested over a wider range of variables.

In working with three phase systems, several researchers (Pandit and Joshi, 1984; Smith et al., 1984; O'Dowd et al., 1987; Saxena et al., 1990a; and Saxena and Chen, 1994) have indicated that the gas holdup can also be correlated with an equation of the form

$$\varepsilon_g = \frac{V_g}{c_1 + c_2 V_g} \tag{2.29}$$

where c_1 and c_2 are constants.

Smith et al. (1984) and O'Dowd et al. (1987) have estimated the valued of c_2 to be 2.0. Pandit and Joshi (1984) on the basis of their data found c_2 to vary from 2.0 to 2.8. Saxena and Chen (1994) calculated the value to be 2.5. Other researchers (Nicklin, 1962; Hills, 1976) have also observed values for c_2 closer to 1.0. Generally, c_1 has been identified as the characteristic terminal rise velocity of a swarm of bubbles ($U_{b\infty}$) in infinite medium. Pandit and Joshi (1984) found $U_{b\infty}$ to vary from 0.22 to 0.55m/s. O'Dowd et al. (1987) found $U_{b\infty}$ to range between 0.36 and 0.50m/s. Saxena and Chen (1994) analyzed several previous studies by Saxena and coworkers to develop the following correlation for $U_{b\infty}$:

$$U_{b\infty} = 1.80C(P_v)(\sigma\rho_{sl}/72)^{0.333}(\mu_{sl})^{0.289} \tag{2.30}$$

Here, $C(P_v)$ is the pressure corresponding to the midpoint of the dispersion in the column. The general equation was developed for small and large columns and for two and three phase systems. Experimental gas holdup results (using

Eq. 2.29) were found to be within 20% from predicted gas holdup values. The range of operating parameters of Saxena and coworkers were as follows:

liquid density	883 - 1000 kg/m^3
liquid viscosity	0.0004 - 0.0559 Pa.s
solids particle size	1.7 - 212 μm
solids concentration	0 - 50 wt%
gas velocity	0.005 - 0.30 m/s
liquid velocity	0 m/s
temperature	298 - 473K

These operating parameters are very similar to the present study. Experimental results of Reilly et al. (1986) and Godbole et al. (1984) were also tested using the correlation of Saxena and Chen (1994) and found to have an average accuracy of +/-10% with a maximum uncertainty of +/-20%.

2.2.5 Gas Holdup Correlations Based on Wake Model

The wake model takes into account the role of the wake behind the gas bubble in liquid flow. The concept considers the three phase fluidized bed to be divided into the gas bubble region, the wake region, and the solid-liquid fluidized region. The overall bed voidage (ε) consists of the total gas holdup (ε_g) and the total liquid holdup (ε_l) which is divided between the wake region (ε_{lw}) and the liquid fluidized region (ε_{lf}).

Bubble wake models have been widely used to predict the bed expansion or contraction behaviors and the phase holdups. General descriptions of the models are given by Epstein (1981), Wild et al. (1984), Muroyama and Fan (1985) and Fan et al. (1987). These models use two key parameters called *k* and *x* where *k* is defined as the ratio of wake volume to bubble volume and *x* is

the ratio of solids holdup in the wake region to the solids holdup in the liquid fluidized region. The mathematical expressions for the two parameters are:

$$k = \varepsilon_w / \varepsilon_g \qquad (2.31)$$

and

$$x = \varepsilon_{sw} / \varepsilon_{sf} \qquad (2.32)$$

The correlations for k have been reviewed by Muroyama and Fan (1985) and Fan et al. (1987). The value of x in general lies between zero (solids-free wake) and unity (wake solid holdup same as solid holdup in liquid fluidized region). Some researchers such as El-Temtamy and Epstein (1978), Dhanuka and Stepanek (1978) assumed that the bubble wakes contained solids while others (e.g. Darton and Harrison, 1975) assumed solids-free wakes.

A generalized wake model was developed by Bhatia and Epstein (1974). The model assumes the relative velocity between the liquid and the solid in the liquid-solid fluidized region is related to the bed porosity by the Richardson and Zaki (1954) equation. The resultant expression for the liquid holdup and bed porosity can be given as:

$$\varepsilon_l = \left[\frac{V_l - V_g k(1-x)}{U_t(1-\varepsilon_g - k\varepsilon_g)}\right]^{1/n}\left[1-\varepsilon_g(1+k-kx)\right] + \varepsilon_g k(1-x) \qquad (2.33)$$

and

$$(1-\varepsilon_s) = \left[\frac{V_l - V_g k(1-x)}{U_t(1-\varepsilon_g - k\varepsilon_g)}\right]^{1/n}\left[1-\varepsilon_g(1+k-kx)\right] + \varepsilon_g(1+k-kx) \qquad (2.34)$$

In order to be able to use Eq. 2.34 to predict solids holdup, methods must be available to estimate U_t, n, k, ε_g and x. For a given gas-liquid-solid system, the values of U_t (particle terminal velocity) and n (Richardson and Zaki constant) are

fixed. In the solids-free wake model, which assumes x=0, the values of k and ε_g need to be known to estimate the phase holdups or bed expansion.

Various empirical correlations have been proposed to estimate the k. This value should depend on the average bubble size, which in turn depends on the prevailing hydrodynamic regime. This has been taken into account only in the correlations proposed by Darton and Harrison (1975) and El-Temtamy and Epstein (1978). The correlation proposed by Darton and Harrison (1975) however assumes a solids-free wake which may not be justified in the beds of fine particles. Wild et al. (1984) have pointed out other limitations of the various correlations for k. Using literature correlations, they have shown that there is a considerable scatter in the predictions of the coefficient k as a function of superficial gas velocity. The equations for k implicitly assume uniform bubble size distribution which is not the case for large gas flowrates in the coalesced bubble flow regime where there are wide distributions of bubble diameters. The validity of these observations need to be tested over a wider range of experimental conditions (Prakash, 1991).

Since the wake model provides only one equation between the three holdups, an extra correlation for gas holdup is required to solve for all holdups. The available correlations for the prediction of the gas holdup have a limited range of applicability. Bhatia and Epstein (1974) have proposed gas holdup estimations based on the bubble rise velocity. These velocities however depend on the bubble diameter for which no accurate correlation or model are available.

Other problems with the wake model include:

- These models implicitly assume a constant bubble rise velocity (i.e. constant bubble diameter) which is not justified at high gas flowrates in the coalesced bubble flow regime.
- All the wake models developed have assumed the bubble wake to be rising at the same velocity as the bubble. Fan et al. (1987) pointed out that due to vortex shedding, the net velocity of the wakes would be lower than that of the bubbles.

2.2.6 Solids Concentration Profiles

The solids mixing behavior in a batch slurry bubble column resembles that in the freeboard region of a gas-liquid-solid fluidized bed containing large or heavier particles (Fan, 1989). The solids concentration shows a decreasing tendency with axial distance. The flow regime also has a strong effect on the axial solids concentration profile. Fan (1989) noted that within the same flow regime (dispersed or coalesced bubble regime), the effect of gas velocity on axial solids concentration distribution is not very significant. Tang and Fan (1989) studied the effects of changing gas velocities on local solids holdup in the dispersed bubble regime and also found that gas velocity has only a slight effect on the holdup distribution. Smith and Ruether (1985), Smith et al. (1986) and O'Dowd et al. (1987) all studied effects of changing gas velocity in the coalesced regime and found no appreciable differences in slurry concentration. Murray and Fan (1989) also confirmed these results using 49μm glass beads, however, they found that for 163μm glass beads, an increase in gas velocity leads to a more uniform concentration distribution.

For batch systems, the solids concentration profile is found to be more uniform for smaller particles (Smith et al., 1986; Murray and Fan, 1989). This was also confirmed by Bukur et al. (1990) who found that 0-5μm particles showed only a slight gradient while 20-44μm particles had a much steeper gradient. This can be explained by a decrease in settling velocity with decrease in particle size. For continuous systems, there is only a very slight effect of particle size on solids distribution profile.

The solids dispersion increases significantly with an increase in the liquid velocity. Bukur et al. (1990) tested 20-44μm iron oxide and silica particles in continuous and batch systems. They observed axial holdup gradients for batch systems, however, when a very small amount liquid circulation was introduced, the profile became uniform and suspension of solids improved significantly. This is not unexpected because a slight flow of liquid will most probably exceed the particle terminal velocity leading to particle dispersion. Murray and Fan (1989) also confirmed these results using glass beads of 49μm and 97μm. They also found that when dealing with a binary mixtures (i.e. two different sized solids in a system), this effect is more significant on the larger particles. Liquid properties like density, viscosity and surface tension and surfactants may also have an effect the solids dispersion (Morooka et al., 1986; Kelkar et al., 1984).

2.2.6.1 Sedimentation-Dispersion Model

The sedimentation-dispersion model has been used extensively to determine the axial solids concentration profiles for batch slurry bubble column systems. The model was originally proposed by Cova (1966) and Suganuma and Yamanishi (1966) however several variations of the model have been proposed for steady-

state conditions. The following assumptions have been made in formulating the model:

- There are no radial gradients in the concentration of solids particles.
- All solids particles are identical in regard to terminal velocity.
- Gas holdup, solids dispersion coefficient and settling velocity of solids are all constant along the column axis.
- Gas and liquid velocities are such that, all solids particles are completely suspended in liquid.

The simplified correlation for axial solids distribution in batch slurry systems may be expressed as

$$C_s(z) = C_{so} \exp\left(\frac{V_p}{E_s} z\right) \qquad (2.35)$$

where V_p is the average solids convective velocity in the particulate fluidization phase and can be directly related to the particle hindered settling velocity (U_p).

As seen in Eq. 2.35, the model is characterized by two parameters - the hindered solids settling velocity (U_p) and the axial solids dispersion coefficient (E_s). Cova (1966) and Suganuma and Yamanishi (1966) determined hindered settling velocities and dispersion coefficients relative to the slurry phase and its cross-sectional area, whereas, Parulekar and Shah (1980) calculated these relative to column cross-sectional area. Various empirical correlations have been proposed in literature to account for these two parameters and several such correlations are summarized in Table 2.2. The dispersion coefficient has been found to be a function of the Peclet Number which in turn is a related to the gas Froude Number,

Table 2.2 Correlations for Solids Axial Dispersion Coefficient and Hindered Settling Velocity in Slurry Bubble Columns

Investigator	Correlation for E_s and U_p (SI Units)	System	Range of Variables
Kato et al. (1972)	$\frac{V_g D_c}{E_s} = 13 Fr_g \left(\frac{\left(1 + 0.009\,\mathrm{Re}_p\, Fr_g^{0.8}\right)}{\left(1 + 8 Fr_g^{0.85}\right)} \right)$ $U_p = 1.33 U_t \left(V_g / U_t \right)^{0.25} \psi_l^{2.5}$	gas: air liquid: water solids: glass beads (75.5 < d_p < 163 μm) ρ_s = 2520 kg/m^3 (perforated plate distributor)	0.0066 < D_c < 0.214 m 2.01 < H_d < 4.05 m 0.02 < V_g < 0.30 m/s 0.02 < V_{sl} < 0.022 m/s 48 < C_s < 202 kg/m^3 (2vol% to 8vol%)
Smith and Ruether (1985)	$\frac{V_g D_c}{E_s} = 9.6 \left(Fr_g^6 / \mathrm{Re}_g \right)^{0.1114} + 0.019\,\mathrm{Re}_p^{1.1}$ $U_p = 1.91 V_g^{0.26} U_t^{0.80} \psi_l^{3.5}$	gas: nitrogen liquid: water, ethanol solids: glass beads (48.5 < d_p < 164 μm) ρ_s = 2420, 3990 kg/m^3 (single bubble cap distributor)	Dc = 0.108 m H_d = 1.94 m 0.03 < V_g < 0.2 m/s 0.0071 < V_{sl} < 0.02 m/s 0 < C_s < 150 kg/m^3 (0vol% to 7.0vol%)
O'Dowd et al. (1987)	$\frac{V_g D_c}{E_s} = 7.7 \left(Fr_g^6 / \mathrm{Re}_g \right)^{0.098} + 0.019\,\mathrm{Re}_p^{1.1}$ $U_p = 1.69 V_g^{0.23} U_t^{0.80} \psi_l^{1.28}$	gas: nitrogen liquid: water solids: glass spheres (88 < d_p < 105 μm) ρ_s = 2420 kg/m^3 (perforated plate distributor)	Dc = 0.108 m H_d = 1.94 m 0.031 < V_g < 0.24 m/s V_{sl} = 0.0077 m/s 0 < C_s < 291 kg/m^3 (0vol% to 12vol%)

Table 2.2 (cont.) Correlations for Solids Axial Dispersion Coefficient and Hindered Settling Velocity in Slurry Bubble Columns

Investigator	Correlation for E_s and U_p (SI Units)	System	Range of Variables
Murray and Fan (1989)	$E_s = 0.022 V_g^{0.938} U_l^{0.702}$ $V_p = V_{lf} - V_s$ V_{lf} is linear liquid velocity V_s is the slip velocity	gas: air liquid: water solids: glass beads ($49 < d_p < 163$ μm) ρ_s = 2450-2990 kg/m^3 (sparger-type distributor)	Dc = 0.076 m H_d = 1.50 m $0.016 < V_g < 0.173$ m/s $0 < V_{sl} < 0.031$ m/s $0 < C_s < 60$ kg/m^3 (0vol% to 2.5vol%)

Peclet Number:

$$Pe_p = \frac{V_g D_c}{E_s} \tag{2.36}$$

Froude Number:

$$Fr_g = \frac{V_g}{(gD_c)^{0.5}} \tag{2.37}$$

Researchers have found Peclet number to increase with increasing Froude number (Kato et al., 1972; Smith and Ruether, 1985; Smith et al., 1986; O'Dowd et al., 1987). They have also observed the Peclet number to decrease with increasing column diameter. Kojima and Asano (1981) and Kojima et al. (1986) developed a correlation to predict Peclet number independent of the column diameter. Their calculated values were higher than most other correlations though. Kato et al. (1972) demonstrated that the axial solids dispersion coefficient was not a function of the liquid velocity or the average solids particle concentration. However, they were able to show that the axial solids dispersion coefficient increases with an increase in superficial gas velocity and is directly proportional to $D_c^{1.0\text{-}1.5}$ (Fan, 1989).

Kato et al. (1972), Smith and Ruether (1985) and O'Dowd et al. (1987) have all determined hindered settling velocities and solids dispersion coefficients using the Suganuma and Yamanishi (1966) model. Their equations are presented in Table 2.2. The range of variables and operating parameters were very similar for all researchers. Kato et al. (1972) developed their equations using air, water and glass beads ($76<d_p<164\mu m$) with varying gas velocities ($0.02<V_g<0.30m/s$) and slurry concentrations (2vol% to 7vol%). Column diameters were varied from 6 to 21 cm and the dispersion height ranged from 2 to 4 m. Smith and Ruether (1985) used a 10cm diameter column with a height of 2 m. Nitrogen, water and ethanol, and glass beads ($76<d_p<163\mu m$) were used with varying superficial gas

velocities ($0.03<V_g<0.20$m/s) and slurry concentrations (0% to 8vol%) to develop their correlations. It should be noted that the original reference article presented by Smith et al (1985) has several typing errors in the equation for hindered settling velocity. These were corrected in a later article. O'Dowd et al. (1987) developed correlations using a 10cm diameter column with dispersion height of 2 m. Nitrogen, water, and glass beads ($88<d_p<105\mu$m) were used with varying superficial gas velocities ($0.03<V_g<0.24$m/s) and slurry concentrations (0% to 12vol%).

Critical reviews of the sedimentation-dispersion model for batch and continuous slurry flow systems are given by Jean et al. (1989) and Fan (1989).

2.2.6.2 Holdup Distribution Model Based on Bubble Wake Phenomenon

Murray and Fan (1989) established this model based on the conceptual framework proposed by Tang and Fan (1989) for solids axial solids distribution in a three phase fluidized bed containing low density particles. One of the characteristics of a three phase fluidized bed of low density particles which most distinguishes it from that of high density particles is the uneven distribution of axial phase holdups. The model takes into account entrainment and de-entrainment in the wake of rising bubbles. There are three distinct phases in the column; the gas bubble phase, the wake phase, and the liquid-solid emulsion phase. As the gas bubbles rise, liquid and solids are entrained into the wake that follows the bubbles. The wake region rises with the bubble at the same velocity as the bubble. Solids in the wake region are discharged through wake shedding. In finalized form, the proposed model is

$$C_s(z) = C_{so} \exp\left(\frac{V_p}{E_s} z\right) \qquad (2.38)$$

The mechanistic model has the same form as the sedimentation-dispersion model (Eq. 2.35) but the authors claim that this model offers significant physical interpretation of model parameters.

Many of the assumptions made in deriving the gas holdup correlations based on the wake model (section 2.2.5) were also extended to this analysis. A full derivation has been presented by Murray and Fan (1989). They were able to correlate the solid velocity in particulate fluidization phase (V_p) as a function of liquid linear velocity (V_{lf}) and slip velocity (V_s):

$$V_p = V_{lf} - V_s \tag{2.39}$$

where

$$V_{lf} = \frac{-V_g k(1 - x\varepsilon_{sf})}{\left(1 - \varepsilon_g - k\varepsilon_g\right)\left(1 - \varepsilon_{sf}\right)} \tag{2.40}$$

and

$$V_s = U_t(1 - \varepsilon_{sf})^{n-1} \tag{2.41}$$

Furthermore, the solids dispersion coefficient was reported by Murray and Fan (1989) as

$$E_s = 0.022 V_g^{0.938} U_t^{-0.702} \tag{2.42}$$

Air, water, and glass beads ($49<d_p<163$mm) were used with varying superficial gas velocities ($0.016<V_g<0.173$m/s). The column diameter and dispersion height were 7.6cm and 1.5m, respectively. Slurry concentration, however, was varied over a limited range (0% to 2.5vol%).

The model was found to fit their experimental data quite well, however, it was not tested with data from other researchers.

2.2.6.3 Hydrodynamic Suspension Model

Kleijntjens et al. (1994) proposed the Hydrodynamic Suspension Model to predict the axial solids holdup distribution. To sustain a state of suspension, solid-liquid two phase stirred reactors are often described by means of a minimum power input. In this state, particles do not remain at the bottom of the reactor for more than 2 seconds. This is known as the Zwietering criterion (Kleijntjens et al., 1994). The Kleijntjens et al. (1994) mathematical model combines the properties of the sedimentation-dispersion model and the Zwietering approach. They theorized that the hydrodynamic state of the suspension, resulting in the specific solids holdup distribution (characterized through the Peclet number), is related to the turbulent liquid fluctuation velocity and the eddy length. These parameters in turn are related to the power input (*P/V*). Thus, the solids holdup profile and power input are related to each other by means of these turbulent parameters.

Turbulence has often been used to describe the interaction between a discrete particle and its surroundings (Hinze, 1972). However, a particle response number must first be identified to determine the hydrodynamic state of particles in turbulent suspension. The particle response number is defined as the ratio of particle response time, τ_p, which gives a measure of the particle inertia, and a characteristic time for the change of motion in turbulent flow, τ_t, (Kleijntjens et al., 1994):

$$\tau_p / \tau_t = \frac{\left[0.04(\rho_s + \beta\rho_l)d_p^{\,2}\right] / \eta_f}{l_e / u'} \qquad (2.43)$$

For particle response numbers of 0.1 or less, the particle inertia is much smaller than the characteristic time of liquid motion indicating that the particle will follow

turbulent flow (i.e. suspension regime). With response numbers above 0.1, complete particle suspension is improbable because the particle is unable to respond to changes in flow. The length of the energy containing eddies, l_e, and the corresponding turbulence fluctuation velocity, u', are also important parameters. Hinze (1959) related both of these parameters to the dispersion coefficient as follows

$$E_z = 2\, u'\, l_e \qquad (2.44)$$

Furthermore, the specific kinetic power dissipation for isotropic turbulent flow, ε_{kin}, can also be described using these two parameters (Batchelor, 1953)

$$\varepsilon_{kin} = u'^3 / l_e \qquad (2.45)$$

This shows that the kinetic energy transfer rate in turbulent flow is determined by the hydrodynamics of energy containing eddies (Kleijntjens et al., 1994). Thus, the mathematical suspension model of Kleijntjens et al. (1994) relates eddy length and fluctuation velocity to parameters used in the sedimentation-dispersion model (namely, E_s and Pe_p).

In order to solve this model, only the eddy length needs to be known. All other parameters can be calculated or estimated. The parameter estimation for l_e can come from a comparison between the predicted average axial solids distribution (according to the model) and the experimentally measured solids holdup.

The mathematical model of Kleijntjens et al. (1994) made several key assumptions. The researchers have played a key role in development of biological slurry reactors for the decontamination of soils and, for this reason, it was decided to develop a tapered reactor system (a Dual Injected Turbulent Separation reactor or DITS). This tapered reactor has the possibility of handling high solids loadings at low power inputs, which is an economic necessity for the soil slurry process. The flow patterns in this reactor primarily resemble that of an

airlift reactor in which the liquid motion is generated by density differences between the bubble containing zone and the liquid zone. Bucyancy forces are thus regarded as being responsible for the bulk motion. In comparing this flow pattern to that in a bubble column, a major difference can be seen. In bubble columns, the flow pattern is highly irregular, while, in the tapered system two relatively stable shear layers are present over the total reactor height (Kleijntjens et al. 1994). The eddy length and turbulent fluctuation velocities are also assumed to be constant over the entire reactor, thus implying that the generated turbulence in the shear layers is distributed quickly by the bulk motion. The size of the eddies is also considered to be small compared to the bulk motion, therefore the turbulence is assumed to be isotropic.

Kleijntjens et al. (1994) carried out experiments in a tapered reactor with height to diameter ratio of 1. This allowed them to make several key assumptions which were highlighted above. The extension of this model to slurry bubble columns is questionable.

3.0 Experimental

3.1 Experimental Setup

Experimental measurements were conducted in a Plexiglas column which had an inner diameter of 0.15m and total height of 2.5m. The column was designed with four sections for easy construction and flexibility (Figure 3.1a). The main support structure was constructed using 2" galvanized piping ensuring that the column was held firmly in place and vertically at times of high vibration (i.e. at high gas velocities).

The gas phase was oil-free compressed air. The filtered air passed through a sonic nozzle and entered the column through a gas distributor at the column bottom. The sonic nozzle provides the advantage of a controlled air flow which is independent of downstream pressure (which may fluctuate during experimental runs). The air flow rate was varied by adjusting the pressure upstream of the sonic nozzle with a pressure regulator. The superficial gas velocity was varied between 0.05m/s and 0.28m/s. The design and calibration of the sonic nozzles is presented in Appendix A. Air exited the column top via a fume hood. Prior to exiting in the fume hood, the air passed through a cyclonic separator and bag filter to remove any fine particulates which may have been entrained.

Tap water was used as the coalescing liquid phase for both two phase (G-L) and three phase (G-L-S) systems. For some experiments, the coalescence behavior of the liquid was altered by adding small amounts (up to 20 vppm) of iso-amyl

Figure 3.1a - Experimental Setup

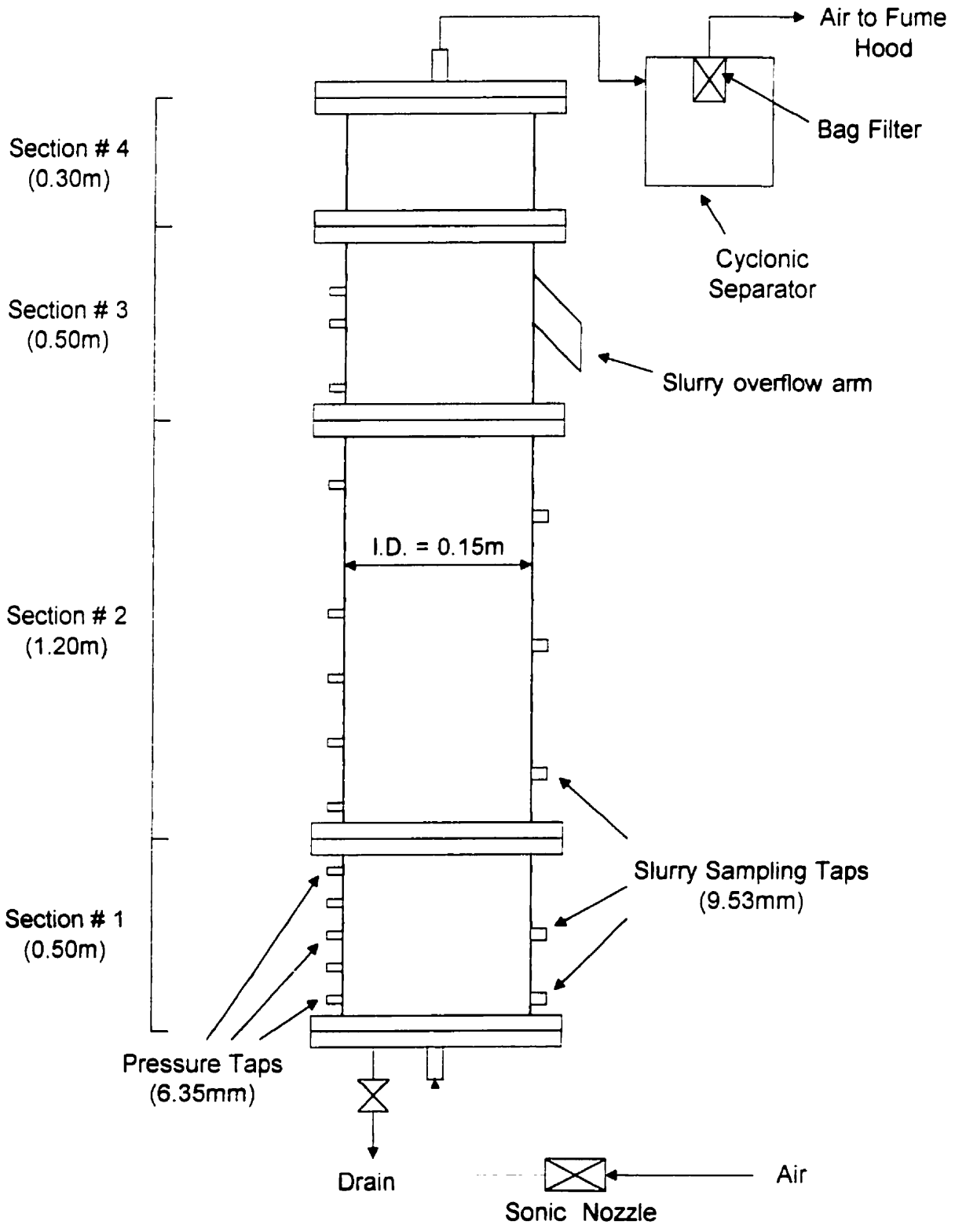

Figure 3.1b - U-Tube Manometer Setup

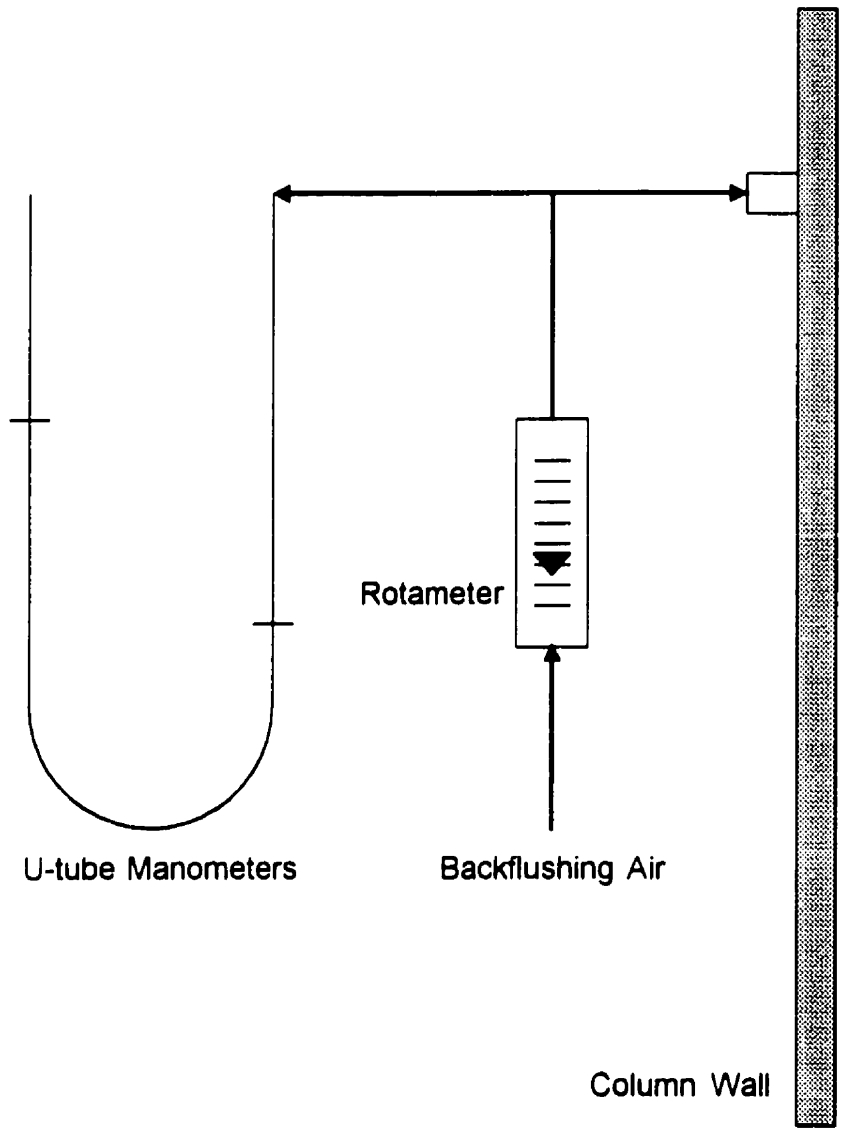

alcohol (a coalescence inhibitor). Initially, a few measurements for gas holdup (in G-L systems) were also obtained with de-ionized water as the liquid phase. Since minute impurities in tap water could have affected gas holdup measurements. The differences in gas holdup between tap water and de-ionized water were found to be negligible (<3%). The static liquid (or slurry) height was mostly maintained at 1.5m above the bottom, though for systems with coalescence inhibitor, this height was reduced to 1.3m due to heavy foaming at the top of the column.

Glass beads of average diameter 35μm and density of 2452 kg/m^3 constituted the solid phase. The particle size distribution and average particle diameter (given in Appendix C) were determined by a particle size analyzer (Brinkman, Model No. 2010). To divide the bulk solids received from the manufacturer (Flex-O-Lite Ltd.) into representative workable fractions, a procedure illustrated in Appendix C was followed. Appendix C also presents the technique used to determine solids density. The liquid and solids were added to the column through the top of the column. To prevent pockets of air from being trapped in the column, water was always added first to the column followed by the solids. The slurry concentration was varied from 5vol% to 40vol% solids.

Due to the large range of flows and slurry concentrations to be studied, a special gas distributor shown in Figure 3.2a was designed. The lower sparger was designed for low gas velocities (<0.15m/s) and the upper sparger for high gas velocities (>0.15m/s). The lower sparger was designed with 4 arms with 5 orifices per arm. The upper sparger was designed with 4 arms with 7 orifices per arm. The orifices diameter was 1.5mm and they were facing vertically downwards (shown in Fig. 3.2b). The design allowed the total gas flow to be split between lower and upper sparger. For this study, however, it was decided to use only the lower sparger due to time constraints. The height of the lower

Fig. 3.2a - Dual Sparger Design (Profile)

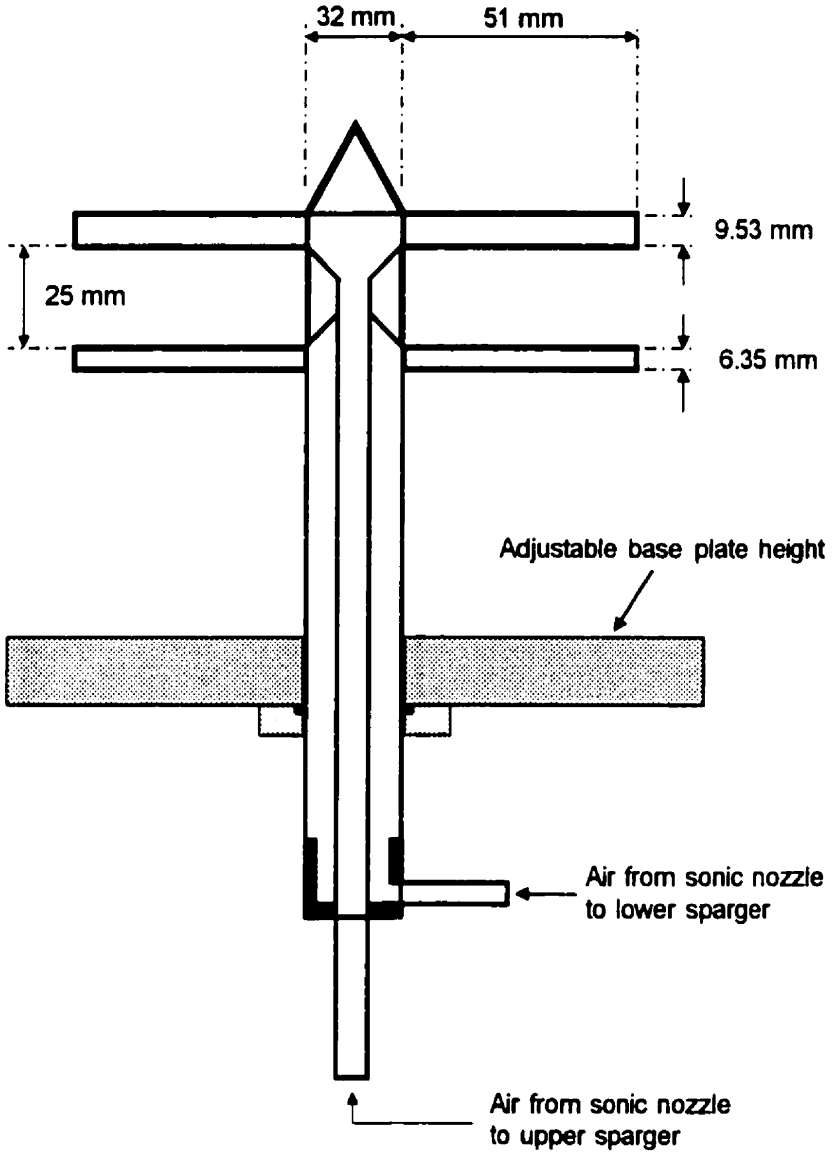

Upper Sparger - 4 arms w/ 7 orifices each
Lower Sparger - 4 arms w/ 5 orifices each
Orifices located on bottom of arms
Orifice diameter = 1.5 mm

Fig. 3.2b - Location of Sparger Orifices (Bottom View)

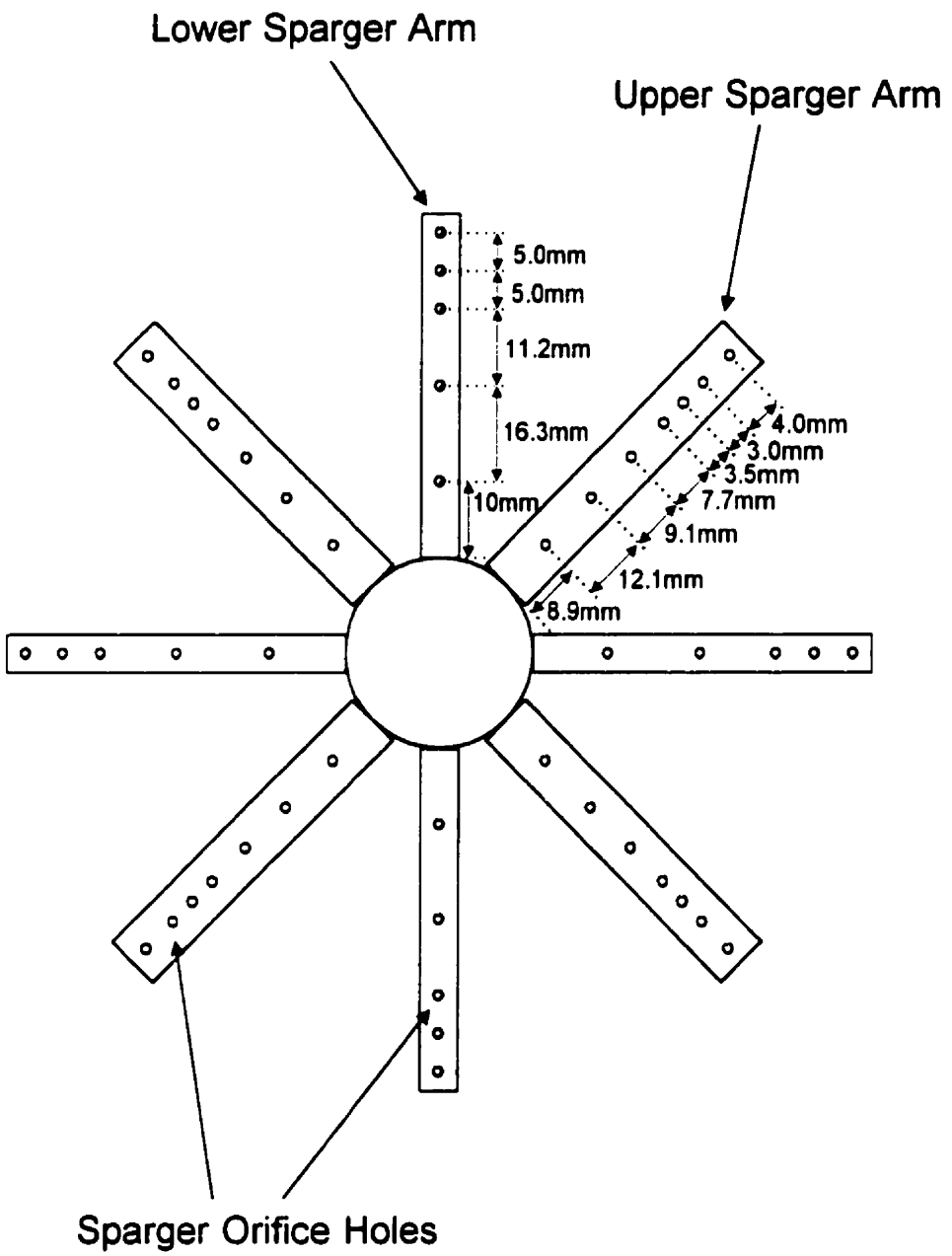

sparger was maintained at 1.5cm above the base plate. A second distributor (shown in Figure 3.3) was also designed to study the effects of sparger height from the column bottom. The height of this sparger could be varied from 1.5 to 45 cm above the column bottom. The design procedure and pressure drop checks for spargers are presented in Appendix B.

3.2 Experimental Techniques

The gas holdup was measured using expanded bed height and pressure profile techniques. Eleven pressure taps were installed along the wall to measure the static pressure along the column height location. The manometers were located at approximately 5, 15, 25, 35, 45, 55, 75, 95, 115, 155, and 205cm, respectively, above the base plate. Two additional taps (located at 175cm and 195cm above the base) were later installed to cover the foam region (see section 3.2.1.3).

Axial solids holdup was measured using the specially designed sampling probe shown in Figure 3.4. Five sampling ports were available along the axial column height to collect slurry samples. They were located at 5, 25, 65, 105, and 145cm (denoted Probes # 1 through #5), respectively, above the base of the column.

3.2.1 Gas Holdup Measurements Techniques

The gas holdup was measured in two manners: 1) by taking the axial pressure profile and 2) by measuring the static and expanded bed heights prior to and during the experimental runs.

Fig. 3.3 - Variable Height Sparger Design (Profile)

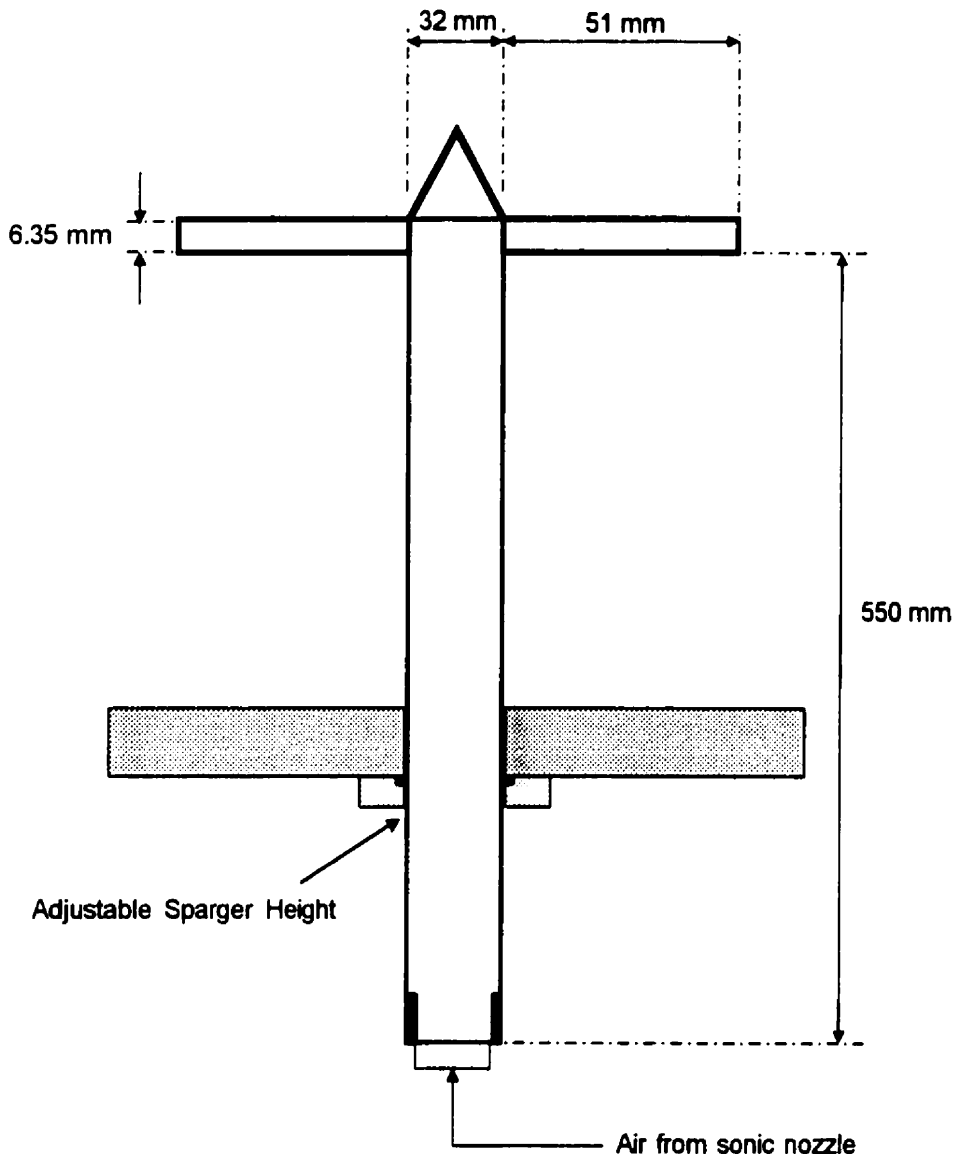

Sparger has 4 arms w/ 5 orifices each
Orifices located on bottom of arms
Orifice diameter = 1.5 mm

Fig. 3.4 - Slurry Sampling Probe

Two probes @ 9 inches
Three probes @ 6 inches

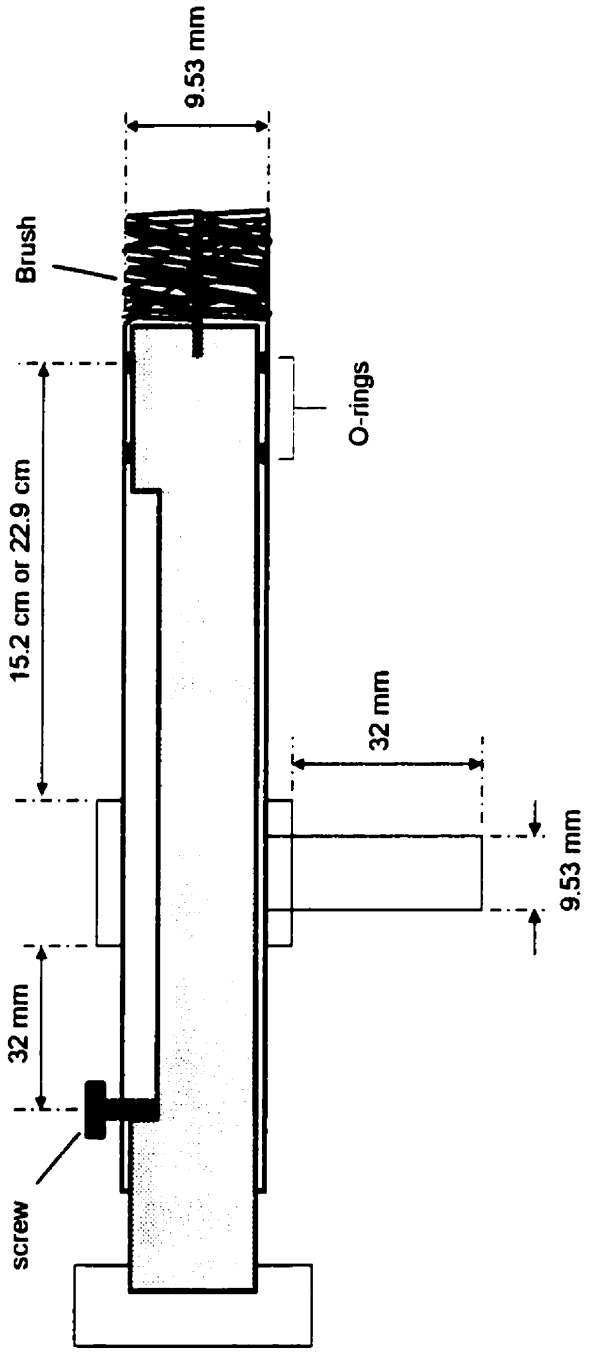

3.2.1.1 Gas Holdup Based on Pressure Profile

The axial gas holdups in the bubble columns were obtained from the static pressure profile measurements along the column height. Initially, the static pressure profile was measured using liquid filled manometers since most literature studies have used liquid filled manometers for gas holdup measurements. Ten measurements were obtained using the probes located from 5cm to 155cm above the base plate. The pressure gradient can be related to the pressure differential (Δy in mm H_2O) to the height difference of the pressure taps (Δz in mm):

$$\frac{\Delta P}{\Delta z} = \rho_l g\left(\frac{\Delta y}{\Delta z} - 1\right) \tag{3.1}$$

However, the pressure gradient is also defined as

$$-\frac{\Delta P}{\Delta z} = g\left(\rho_l \varepsilon_l + \rho_g \varepsilon_g\right) \tag{3.2}$$

Neglecting the ($\rho_g \varepsilon_g$) term in Eq. 3.2, gas holdup between two adjacent taps can be directly correlated from Eqs. 3.1 and 3.2

$$\varepsilon_g = \left(\Delta y / \Delta z\right) \tag{3.3}$$

A full derivation of this equation is presented in Appendix D.

The system worked well with gas-liquid bubble columns but problems arose when dealing with slurry systems due to plugging of manometer lines. Porous polyethylene filters (1.6mm thick) were initially tested to prevent solids from entering the manometer lines. However, it was soon discovered that the solids would plug the filters and dramatically reduce the manometer response time. A new system therefore had to be developed to measure the gas holdups.

The idea of using air to backflush the purge lines was then tested. This could be accomplished by adding flow purge Rotameters to each pressure tap. The setup is shown in Figure 3.1b. Since air was being used, the original manometers were to be changed to U-tube manometers. Each Rotameter would allow a very small amount of air to enter the column, thereby preventing liquid and/or solids from entering the lines. Ideally, the pressure in the entire line should be the equal, so the pressure measured by the U-tube manometers should be equal to that at the column wall. The only noticeable problem would have been the frictional pressure drop in the line from the Rotameter to the column wall. To minimize this error, the length of tubing from the tee splitter to the column wall was minimized to approximately 50cm. This was done for all pressure taps to maintain consistency. The idea was tested and found to work successfully for both bubble column and slurry bubble column systems. Due to limited availability of Rotameters and manometers, the number of pressure taps used for local measurements were reduced from ten to five. The new pressure taps employing the U-tube technique with backflushing were located at 5, 25, 45, 75 and 115cm above the base plate.

Initially, a trap system was also set up to prevent slurry from entering the manometer lines, however, no backflow of slurry was observed. Since several leaks were also discovered, the system was disconnected. At high gas flowrates, there were large fluctuations of liquid levels in the manometers. In order to dampen the oscillations, capillary restrictions (0.8mm diameter and 50mm long) were used in each of the tubes connecting the manometer lines to the system. Extensive testing has shown that measured average pressures are not affected by the restrictions (Prakash, 1991).

A full derivation for obtaining gas holdup was performed for the U-tube manometers and is presented in Appendix D. The pressure gradient can be related to the pressure differential (Δy in mm H_2O) to the height difference of the pressure taps (Δz in mm) as follows:

$$\frac{\Delta P}{\Delta z} = \rho_f g\left(\frac{\Delta y}{\Delta z}\right) \tag{3.4}$$

Where ρ_f is the density of the fluid in the manometer. And the pressure gradient is defined as

$$-\frac{\Delta P}{\Delta z} = g\left(\rho_l \varepsilon_l + \rho_s \varepsilon_s + \rho_g \varepsilon_g\right) \tag{3.5}$$

The dispersion density (ρ_d) in the column is given by

$$\rho_d = \left(\rho_l \varepsilon_l + \rho_s \varepsilon_s + \rho_g \varepsilon_g\right) \tag{3.6}$$

Assuming water is used as the manometer fluid, and by substituting and simplifying, one can obtain the relationship between dispersion density and pressure profile

$$\rho_d = -\rho_w\left(\Delta y / \Delta z\right) \tag{3.7}$$

For bubble column systems, the gas holdup between two adjacent pressure taps can be directly correlated from the ratio of pressure differential to the height difference of the pressure taps,

$$\varepsilon_g = 1 + \left(\Delta y / \Delta z\right) \tag{3.8}$$

For slurry systems, the process is more complicated. A second variable which would also have to be known is the axial slurry density (ρ_{sl}) based on liquid-solid only. The slurry density would be found by taking slurry samples along the

height of the column and plotting an axial density profile. Finally, the gas holdup could be calculated by taking a ratio of the dispersion density to slurry density,

$$\varepsilon_g = \left(1 - \frac{\rho_d}{\rho_{sl}}\right) \qquad (3.9)$$

The slurry sampling procedure and calculation of slurry density is described in section 3.2.2.

The average gas holdup in the column was also calculated by taking the average pressure profile between the bottom and top pressure taps (located at 5cm and 115 cm, respectively). For slurry systems, the slurry density (ρ_{sl}) was assumed to be average slurry concentration in the column.

3.2.1.1.1 Effect of Backflushing on Gas Holdup

Since backflushing introduced a small amount of air into the system, tests were performed to measure the effect of backflushing on average gas holdups. Measurements were made for a gas-liquid system with air backflushing and with backflushing turned off. As shown in Fig. 3.5, the effects of backflushing were negligible. The average error was determined to be about 1%. As a further check, the main gas flow (via the sparger) was cut off and the expanded bed height was measured with only air backflushing. Results showed that average gas holdup was only 0.3% higher, which again is well within experimental error.

Fig. 3.5 Comparison of Gas Holdups measured with air backflushing and without air backflushing for a gas-liquid system

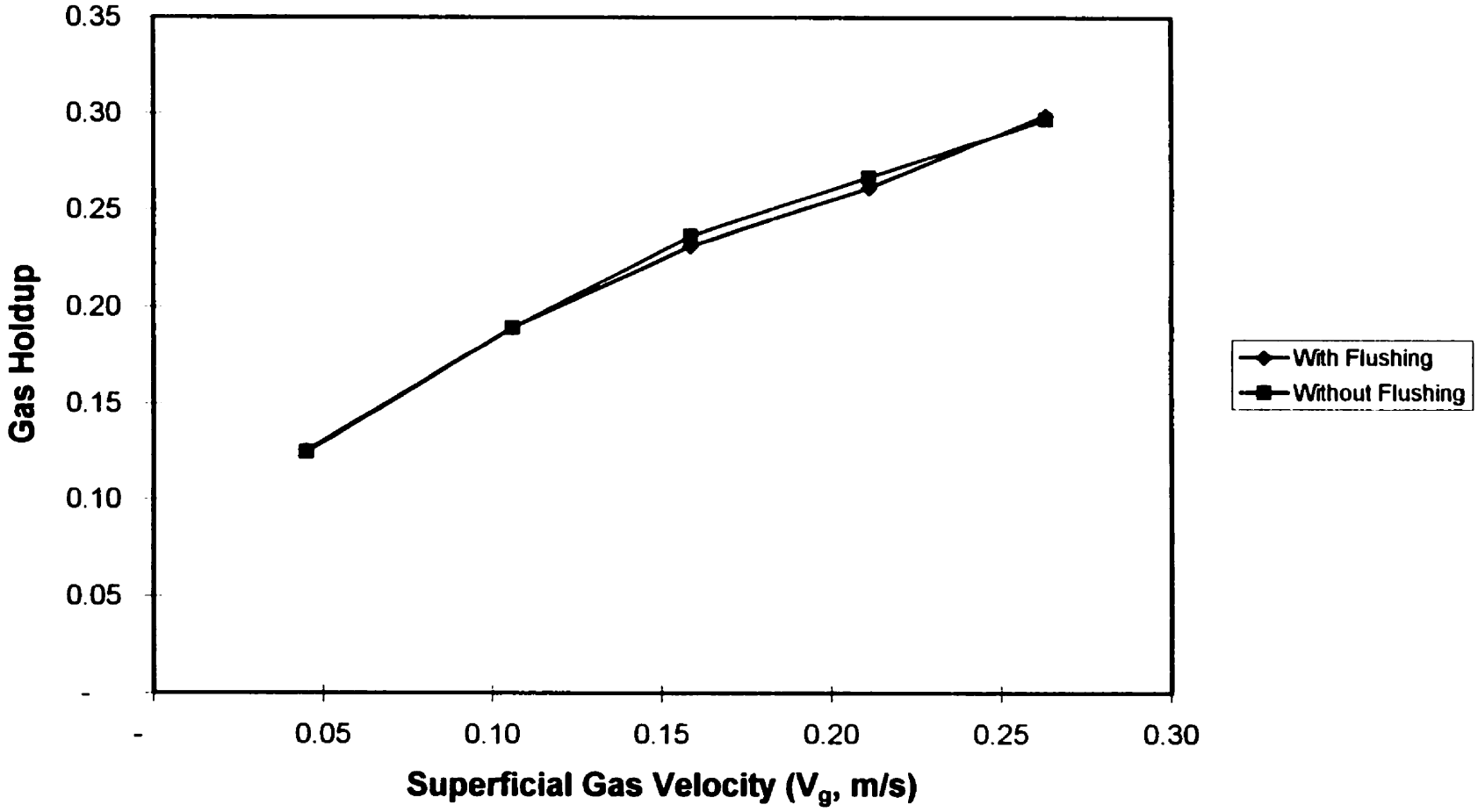

3.2.1.2 Gas Holdup Based on Static and Expanded Bed Heights

The average gas holdup in the column was also calculated by measuring the static and expanded bed heights prior to and during the experimental runs (as shown by Eq. 2.5).

$$\varepsilon_g = \frac{(H_d - H_s)}{H_d} \qquad (3.10)$$

To measure bed heights accurately, a clear tape was placed along the length of the column. A volume calibration chart was produced and comparison to theoretical volumes showed errors less than 1%.

During experimental runs, large fluctuations in the expanded bed heights were observed. To minimize measurement error, three readings of bed heights were taken at different times during an experimental run. The first reading would be taken after allowing approximately 15 minutes of mixing time. Each subsequent reading would be taken in 5 minutes intervals. The average of these three readings was used to estimate the final expanded bed height. To check the accuracy of these results, a pressure profile plot (for above and below the bed height) was produced for several experimental runs. The pressure should decrease linearly as one moves up the column. Above the bed, the pressure should remain constant. The point at which these two lines intercept would be the expanded bed height. The results are shown in Figs. 3.6a and 3.6b which correspond to 0% and 40vol% solids systems, respectively. For the gas-liquid system shown in Fig. 3.6a, the range of error between measured bed height and that calculated through the pressure profile varies from 1.0% to 3.8% (for differing superficial gas velocities). For the 40vol% solids system, the error range is 0.6% to 1.4%. There is a general tendency for the average error to decrease as the average solids concentration in the column increases. This

Fig. 3.6a Pressure Profile Measurements for a Gas-Liquid system

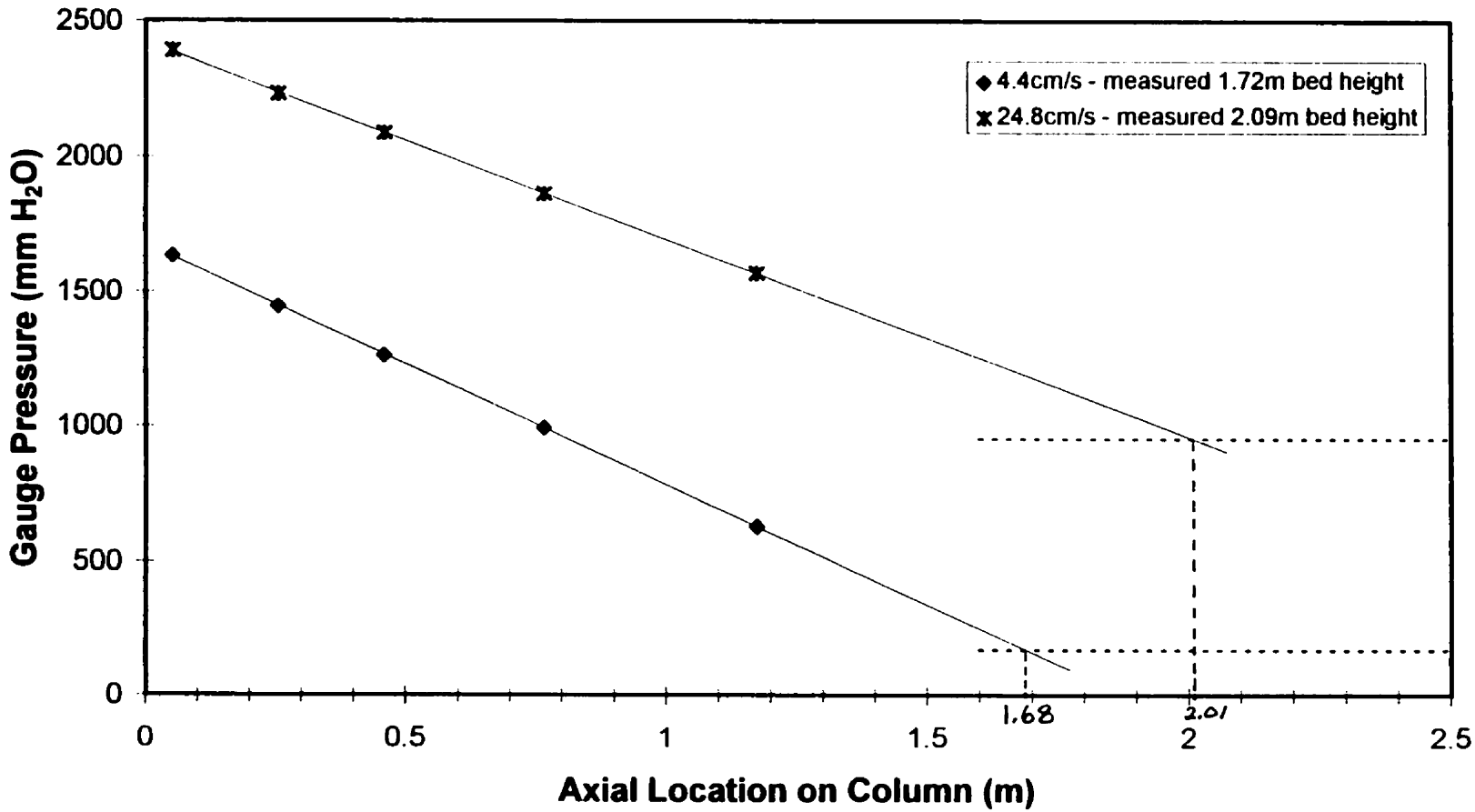

Fig. 3.6b Pressure Profile Measurements for a Gas-Liquid-Solids system containing 40% average solids concentration

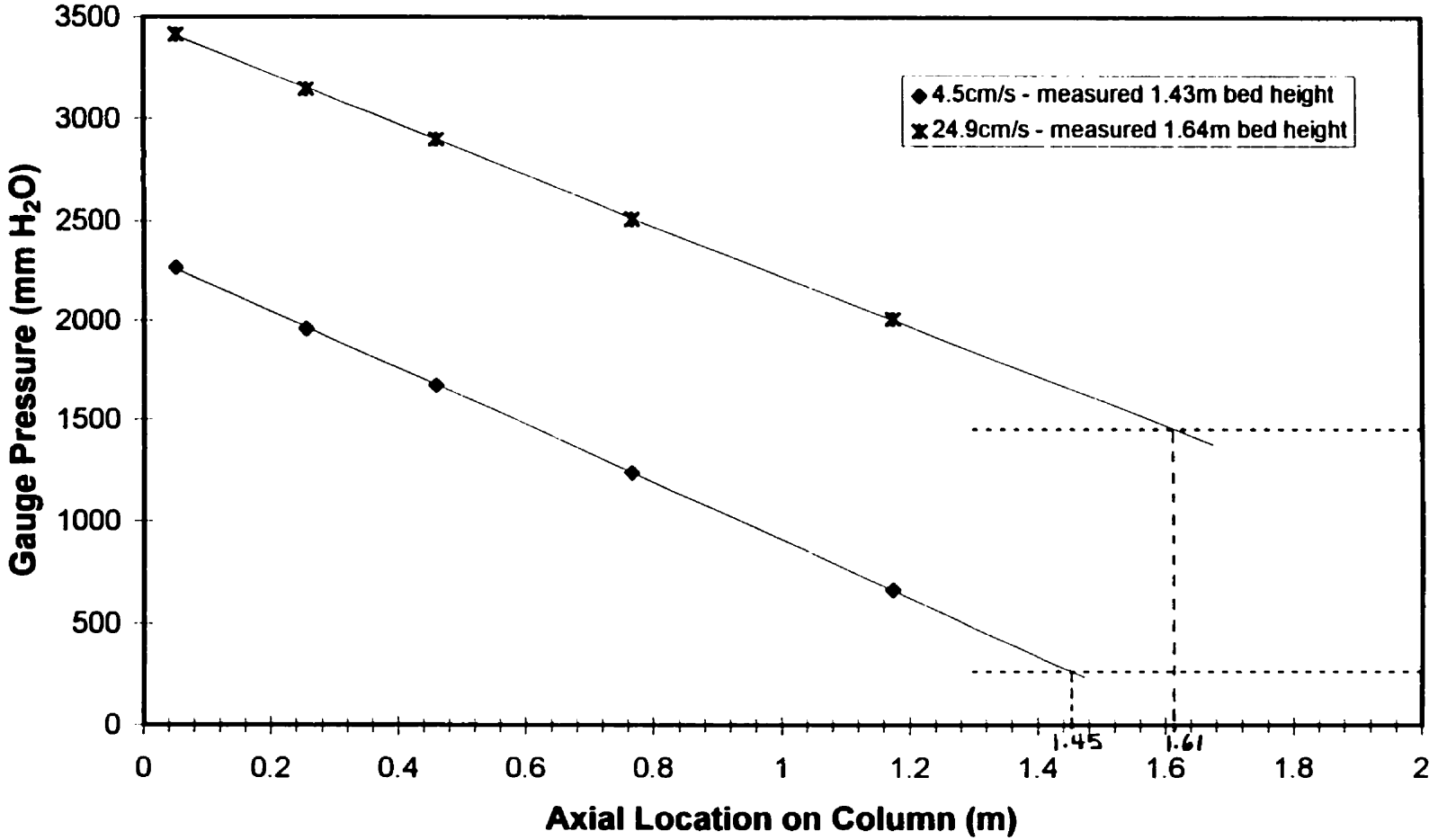

could be due to less foam formation with increasing solids concentration, making it easier to get accurate bed height readings.

3.2.1.3 Comparison of two Average Gas Holdup Measurement Techniques

The gas holdup data obtained by the two techniques were compared. The gas holdups measured by the average pressure profiles were consistently lower (3% to 20%) than those determined by static and expanded bed heights. Several replicates were performed for the gas-liquid only system (7 replicates) and the 30vol% solids system (6 replicates). An error analysis was performed for each case to determine whether the differences were statistically significant; the 90% confidence intervals are shown in Figs. 3.7a and 3.7b. For the gas-liquid system, the error range was 6% to 15%. For the 30vol% solids system, the error range was 1% to 6%, most probably due to decreased foaming and smaller fluctuations in bed height. The error was still statistically significant (especially for systems with lower solids concentrations). Since results obtained through expanded bed height measurements were comparable to those of other researchers (who also use the expanded bed height technique to measure average gas holdups), it was decided to further investigate calculation of the average pressure profile.

Since foaming was observed near the top section of the column, two additional pressure taps were installed at the top of the column to measure gas holdup in this region. Testing was conducted in a gas-liquid system (where the error was most significant). Two separate experimental runs were performed and a plot of the axial gas holdup profile for the first run is shown in Fig. 3.8. The gas holdup in the top section of the column was found to increase significantly for gas velocities of 0.10m/s to 0.25m/s, indicating the presence of a foaming region. At

Fig. 3.7a Gas Holdup Error Analysis for a Gas-Liquid system using t-Test with 90% confidence intervals

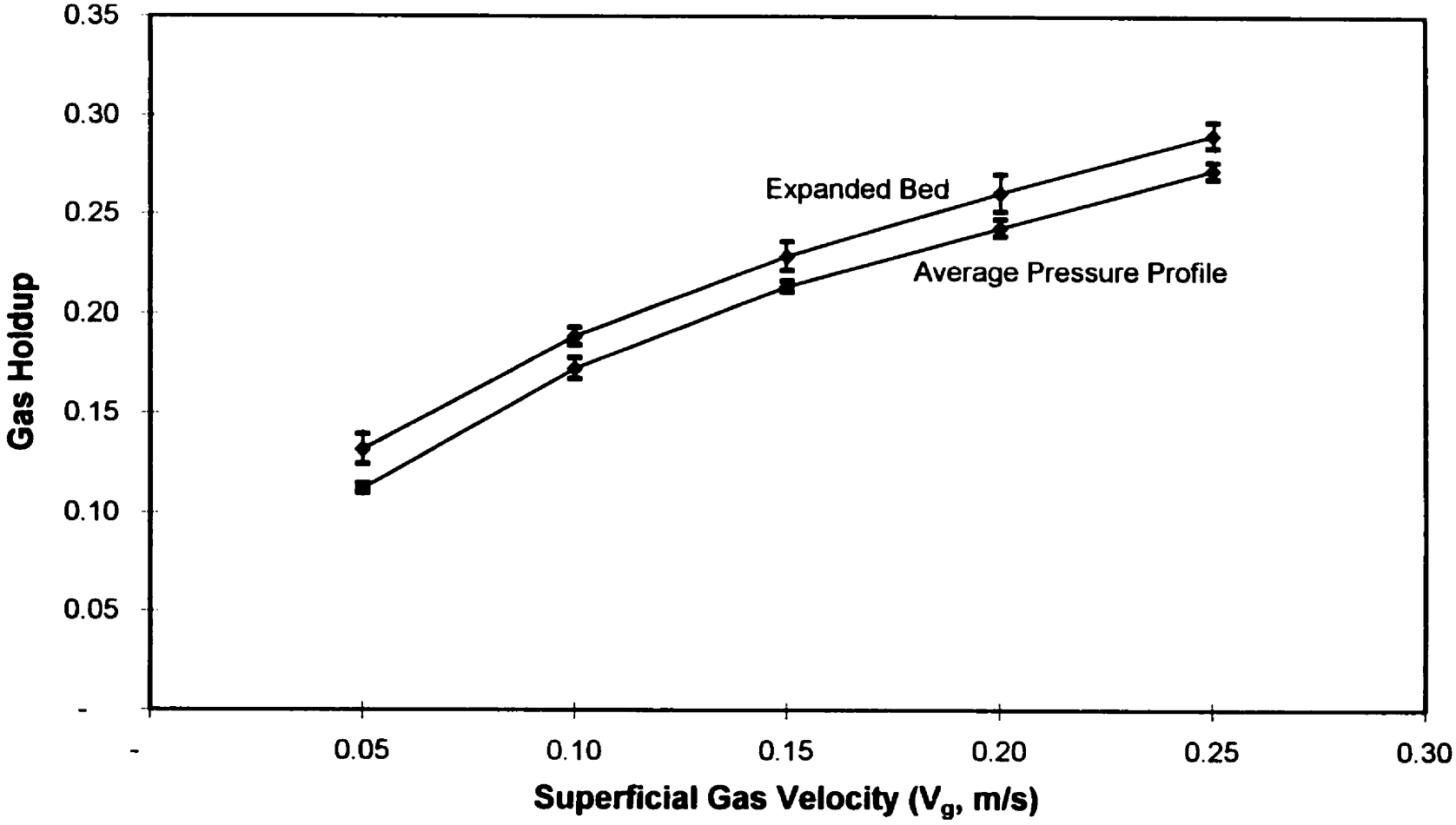

Fig. 3.7b Gas Holdup Error Analysis for a 30vol% solids system using t-Test with 90% confidence intervals

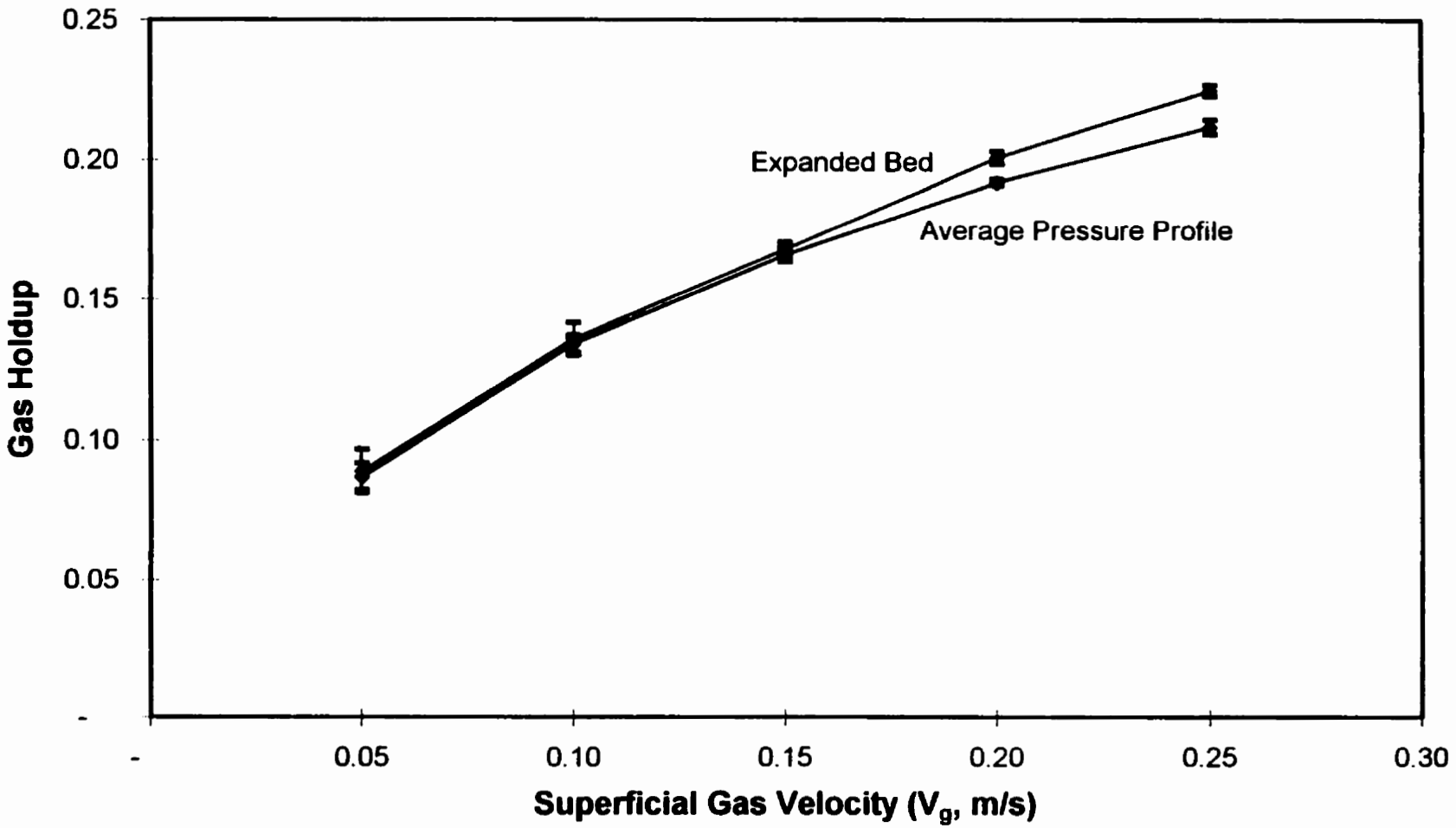

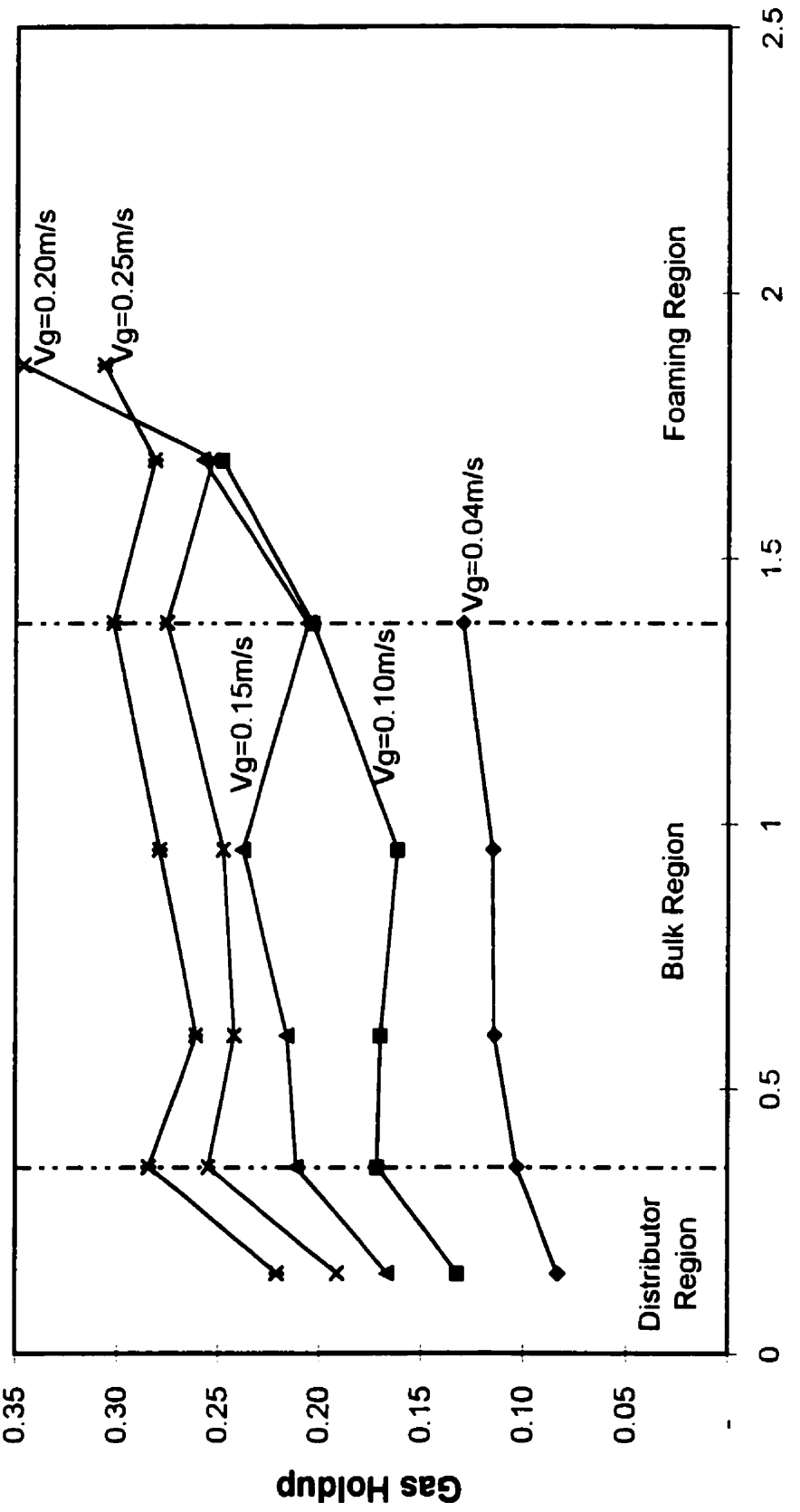

Fig. 3.8 Axial Gas Holdup Profile for a Gas-Liquid system with higher pressure taps installed

a gas velocity of 0.04m/s, the expanded bed height dropped below the new pressure taps consequently readings for the top section were not taken. A comparison of average gas holdups measured using the expanded bed height and new pressure profile (incorporating the new probes) is presented in Fig. 3.9 for the first experimental run. The error range between two techniques was found to be 0.1% to 5.4% with an average error less than 3%. Results were similar for the second run. These are well within the experimental error range of the expanded bed height defined in section 3.2.1.2. Thus, foaming does play a significant role in measurement of average gas holdup.

The average gas holdup through pressure profile can therefore calculated in two manners; 1) by adding pressure taps near the top and bottom regions of the column, accounting for both the low gas holdup distributor region and the high gas holdup foaming region (the average of which should be close to the gas holdup for the bulk region), or 2) by taking the average pressure profile for the bulk section of the column only. The second method was tested by ignoring the bottom pressure tap and results are shown in Fig. 3.10. The error range for superficial gas velocities of 0.10m/s and higher was 1.3% to 6.4%, which corresponds with the above results. However, the error for 0.05m/s gas velocity was significantly higher at 11.7%. This can be attributed to expanded distributor region effects. Pressure profile results for the remainder of this study were obtained by ignoring the bottom pressure tap (step 2 above).

Fig. 3.9 Comparison of Average Gas Holdups calculated using Expanded Bed Height and Average Pressure Profile Techniques (Gas-Liquid system using new, higher probes)

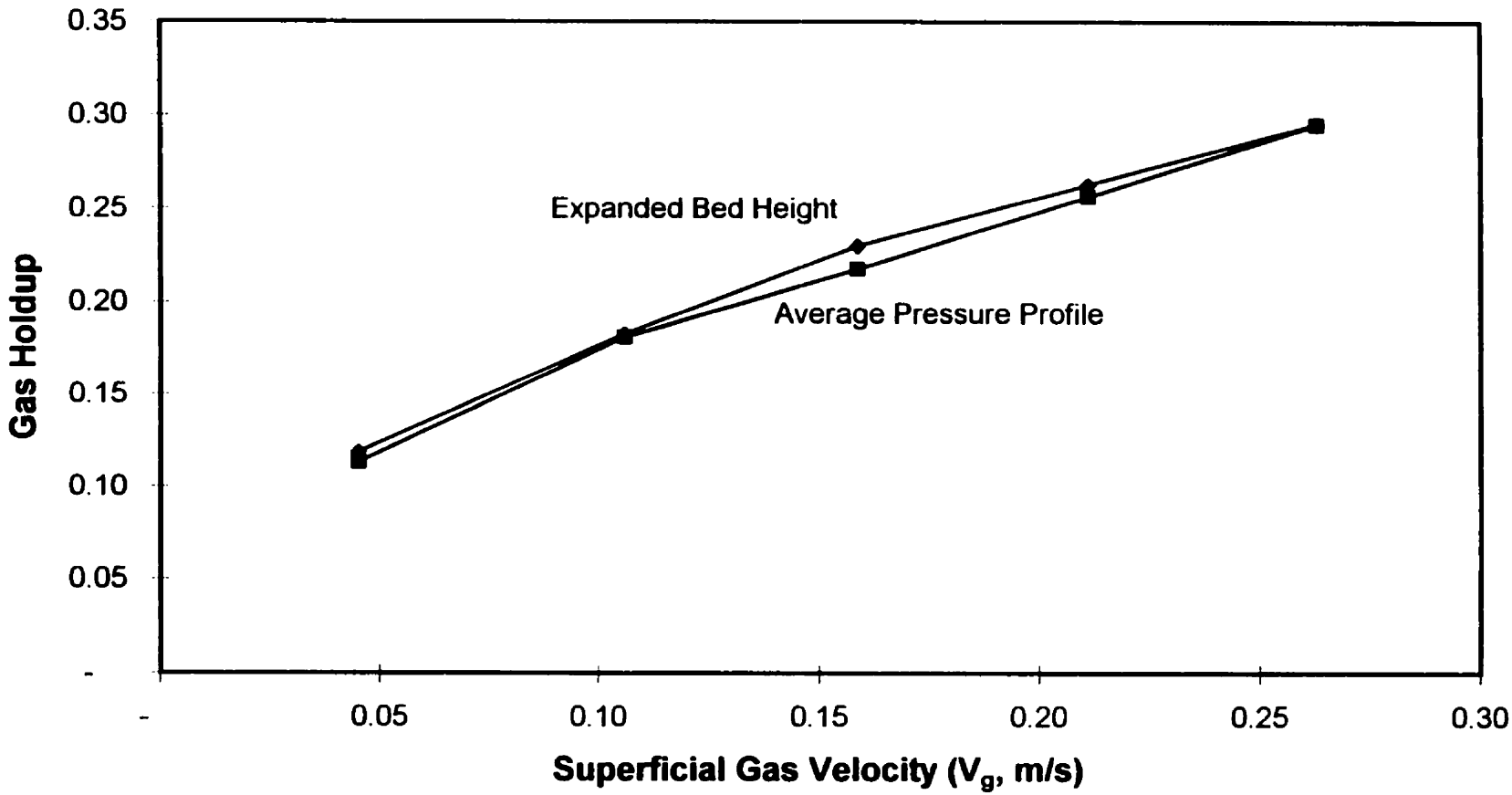

Fig. 3.10 Comparison of Average Gas Holdups measured by Expanded Bed Height and Pressure Profile (using middle taps only) techniques for a Gas-Liquid system

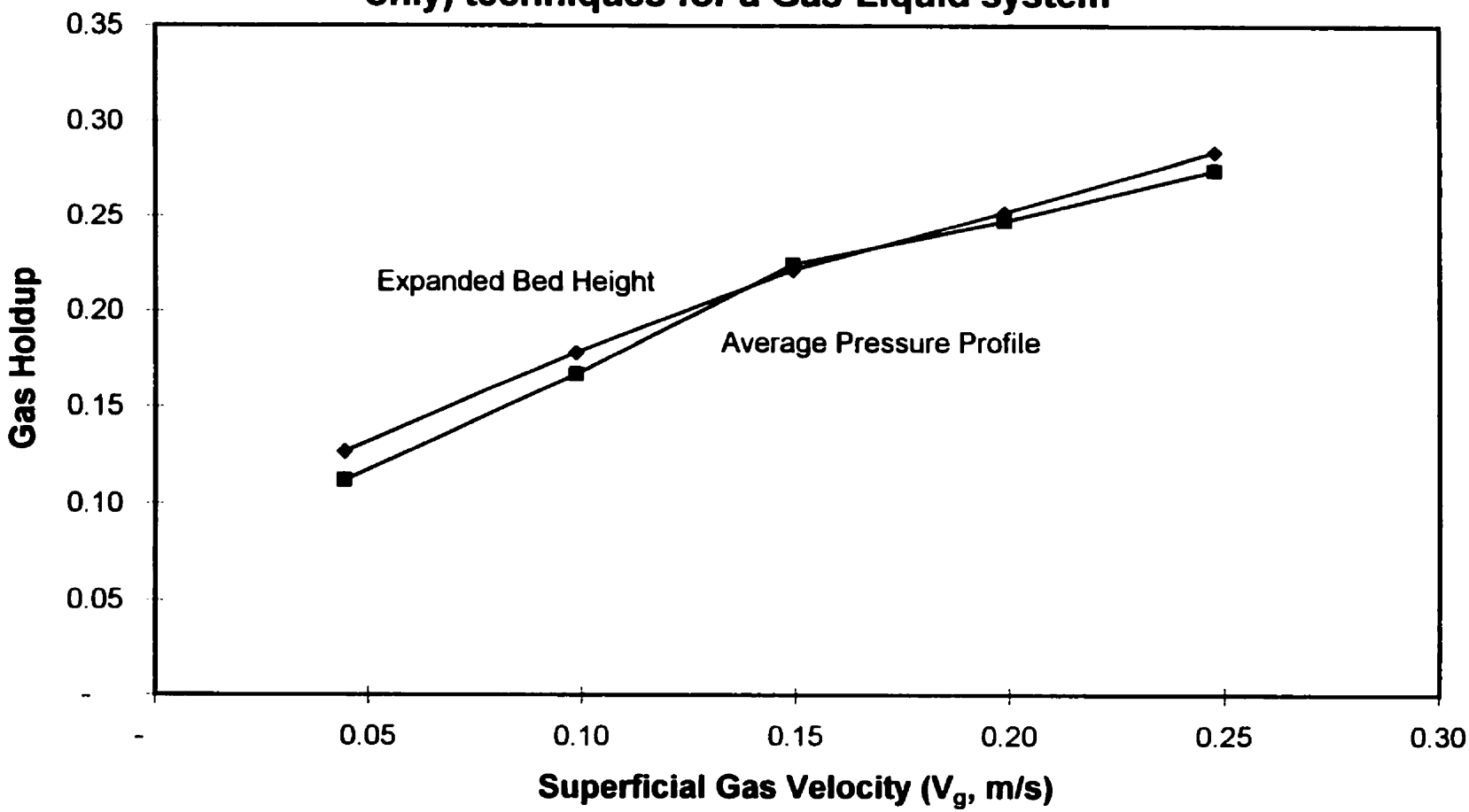

3.2.2 Axial Solids Holdups Measurements

3.2.2.1 Slurry Sampling Probe Design

As mentioned in section 3.2, five sampling ports were available along the axial column height to collect slurry samples. The sampling probe was designed so as to avoid entrainment of gas bubbles in the lines. Since radial sampling was also to be conducted, the sampling probe had to have an easy mechanism for withdrawal and insertion to various points of the column. Fig. 3.4 shows a schematic of the final slurry sampling probe used. Five sampling probes were made in total - three probes were made with a 15.2cm long shaft (which would be used for sampling up to center of column) and two probes were made with a 22.9cm long shaft (which could be used for sampling from wall to wall).

Several designs were tested before the final design was selected. Initially, a probe was designed with a 2mm mesh attached at the tip (and no inside shaft). The sampling would be controlled by solenoid valves opening and closing simultaneously. However, it was determined that solids would settle in the lines and affect sampling results. Since the cost of the solenoid valves was also high, it was decided to design a probe which could be operated manually in a piston-type manner. A solid rod inside the shaft could be withdrawn to remove a sample. After sampling the rod would be re-inserted, leaving no volume for the solids to settle in. A brass shell with polyethylene insert rod was constructed. Two O-rings were added to the tip of the polyethylene insert to allow for easy sliding. A notch was also designed into the rod where a screw could be placed to prevent excessive withdrawal or re-insertion. The sampling probe was tested and worked successfully for lower concentration systems. However, after prolonged use, several inserts were becoming more and more difficult to

remove. This was due to extra friction created by; 1) solids becoming trapped in between the insert rod and the shaft, and 2) the polyethylene inserts began to absorb water and expanded. Removing and cleaning sampling probes in between experimental runs helped reduce the first problem but the second problem persisted. A new brass insert rod was therefore designed and used. The possibility of expansion was reduced but problems associated with entrapped solids persisted. To minimize this problem, brushes were also placed on the tips of the insert rods to move the entrapped solids back into the column. This modified sampling probe (which was previously shown in Fig. 3.4) was tested and worked successfully. Five probes were designed and installed.

3.2.2.2 Slurry Sampling Procedure

In addition to axial sampling for all five probes, radial slurry samples were also obtained for Probes # 2, 4 and 5. Samples would be taken at five axial locations; -R, -R/2, 0, +R/2, and +R (with R representing the radius of the column and 0 representing the center of the column). Samples sizes of 75mL to 100mL were taken in 125mL Erlenmeyer Flasks.

The solids concentrations were initially measured using a filtering-drying technique. First, the mass of withdrawn slurry samples (m_{sl}) would be measured. The water would then be filtered off using a vacuum and 1μm filter paper in a Buchner Funnel. The filtered solids would be dried in an oven overnight and re-weighed to obtain the mass of solids (m_s). Since the densities for both water and glass beads are known, it is possible to calculate the slurry concentration (ψ_s) and density (ρ_{sl}):

$$\psi_s = \frac{\left(m_s/\rho_s\right)}{\left(m_s/\rho_s + (m_{sl} - m_s)/\rho_l\right)} \qquad (3.11)$$

and

$$\rho_{sl} = \frac{m_s + (m_{sl} - m_s)}{\left(m_s/\rho_s + (m_{sl} - m_s)/\rho_l\right)} \tag{3.12}$$

The mass of water and solids removed from the column (due to sampling) was replaced prior to running the next experiment. The procedure worked well but had one major drawback - only one run could be performed per day because of the long solids drying time. In total, 14 samples were being removed from the column per experimental run. The total volume of slurry withdrawn was about 1.4L, representing about 5% of the slurry volume in the column. This technique was used for slurry systems up to 20vol% solids. For higher slurry concentrations, the filtering time was becoming much longer, therefore a new procedure based on the pycnometric technique was used. This technique involves weighing the sample (m_{sl}) and then transferring it to a 100mL volumetric cylinder. Using Burettes, additional water is added to the volumetric cylinder bringing it to the 100mL mark. Since the volume of the extra water added (V_{refill}) is known, therefore the volume of the sample (V_{slurry}) can be determined and the slurry concentration (ψ_s) and density (ρ_{sl}) can again be calculated:

$$\psi_s = \frac{\left(m_{sl} - \rho_l V_{slurry}\right)}{V_{sl}(\rho_s - \rho_l)} \tag{3.13}$$

and

$$\rho_{sl} = \frac{m_{sl}}{\left(0.1 - V_{refill}\right)} \tag{3.14}$$

This procedure was also found to work well and reduced the time taken to perform an experimental set of runs from 5 days to 2 days. Samples for all remaining experiments (including non-coalescing systems and sparger height variation systems) were taken using this technique. Before starting the next experiment, the withdrawn liquid and solids were placed back into the column.

3.2.2.3 Accuracy of Solids Sampling

To check accuracy of the solids sampling (pycnometric) technique, several replicates were taken for a 30% solids system. In total, 6 replicates were performed and the results of the t-Test analysis with 95% confidence intervals for three superficial gas velocities are presented in Figures 3.11a through 3.11c. There is no relationship between superficial gas velocity or axial column location to the specific error as the error is randomly distributed. The average error from the mean for all runs was calculated to be +/-1.7% with a maximum of +/-3.5%. This indicates that the sampling procedure itself was adequate.

3.2.2.4 Effect of Probe Rotation on Solids Sampling

Due to the unique solids sampling probe design, it was decided to investigate the effects of probe rotation on the solids sampling. During regular experimental runs, for each superficial gas velocity and solids concentration (up to 25vol% solids), Probe # 3 (located 65cm above the base plate) was rotated 90° and then re-sampled. A comparison of samples is presented in Fig. 3.12. The error range was found to be -1.3% to +2.4% with an average absolute relative error of 0.7% which is well within the bounds of experimental error. We can conclude that the effects of probe rotation on slurry sampling concentrations are negligible. Studying the effects of probe rotation was discontinued for slurry systems of 30vol% to 40vol% solids.

Fig. 3.11a Solids Sampling Error Analysis for a 30vol% solids system using t-Test with 95% confidence intervals (V_g = 0.05m/s)

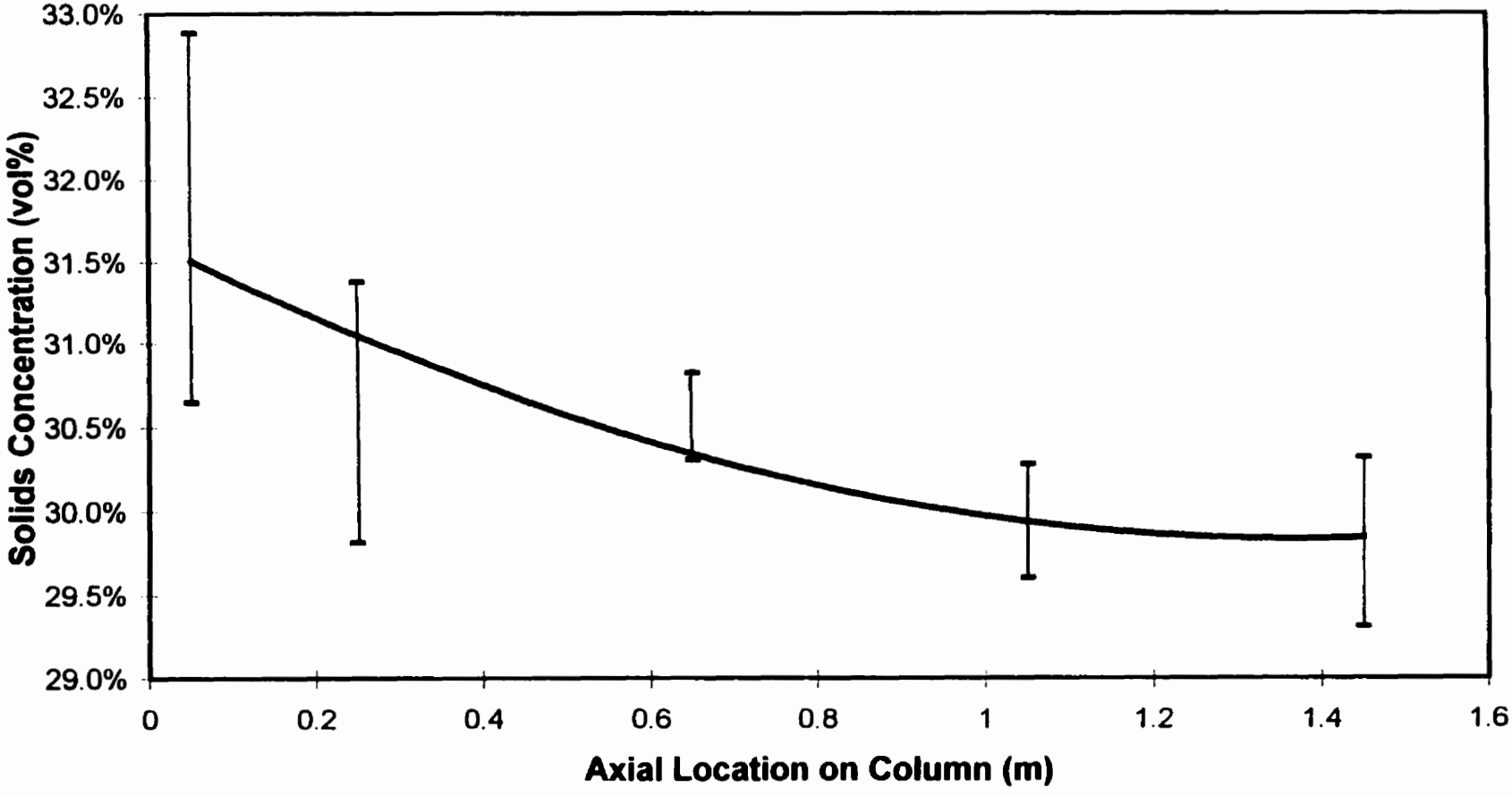

Fig. 3.11b Solids Sampling Error Analysis for a 30vol% solids system using t-Test with 95% confidence intervals (V_g = 0.15m/s)

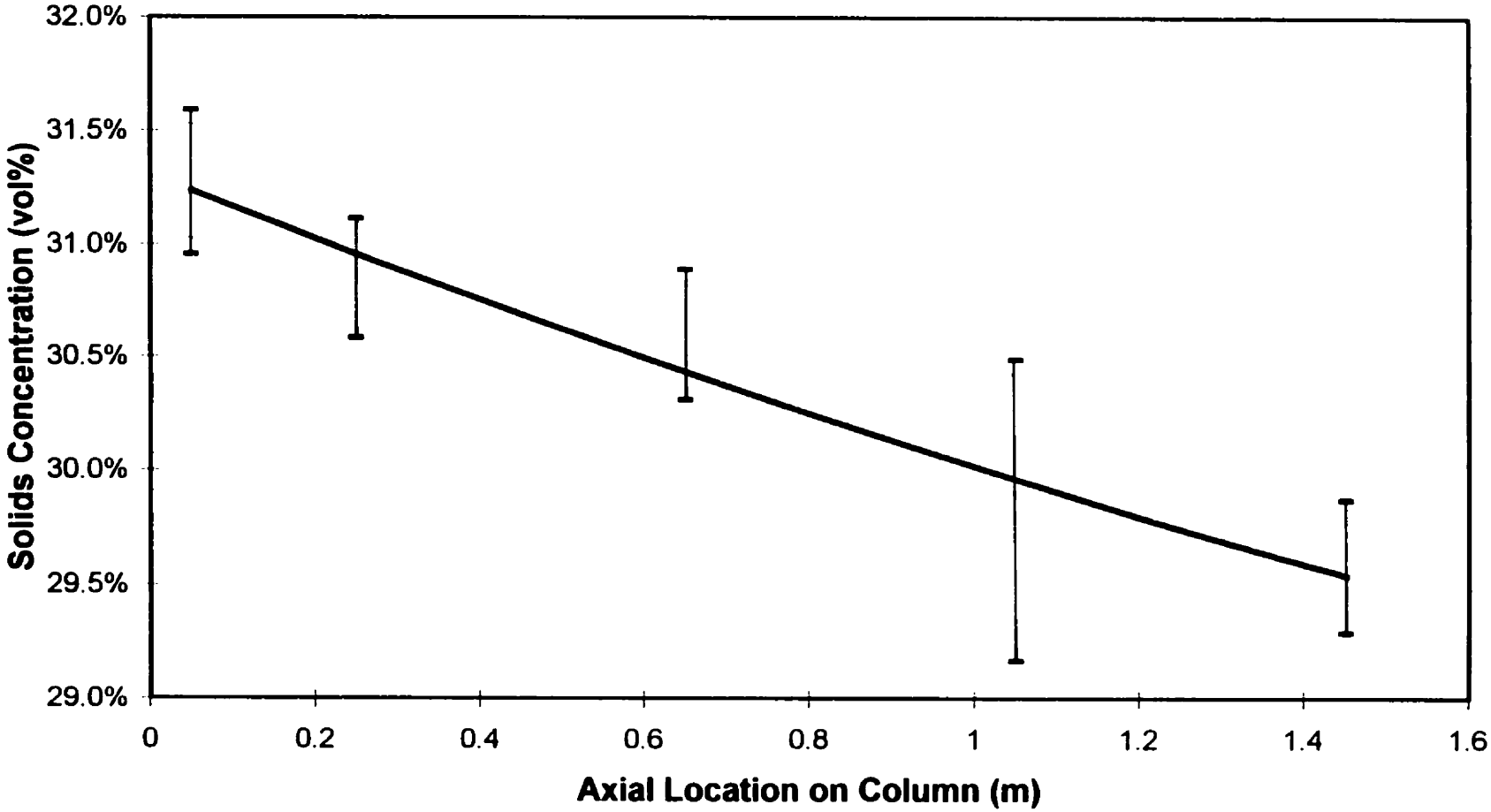

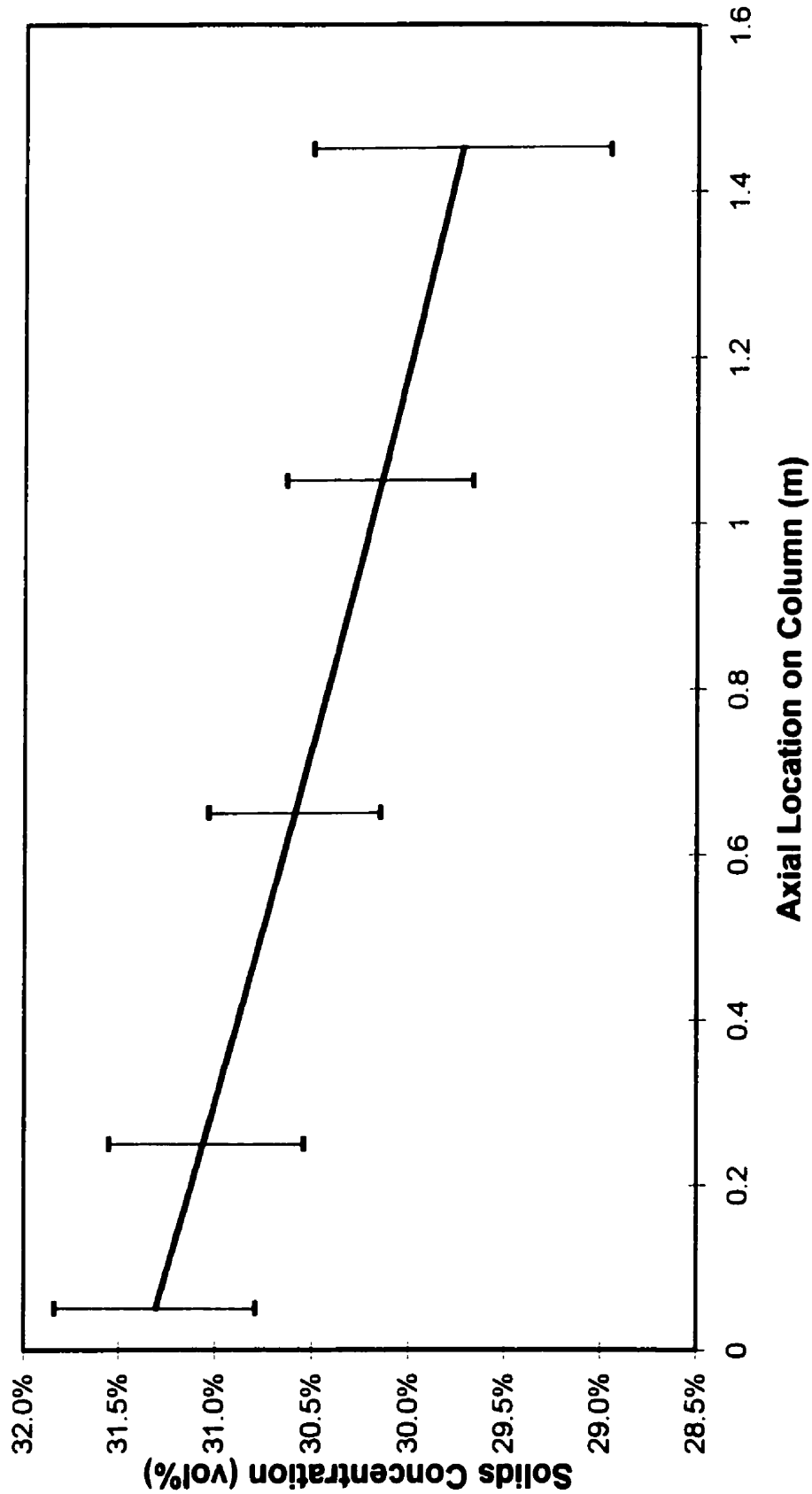

Fig. 3.11c Solids Sampling Error Analysis for a 30vol% solids system using t-Test with 95% confidence intervals (V_g = 0.25m/s)

Fig. 3.12 Comparison of Rotated Solids Sampling Probe versus Unrotated Probe for Varying Superficial Gas Velocities

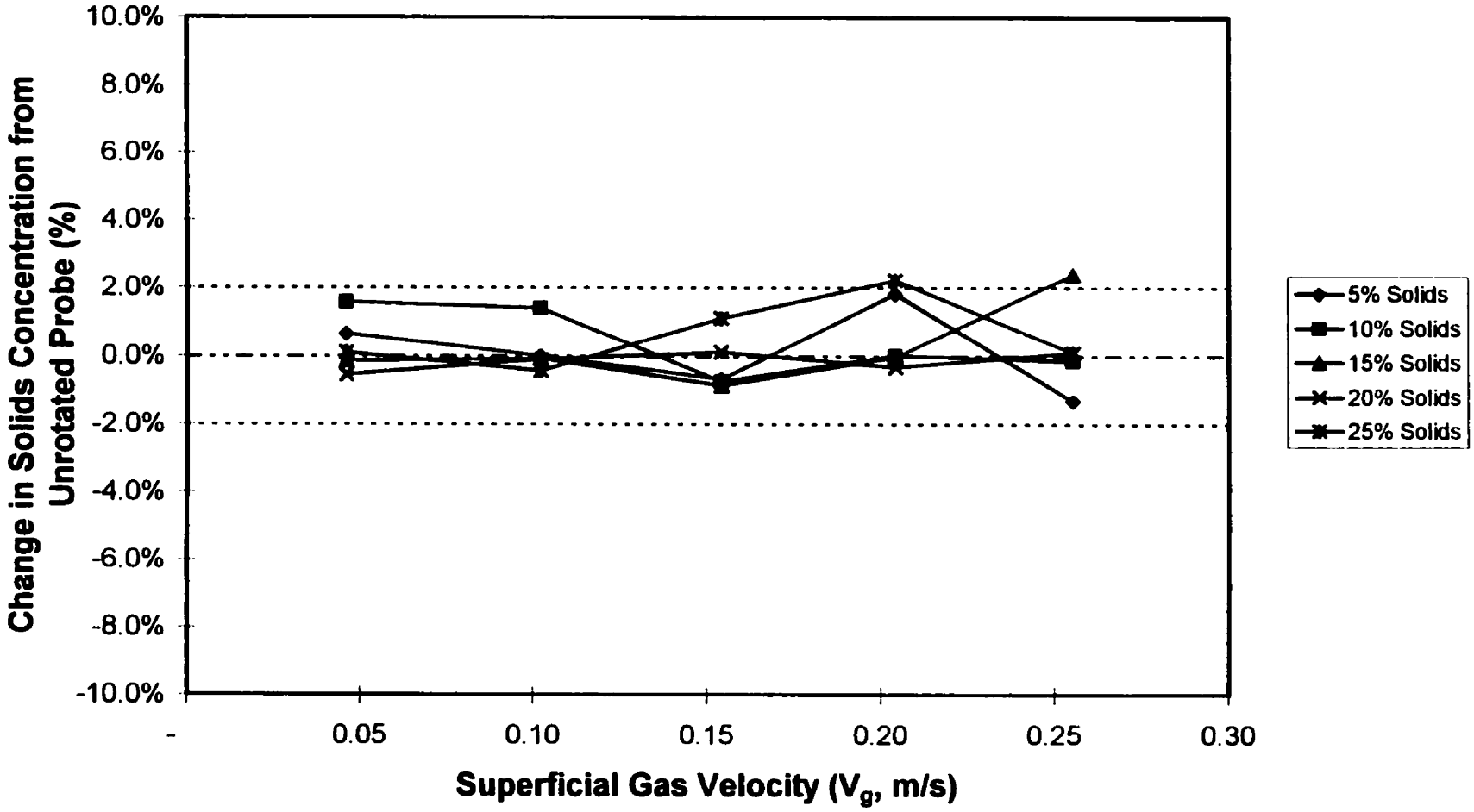

3.3 Experimental Procedure

The experimental procedure consisted of the following main steps:

1. Record initial static bed height.
2. Determine which sonic nozzle and the pressure regulator setting to use from the calibration charts. Open regulator to 10psig setting and then open the valve directly beneath the sparger. Since pressure has already built up in the line, there was no backflow of slurry through the sparger. Adjust regulator to desired setting. This step is done to prevent forming of large initial slugs in the column.
3. Open air backflushing lines to the column only. Set air backflushing flowrate to approximate 3 liters per min (lpm) or 1 SCFM. At these flowrates, the air should be mildly bubbling into the column.
4. Add a slight backpressure to the manometers and then open the manometer lines to the column. Increase manometer backpressure, if necessary, to keep in range.
5. After 10-15 minutes, measure the expanded bed heights in 5 minute increments (for a total of 3 readings). At 25-30 minutes, record the pressure profile, manometer backpressure, pressure above bed, and sparger upstream pressure.
6. Take slurry samples, if necessary. Once slurry measurements are complete, replace samples in column (from the top).
7. Shut the system down temporarily and record the final static slurry height for the run (which is also the initial slurry height for the next velocity). Move onto next superficial gas velocity.

One experimental set would consist of 5 gas velocities. At the beginning of an experimental set (i.e. with a new solids concentration), solids and liquids would be inserted at the top of the column. When switching from a lower to higher solids concentrations, rather than removing the entire slurry and replacing with fresh slurry, the liquid from the top of the column was decanted and the correct mass of solids was added to bring to the desired concentration. For this case, the solids were left to settle overnight. A study on solids settling characteristics is presented in Appendix C. This procedure was consistent for both coalescing and non-coalescing experiments. For sparger height variation experiments, rather than changing the slurry concentration, the sparger height was varied after an experimental set.

For startup of higher concentration slurry systems (20vol% solids and higher), the bed of settled solids particles could not be dispersed by simply switching on the desired gas flow. For these higher concentrations, solids plugs were forming and moving up the column without solids dispersion. The plugs would form because the critical length (L) for settled solids was exceeded (discussed in more detail in the section 4.2.1). A special method was therefore developed to disperse the solids. Rather that installing new equipment, this was accomplished by using the air from the manometer purge lines to disperse the solids in smaller fractions. The uppermost tap (within the settled bed) was first opened with a significantly increased air flow. Once solids in the region were dispersed, the next tap was opened. This was continued until dispersion was possible from the gas distributor itself. The approximate time of dispersion was 30 minutes for a 20vol% solids system to 2 hours for a 40vol% solids system.

4.0 Results and Discussion

The results of this study are presented in two main sections (4.1 and 4.2). Section 4.1 reviews the gas holdup and solids dispersion data obtained with the gas distributor fixed at 1.5cm above the column bottom. Section 4.2 discusses issues of practical importance including the results obtained by varying the axial position of the gas distributor in the column.

4.1 Effects of Operating Parameters on Column Hydrodynamics

Effects of gas velocity and solids concentration on gas holdups (average and axial) and solids dispersion (axial and radial) were investigated.

4.1.1 Axial Gas Holdup Profiles

As discussed in section 3.2.1.1, the axial gas holdup profiles were estimated from measured axial pressure profiles and axial slurry concentrations. The measured axial gas holdup profiles can generally be divided into three main regions. These are the distributor region (near column bottom), the bulk region and the foam region at the column top (refer to Figure 3.8). The relative size and significance of each region varied depending on operating conditions. In general, gas holdups were low in the distributor region, relatively constant in the bulk region and high in the foam region. These observations are generally in agreement with literature (Saxena and Chen, 1994). The gas holdup behavior in the distributor region was analyzed for the effects of gas velocities and slurry concentrations.

Fig. 4.1 shows that in the solids-free bubble column, the gradient in the distributor region increased with increasing gas velocity. The gradient here essentially represents the increase in gas holdup due to bubble break-up. A smaller gradient represents a low bubble break-up rate and a higher gradient represents increased bubble break-up. The gas holdup in the distributor region itself is a net result of the processes of bubble formation, bubble coalescence and bubble break-up. The process of bubble formation has been studied by a number of researchers (Leibsan et al., 1956; Miyahara et al., 1983; Klug and Vogelpohl, 1986). It is a function of several factors including gas flowrate, orifice diameter, orifice spacing and physical properties of the liquid. With increasing gas velocity, there is a transition from nearly uniform bubbling to bubble coalescence leading to the formation of gas jet columns (Leibsan et al., 1956; Klug and Vogelpohl, 1986). The transition from uniform bubbling to bubble coalescence and gas jetting is observed to occur with the onset of turbulence, above a Reynolds number of 2100 (Leibsan et al., 1956). The orifice Reynolds number for this study were in the range of 2700 to 14,000 indicating operation in the turbulent regime. For a superficial gas velocity of 0.05m/s (with a orifice Reynolds number of 2700), operation was in the bubble coalescing regime. Transition to gas jetting regime occurred at a gas velocity of 0.10m/s (which corresponds to a orifice Reynolds number of 5500) as observed by Leibsan et al. (1956). Gas jetting for velocities of 0.10m/s and greater were also confirmed by the Zenz (1968) correlation for downward vertical jets and by visual observations for the gas-liquid system. The large, unstable bubbles formed at the tip of the gas jets break-up to form smaller bubbles as they move up the distributor region to the bulk region. The bubble break-up rate would depend on the column turbulence which would increase with increasing gas velocity. Thus, in the distributor region, the gradient of gas holdup increases with increasing gas velocity due to a higher bubble break-up rate.

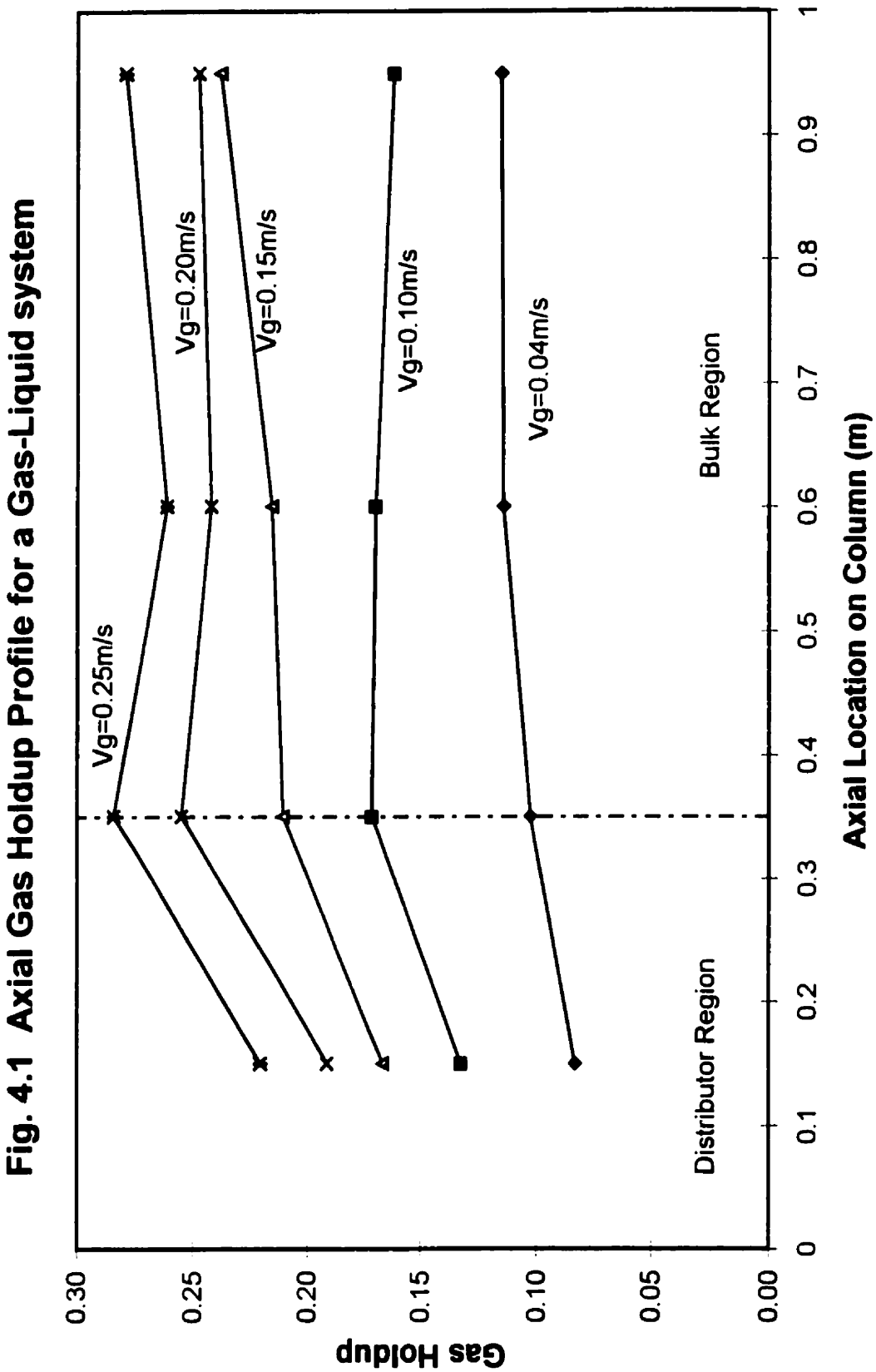

Fig. 4.1 Axial Gas Holdup Profile for a Gas-Liquid system

The effects of slurry concentration on axial gas holdup profiles are shown in Figs. 4.2a and 4.2b for gas velocities of 0.20m/s and 0.25m/s, respectively. The effects of slurry concentration were observed to be more significant for higher gas velocities (≥0.15m/s). Figs. 4.2a and 4.2b clearly show a significant drop in gradient in the distributor with the addition of solids. This is due to the decreased bubble break-up rate in the presence of solids. It is interesting to note that gas holdup close to the distributor is practically the same for solids-free and 10vol% solids systems for both gas velocities. This indicates that average bubble size above the distributor was not influenced by low slurry concentrations. There is, however, a decrease in the distributor region gas holdup for higher slurry concentrations as the increased presence of solids leads to slightly larger bubbles being formed.

It can also be noted that increasing the slurry concentration from 30vol% to 40vol% solids results in a much larger drop in the distributor region gas holdup and a sharper gradient. The lower gas holdup indicates formation of much larger bubbles at the distributor. This increase can be attributed to the increase in suspension 'pseudo-viscosity' with increasing slurry concentration (Kara et al., 1982; Fan, 1989). The pseudo-viscosity of suspensions can be estimated from literature correlations. The following commonly used equation from Barnea and Mizrahi (1973) was used to estimate the pseudo-viscosity:

$$\mu_{sl} = \mu_l \exp\left(\frac{\left(5/3\right)\psi_s}{\left(1-\psi_s\right)}\right) \qquad (4.1)$$

A plot of estimated slurry viscosity for varying slurry concentrations for this study is presented in Fig. 4.3. It can be seen that the slurry viscosity increases linearly with slurry concentration up to about 30vol% solids. Above 30vol% solids, the slurry viscosity begins to increase exponentially. A plot of distributor

Fig. 4.2a Effect of Slurry Concentration on Axial Gas Holdup Profile (V_g = 0.20 m/s)

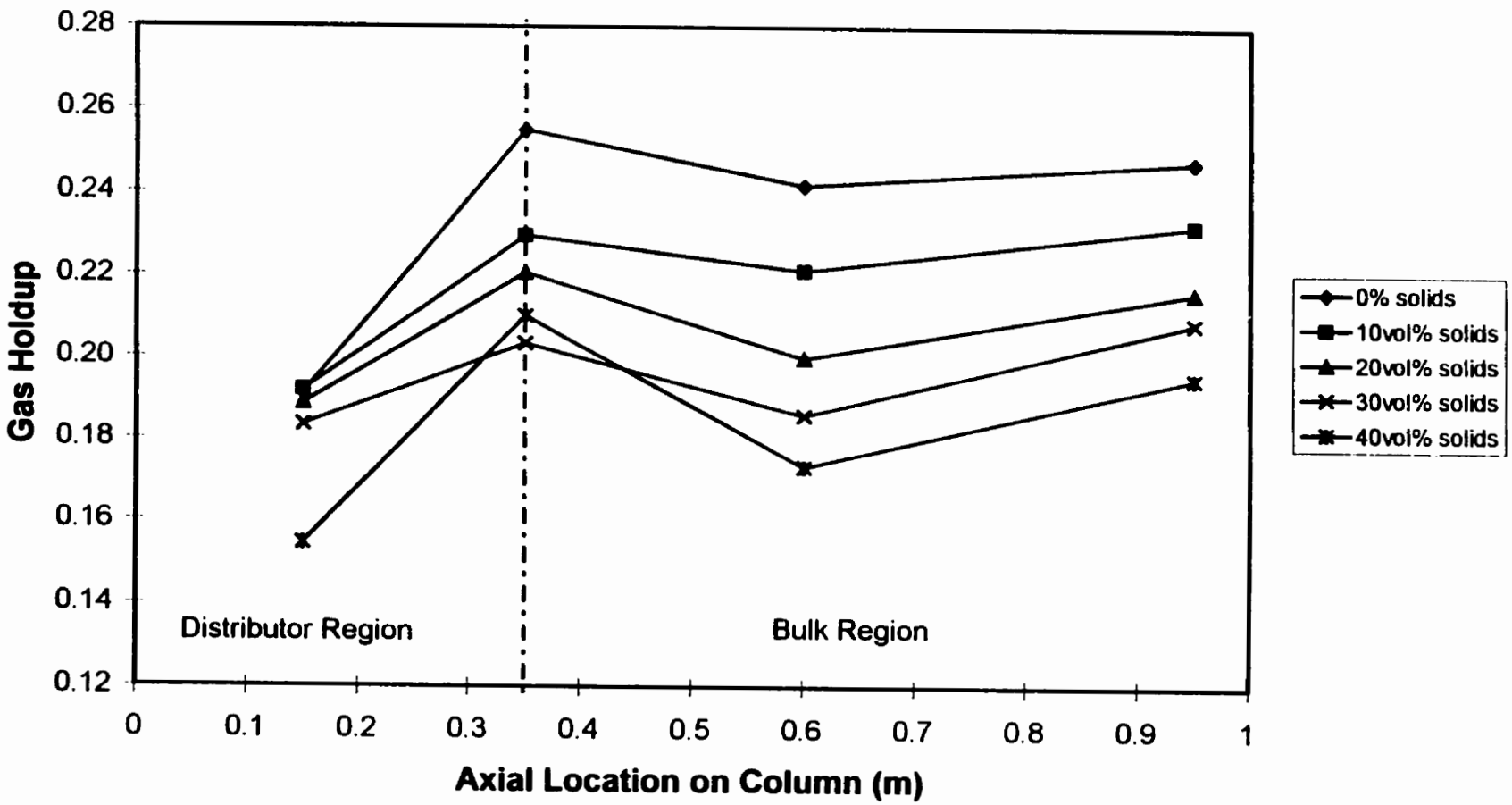

Fig. 4.2b Effect of Slurry Concentration on Axial Gas Holdup Profile (V_g = 0.25 m/s)

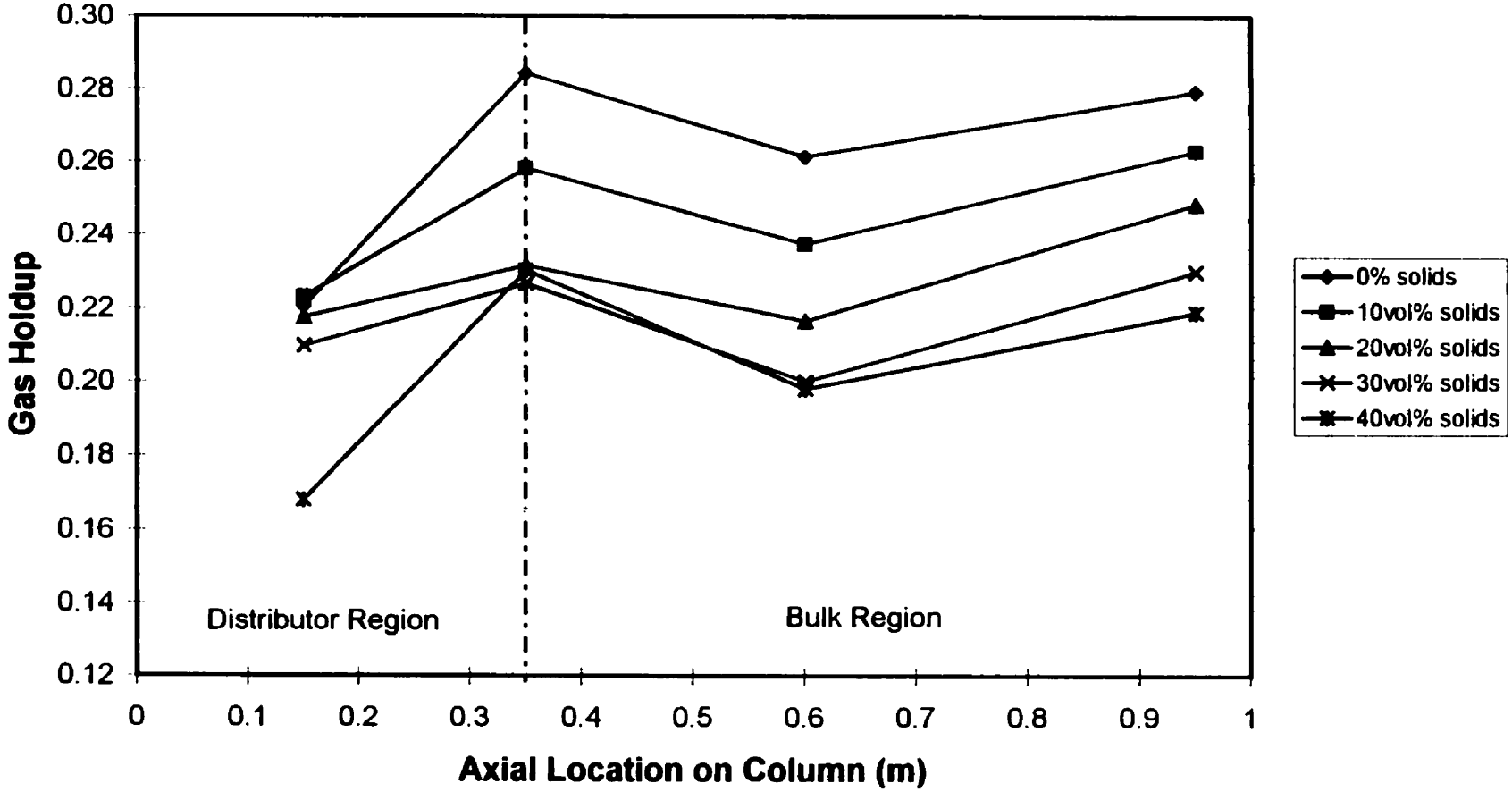

Fig. 4.3 Slurry Viscosity as a function of Slurry Concentration (Barnea and Mizrahi, 1973)

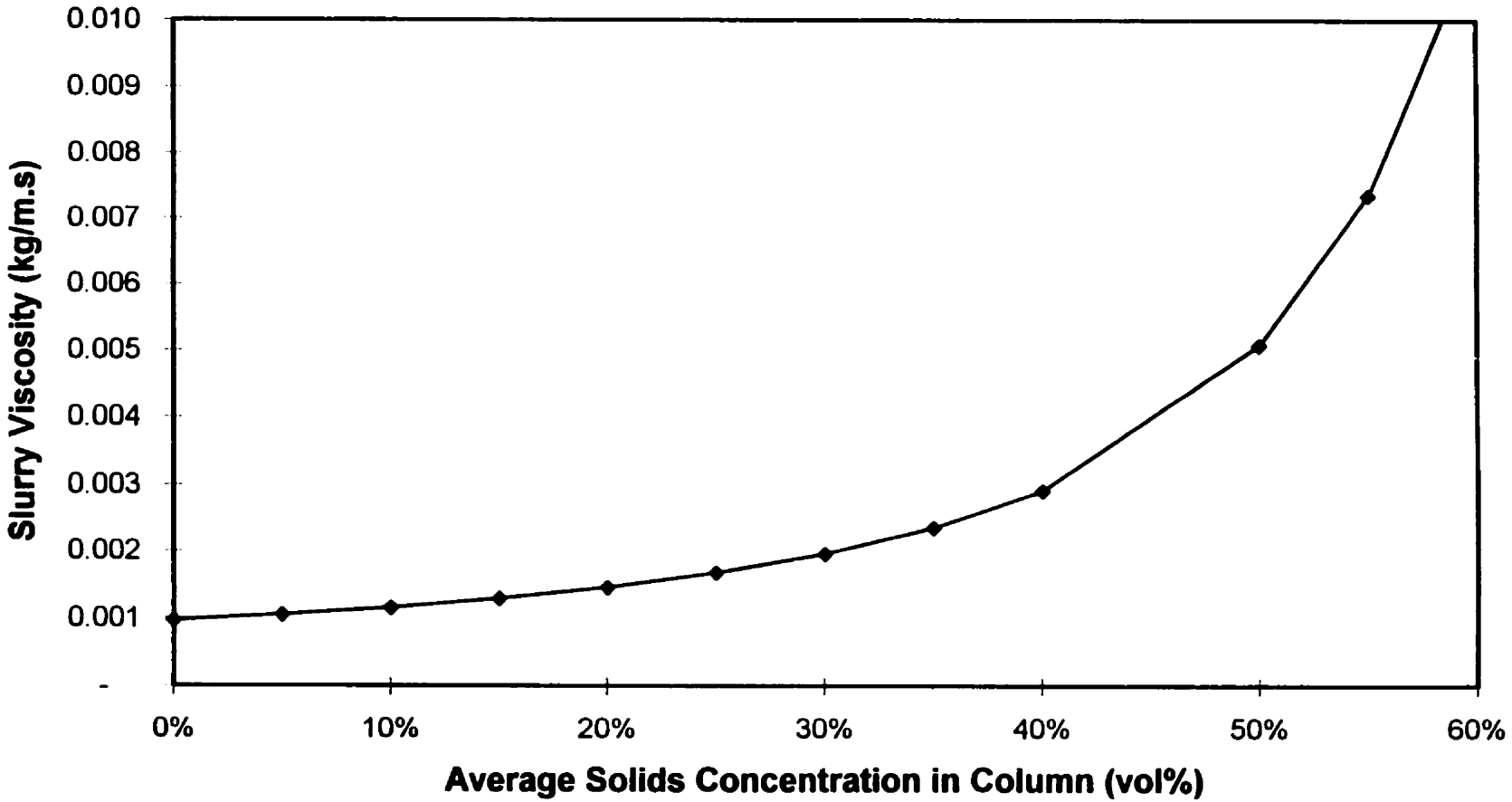

region gas holdup for varying slurry viscosities (Fig. 4.4) also reveals a significant drop in gas holdup for viscosities greater than 0.0020 kg/m.s (which corresponds to a 30vol% solids system). We can therefore conclude that for higher slurry concentrations (≥30vol% solids), the physical properties of the slurry change dramatically. Furthermore, the sharp increase in gradient is probably a result of slower rising small bubbles due to the significant changes in slurry properties.

As observed in Figs. 4.2a and 4.2b for higher velocity systems, there is a slight decrease of gas holdup initially in the bulk region followed by another slight increase in gas holdup. The decrease in gas holdup can be attributed to mild bubble coalescence. As seen in Fig. 4.1, this decrease in gas holdup is not observed for lower gas velocities (≤0.10m/s) due to low bubble concentrations. The slight increase in gas holdup is probably due to the high gas holdup in foaming region extending further down the column for higher velocities.

4.1.2 Average Gas Holdups

The average gas holdups were measured to study mainly the effects of superficial gas velocity and slurry concentration. The average gas holdups presented in this section were obtained from pressure profile readings unless otherwise stated. The average pressure profile was obtained for the bulk section of the column only (as mentioned in section 3.2.1.3).

As shown in Figure 4.5, the average gas holdups increased with increasing superficial gas velocity for all solids concentrations and generally decreased with increasing solids concentrations. The effects of slurry concentrations on gas holdup is better presented in Figure 4.6. Here, the gas holdups are plotted

Fig. 4.4 Distributor Region Gas Holdup for Varying Slurry Viscosities

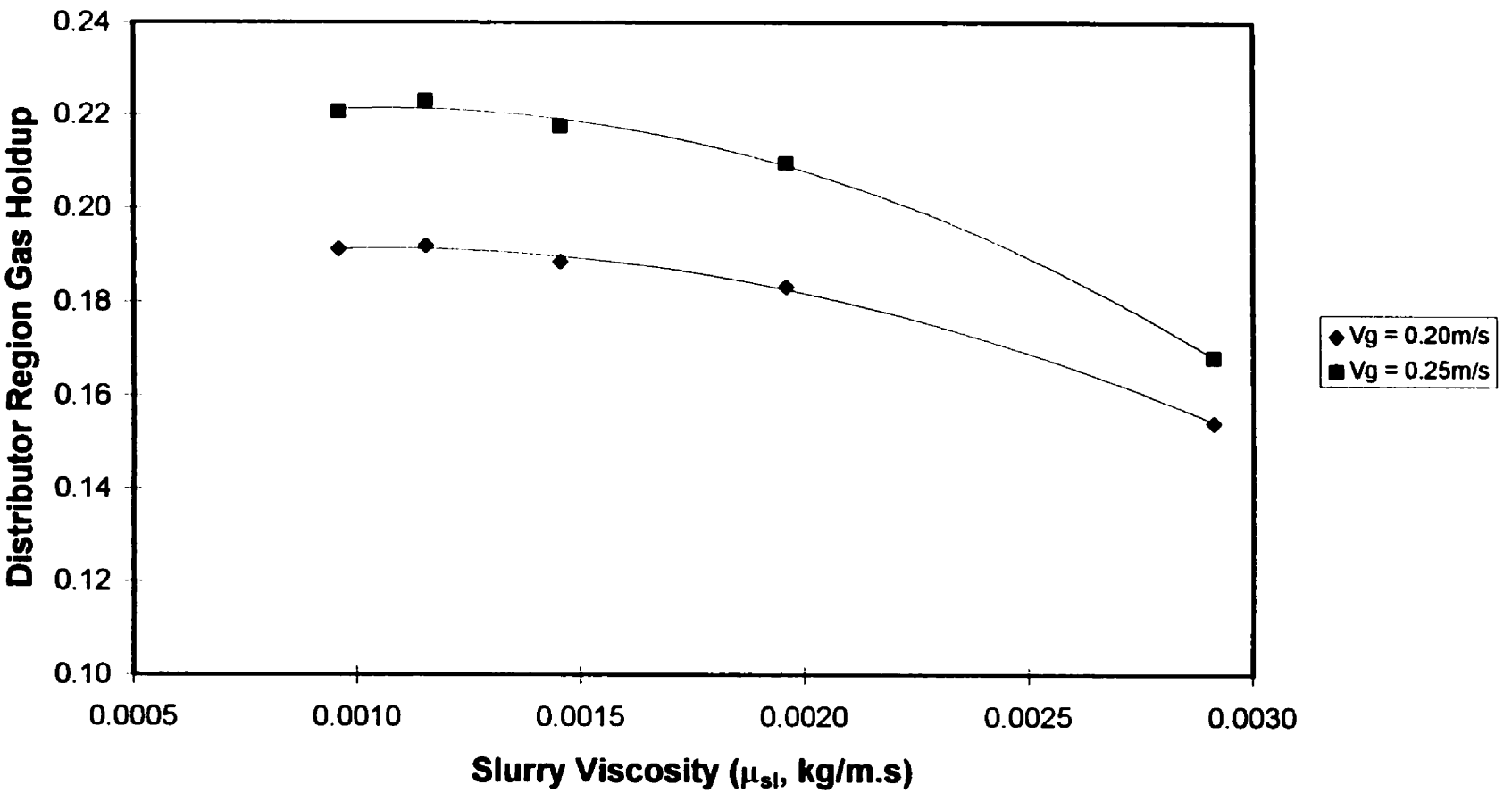

Fig. 4.5 Average Gas Holdup for varying Superficial Gas Velocities and Slurry Concentrations (based on pressure profile)

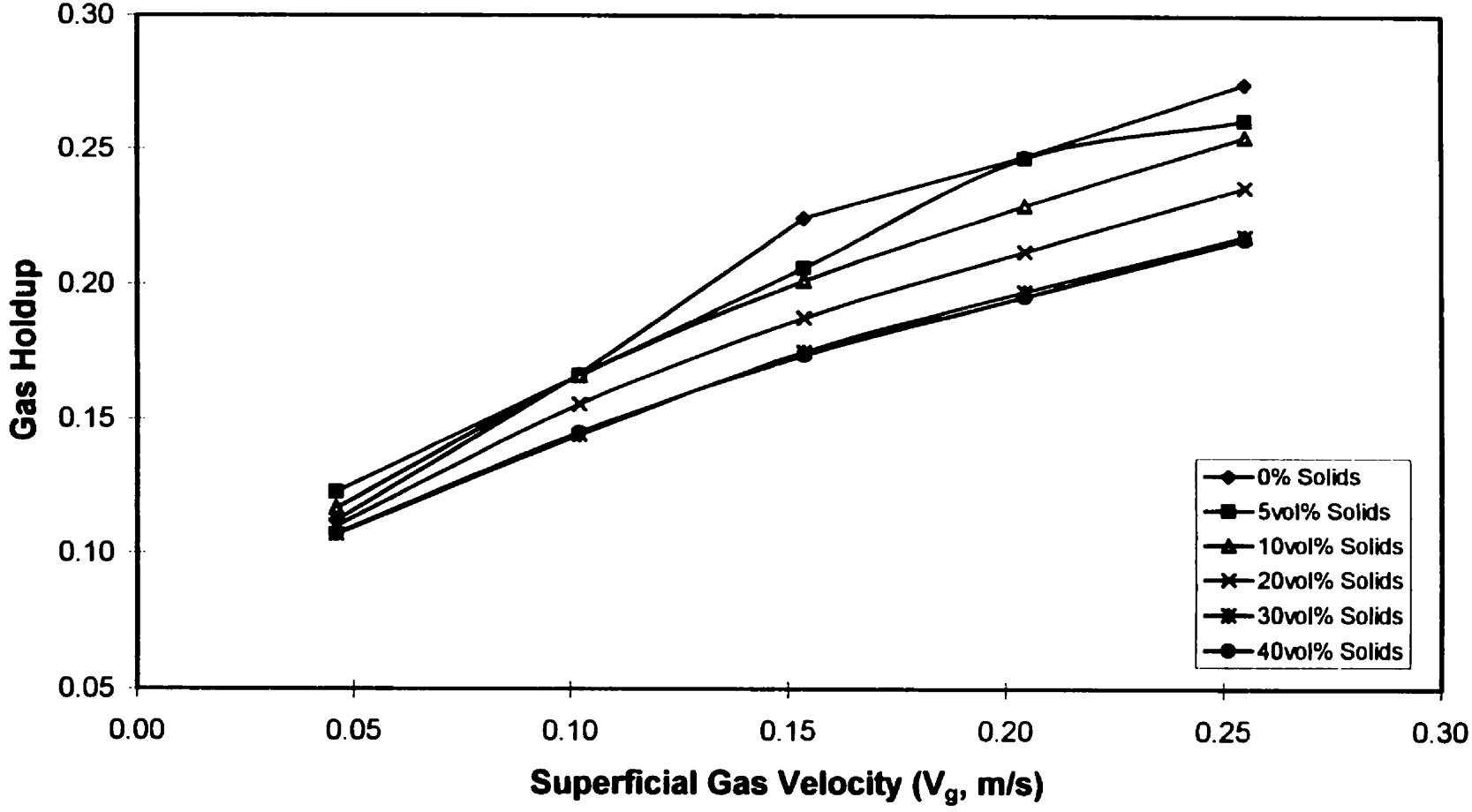

Fig. 4.6 Average Gas Holdup for varying Slurry Concentrations

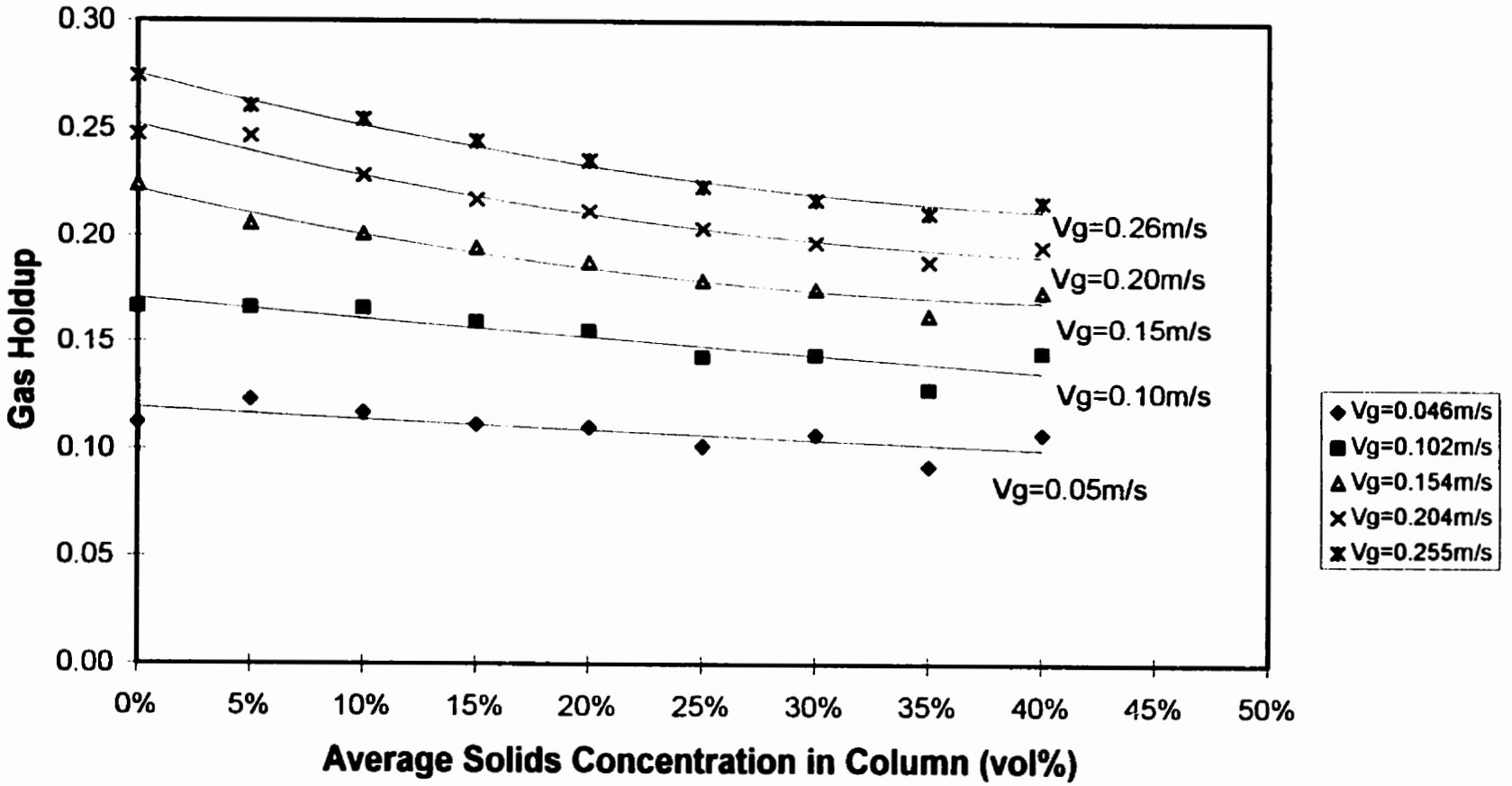

as a function of slurry concentration for given gas velocities. It can be seen that gas holdups decreased with increasing slurry concentration up to 35vol%, followed by a slight tendency to increase at higher slurry concentration (40vol%). The rate of decrease of gas holdup with increasing slurry concentration also seems to depend on operating gas velocity. Approximate absolute gradients for the gas holdup (i.e. change in gas holdup per unit change in slurry concentration) were calculated for each superficial gas velocity for slurry concentrations up to 30vol% and are plotted in Fig. 4.7. It can be seen that the gradient increases with increasing gas velocity. This shows that the rate of decrease of gas holdup with slurry concentration was higher for higher gas velocities. The decrease in gas holdup can be attributed to either an increase in bubble coalescence rate or a reduction in bubble break-up rate. The high gas holdups obtained at high gas velocities can be attributed to the higher rates of bubble break-up with increasing turbulence. The break-up is caused by interactions of turbulent eddies with bubbles (Prince and Blanch, 1990). The addition of solids has a dampening effect on the bubble break-up rate due to higher suspension viscosity. The bubble break-up rate is expected to be low at low gas velocities (<0.10m/s), therefore the rate of decrease of gas holdup with increasing slurry concentration is also low for lower gas velocities (as seen in Fig. 4.7).

4.1.2.1 Non-Coalescing Systems

Several experiments were also conducted to observe the behavior of differing slurry concentrations with non-coalescing systems. Iso-amyl alcohol (20 vppm in aqueous solution) was used to inhibit coalescence.

Fig. 4.7 Change in Gas Holdup Gradient for Varying Superficial Gas Velocities

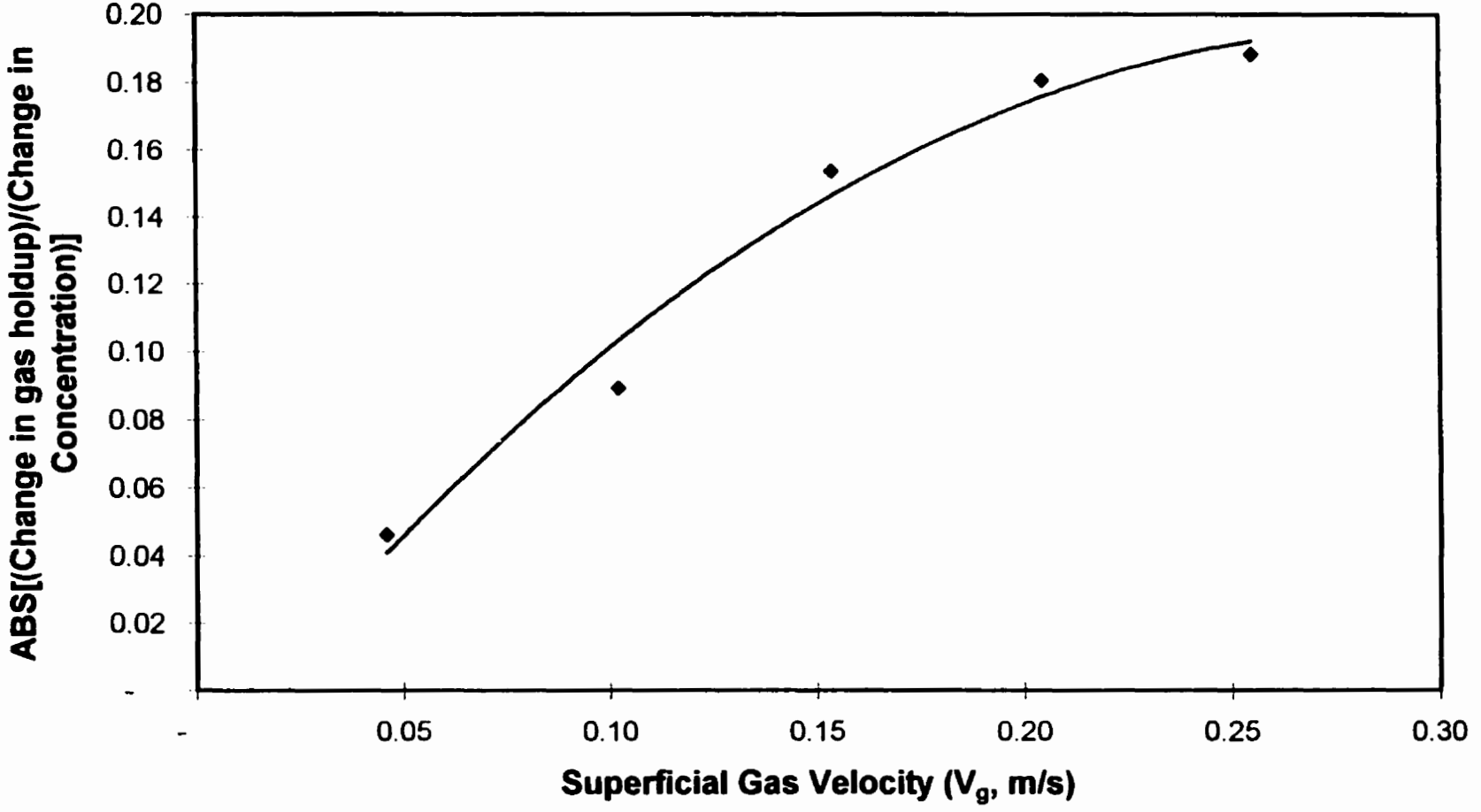

As found with coalescing systems, the average gas holdup was found to increase with increasing superficial gas velocity for all solids concentrations and decrease with increasing solids concentrations (as shown in Fig. 4.8). For higher gas velocities, however, the increase is more significant due to the presence of iso-amyl alcohol. Normally for higher gas velocities, due to turbulence, the rate of bubble break-up increases and bubble coalescence would also increase due to higher bubble concentration (Prince and Blanch, 1990). However, the presence of the coalescence inhibitor prevents coalescence, leading to much higher holdups for higher velocities. The effect of slurry concentration on gas holdup is better illustrated in Fig. 4.9. Gas holdups were again found to decrease with increasing slurry concentration up to 30vol%. For 40vol% solids, as before, there was a slight increase in the gas holdup. The largest rate of decrease of gas holdup occurred at the highest gas velocities. The decrease in gas holdup can be attributed to a reduction in bubble break-up rate caused by the presence of solids (and apparent slurry viscosity). At lower gas velocities, since the bubble break-up rate is already low, therefore the rate of decrease of gas holdup with increasing slurry concentration is also low.

Figure 4.10 compares the gas holdups obtained with coalescing and non-coalescing systems. Gas holdups obtained with gas velocities of 0.05m/s, 0.15m/s and 0.25m/s are shown. For slurry concentrations below 30vol%, the gas holdup is much higher for non-coalescing systems compared to coalescing slurry systems. Again, this is due to significantly reduced rates of bubble coalescence caused by presence of the coalescence inhibitor. For higher gas velocities and higher slurry concentrations, differences in gas holdups between coalescing and non-coalescing systems tend to disappear. At these high slurry concentrations, larger bubbles formed reduce gas holdup, however, bubble coalescence would also reduce as a result of low bubble concentrations and low turbulence. For a gas velocity of 0.05m/s, the difference in gas holdups for the

Fig. 4.8 Average Gas Holdup for varying Superficial Gas Velocities and Slurry Concentration with 20 vppm Coalescence Inhibitor (based on pressure profile)

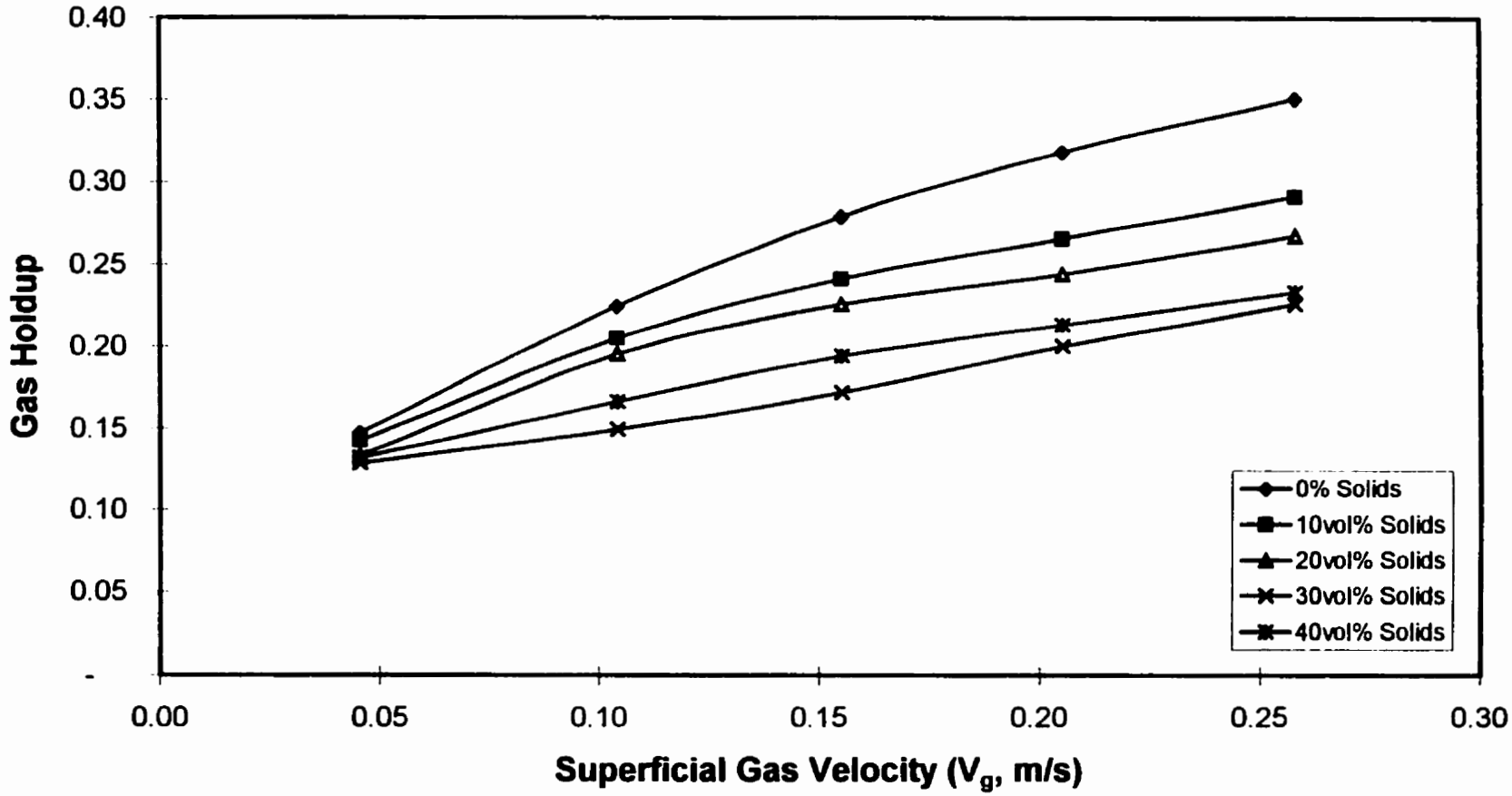

Fig. 4.9 Average Gas Holdup for varying Slurry Concentrations with 20 vppm Coalescence Inhibitor

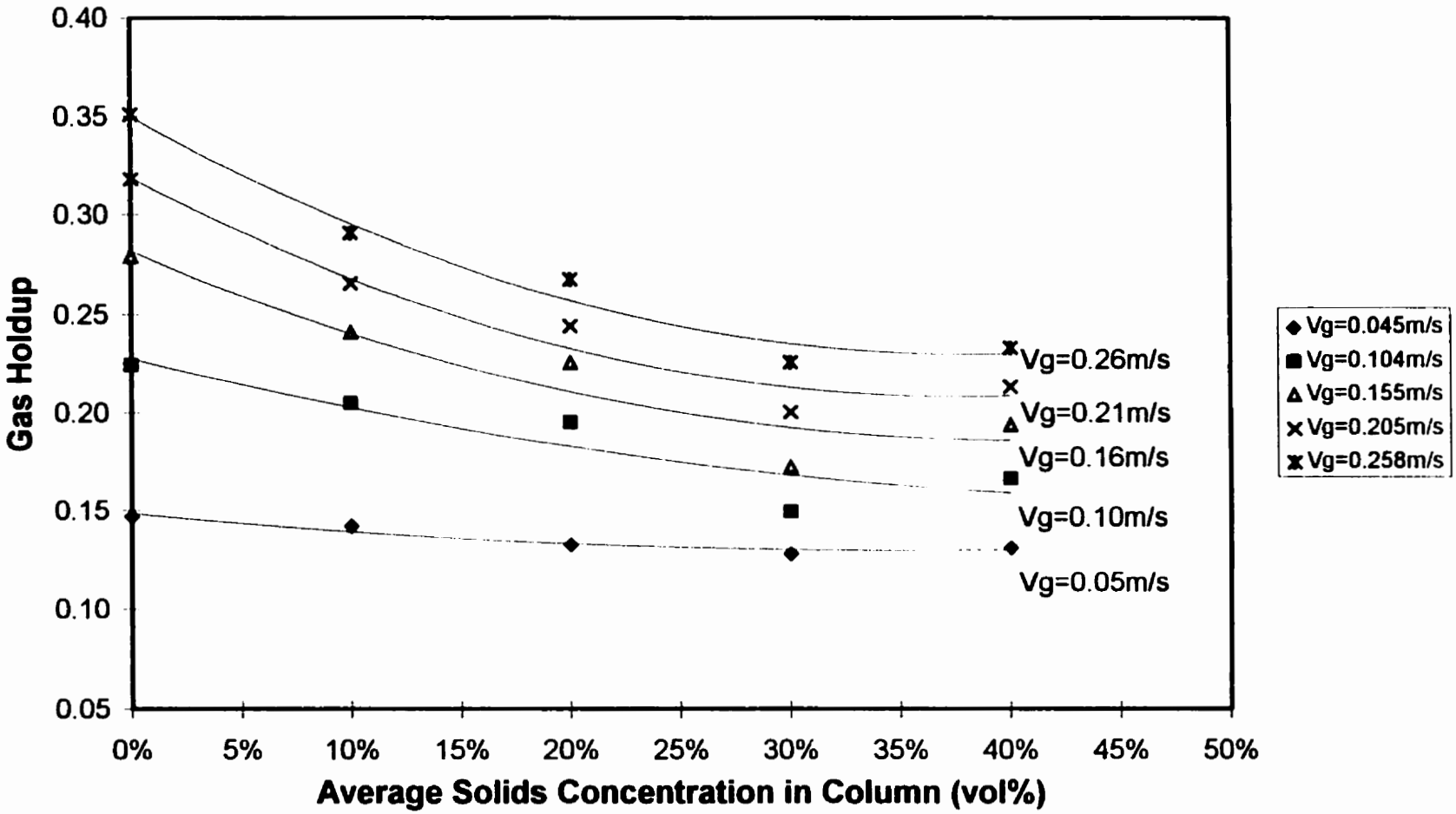

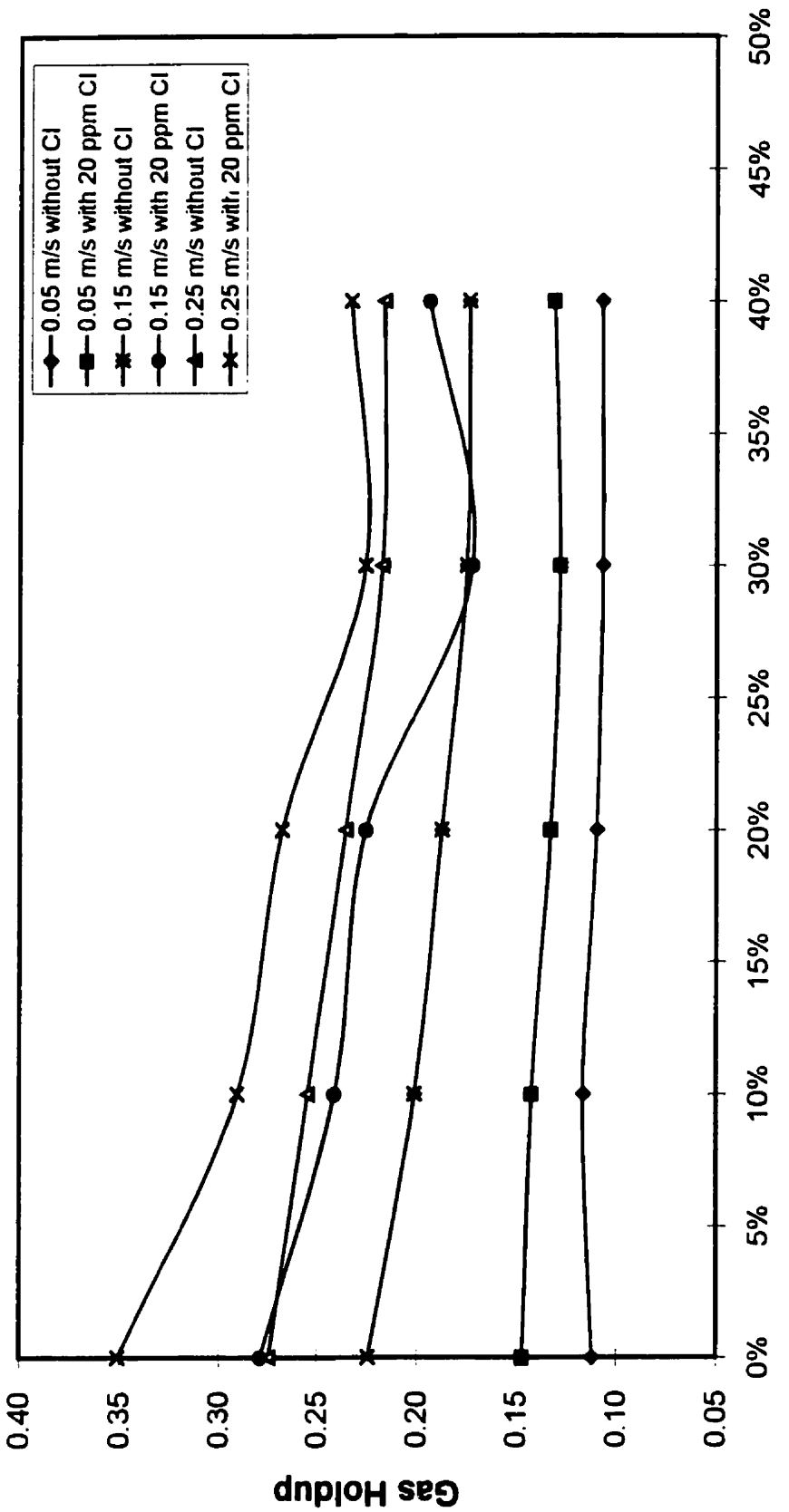

Fig. 4.10 Comparison of Average Gas Holdups for varying Slurry Concentrations with and without a coalescence inhibitor

two systems is practically constant for all slurry concentrations, due to low gas holdups to start with and lower turbulence levels.

The differences between coalescing and non-coalescing systems disappear at around 30vol% then slightly increase again at the highest slurry concentration (40vol%). A plot of the gas holdup as a function of slurry concentration for gas velocities of 0.15m/s and 0.25m/s is presented in Fig. 4.11. For each velocity, there is a decrease in the gas holdup as the slurry concentration is increased from 20vol% to 30vol%. This is due to the presence of solids reducing the rate of bubble break-up for each case. However, from 30vol% to 40vol%, there is a slight increase in gas holdup. As mentioned in section 4.1.1, this is due to the changing physical properties of the slurry. It appears as though smaller bubbles are rising slower in this highly viscous slurry. Since there are more smaller bubbles present in a non-coalescing system, therefore the holdup increases more significantly for the non-coalescing system.

4.1.2.2 Comparison of Average Gas Holdup Data with Literature Correlations

The various empirical literature correlations developed for the prediction of phase holdup in bubble columns and slurry bubble columns were reviewed in chapter 2.2.3. Correlations of Akita & Yoshida (1973), Hikita et al. (1980), Hughmark (1967), Hughmark modified by Smith et al. (1984), and Wilkinson et al. (1992) were tested for the solids-free system and results are summarized in Table 4.1. The correlations of Hughmark (1967), Akita and Yoshida (1973), Hikita et al. (1980), and Hughmark modified by Smith et al. (1984) were all found to predict gas holdups well within 10%, as shown in Fig. 4.12. This is probably due to the fact that all of these correlations were developed over a wide range of variables which included the range for this study. The Hughmark correlation

Fig. 4.11 Comparison of Average Gas Holdups for varying Slurry Concentrations with and without a coalescence inhibitor (for higher slurry concentrations and gas velocities only)

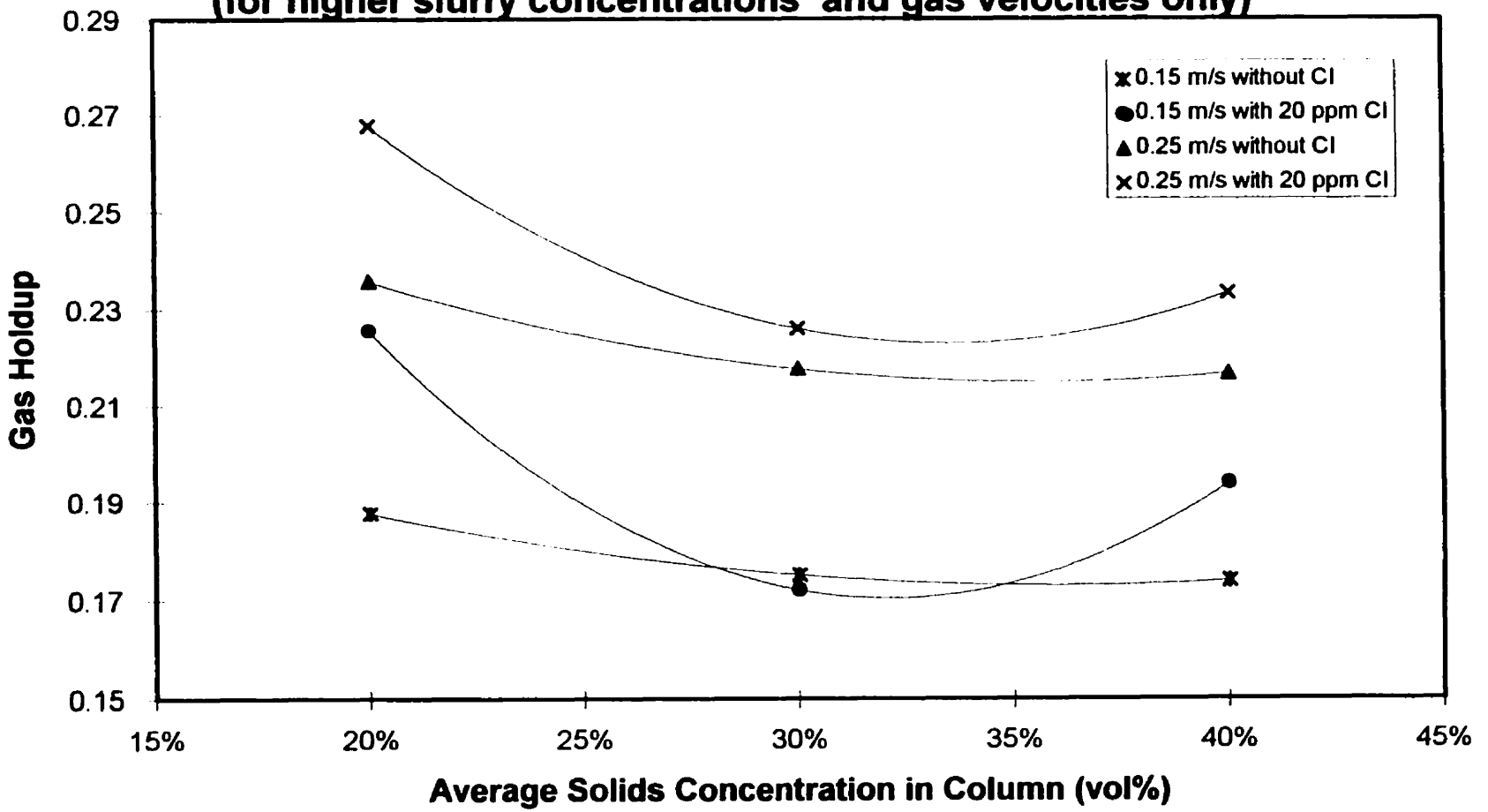

Table 4.1 - Summary of comparison between experimental gas holdup values and those obtained through literature correlations for gas-liquid systems

Summary of Results	Average Absolute Relative Error (%)	Average Relative Error (%)	Error Range (%)
Akita & Yoshida (1973)	6.7%	-6.7%	-11.0% to -1.6%
Hikita et al. (1980)	7.7%	-7.7%	-12.2% to -3.1%
Hughmark (1967)	6.9%	2.9%	-9.9% to 7.9%
Hughmark modified by Smith et al. (1984)	6.0%	5.2%	-2.0% to 12.5%
Wilkinson et al. (1992)	20.4%	-20.4%	-23.6% to -16.4%

Fig. 4.12 Comparison of experimental gas holdups with various literature correlations for a gas-liquid system

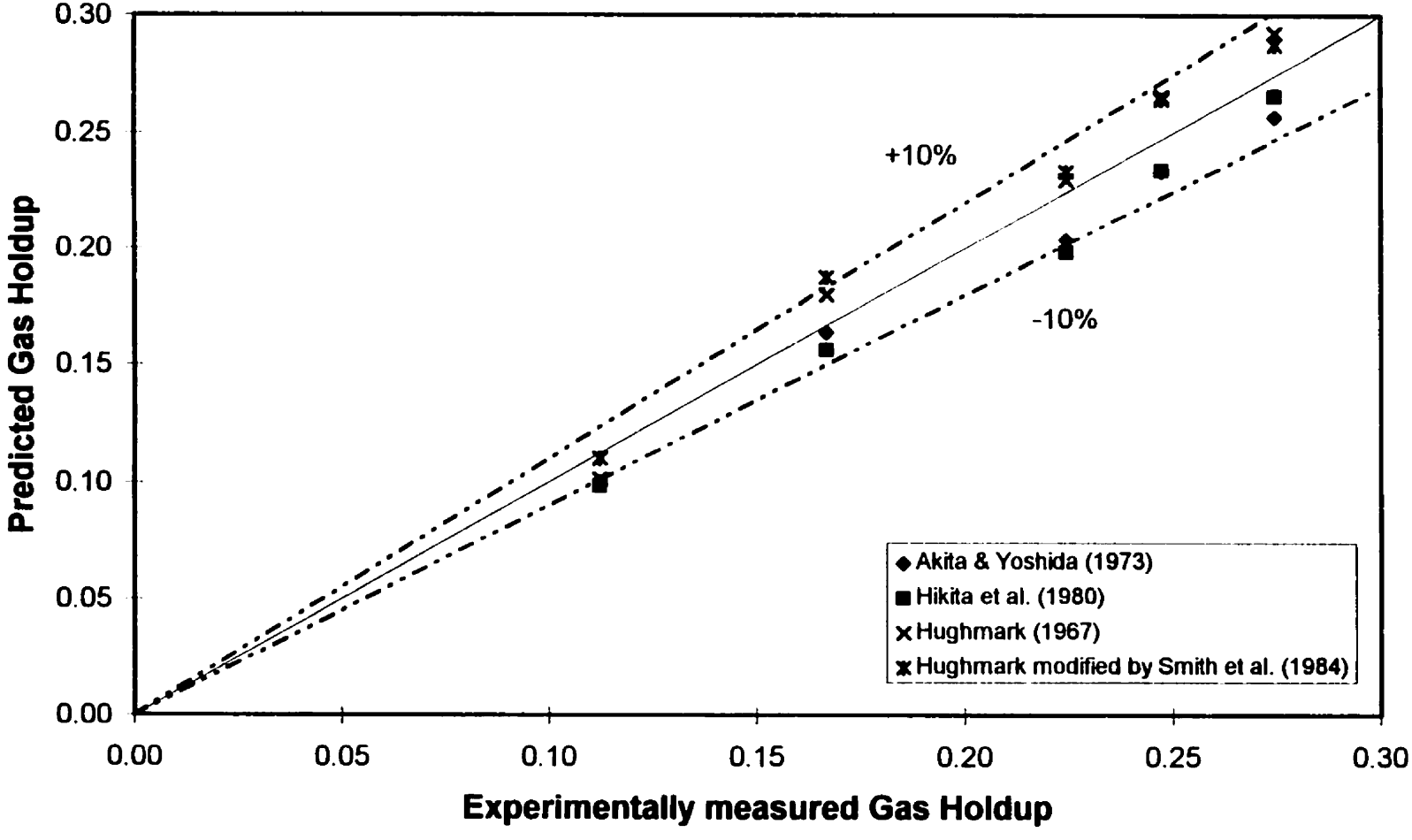

modified by Smith et al. (1984) was found to give the best prediction of experimental data with an average absolute relative error of only 6.0%. This correlation was developed for the coalesced bubble regime ($0.03<V_g<0.20$m/s) only, which closely approximates the operating range for this study. The correlations of Akita and Yoshida (1973, Hikita et al. (1980) and Hughmark (1967) were all developed over larger gas velocity ranges ($0.004<V_g<0.45$m/s) which correspond to both dispersed and coalesced bubble regimes. The correlation Wilkinson et al. (1992), which had an absolute error of over 20%, was developed for high pressure systems over a very small velocity range. Therefore, the Hughmark correlation modified by Smith et al. (1984) is the best correlation to estimate gas holdup for this gas-liquid system.

Literature correlations developed for slurry systems were also tested. Experimental data was compared with correlations by Kara et al. (1982), Koide et al. (1984), Hughmark modified correlation by Smith et al. (1984), Sauer & Hempel (1987), and Sada et al. (1986b). The Hikita et al. (1980) correlation modified for slurry viscosity using the Barnea and Mizrahi (1973) equation was also tested. The results are summarized in Table 4.2. Only a few of the correlations followed the observed downward gas holdup gradient with increasing slurry concentration. These included the correlations of Kara et al. (1982), Sada et al. (1986b) and Sauer & Hempel (1987). For the low gas velocity (0.05m/s), the Hughmark correlation modified by Smith et al. (1984) was also found to fit the gradient well. Figures 4.13a through 4.13c compare these correlations with experimentally measured gas holdups for three varying gas velocities. Errors bars are included on experimental data using a simple linear regression with 95% confidence intervals from the mean. The linear regression was found to fit experimental data well (since $R^2 > 0.95$). The correlation of Sada et al. (1986b) had the best fit with an average absolute relative error of 8.6%. This correlation compared quite well with experimental data for higher gas velocities (0.10m/s and higher). This is probably due to the fact that the

Table 4.2 - Summary of comparison between experimental gas holdup values and those obtained through literature correlations for slurry bubble columns

Summary of Results	Average Absolute Relative Error (%)	Average Relative Error (%)	Error Range (%)
Hikita et al. (1980) modified for slurry viscosity	10.3%	5.4%	-16.2% to 23.3%
Hughmark modified by Smith et al. (1984)	17.2%	15.6%	-9.0% to 34.9%
Kara et al. (1982)	11.1%	-7.9%	-33.5% to 28.1%
Koide et al. (1984)	22.3%	-22.3%	-46.3% to -13.6%
Sada et al. (1986b)	8.6%	-4.4%	-34.8% to 7.7%
Sauer & Hempel (1987)	10.0%	6.1%	-27.7% to 18.2%

Fig. 4.13a Comparison of experimentally measured gas holdups with literature correlations for slurry bubble columns (V_g=0.05m/s)

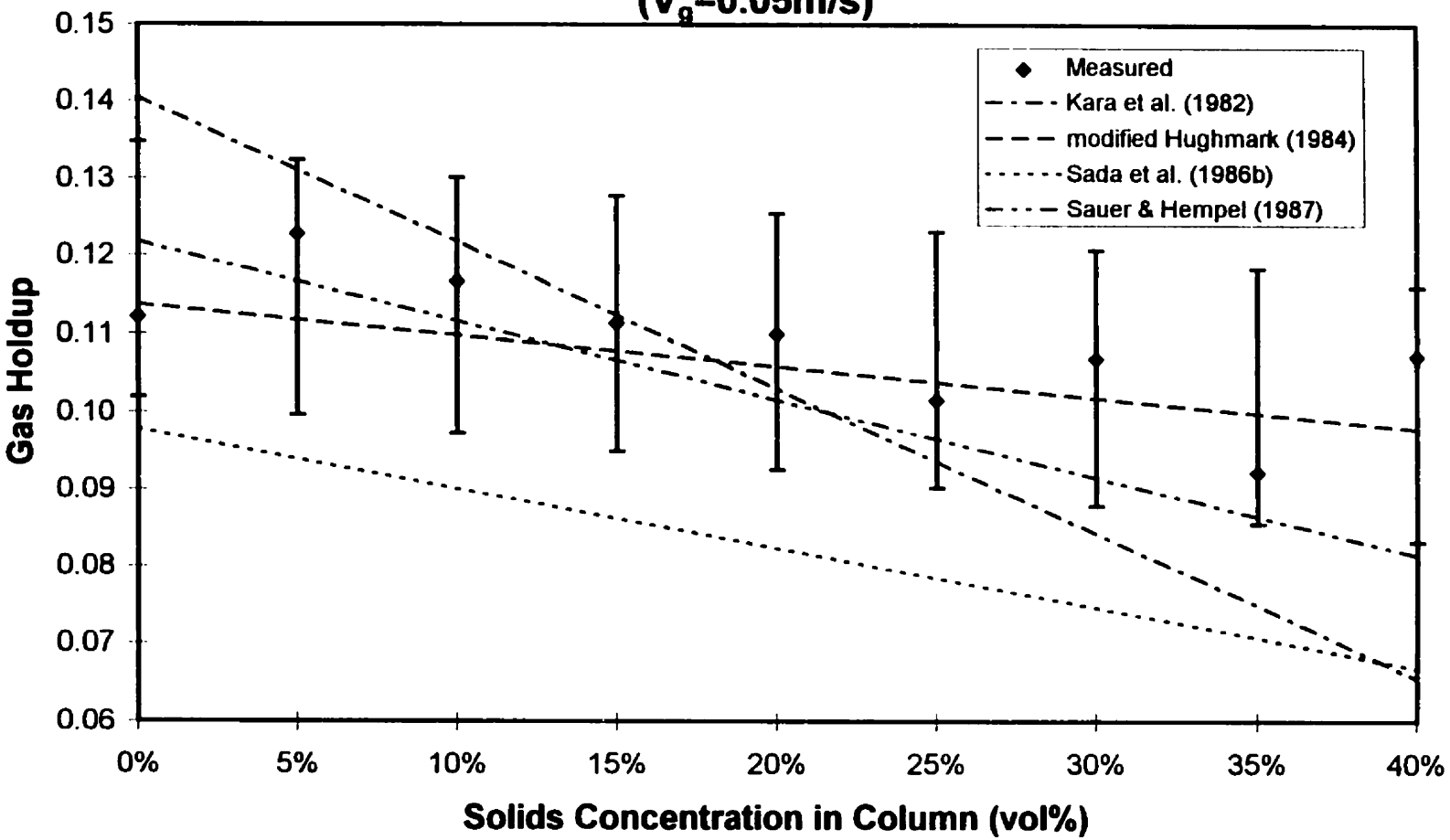

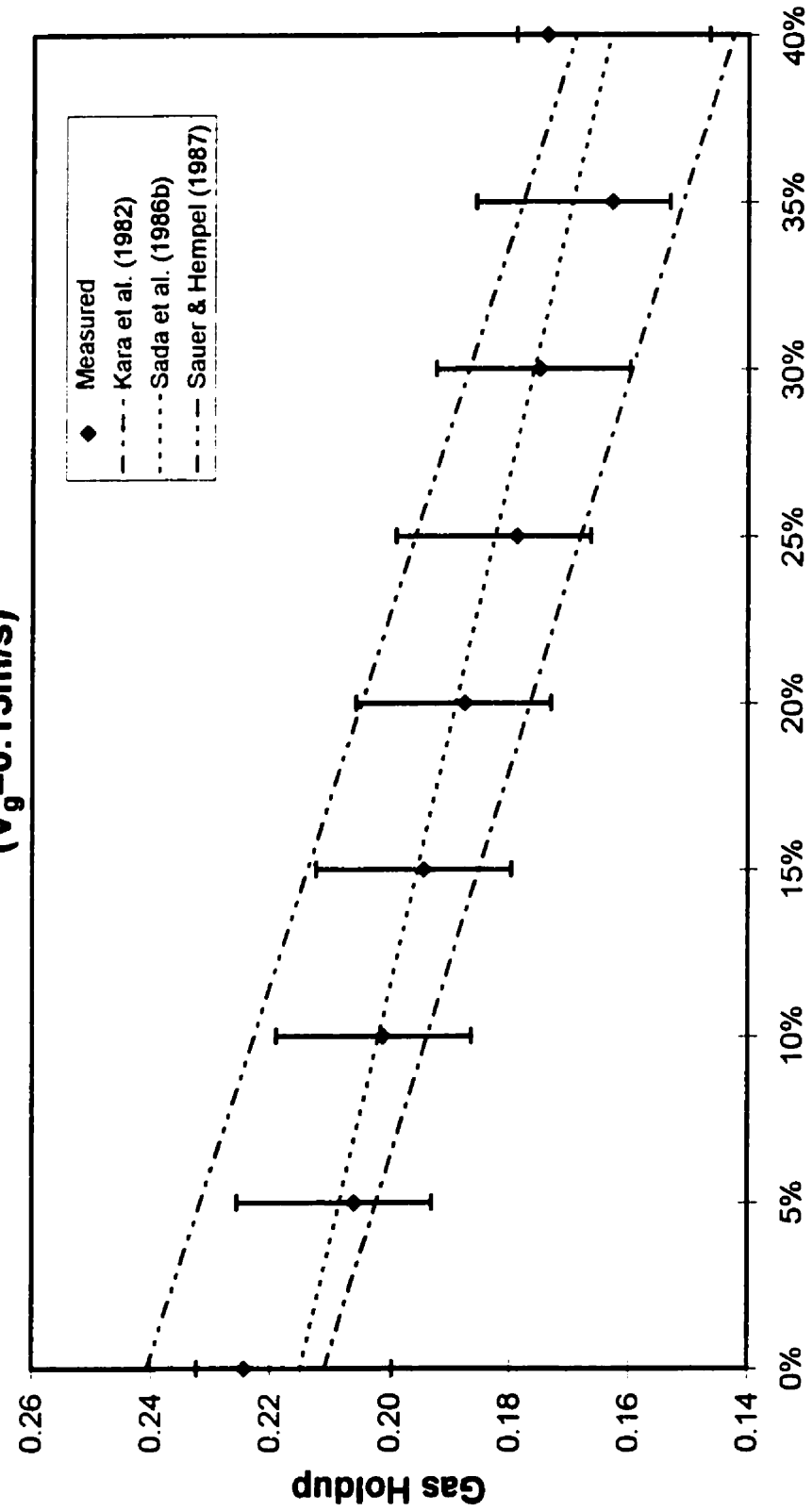

Fig. 4.13b Comparison of experimentally measured gas holdups with literature correlations for slurry bubble columns (V_g=0.15m/s)

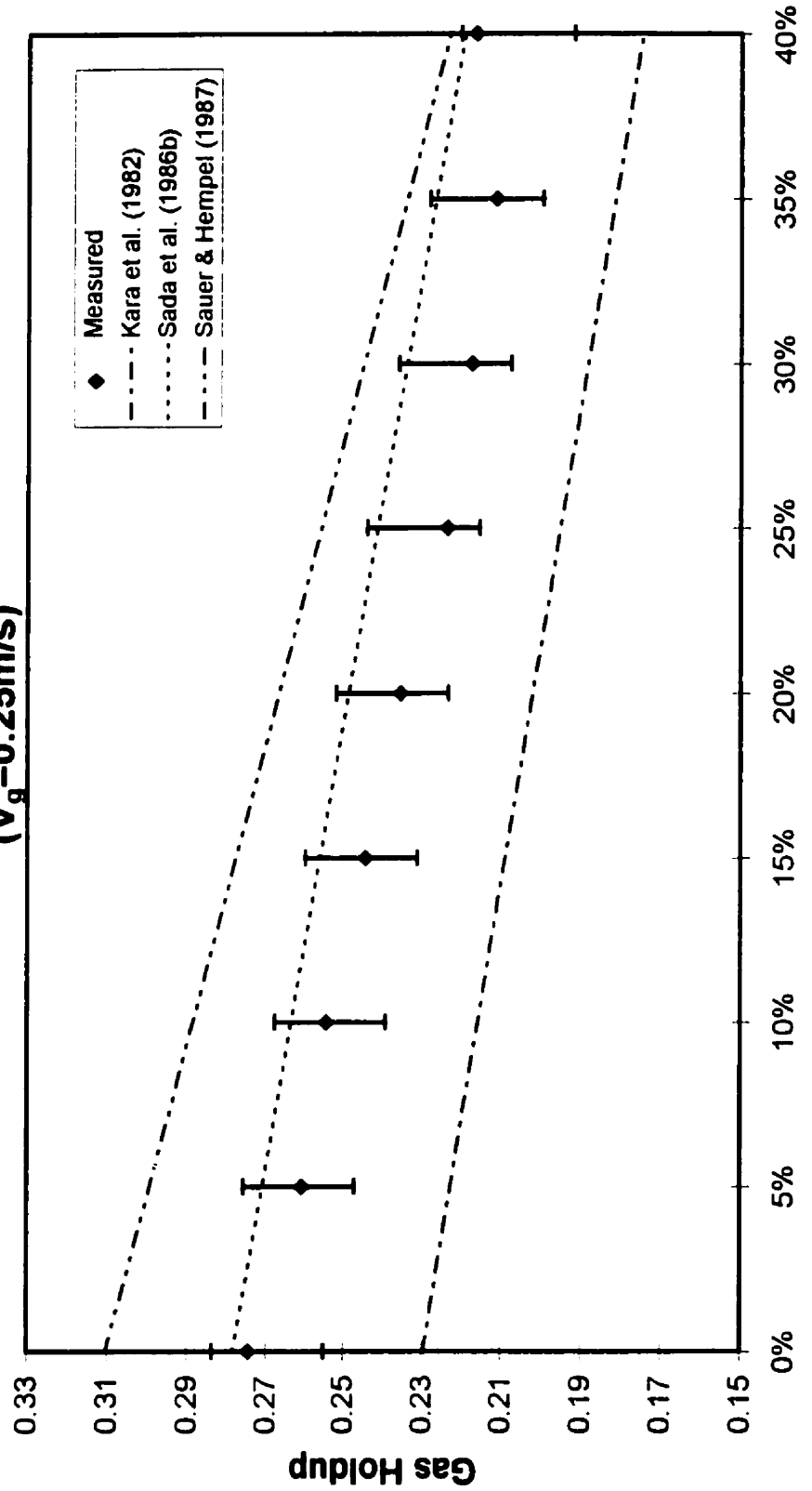

Fig. 4.13c Comparison of experimentally measured gas holdups with literature correlations for slurry bubble columns (V_g=0.25m/s)

correlation does take into account the effect of particle size and slurry concentration and was developed using similar gas velocities and particle sizes. For a superficial gas velocity of 0.05m/s, the correlation of Hughmark modified by Smith et al. (1984) was found to give best fit with a relative error of 10% (as seen in Fig. 4.13a). This is most probably due to the fact that the change in gas holdup gradient for the low gas velocity was minimal (as mentioned in section 4.1.2 and shown in Fig. 4.6), thus the slurry system operated much like a solids-free system. The correlations of Kara et al. (1982) and Sauer and Hempel (1987) were also found to fit well. Kara et al. (1982) was found to have an absolute relative error of 11.1%. The correlation did take into account the effect of particle size and slurry concentration and operating ranges were similar to that of our system, however, the values for coefficients B_1 through B_4 (based on dried mineral and coal) were specific to their system and could not be adequately estimated for glass beads. The range of error for these coefficients was as high as 100%. The correlation of Sauer and Hempel (1987) had an absolute relative error of 10%. This correlation did take into account the effective slurry viscosity and column diameter, however, particle size was not considered. The range of operating parameters used to derive this equation were also much different from this study. Thus for higher gas velocities, the correlation of Sada et al. (1986b) was found to give the best fit of experimental data, while for a gas velocity of 0.05m/s the Hughmark correlation modified by Smith et al. (1984) was found to give the best fit.

4.1.2.3 Correlations Based on Drift Flux

The drift flux model and various correlations were reviewed in section 2.2.4. Since Saxena and coworkers have developed drift flux correlations over operating ranges similar to this study, it is worthwhile to test their correlation. To predict gas holdup, Saxena and Chen (1994) modified Eq. 2.29 as follows:

$$\varepsilon_g = \frac{V_g}{U_{b\infty} + 2.5V_g} \tag{4.2}$$

where $U_{b\infty}$ represents the characteristic terminal rise velocity of a swarm of bubbles and

$$U_{b\infty} = 1.80C(P_v)(\sigma\rho_{sl}/72)^{0.333}(\mu_{sl})^{0.289} \tag{4.3}$$

where $C(P_v)$ is the pressure corresponding to the midpoint of the dispersion in the column. The full range of operating parameters used to develop Eqs. 4.2 and 4.3 are presented in section 2.2.4. It should be noted that the $U_{b\infty}$ is independent of the superficial gas velocity.

The characteristic terminal rise velocities were first calculated using Eq. 4.3. The results were then substituted into Eq. 4.2 and are summarized in Table 4.3. For the coalescing systems, the average absolute relative error was found to be 15.5%, however, the range or error was quite large. For non-coalescing systems, the average absolute relative error was 10.0%, but again the range of error was large. Since bubble swarm velocity is the only unknown parameter in Eq. 4.2, it was decided to recalculate $U_{b\infty}$ values based on experimental data and then compare with predicted values. Results are summarized in Table 4.4. For the coalescing system the average absolute relative error was 35.9%, and for the non-coalescing system, the average absolute relative error was 21.0%, indicating that the prediction of $U_{b\infty}$ was insufficient. These differences can be related to the range of superficial gas velocities ($0.005<V_g<0.30$m/s) used by Saxena and coworkers to develop their correlation. The correlation itself does not take into account gas velocity, however, it is known that the lower gas velocities (<0.10m/s) correspond to the dispersed bubble regime which has much smaller bubbles and, therefore, lower $U_{b\infty}$ values. Since the majority of gas velocities used for this study correspond to the coalesced bubble regime,

Table 4.3 - Comparison of Predicted Gas Holdups (using the Drift Flux Model proposed by Saxena and Chen (1994)) with Experimentally Measured Gas Holdups

	Average Absolute Relative Error (%)	Average Relative Error (%)	Error Range (%)
Coalescing System	15.5%	14.4%	-16.8% to 27.3%
Non-Coalescing System	10.0%	-2.8%	-32.2% to 23.3%

Table 4.4 - Comparison of Predicted Bubble Swarm Velocities (using the Model proposed by Saxena and Chen (1994)) with Calculated Values from Eq. 4.3

	Average Absolute Relative Error (%)	Average Relative Error (%)	Error Range (%)
Coalescing System	35.9%	-34.5%	-63.0% to 21.7%
Non-Coalescing System	21.0%	4.1%	-49.7% to 59.1%

the applicability of the correlation was in question. It was therefore decided to abandon this version of the drift flux model.

A new model was developed (based on Eq. 2.26) which could adequately predict the gas holdup. Eq. 2.26 can be modified for a batch slurry system as follows:

$$\frac{V_{gl}}{\varepsilon_g} = \frac{V_g}{\varepsilon_g} - \frac{V_g}{\varepsilon_g + \varepsilon_l} \tag{4.4}$$

which can be rearranged to be rearranged as follows

$$\varepsilon_g = \frac{(1-\psi_s)(V_{gl}/V_g)}{(V_{gl}/V_g)+(1-\psi_s)(1-(V_{gl}/V_g))} \tag{4.5}$$

where liquid holdup (ε_l) was correlated with the following

$$\varepsilon_l = (1-\psi_s)(1-\varepsilon_g) \tag{4.6}$$

To predict drift flux velocity (V_{gl}), Nacef et al. (1988) proposed the following correlation:

$$V_{gl} = b_1(V_g)^{b_2} \tag{4.7}$$

The following correlations were therefore developed for drift flux velocity for coalescing and non-coalescing systems using regression of experimental data

Coalescing system:

$$V_{gl} = 0.6271(V_g)^{0.8934} \qquad R^2 = 0.998 \tag{4.8}$$

Non-coalescing system:

$$V_{gl} = 0.5999(V_g)^{0.8936} \qquad R^2 = 0.998 \tag{4.9}$$

Figs. 4.14a and 4.14b show the plots of drift flux velocity as a function of gas velocity, based on the above correlations. It can be seen that the proposed correlations predict the drift flux velocity very well. It should also be noted that

Fig. 4.14a Prediction of the Drift Flux Velocity as a function of Superficial Gas Velocity for all Coalescing Slurry Systems

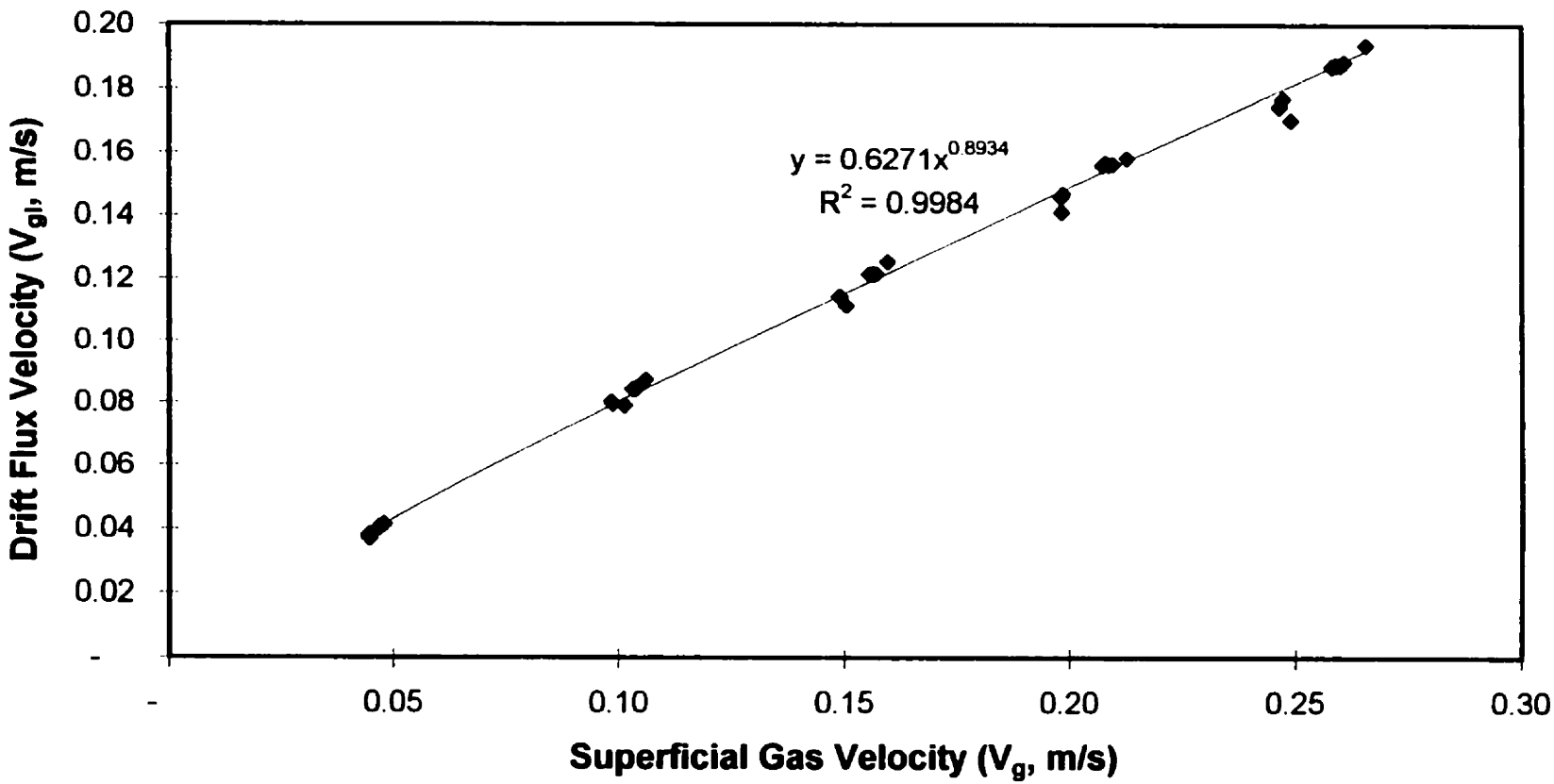

Fig. 4.14b Prediction of the Drift Flux Velocity as a function of Superficial Gas Velocity for all Non-Coalescing Slurry Systems

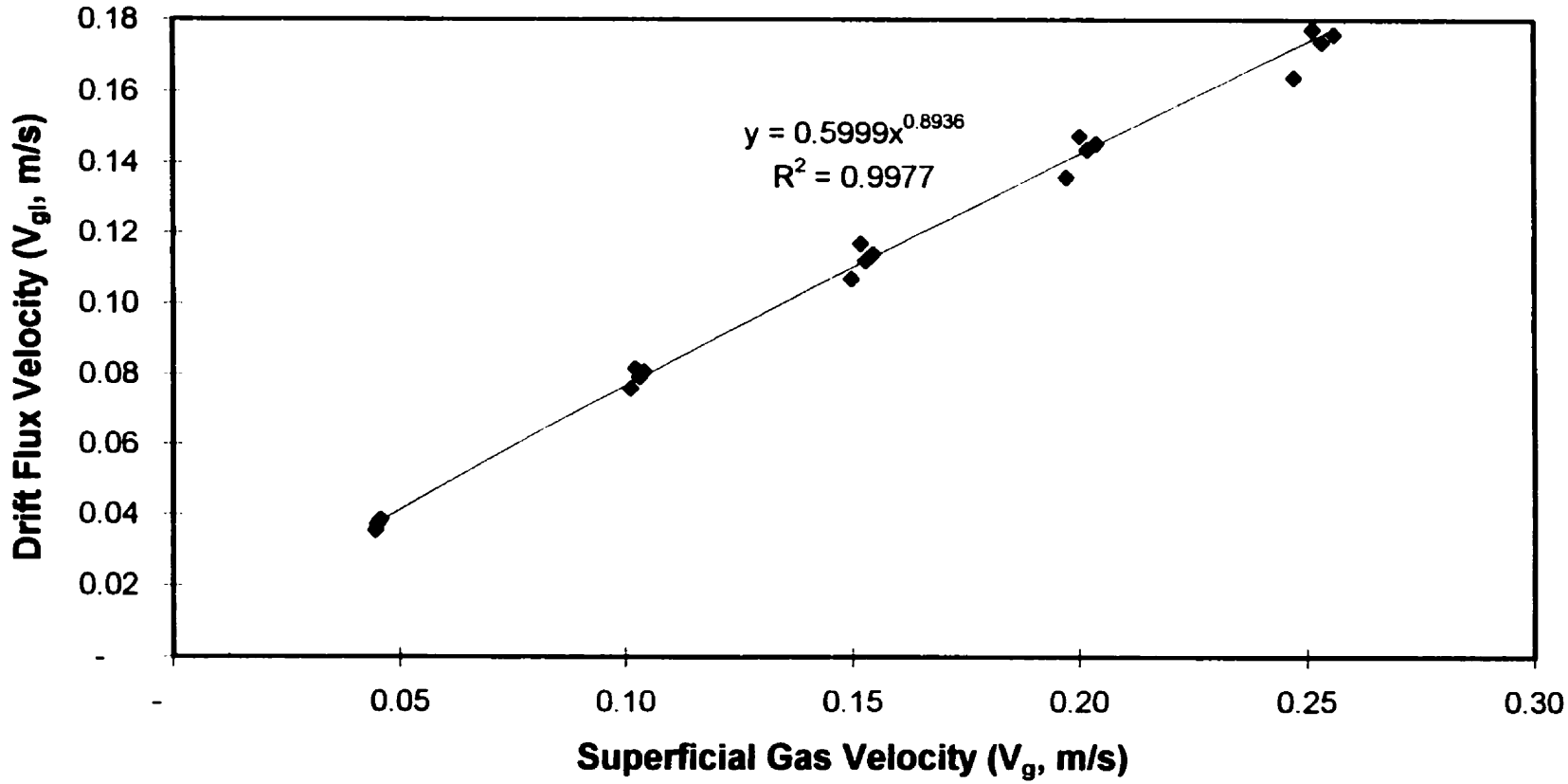

the data was plotted over the entire range of slurry concentrations (0-40vol%) with the slurry concentration having negligible on the overall drift flux velocity (because of the high R^2 values). As an additional check, correlations were determined for individual slurry concentrations (5vol% and 40vol% solids) and results were compared for superficial gas velocities of 0.05m/s and 0.25m/s. The range of error was found to be from 0.9% to 5.2%. This indicates that the drift flux does not depend on the slurry concentration and hence, slurry viscosity. Results from Eqs. 4.7 and 4.6 were substituted into Eq. 4.5 and gas holdups were calculated for both coalescing and non-coalescing systems. A comparison of measured and calculated gas holdups are presented in Figs. 4.15a and 4.15b and Table 4.5. For the coalescing system the average absolute relative error was found to be 6.5%, and for the non-coalescing system the average absolute relative error was determined to be 7.2%, both of which are excellent fits.

Finally, the applicability of the new gas holdup model was tested with experimental data of Saxena and coworkers. The average absolute relative error was 15.2%, however, many of the larger deviations from predicted values occurred for lower gas velocities (<0.10m/s). A significant portion of the experimental data of Saxena and coworkers was obtained at low gas velocities (which correspond to the dispersed bubble and transitional regimes). Ignoring these lower velocities reduced the average absolute relative error to 10.2%. We can therefore conclude that the drift flux model equations developed for predicting gas holdup are adequate for the coalesced bubble regime (with superficial gas velocities of 0.10m/s and higher) for coalescing and non-coalescing systems. A different model, however, is required for lower gas velocities and the dispersed bubble flow regime.

Fig. 4.15a Comparison of Experimental Gas Holdup Data with Calculated Gas Holdups using the Drift Flux Model for all Coalescing Systems

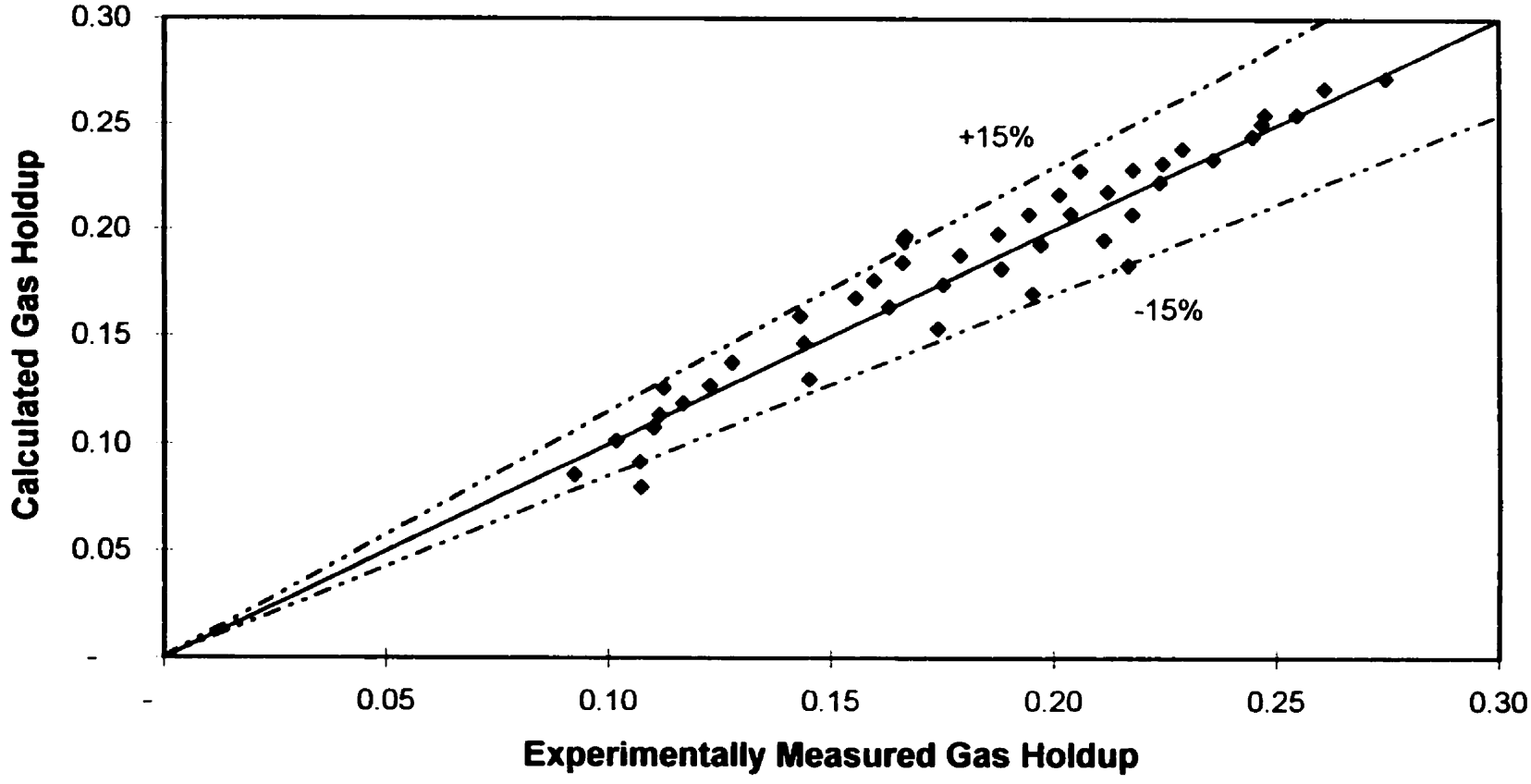

Fig. 4.15b Comparison of Experimental Gas Holdup Data with Calculated Gas Holdups using the Drift Flux Model for all Non-Coalescing Systems

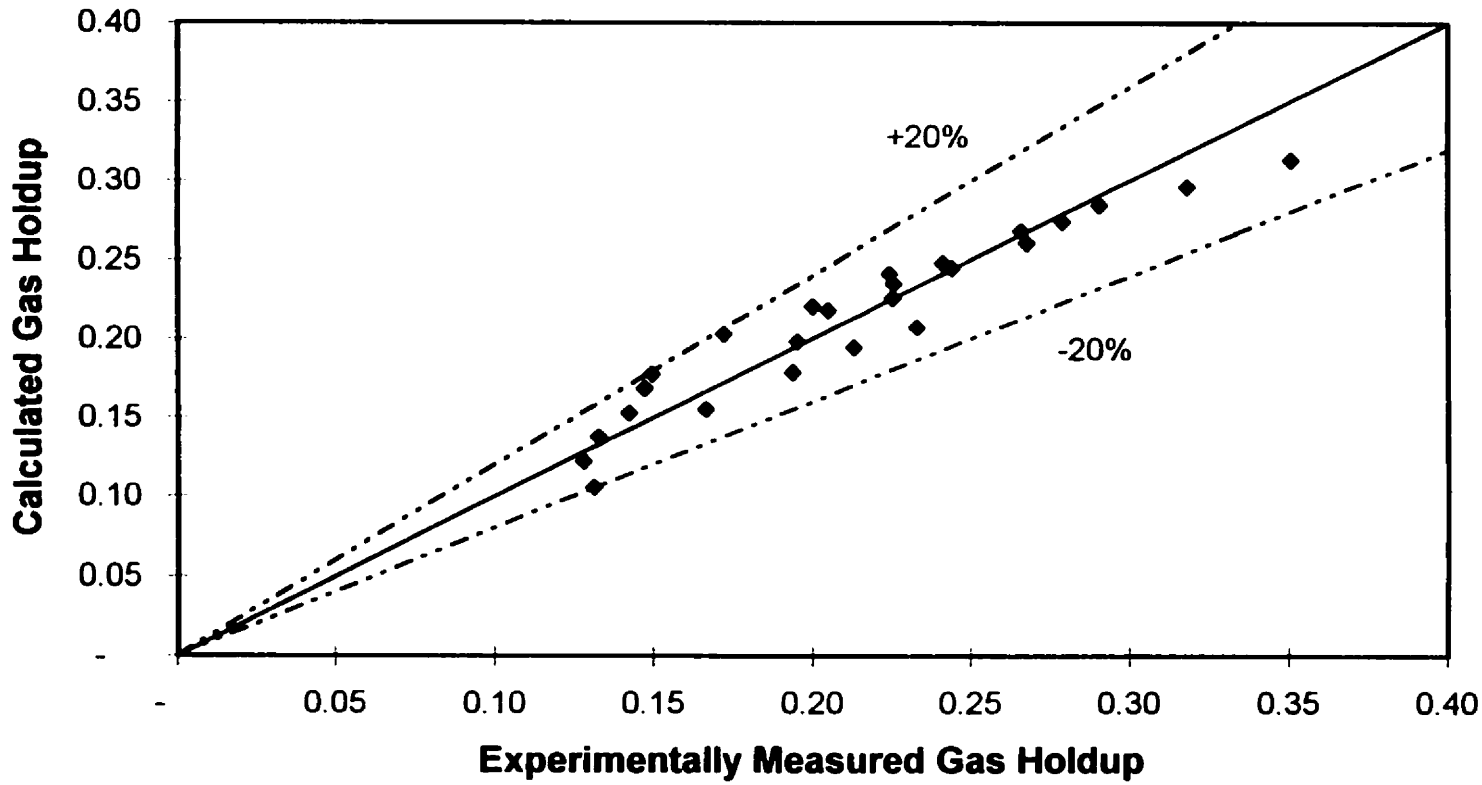

Table 4.5 - Comparison of Predicted Gas Holdups with Experimentally Measured Gas Holdups using developed Drift Flux Model

	Average Absolute Relative Error (%)	Average Relative Error (%)	Error Range (%)
Coalescing System	6.5%	0.3%	-34.2% to 15.5%
Non-Coalescing System	7.2%	-0.3%	-24.1% to 15.7%

4.1.3 Axial Solids Holdup Profiles

Local solids holdups were measured using five different sampling probes (denoted Probes # 1 through 5) placed at several axial positions on the column (z=5, 25, 65, 105, and 145 cm, respectively) above the base plate. The solids sampling probe design and dimensions have been summarized in the experimental section of this thesis. The local axial and radial solids concentrations were determined using both the filtering-drying and pycnometric techniques (also described in the experimental section). A batch system was employed with respect to the liquid/slurry.

Axial solids concentration profiles for 10vol% through 40vol% solids systems are presented in Figs. 4.16a through 4.16d, respectively. There is a downward sloping solids concentration profile (gradient) for all solids concentrations. This gradient can be explained by the settling effect of gravity on solids particles. Since solids are denser than the liquid and gas, they tend to settle to the bottom of the column. However, due to the turbulence created by the flow of gas and liquid circulation, there is also an upward lift force acting on the particles. When the net upward force exceeds the particle settling velocities, the particles are dispersed. The lift is a function of slurry kinetic energy which in turn is related to column turbulence and bubble wake phenomenon. Since this is a batch system with respect to liquid and slurry, we would also expect this gradient to cross the average slurry concentration line to obey the law of conservation of mass. The gradient is observed to cross the average concentration line between 0.40m and 0.80m. It may also be noted from Figs. 4.16a through 4.16d that the effect of superficial gas velocity on solids concentration profile is not very significant.

Fig. 4.16a Axial Slurry Concentration Variation (with 10vol% average solids concentration in column)

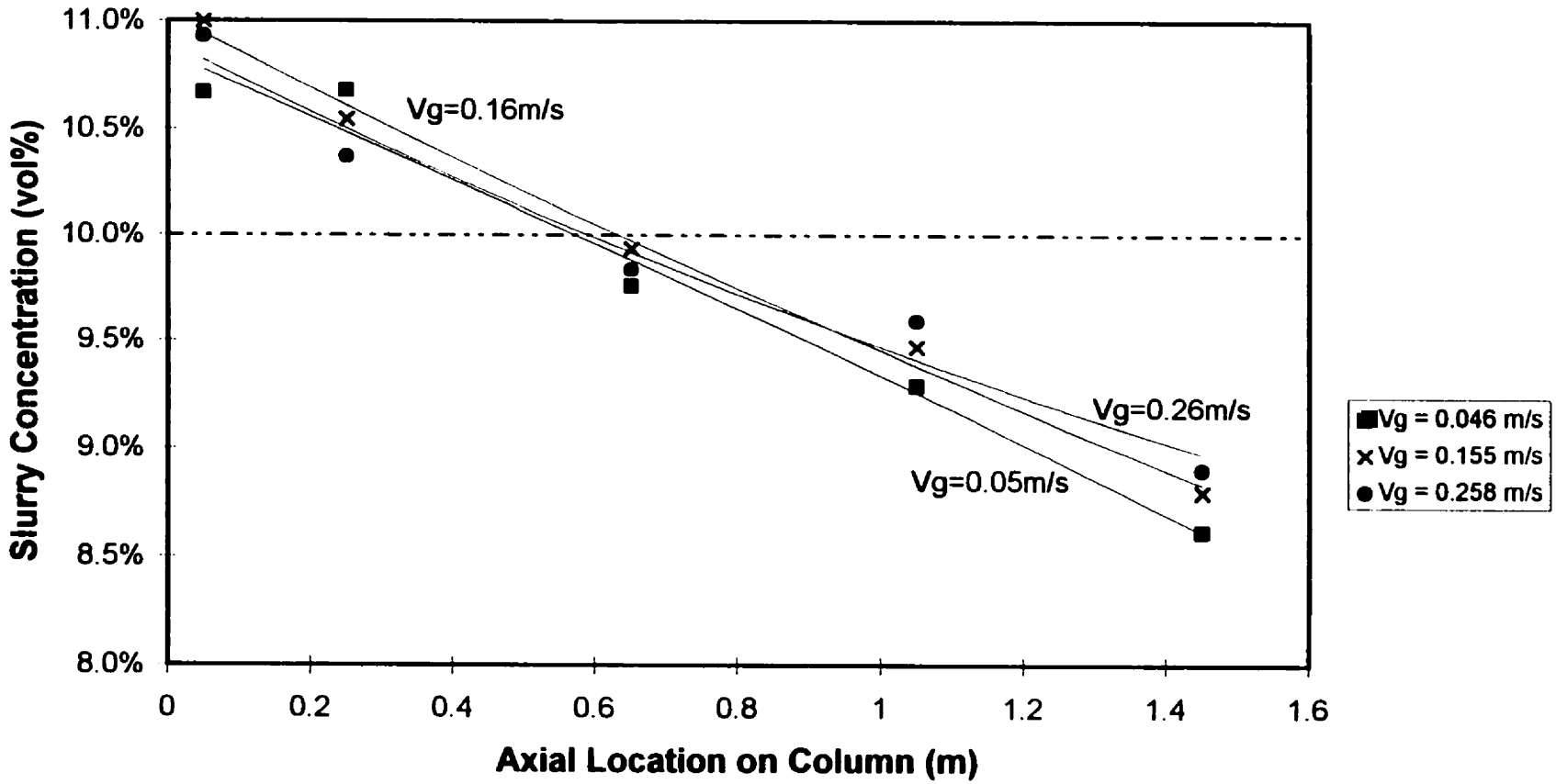

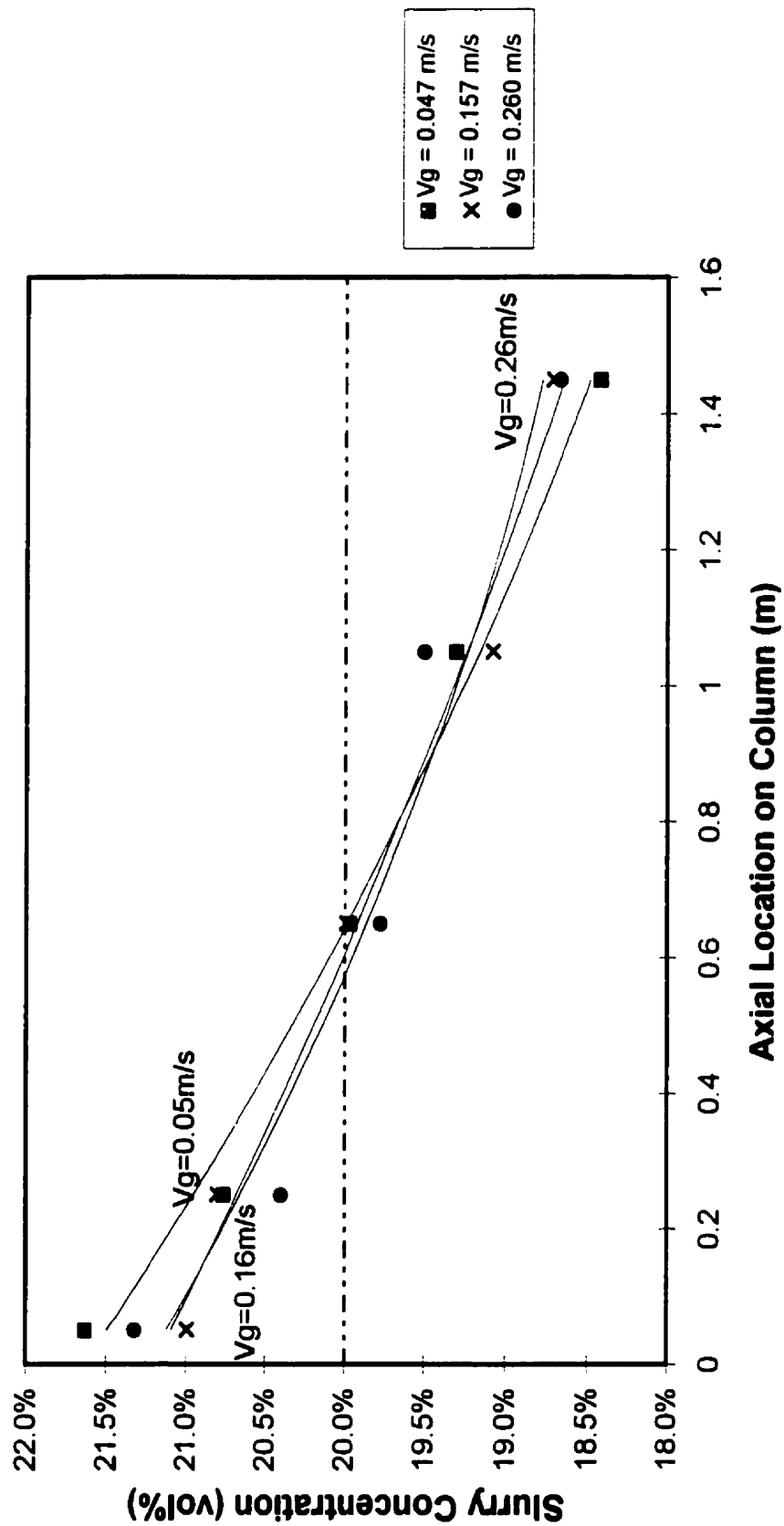

Fig. 4.16b Axial Slurry Concentration Variation (with 20vol% average solids concentration in column)

Fig. 4.16c Axial Slurry Concentration Variation (with 30vol% average solids concentration in column)

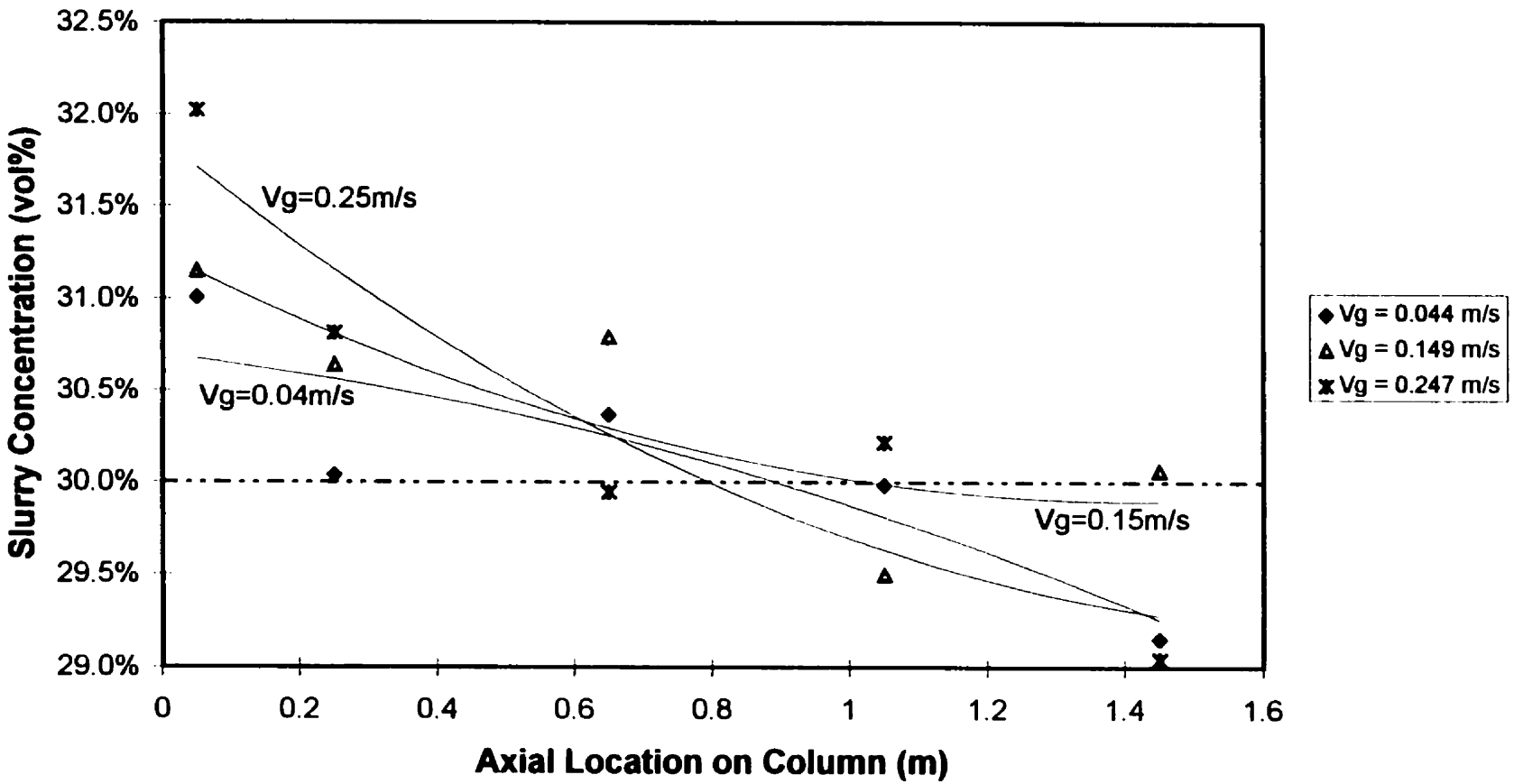

Fig. 4.16d Axial Slurry Concentration Variation (with 40vol% average solids concentration in column)

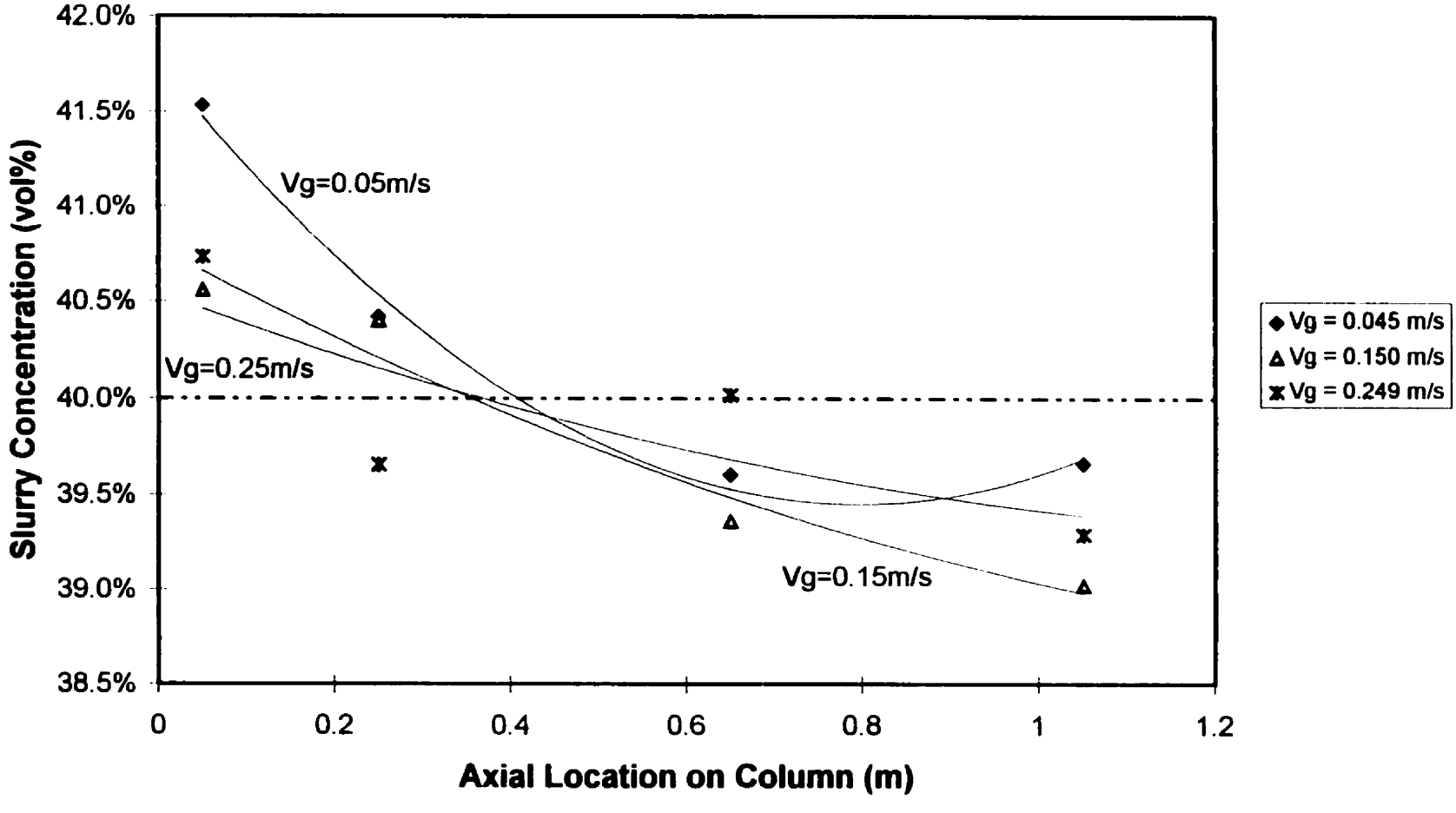

In order to clarify, the effects of varying superficial gas velocities were further studied for different slurry concentrations. Figures 4.17a through 4.17d show the effect of varying gas velocities (0.05m/s to 0.26m/s) on the normalized axial solids holdup profile for different sampling probe locations and solids systems (10vol% to 40vol%). The relatively flat slopes indicate that the effect of superficial gas velocity on the axial solids concentration profile is generally small. Most observed gradients have a normalized slurry concentration range of approximately 1% to 4%, which fall within the sampling error range highlighted in section 3.2.2.3. This negligible effect of gas velocity on axial solids concentration distribution was also observed by Smith and Ruether (1985), Smith et al. (1986), O'Dowd et al. (1987) and Murray and Fan (1989). They explained that this effect was a result of offsetting effects of parameters. Both solids dispersion (E_s) and hindered setting velocity (U_p) increase as gas velocity increases. Since axial solids distribution is a function of U_p/E_s, therefore an increase in V_g will only minimally affect the axial slurry concentration. However, this effect can also be explained in terms of the potential energy required to keep a particle in suspension. The incoming buoyant power, which is primarily a function of a gas volumetric flowrate, is used for the generation of bulk motion and can be calculated as follows (Lamont, 1958):

$$P_{in,g} = P_o Q_{o,g} \ln\left(\frac{P_o + \rho_{sl} g H_c}{P_o}\right) \qquad (4.10)$$

Turbulence is generated as a result of this bulk motion and quickly spreads throughout the reactor. Kleijntjens et al. (1994) reported that a portion of the turbulent power generated is used to maintain the potential energy of the particles in suspension and the remainder maintains slurry motion (kinetic energy). Therefore,

$$P_{in,g} = \left(\frac{dE_{pot,p}}{dt}\right)_{tot} + \varepsilon_{kin} V_R \rho_{sl} \qquad (4.11)$$

Fig. 4.17a Comparison of Axial Solids Concentration for Varying Probe Locations and Superficial Gas Velocities (with 10vol% average solids concentration in system)

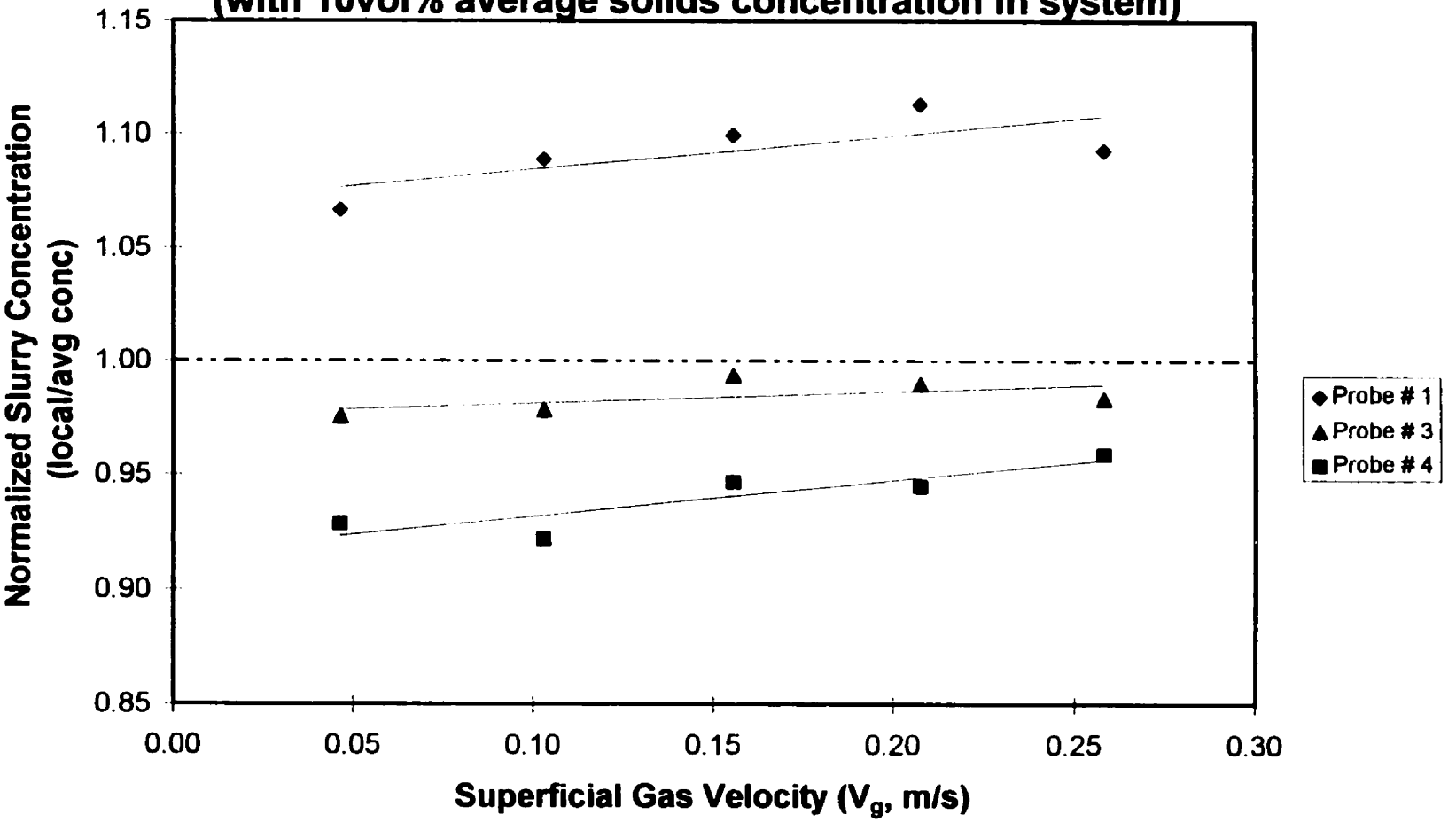

Fig. 4.17b Comparison of Axial Solids Concentration for Varying Probe Locations and Superficial Gas Velocities (with 20vol% average solids concentration in system)

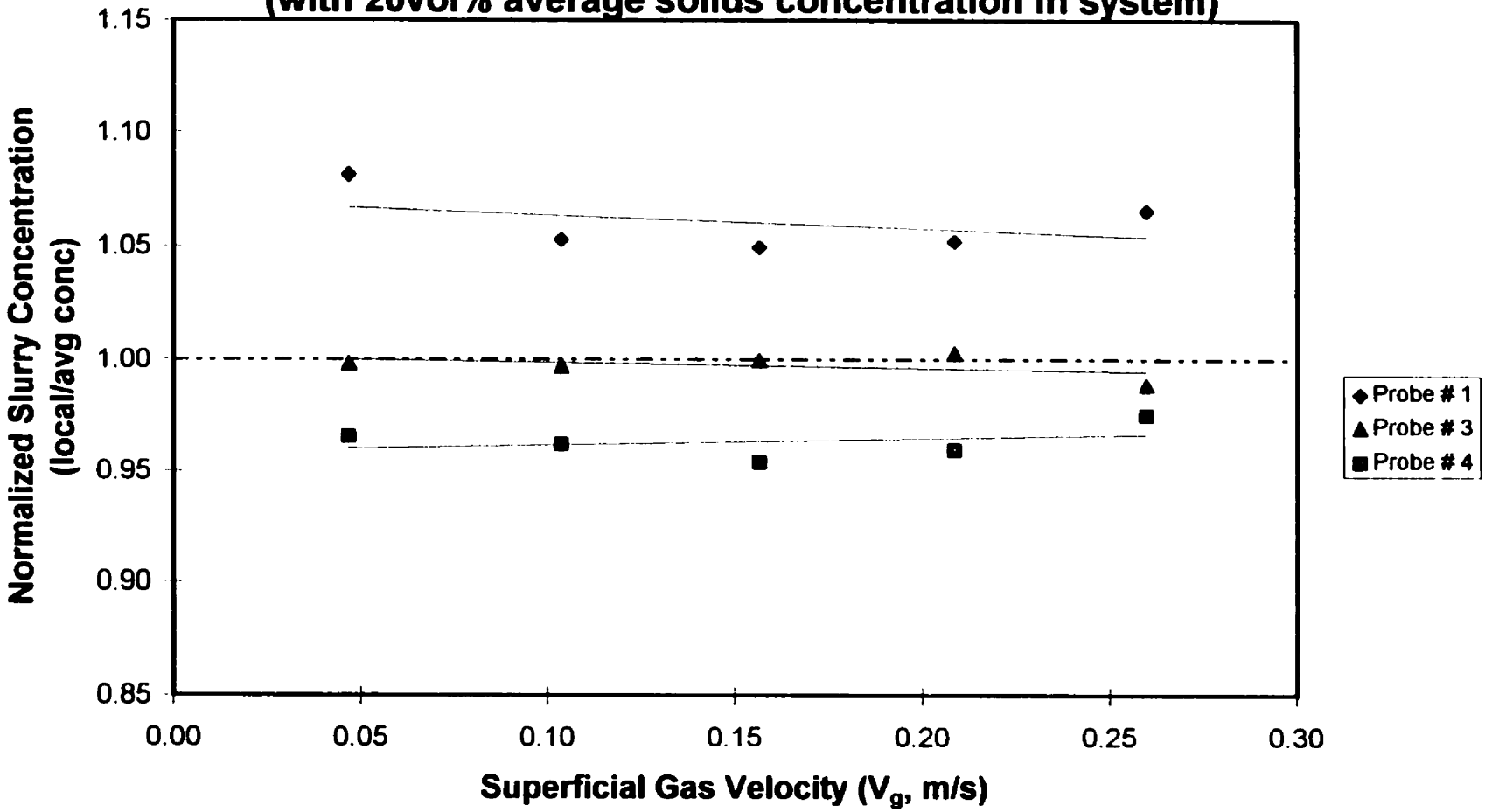

Fig. 4.17c Comparison of Axial Solids Concentration for Varying Probe Locations and Superficial Gas Velocities (with 30vol% average solids concentration in system)

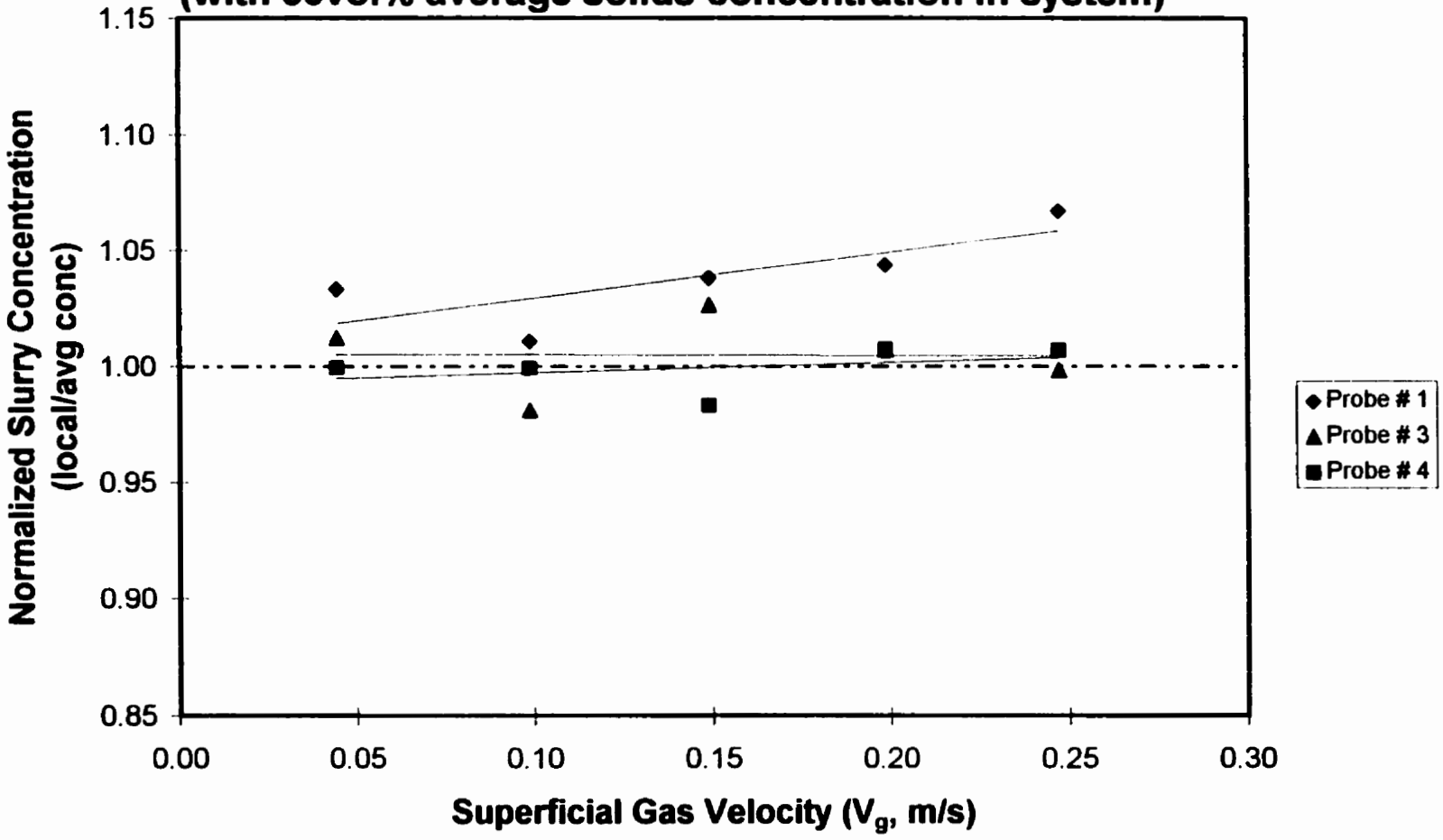

Fig. 4.17d Comparison of Axial Solids Concentration for Varying Probe Locations and Superficial Gas Velocities (with 40vol% average solids concentration in system)

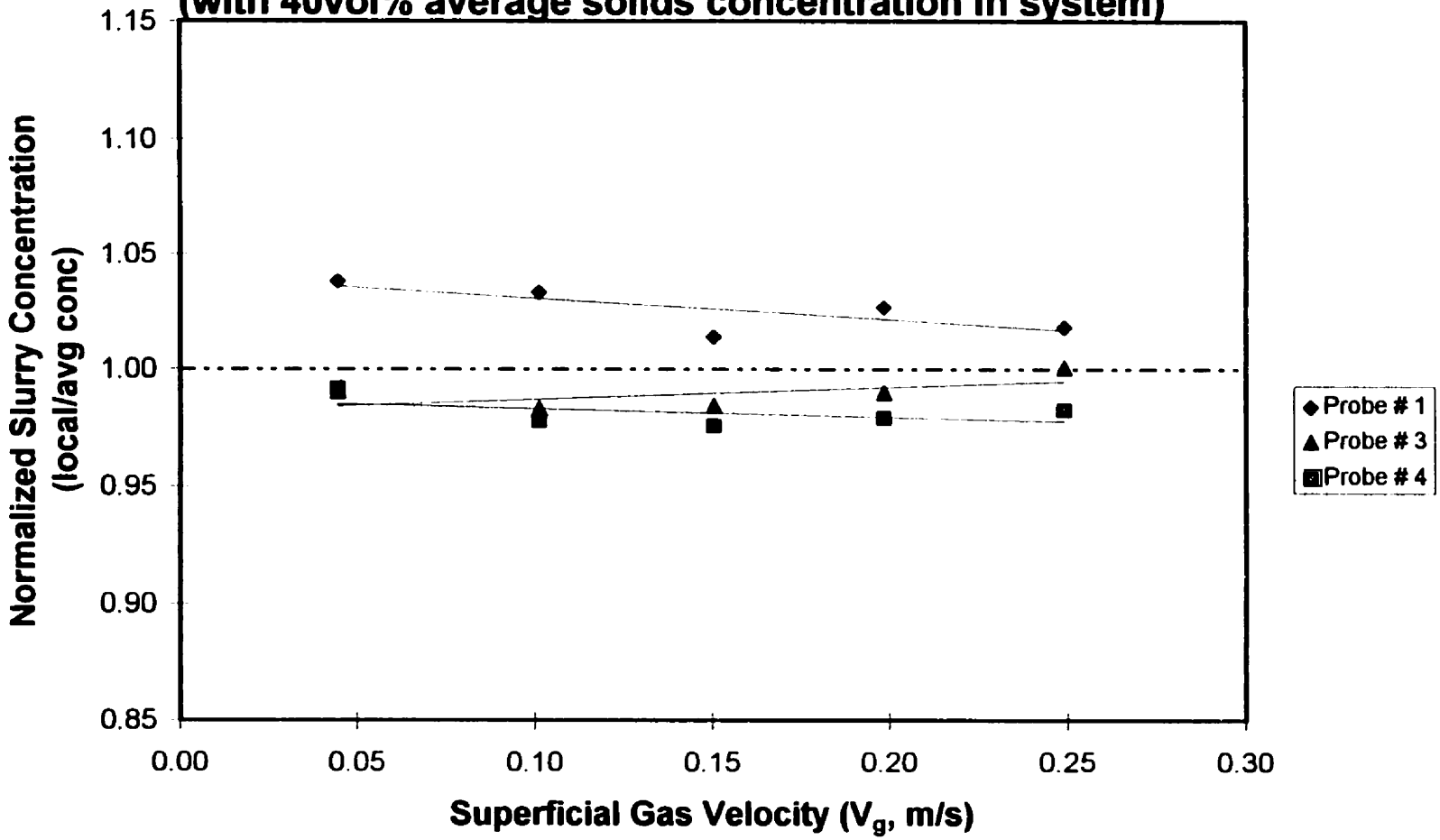

For the range of gas flowrates in this study ($0.05<V_g<0.25$m/s), the incoming power was calculated by the above correlation (Eq. 4.10) to range from 15 to 115 W. However, the corresponding potential energy required to keep particles in suspension was calculated to be only 0.06 to 0.20 W. Thus, there was an abundant amount of energy available to keep particles in suspension. Since the particles were already in suspension at lower gas velocities, the effect of increasing gas velocity was negligible.

The effect of varying average solids concentration (10vol% to 40vol%) can also be studied from Figs. 4.17a through 4.17d. In Fig. 4.17a, we observe that for a 10vol% solids system, the normalized concentration profile ranges from approximately 0.93 to 1.10. This represents a range of variation of 17% from the normalized slurry concentration. As the solids concentration is increased, this range decreases significantly. For the 20vol% solids system shown in Fig 4.17b, the range of variation is 11%. For the 30vol% and 40vol% solids systems, the range of variation is only 5%. Therefore, an increase in solids concentration leads to an overall flatter axial solids concentration profile. Similar observations were made by O'Dowd et al. (1987). This can be attributed to decrease in hindered settling velocity as slurry concentration increases. For higher slurry concentrations (30vol% and 40vol%), the change in hindered settling velocity was calculated to be minimal, therefore the profile remained the same.

4.1.3.1 Comparison of Axial Solids Distribution in Coalescing and Non-Coalescing Systems

Figs. 4.18a through 4.18d compare axial gas holdups for coalescing and non-coalescing systems. Several observations made for non-coalescing systems were similar to those made for the coalescing systems. As before, there is

Fig. 4.18a Comparison of Axial Solids Concentration for Coalescing and Non-Coalescing Systems (with 10vol% average solids concentration)

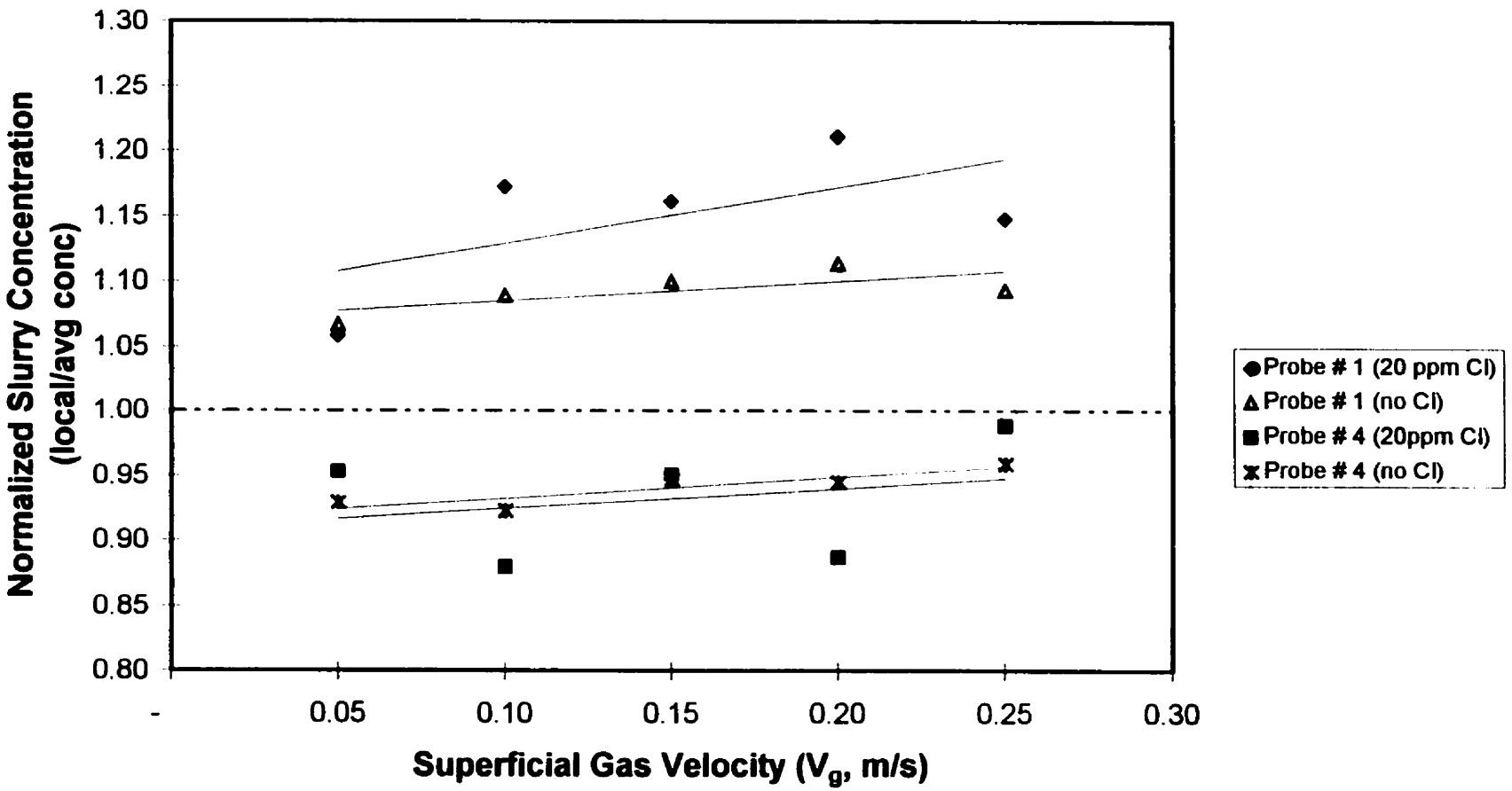

Fig. 4.18b Comparison of Axial Solids Concentration for Coalescing and Non-Coalescing Systems (with 20vol% average solids concentration)

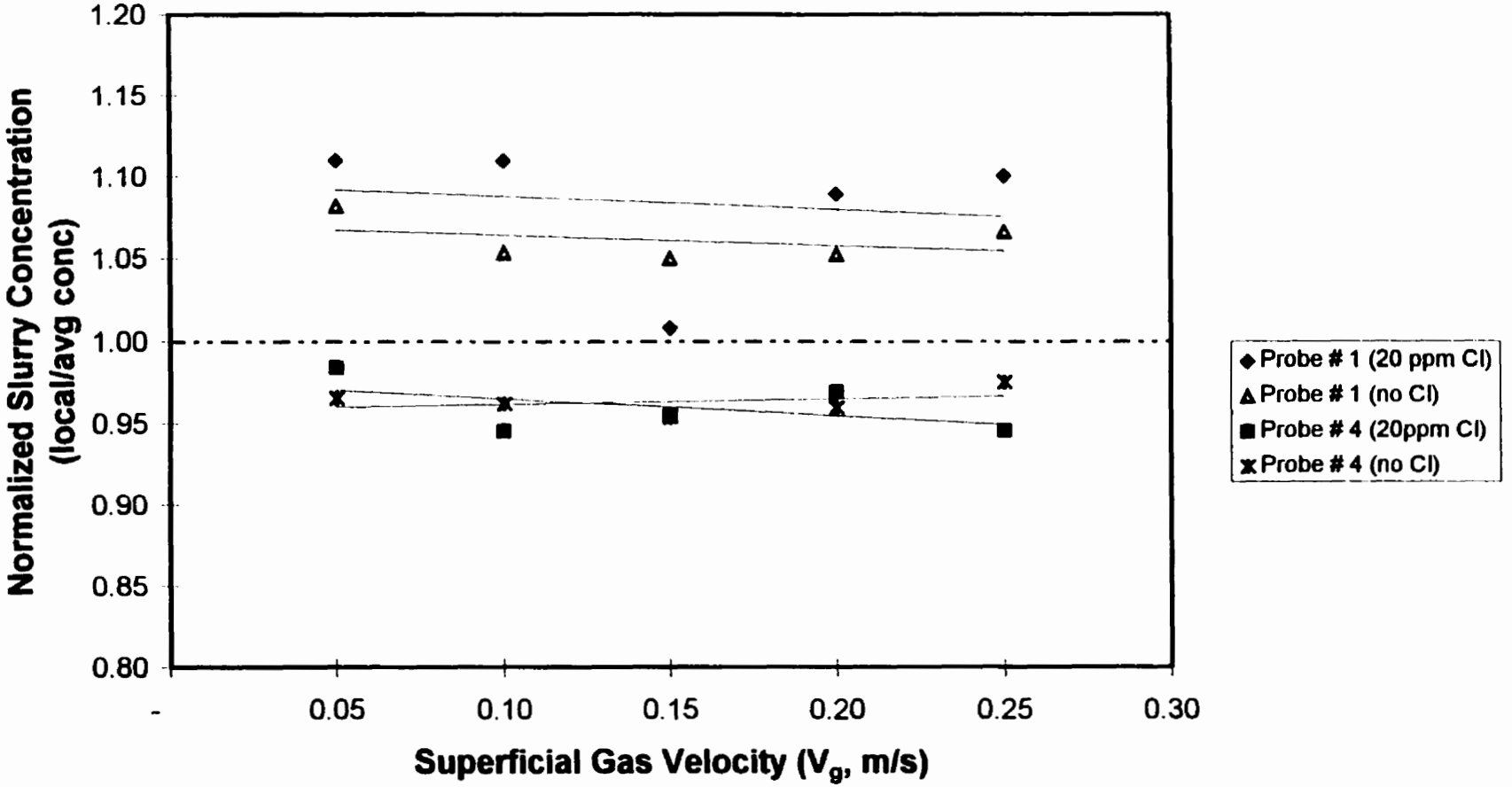

Fig. 4.18c Comparison of Axial Solids Concentration for Coalescing and Non-Coalescing Systems (with 30vol% average solids concentration)

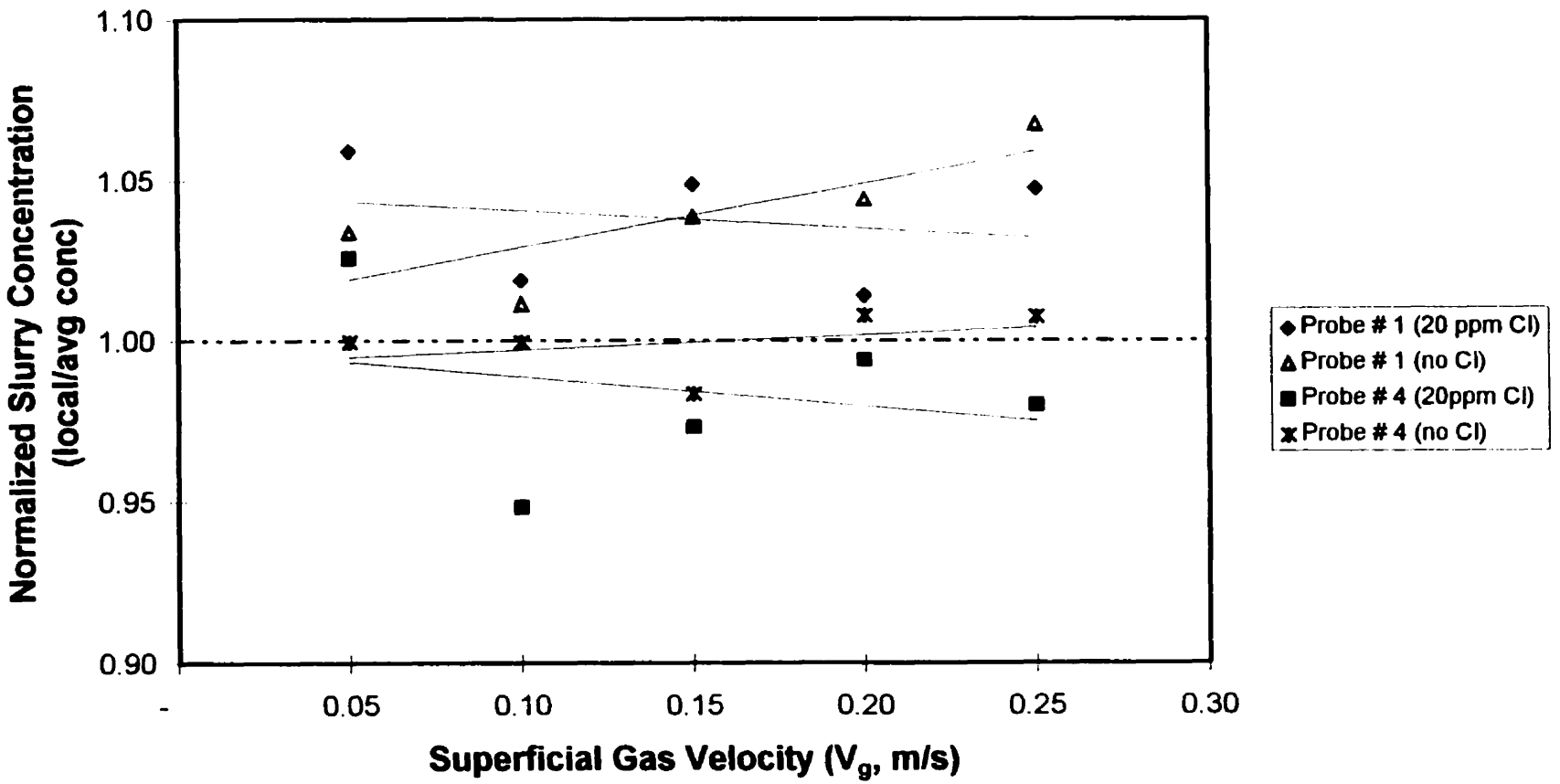

Fig. 4.18d Comparison of Axial Solids Concentration for Coalescing and Non-Coalescing Systems (with 40vol% average solids concentration)

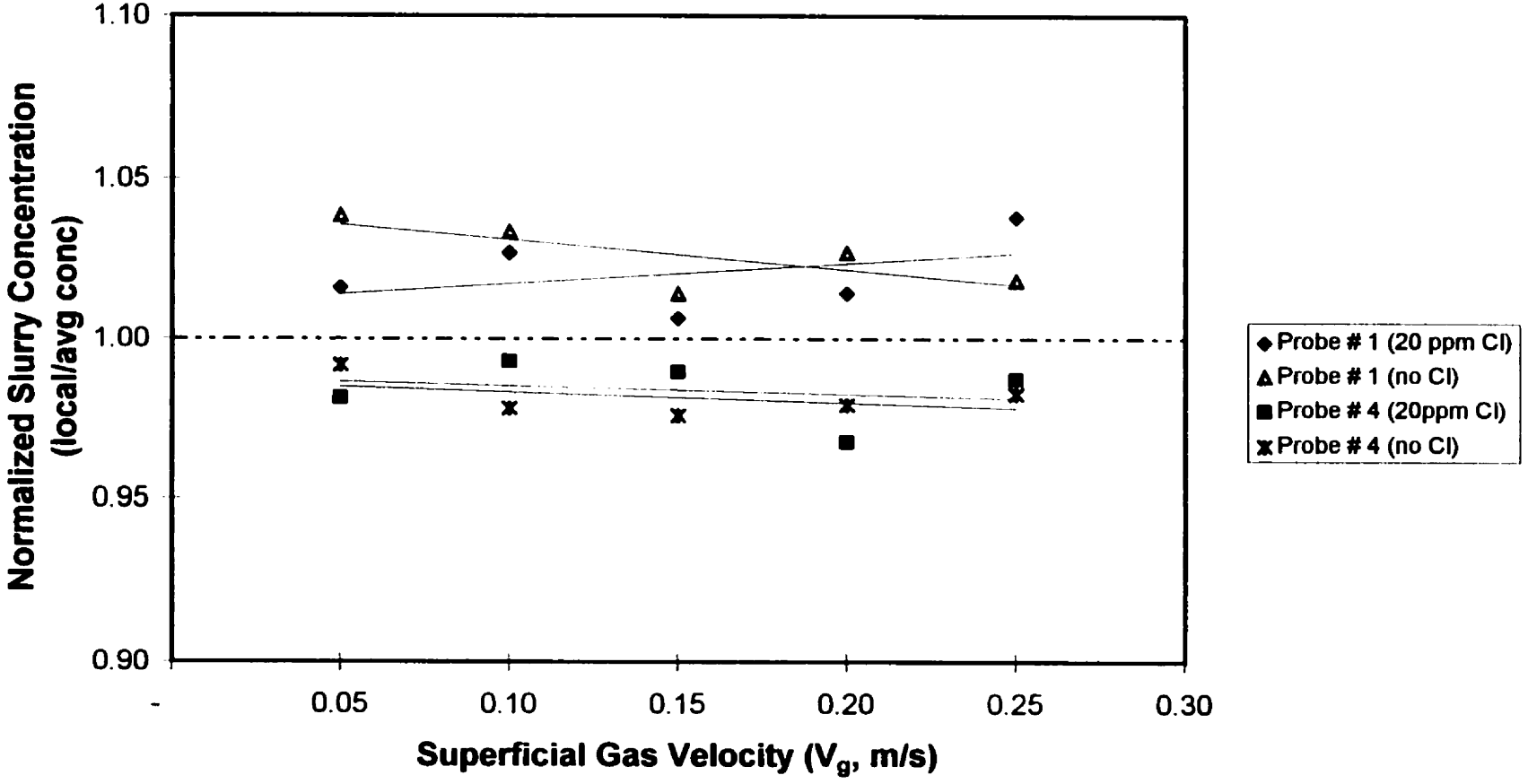

general tendency for the axial solids concentration to decrease as axial height increases (downward gradient). Also, the effects of superficial gas velocity on the axial slurry concentration profile were found to be generally small. We also observe an axial solids concentration gradient to be much greater for lower average solids concentration (10vol%) systems than for higher average solids (40vol%) systems. The range of variation of the normalized slurry concentration gradient is approximately 30% for a 10vol% solids system. This range gradually decreases to 5% for a 40vol% system. The increase in gradient for lower concentration systems can be related to the average bubble size in the column. For lower concentration systems, the number of small bubbles is significantly higher (as indicated by high gas holdups in Fig. 4.9). This diminishes the possibility of entrainment of solids in the bubble wake. As a result, the entrainment rate decreases and fewer particles are distributed up the column, leading to a much larger gradient along the column height. As the slurry concentration increases, bubble size increases and the influence of coalescence inhibitor decreases (Fig. 4.9). With larger bubbles, the entrainment rate increases and a flatter profile results.

The axial solids concentration profile for the non-coalescing system exhibits a larger range of variation (gradient) than the coalescing system. This is clearly seen in Fig 4.18a with a 10vol% solids system. The range of variation for the coalescing system is approximately 17% while that of the non-coalescing system is closer to 30%. For the 20vol% slurry system shown in Fig. 4.18b, there is still a significant difference in ranges (11% for coalescing system versus 18% for non-coalescing systems). For 30vol% and 40vol% solids systems, this difference becomes negligible. This may be explained in terms of average bubble sizes again. For lower concentration systems, the number of smaller bubbles is significantly higher in non-coalescing systems then in coalescing systems (as indicated by gas holdups seen in Fig. 4.10). This reduces the entrainment rate and fewer particles are distributed up the column, leading to a

larger gradient along the column height. As the slurry concentration increases, bubble size increases. The average bubble sizes for coalescing and non-coalescing become virtually equal (as described in section 4.1.2.1 in terms of gas holdups being equal at these higher concentrations). Thus, the entrainment rates are also equal leading to similar axial gradients.

4.1.3.2 Comparison of Axial Solids Concentration Profile with Literature Correlations and Models

Various literature correlations and models developed for predicting the axial solids concentration profile for slurry bubble columns have been reviewed in section 2.2.6.

The experimental data of this study were compared with correlations of Kato et al. (1972), Smith and Ruether (1985), O'Dowd et al. (1987), and Murray and Fan (1989). As discussed in section 2.2.6, the first three research groups used the Sedimentation-Dispersion model to develop their correlations, while Murray and Fan (1989) developed their correlation based on the bubble wake model. The summary of results are presented in Tables 4.6 and 4.7. Table 4.6 shows a direct comparison of experimental solids holdup profile values to correlated values, while Table 4.7 shows a comparison of differences relative to the average solids concentration in the column. It can clearly be seen that the differences relative to average solids concentration in the column are significantly larger. Also, comparisons of literature correlations with experimental solids holdup results for a gas velocity 0.15m/s and solids concentrations of 5vol% and 40vol% are presented in Figs. 4.19a through 4.19b. As done with the gas holdup analysis, errors bars are included on experimental data using a simple linear regression with 95% confidence intervals from the

Table 4.6 - Summary of comparison between experimental solids holdup profile and literature correlations (using a direct comparison of measured and calculated values)

Literature Correlation	Average Absolute Relative Error (%)	Average Relative Error (%)	Error Range (%)
Coalescing System			
Kato et al. (1972)	2.0%	0.2%	-7.6% to 5.9%
Smith & Ruether (1985)	2.0%	-0.6%	-6.8% to 5.8%
O'Dowd et al. (1987)	2.2%	1.2%	-5.9% to 8.6%
Murray & Fan (1989)	5.6%	5.1%	-4.8% to 23.1%
Non-coalescing System			
Kato et al. (1972)	2.6%	0.8%	-10.4% to 11.8%
Smith & Ruether (1985)	2.7%	-0.2%	-11.2% to 11.7%
O'Dowd et al. (1987)	2.9%	1.8%	-8.9% to 13.2%
Murray & Fan (1989)	6.2%	5.6%	-6.9% to 21.1%

Table 4.7 - Summary of comparison between experimental solids holdup profile values and literature correlations (comparison of differences relative to the average solids concentration in column)

Literature Correlation	Average Absolute Relative Error (%)	Average Relative Error (%)
Coalescing System		
Kato et al. (1972)	237%	-31%
Smith & Ruether (1985)	181%	-83%
O'Dowd et al. (1987)	367%	63%
Murray & Fan (1989)	1158%	132%
Non-coalescing System		
Kato et al. (1972)	520%	-321%
Smith & Ruether (1985)	720%	-422%
O'Dowd et al. (1987)	477%	-297%
Murray & Fan (1989)	1024%	203%

Fig. 4.19a Comparison of Various Literature Correlations with Experimental Results for Coalescing Systems (V_g=0.15m/s and avg slurry conc = 5vol%)

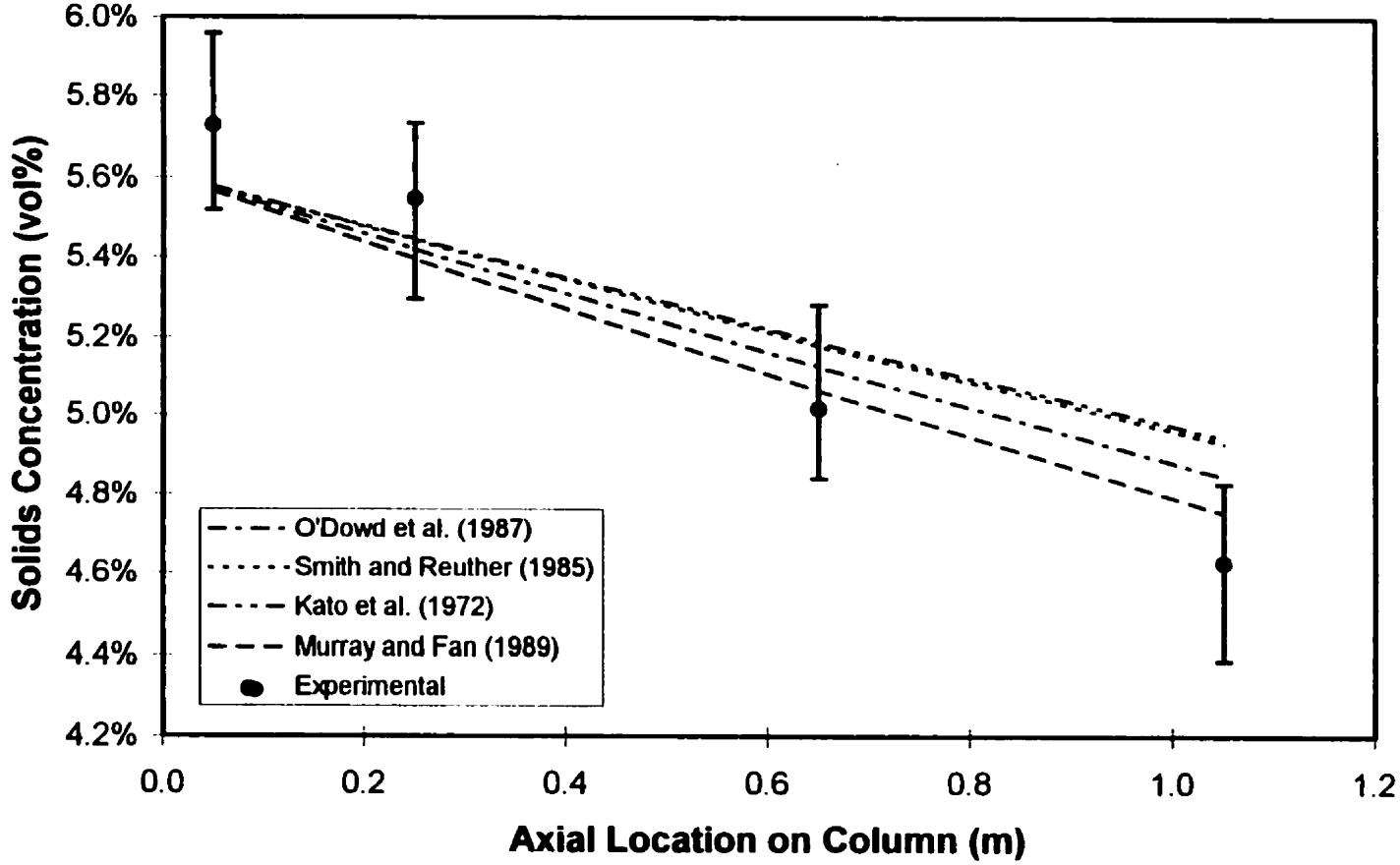

Fig. 4.19b Comparison of Various Literature Correlations with Experimental Results for Coalescing Systems (V_g=0.15m/s and avg slurry conc = 40vol%)

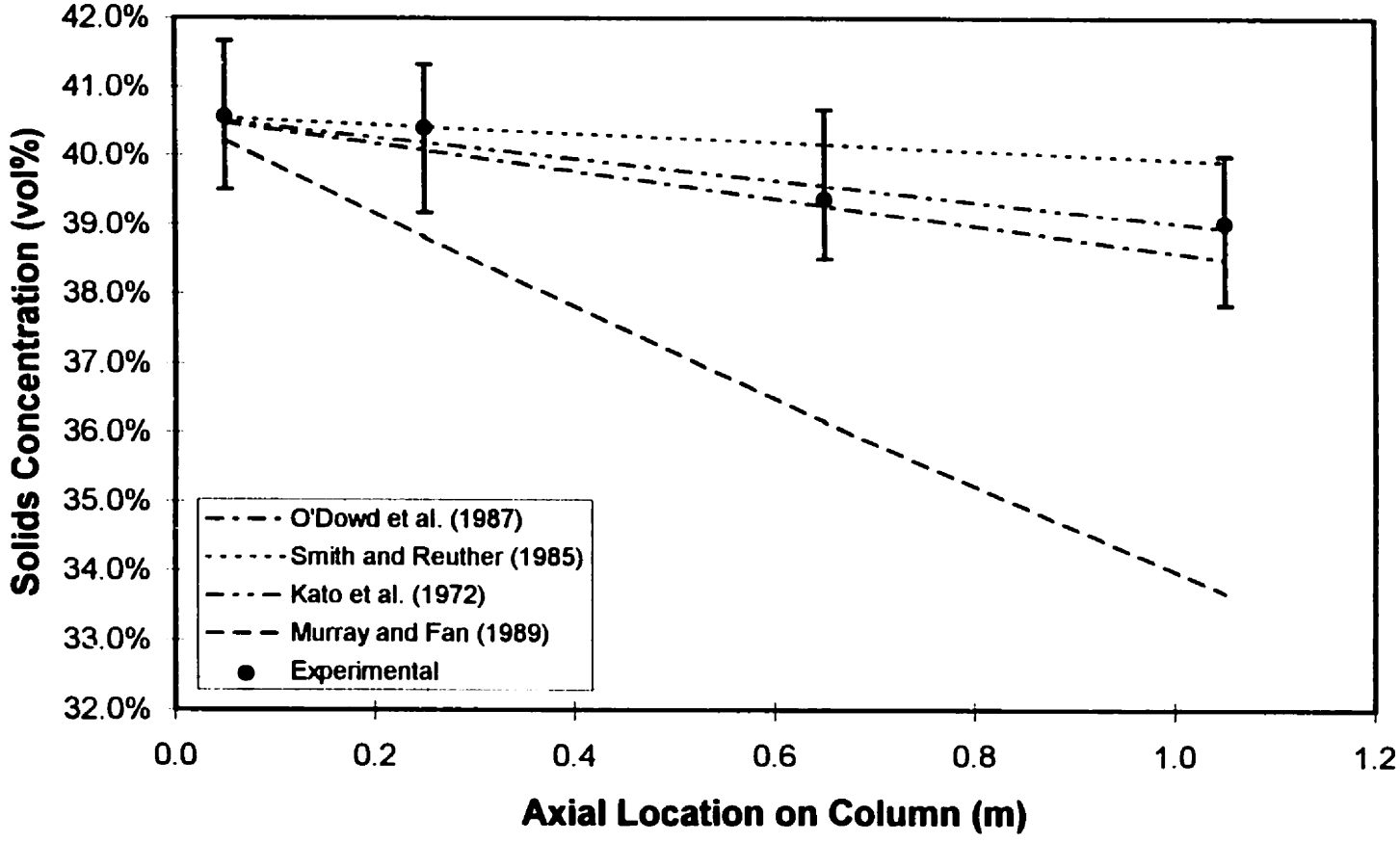

mean. Once again, the linear regression was found to fit the experimental data well (with $R^2 > 0.95$).

4.1.3.2.1 Sedimentation-Dispersion Model Derivation and Results

A review of the sedimentation dispersion model is presented in section 2.2.6.1. If we consider a horizontal cross sectional element of a slurry bubble column having a thickness Δz, a differential mass balance in the vertical z-direction with respect to solids particles gives:

Rate of accumulation within volume element	=	Rate of (mass in - mass out) due to dispersion	+	Rate of (mass in - mass out) due to convective flow of slurry	+	Rate of (mass in - mass out) due to the settling of solids

The effects of gravitational and buoyant forces are taken into account in the last term on the right hand side of this equation. By taking the limit as Δz approaches zero, the following equation is obtained:

$$\frac{\partial C_s}{\partial t} = -\frac{\partial n_d}{\partial z} - \frac{\partial}{\partial z}\left(\frac{V_{sl}}{1-\varepsilon_g} C_s\right) + \frac{\partial}{\partial z}\left(U_{st} C_s\right) \qquad (4.12)$$

where U_{st} is the generalized solids settling velocity, and the flux of solids particles due to dispersion, n_d, is given by

$$n_d = -E_s \frac{\partial C_s}{\partial z} \qquad (4.13)$$

Substituting Eq. 4.13 into Eq. 4.12 yields the sedimentation-dispersion model in its original form (Parulekar and Shah, 1980)

$$\frac{\partial C_s}{\partial t} = \frac{\partial}{\partial z}\left(E_s \frac{\partial C_s}{\partial z}\right) - \frac{\partial}{\partial z}\left(\frac{V_{sl}}{1-\varepsilon_g} - U_{st}\right) C_s \qquad (4.14)$$

The term U_{st} has been interpreted differently by many investigators in literature as previously mentioned. It has been interpreted as the particle terminal velocity or as the hindered settling velocity of a swarm of particles. Smith and Ruether (1985) defined U_{st} as the solids velocity relative to the liquid (slurry). The sedimentation-dispersion model in volume averaged form is therefore given by

$$\frac{\partial C_s}{\partial t} = \frac{\partial}{\partial z}\left[E_s \frac{\partial C_s}{\partial z} - \left(\frac{V_{sl}}{1-\varepsilon_g} - \psi_l U_p\right) C_s\right] \tag{4.15}$$

The volume averaged superficial slurry velocity (V_{sl}) can also be defined as

$$V_{sl} = V_p \varepsilon_s + V_l \varepsilon_l \tag{4.16}$$

In addition, the average solids convective velocity in the particulate fluidization phase (V_p) can be related to the slip velocity (V_s) between liquid and solids by

$$V_s = V_l - V_p \tag{4.17}$$

Therefore, from Eq. 4.16 and Eq. 4.17, V_p can then be related to the average solids-liquid relative velocity by

$$V_p = \frac{V_{sl}}{1-\varepsilon_g} - \psi_l U_p \tag{4.18}$$

where

$$\psi_l = \frac{\varepsilon_l}{\varepsilon_s + \varepsilon_l} \tag{4.19}$$

Substituting Eq. 4.18 in Eq. 4.15 yields the following

$$\frac{\partial C_s}{\partial t} = \frac{\partial}{\partial z}\left[E_s \frac{\partial C_s}{\partial z} - V_p C_s\right] \tag{4.20}$$

Equation 4.20 can be simplified for steady state operation. At steady state, the L.H.S. of the Eq. 4.20 is equal to zero. Also, under the assumption that the solids dispersion coefficient (E_s), gas holdup (ε_g), and solids settling velocity (U_{st})

are constant in the vertical direction of the column (Smith and Ruether, 1985), Eq. 4.20 may be written in the following simplified form

$$E_s \frac{d^2C_s}{dz^2} - V_p \frac{dC_s}{dz} = 0 \qquad (4.21)$$

Furthermore, for semi-batch operation with respect to liquid and solids, the solids convective velocity in Eq. 4.18 (with $V_{sl} = 0$) reduces to

$$V_p = -\psi_l U_p \qquad (4.22)$$

Thus the general solution of the second order differential equation in Eq. 4.21 is

$$C_s = F_1 + F_2 \exp\left(\frac{-\psi_l U_p}{E_s} z\right) \qquad (4.23)$$

The coefficients can then be evaluated using boundary conditions. The first boundary condition, as $z \rightarrow \infty$, $C_s = 0$ leads to $F_1 = 0$. The second boundary condition, as $z \rightarrow 0$, $C_s = C_{so}$ leading to $F_2 = C_{so}$. Thus for a batch slurry system, the correlation for axial solids distribution may be expressed as

$$C_s(z) = C_{so} \exp\left(\frac{V_p}{E_s} z\right) \qquad (4.24)$$

where C_{so} is the slurry concentration at the bottom of the column and can be correlated with (Smith and Ruether, 1985)

$$C_{so} = \frac{-C_s \psi_l U_p H_d}{E_s\left[\exp\left(-\psi_l U_p H_d / E_s\right) - 1\right]} \qquad (4.25)$$

In analyzing results for the coalescing system, it can be seen that all three sedimentation-dispersion correlations are able to predict the axial solids holdup distribution profile more closely than the bubble wake based model of Murray and Fan (1989). The correlations of both Kato et al. (1972) and Smith & Ruether (1985) give the best fit of the experimental data. Both correlations were found to

have average absolute relative errors of only 2.0%. The error ranges were also narrow. A graph of experimental solids holdup data versus predicted solids holdup data using the correlation of Kato et al. (1972) for coalescing systems is shown in Fig. 4.20. We observe that most predicted data fits within +/-5% from experimental data. Figs. 4.19a through 4.19d show a comparison of literature correlations with experimental data.

The results for the non-coalescing system were similar to those of the coalescing system with a slightly larger error range. All sedimentation-dispersion correlations were again adequately able to predict the solids holdup distribution with the correlations of Smith and Ruether (1985) and Kato et al. (1972) having the best fit of experimental data. Kato et al. (1972) were able to predict the holdup distribution with an average absolute relative error of 2.6%. Smith and Ruether (1985) were able to predict the solids holdup distribution with an average error of 2.7%. A graph of experimental data versus predicted solids holdup data for the Smith and Ruether (1985) correlation for non-coalescing systems is presented in Fig. 4.21. Again, we observe most predicted data to fit within +/-5% of experimental data.

The excellent fit of experimental data can be attributed the systems used by the researchers develop their correlations. The media used were similar to those of this study. Gas velocity ranges ($0.02<V_g<0.30$m/s) were also comparable. Fine glass beads were used in their study as well as ours. The only noticeable difference was the range of solids concentrations tested (0% to 12vol%).

Fig. 4.20 Comparison of Experimental Solids Holdup Data for all coalescing solids systems and probe locations with Predictions of Kato et al. (1972) Correlation

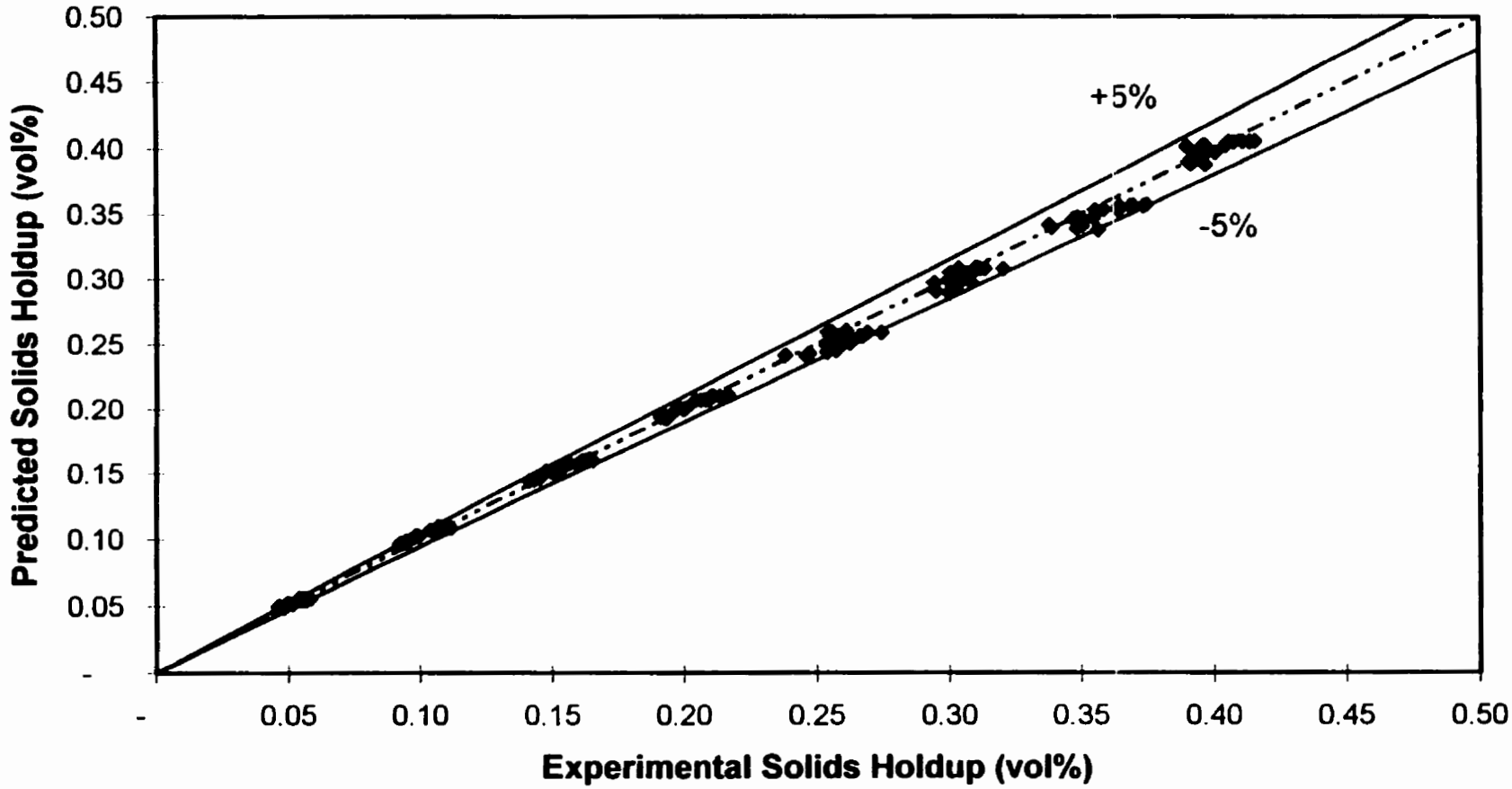

Fig. 4.21 Comparison of Experimental Solids Holdup for all non-coalescing solids systems and probe locations with Predictions of Smith & Ruether (1985) Correlation

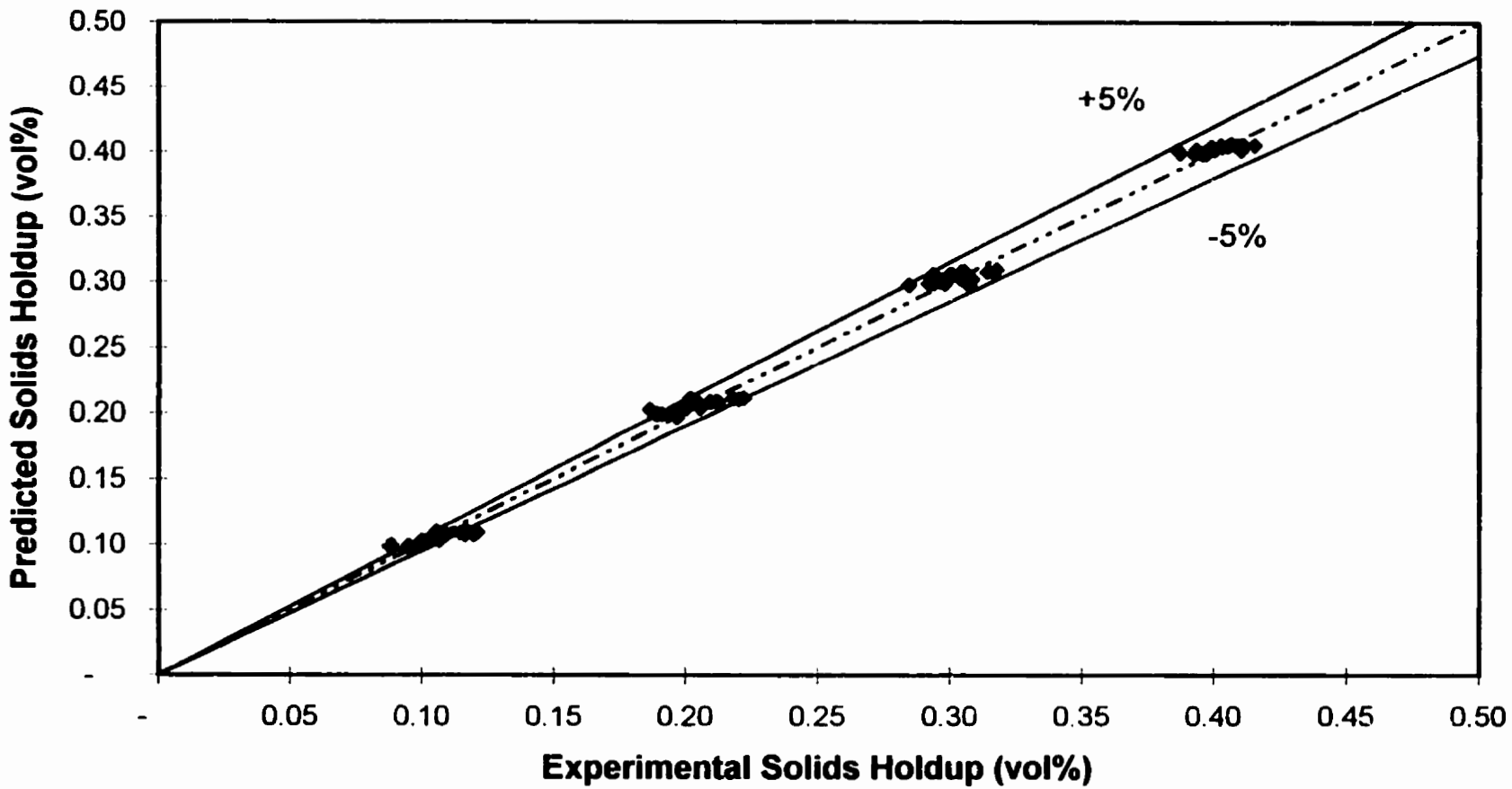

4.1.3.2.2 Holdup Distribution Based on Bubble Wake Phenomenon - Model Derivation and Results

A review of this model is presented in section 2.2.6.2. A mass balance around the wake phase associated with each bubble gives

Rate of accumulation of solids in the engagement phase = Solids entrainment into the engagement phase + Solid discharge from the engagement phase

which for continuous slurry operation yields

$$V_R \frac{\varepsilon_w}{N_b} \frac{d\varepsilon_{sw}}{dt} = V_e A_e \varepsilon_{sf} - V_d A_d \varepsilon_{sw} \qquad (4.26)$$

where V_R is the volume of the reactor, N_b is the total number of bubbles and ε_w is the total volume fraction of the wake region and is related to the overall gas holdup by

$$k = \varepsilon_w / \varepsilon_g \qquad (4.27)$$

The two terms on the right hand side of Eq. 4.26 account for solids entrainment into and de-entrainment out of the wake region. Under the assumption of no interaction between bubbles, the axial position of the bubble is related to the time coordinate by

$$U_b \, dt = dz \qquad (4.28)$$

At steady state, a differential mass balance of solids across the bed yields

$$U_b \varepsilon_w \frac{d\varepsilon_{sw}}{dz} + \varepsilon_f \frac{d\left(V_p \varepsilon_{sf}\right)}{dz} = 0 \qquad (4.29)$$

where V_p is the velocity of solids in the particulate fluidization phase and can be related to the slip velocity (V_s) by

$$V_p = V_{lf} - V_s \qquad (4.30)$$

By integrating Eq. 4.29 and substituting in boundary conditions, the following equation results

$$U_b \varepsilon_w \varepsilon_{sw} + V_p \varepsilon_{sf} \varepsilon_f = V_{sl} \varepsilon_s^f \tag{4.31}$$

The ratio of solids holdup in the wake phase to the solids concentration in the particulate fluidization phase can be represented by the fraction

$$x = \varepsilon_{sw} / \varepsilon_{sf} \tag{4.32}$$

It can be considered that x and k are only weak functions of axial position and may be assumed constant with respect to axial position (El-Temtamy and Epstein, 1980). Thus, differentiating Eq. 4.32 with respect to z and substituting in Eq. 4.28 yields

$$\frac{d\varepsilon_{sw}}{dt} = U_b x \frac{d\varepsilon_{sf}}{dz} \tag{4.33}$$

Substituting Eqs. 4.31, 4.32 and 4.33 into Eq. 4.26 yields

$$E_s \frac{d\varepsilon_{sf}}{dz} = V_p \varepsilon_{sf} + P' V_{sl} \varepsilon_s^f \tag{4.34}$$

where

$$E_s = \frac{V_R U_b \varepsilon_w x}{N_b \left[\frac{V_e A_e}{V_p} + \frac{V_d A_d \varepsilon_f}{U_b \varepsilon_w} \right]} \tag{4.35}$$

and

$$P' = \frac{V_d A_d}{U_b \varepsilon_w \left[\frac{V_e A_e}{V_p} + \frac{V_d A_d \varepsilon_f}{U_b \varepsilon_w} \right]} \tag{4.36}$$

The solids concentrations, ε_{sf} and ε_s are interrelated by the following mass balance

$$\varepsilon_{sf} = \frac{\varepsilon_s}{xk\varepsilon_g + \left(1 - \varepsilon_g - k\varepsilon_g\right)} \tag{4.37}$$

Now, considering ε_g to be independent of z (Smith and Ruether, 1985), and substituting Eq. 4.37 into Eq. 4.34, we get

$$E_s \frac{dC_s}{dz} = V_p C_s + P' V_{sl} C_s^f \left[xk\varepsilon_g + (1 - \varepsilon_g - k\varepsilon_g)\right] \tag{4.38}$$

Finally, by integrating and setting boundary conditions, the correlation for a batch slurry system simplifies to

$$C_s(z) = C_{so} \exp\left(\frac{V_p}{E_s} z\right) \tag{4.39}$$

As shown in Table 4.6, for coalescing systems the correlation of Murray and Fan (1989) predicted the axial solids holdup distribution with an average absolute relative error of 5.6%. A plot of experimental data versus predicted values of Murray and Fan (1989) for coalescing systems is presented in Fig. 4.22. Most of the predicted values for solids holdup are observed to be less than experimental values. Furthermore, we observe the error increases with increasing solids concentration and axial height, as seen in Figs. 4.19b. The error was calculated to be 2.9% for systems with 20vol% solids or less, and 8.3% for systems with greater than 20vol% solids. This indicates that there is a systematic problem with this model to estimate axial solids holdup. The correlation for solids dispersion coefficient was obtained through regression of experimental data by Murray and Fan (1989). However, their system consisted of fine particles of low slurry concentrations (0% to 2.5vol%). It has been observed by several researchers (Kelkar et al., 1984; Sada et al., 1986b; Sauer and Hempel, 1987; and Wolff et al., 1990) that a slurry bubble column with fine particles in suspension with low concentrations will operate similar to a solids-free system. As we have already discussed in section 4.1.3.1, due to reduced entrainment

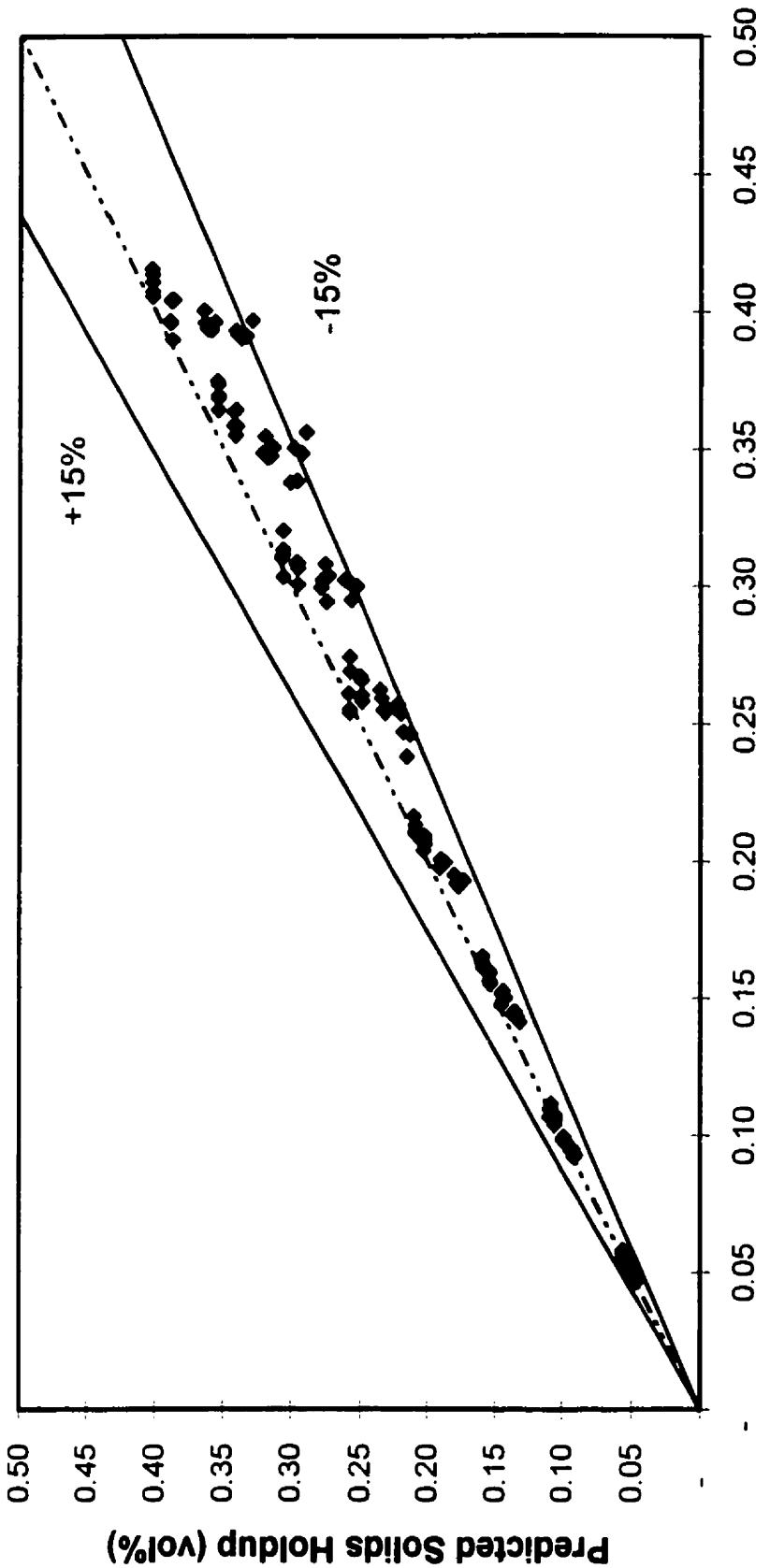

Fig. 4.22 Comparison of Experimental Solids Holdup Data for all coalescing solids systems and probe locations with Predictions of Murray and Fan (1989) Correlation

rates, smaller bubbles will lead to a larger axial solids gradients. The solids dispersion coefficient should have been correlated over a wider range of slurry concentrations by the researchers. Results for the non-coalescing system were similar.

4.1.4 Radial Solids Holdup Profiles

Radial slurry sampling was also performed for Probes # 2, 4 and 5. Samples were taken at five different locations (-R, -R/2, 0, +R/2, and +R) with R representing the radius of the column and '0' representing the center of the column. The effects of average slurry concentration, superficial gas velocity and probe location on radial concentration profiles were all studied for coalescing systems only.

Figures 4.23a through 4.23f show the effect of slurry concentration and superficial gas velocity on the radial concentration profile for different probe locations. For most cases, the radial solids holdup has a parabolic profile with a maximum concentration at the walls and a minimum at the center of the column, as observed by Pandit and Joshi (1984). This profile is the exact opposite of the radial gas holdup profiles that have been observed by researchers for coalescing bubble regime (Nottenkaemper et al., 1983; Wachi et al., 1987). This variation is expected if the liquid velocity patterns in the bubble column are studied. At the center of the column, liquid moves up the column at high velocities due to large gas bubbles. At the column walls, liquid recirculates back down the column at much lower velocities. The center of the column is therefore a much more turbulent region than the walls. In turn, solids particles will migrate from the column center to the column walls where there is less turbulence. This results in the parabolic profile describe above.

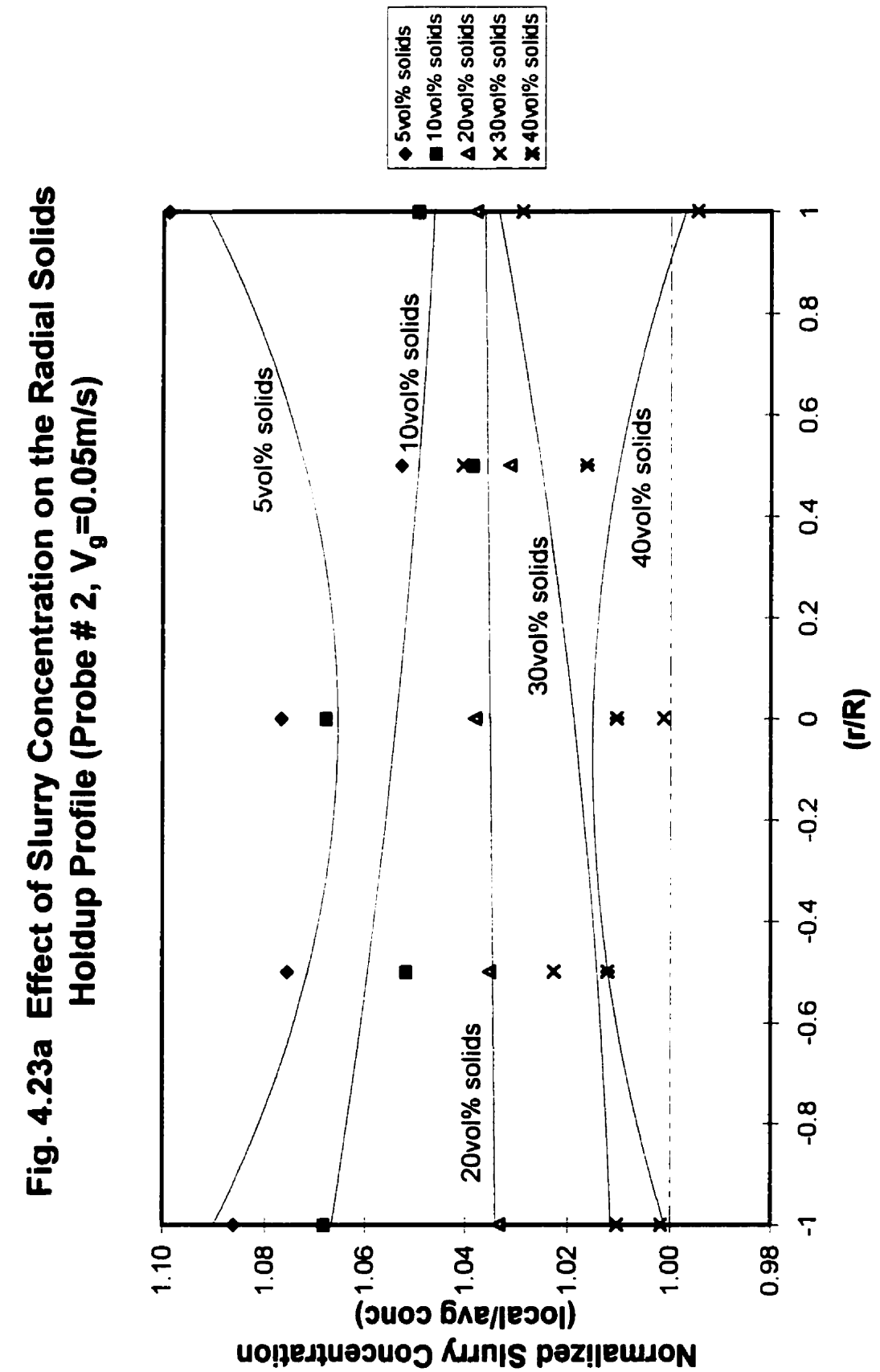
Fig. 4.23a Effect of Slurry Concentration on the Radial Solids Holdup Profile (Probe # 2, V_g=0.05m/s)
5vol% solids
10vol% solids
20vol% solids
30vol% solids
40vol% solids
Normalized Slurry Concentration (local/avg conc)
(r/R)
1.10
1.08
1.06
1.04
1.02
1.00
0.98
-1
-0.8
-0.6
-0.4
-0.2
0
0.2
0.4
0.6
0.8
1

Fig. 4.23b Effect of Slurry Concentration on the Radial Solids Holdup Profile (Probe # 2, V_g=0.15m/s)

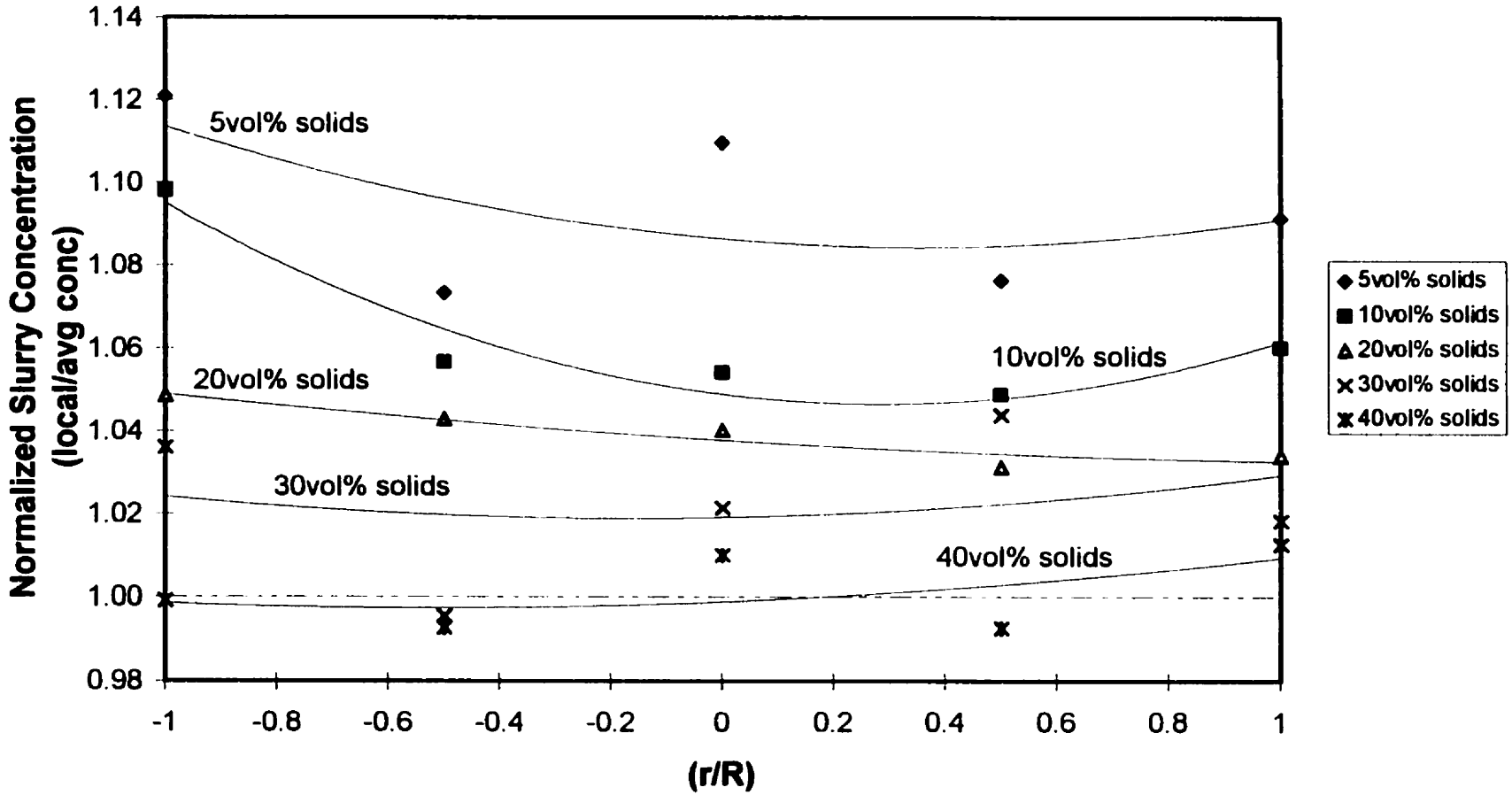

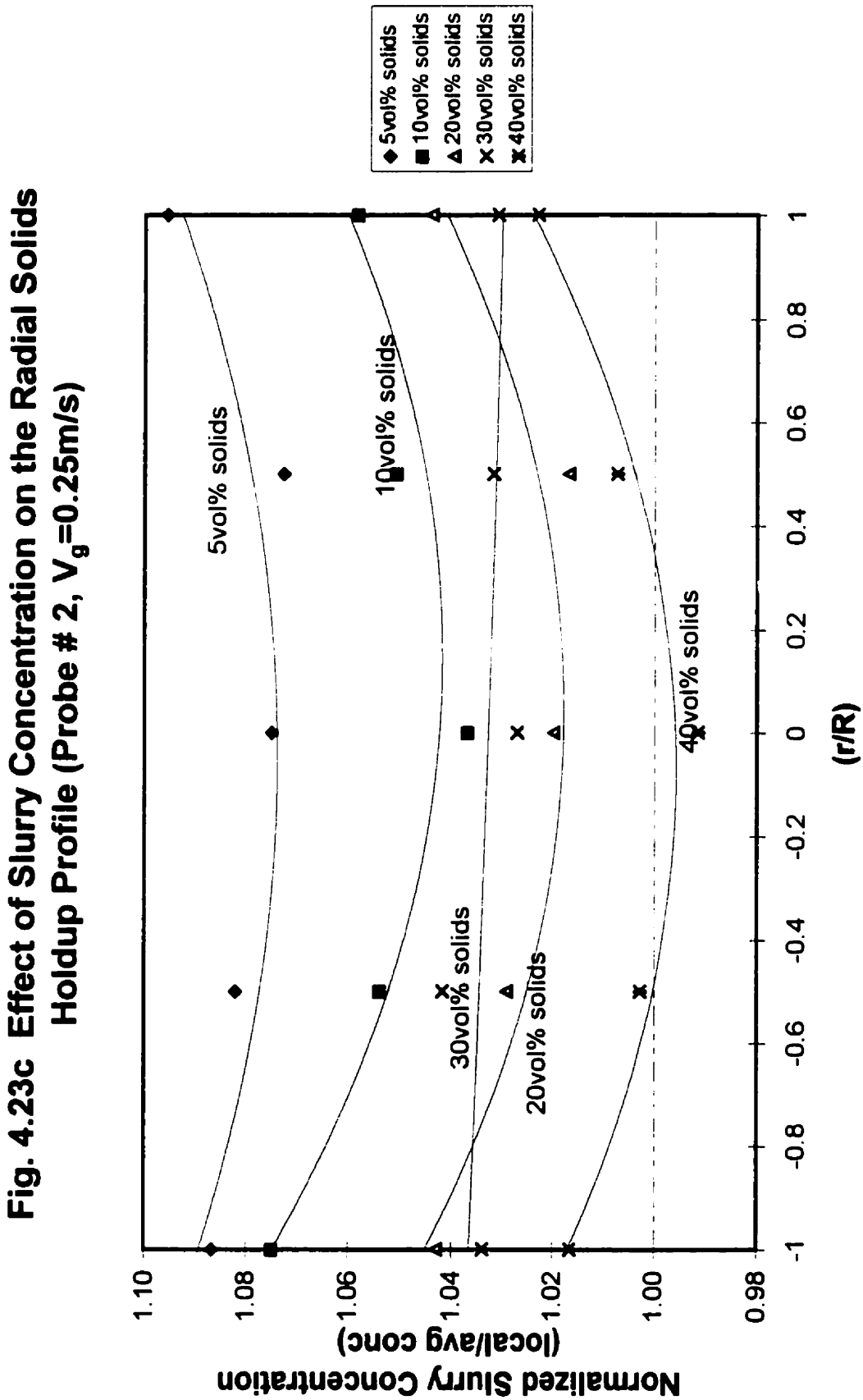

Fig. 4.23c Effect of Slurry Concentration on the Radial Solids Holdup Profile (Probe # 2, V_g=0.25m/s)

Fig. 4.23d Effect of Slurry Concentration on the Radial Solids Holdup Profile (Probe # 5, V_g=0.05m/s)

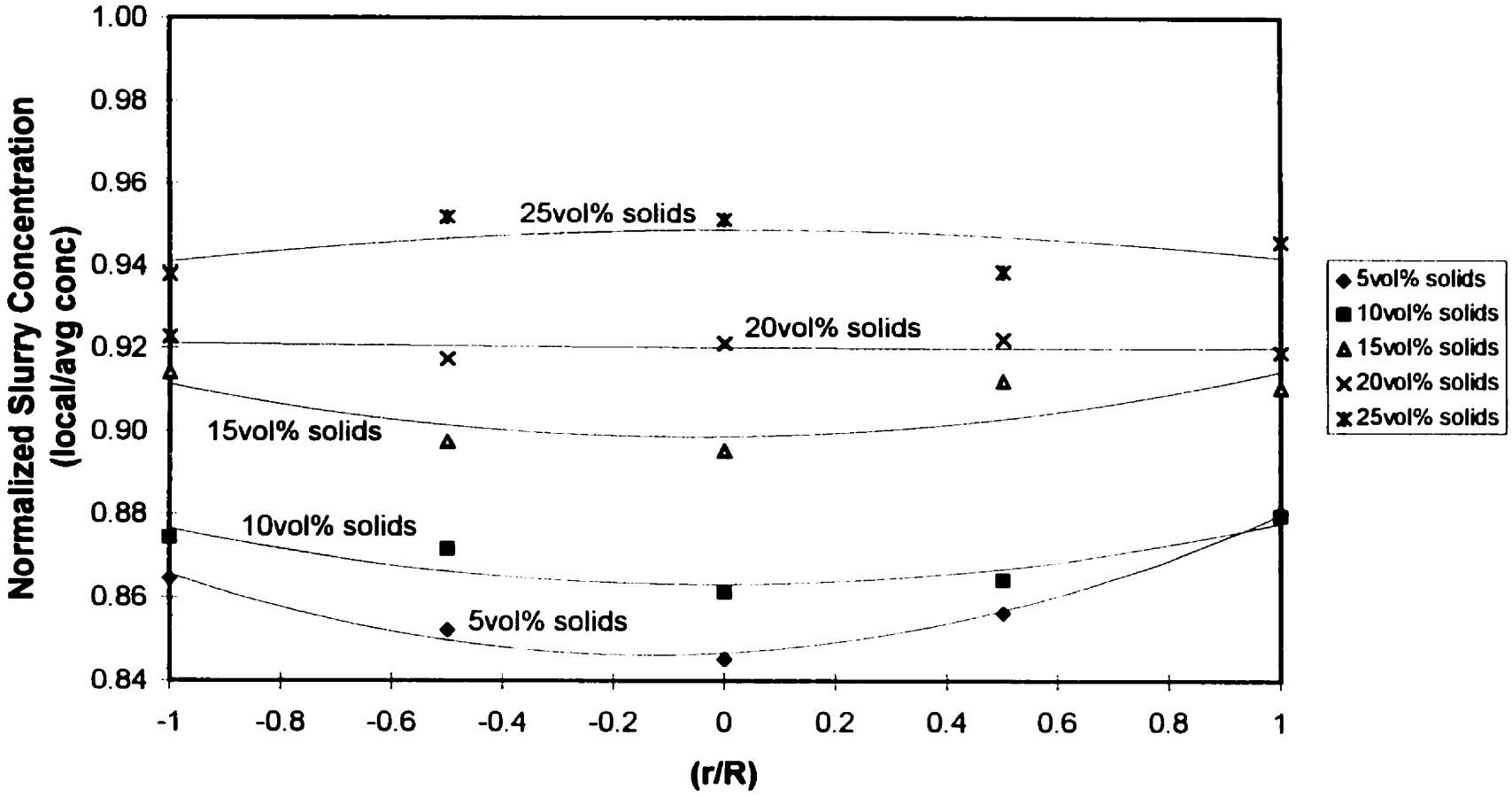

Fig. 4.23e Effect of Slurry Concentration on the Radial Solids Holdup Profile (Probe # 5, V_g=0.15m/s)

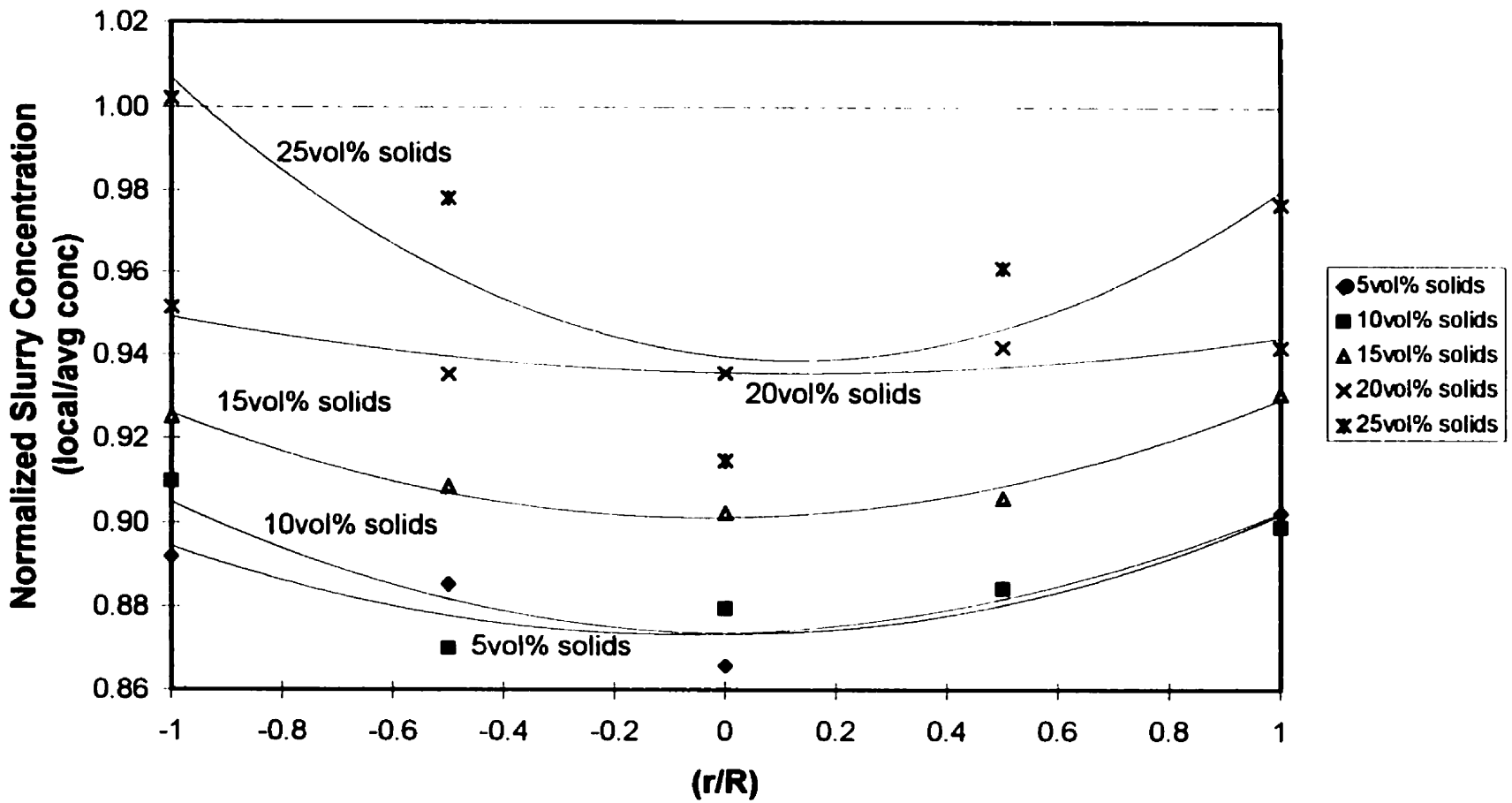

Fig. 4.23f Effect of Slurry Concentration on the Radial Solids Holdup Profile (Probe # 5, V_g=0.25m/s)

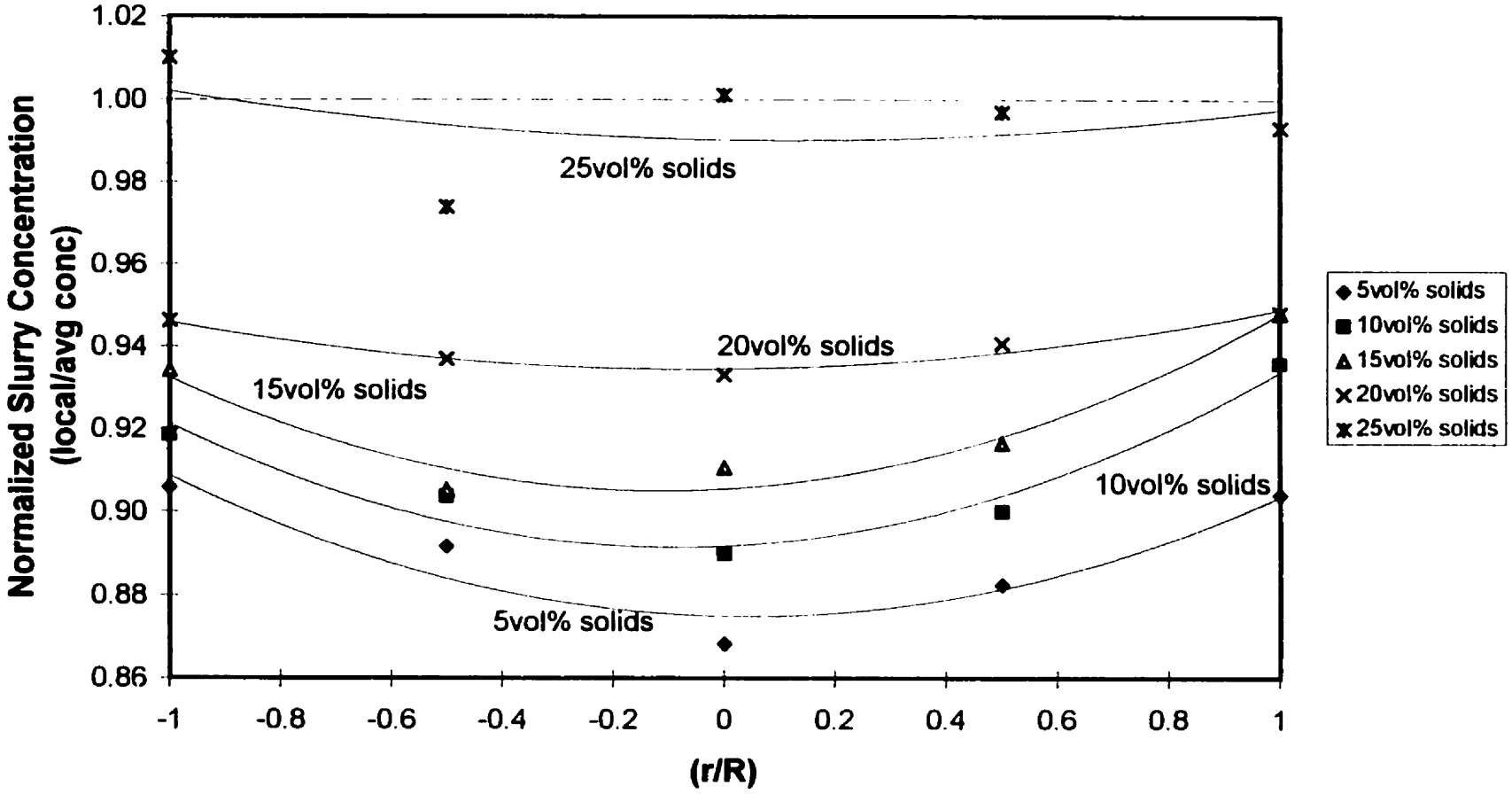

An increase in slurry concentration (to about 20vol% solids) at lower gas velocities was found to make the radial solids concentration profile flatter as also observed by Pandit and Joshi (1984). However, a reversal of the profile is also observed for higher concentrations (>25vol% solids). This can be observed in Figs. 4.23a and 4.23d. This can also be related to the mixing patterns in the column. At higher solids concentration with low velocities, there is significantly less turbulence in the column, therefore the movement of solids from column center to the wall will be reduced, leading to a flatter profile. Since gas and liquid carry the solids up the center of the column, we would expect the profile to reverse at very high solids concentrations, where very little turbulence is encountered. The reversal in profile was not observed by Pandit and Joshi (1984) because their research was performed on slurry systems only up to 15vol% solids. For higher gas velocities (0.15m/s and greater), the flattening and reversal was not observed due to higher turbulence. Thus, superficial gas velocity has no real effect on low solids concentration systems (<20vol%), but a decrease in gas velocity leads to a flattening and reversal of the solids holdup profile for higher solids systems (>20vol%).

4.2 Issues of Practical Significance

During the experimental runs, a few important problems of practical significance were identified, including; 1) formation of solids plugs for high concentration systems, 2) pitting of the column base plate, and 3) plugging of the sparger and erosion of its orifices.

4.2.1 Solids Plug Formation

It was observed that above slurry concentrations of 15vol%, solids plugs were formed during the startup operation of solids dispersion (refer to Fig. 4.24). As discussed in section 3.3, these plugs moved up the column. The plug formation can cause a number of problems which include; 1) high pressure buildup near the column bottom and 2) damage of internals and recirculating pumps.

The problem of plug formation in three phase gas-liquid-solid systems has not been reported in the literature. However, the problem of plug formation is well documented in dense phase pneumatic conveying (gas-solid) systems (Zenz, 1949; Zenz and Othmer, 1960; Leung, 1980; Rizk, 1983). The solids particles form a plug as the gas velocity is reduced for fixed solid flow with transition occurring from dilute phase transport to dense-phase (Leung, 1980). Plug formation in gas-solid systems has been related to the angle of internal friction (α) for granular solids (Zenz and Othmer, 1960). It is a measure of the angle below which solids will not pour from a bin or a container as shown in Fig. 4.25. The angle of internal friction can be related to the angle of repose (θ):

$$\alpha = \theta + 27^{o} \qquad (4.40)$$

For the free flowing glass beads, the angle of repose is approximately 26° (Zenz and Othmer, 1960) which corresponds to an angle of internal friction of 53°. The critical length (L) at which plugs or slugs will begin to form in a cylindrical tube can be calculated using:

$$L = D_c \tan(\alpha) \qquad (4.41)$$

The above equation gives a theoretical critical length for a 15cm diameter column to be 20cm for gas-solids system.

Fig. 4.24 - Diagram of Plug Formation

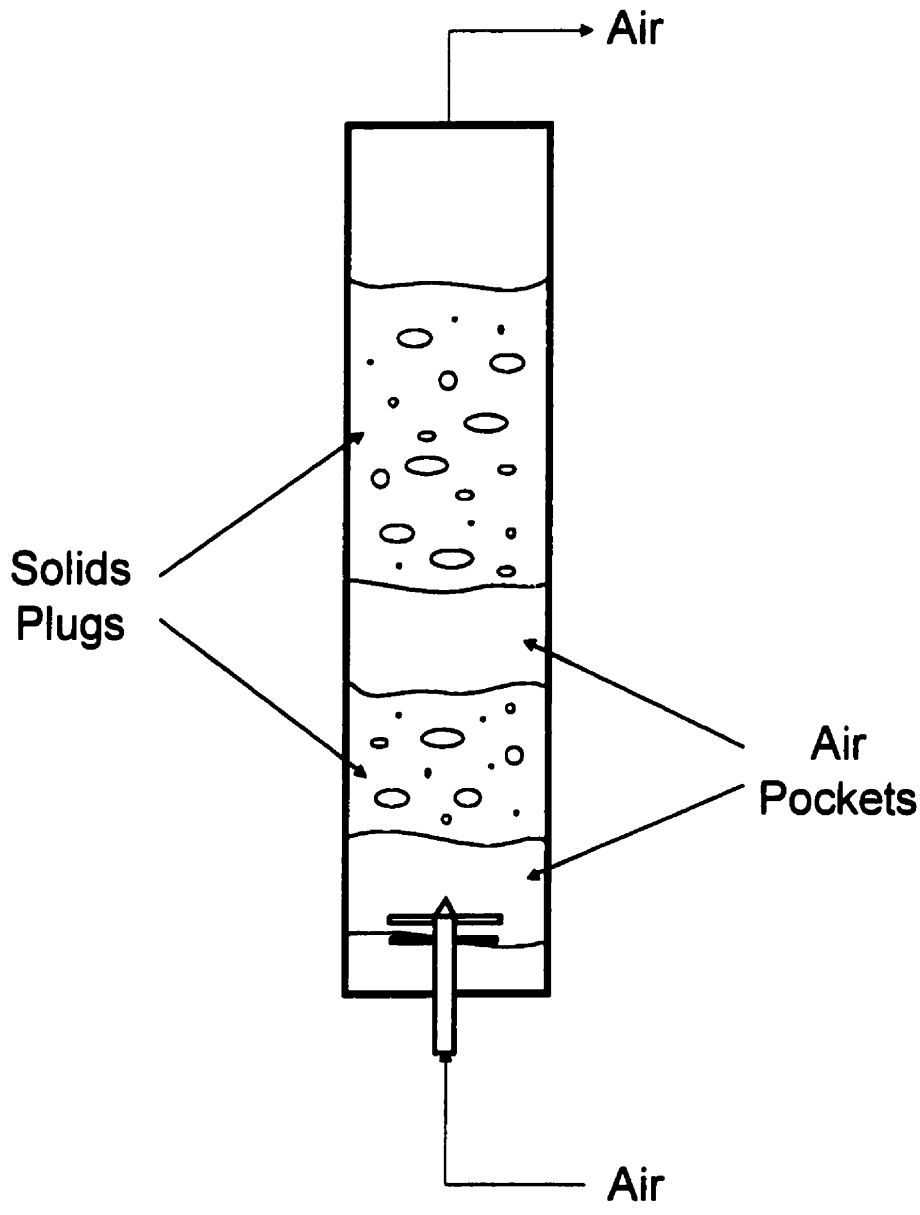

Fig. 4.25 - Angle of Internal Friction

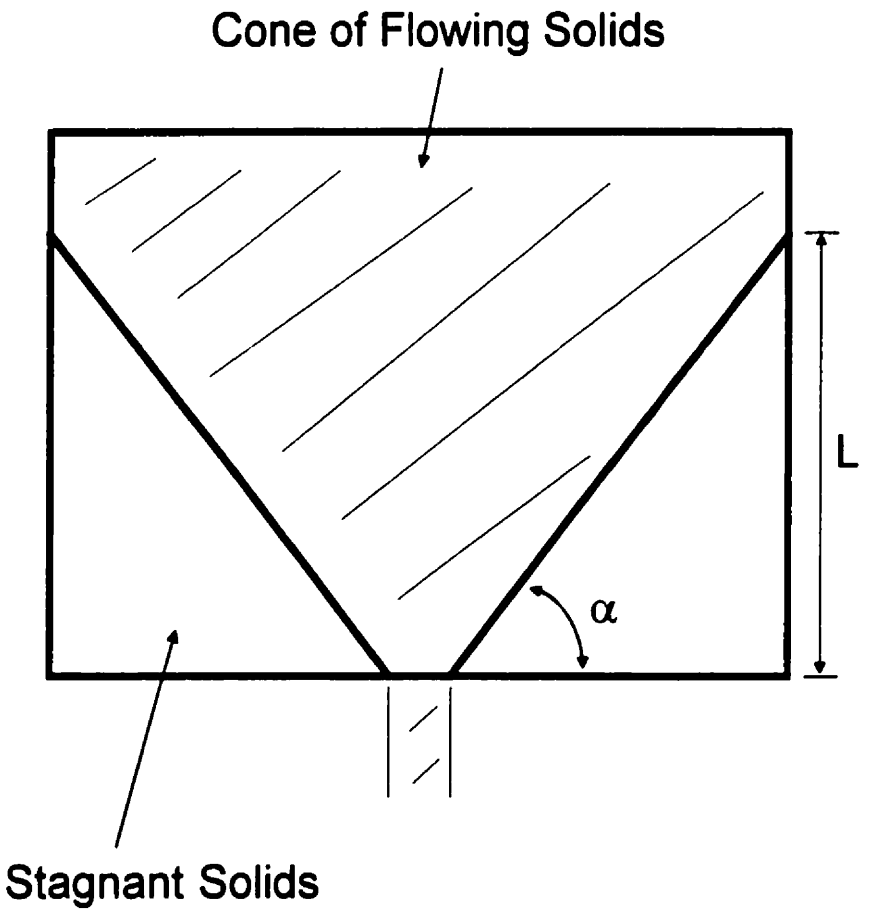

The plug formation in the three phase system of this study was observed at the settled solids height of 45cm which corresponds to a slurry concentration of 20vol%. In fact, plug formation may have started between slurry concentrations of 15vol% and 20vol% (or settled bed heights of about 38cm to 45cm) since the next lower slurry concentration used was 15vol%. For conservative estimates, the plug formation was assumed to start at a slurry concentration of 15vol%. The initial settled solids height for this concentration was measured at 36.5cm above the sparger. Using Eq. 4.41, this corresponds to an angle of internal friction of 68°, which is significantly higher that the value for gas-solids systems. It should be noted that there is greater particle-fluid friction in the presence of liquid (higher cohesiveness) than with gas which would increase resistance to flow of solids. The maximum height of settled solids above the sparger for any given diameter column can be calculated using the calculated internal angle of friction. Further investigations are, however, required to cover a wider range of solids characteristics.

4.2.2 Pitting of the Column Base Plate

During inspection of column internals after a series of experiments, significant pitting was observed on the column base plate (as shown in Fig. 4.26). The pitting was primarily attributed to jet impingement on the base plate. As detailed in Appendix B, the gas distributor orifices were facing vertically downwards and were set at 1.5cm above the base plate for most of the experiments. This low height was initially selected to minimize the formation of defluidized zones near the distributor. However, the jet impact can be reduced by raising the sparger height above the column base. In order to investigate the problem further, it was decided to conduct experiments with varying sparger heights. A new gas distributor (see Fig. 3.3) was designed which could be moved up and down to vary the orifice distance from base plate from 1.5cm to 45cm. Measurements

Fig. 4.26 - Location of Base Plate Pitting Marks

(diameter,depth)

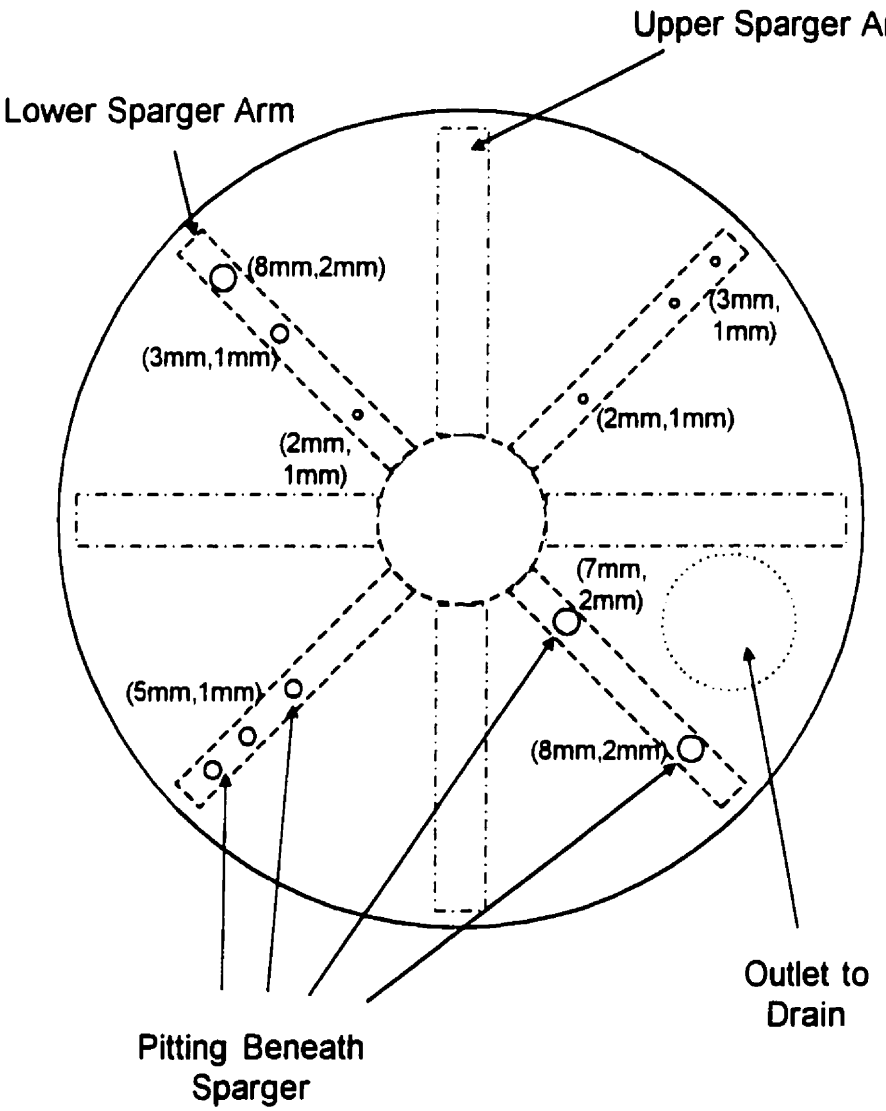

were conducted for solids dispersion and gas holdup. All experiments were performed with a 15vol% solids system which had an initial settled bed height of 38cm above the base plate. Local slurry samples were taken at Probes # 2-5 (whenever possible).

For a quick approximation of the fraction of dispersed solids, the local dispersed slurry concentration (measured at Probe # 4) was plotted for varying superficial gas velocities and sparger heights, and results are presented in Fig. 4.27. However, it should be noted that these are local (and not average) measurements which can vary along the column height (as discussed in section 4.1.3). To determine the average dispersed slurry concentration, the ratio of dispersed solids to initial settled solids was calculated. During previous experimental runs, settled static solids heights were recorded and a calibration curve of static solids height to slurry concentration was produced (see Appendix C). Thus, the average dispersed slurry concentration can easily be found by relating to settled solids height. The results are shown in Fig. 4.28. Results for both techniques are comparable within experimental error.

As seen in Fig. 4.28, there was an increase in the dispersed solids concentration as the sparger height was gradually lowered, as would be expected. At a sparger height of 45cm above base, for example, the dispersed slurry concentration was only 0-2vol% depending on gas velocity. At an intermediary height of 25cm, this concentration had increased to about 7-10vol% and for a sparger height of 1.5cm, full dispersion (15vol%) was observed. We also find that, for a given sparger height, an increase in superficial gas velocity increases the dispersed slurry concentration. However, the gradient of increase was constant for most sparger heights except 1.5cm and 5cm. At these heights, once full dispersion (15vol%) was achieved, the gradient of increase became flat. A plot of average dispersed slurry concentration as a function of sparger

Fig. 4.27 Local Dispersed Solids Concentration for varying sparger heights with 15vol% average solids concentration in system (Probe # 4)

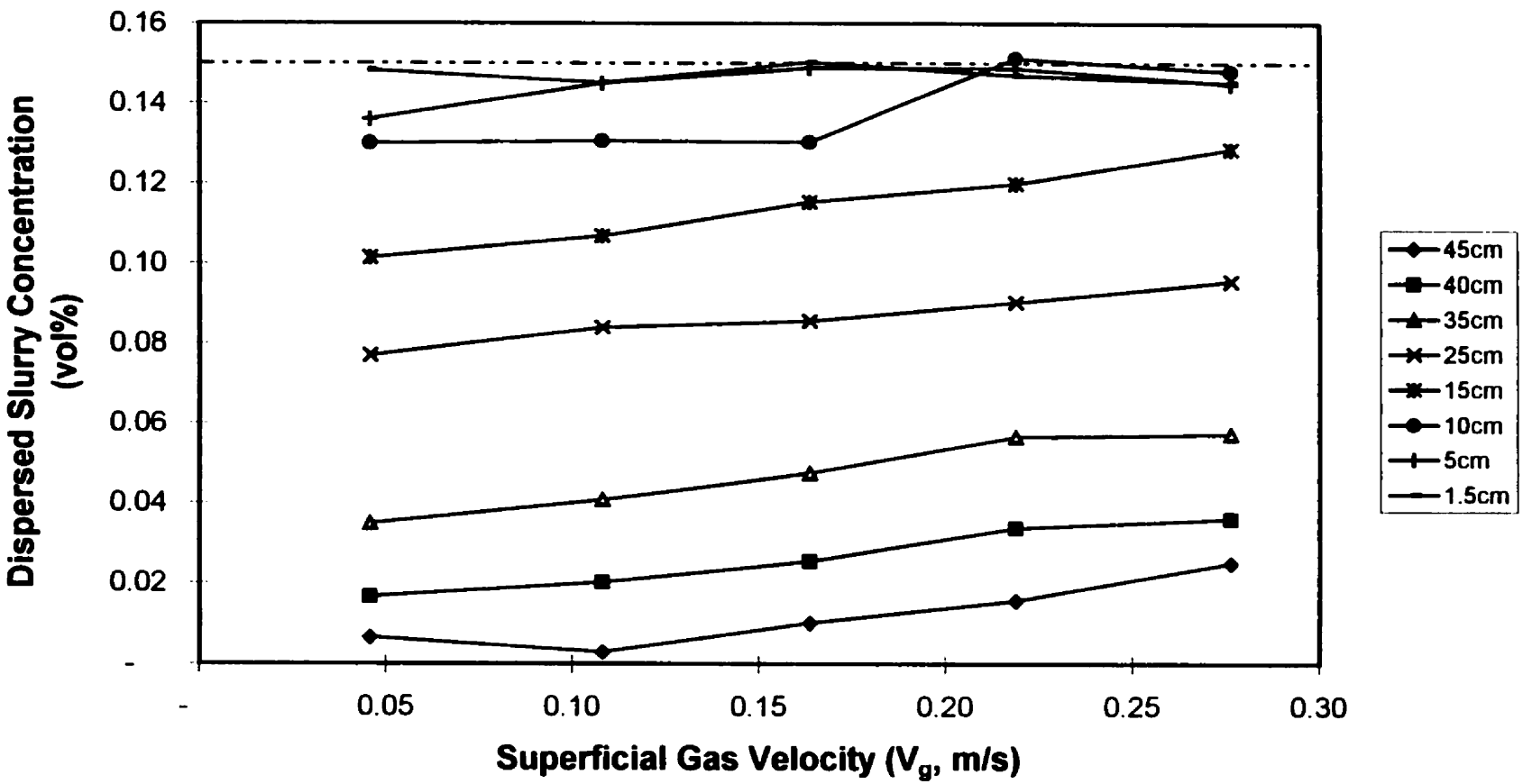

Fig. 4.28 Average Dispersed Solids Concentration for varying sparger heights with 15vol% average solids concentration in system (calculated using calibration curve)

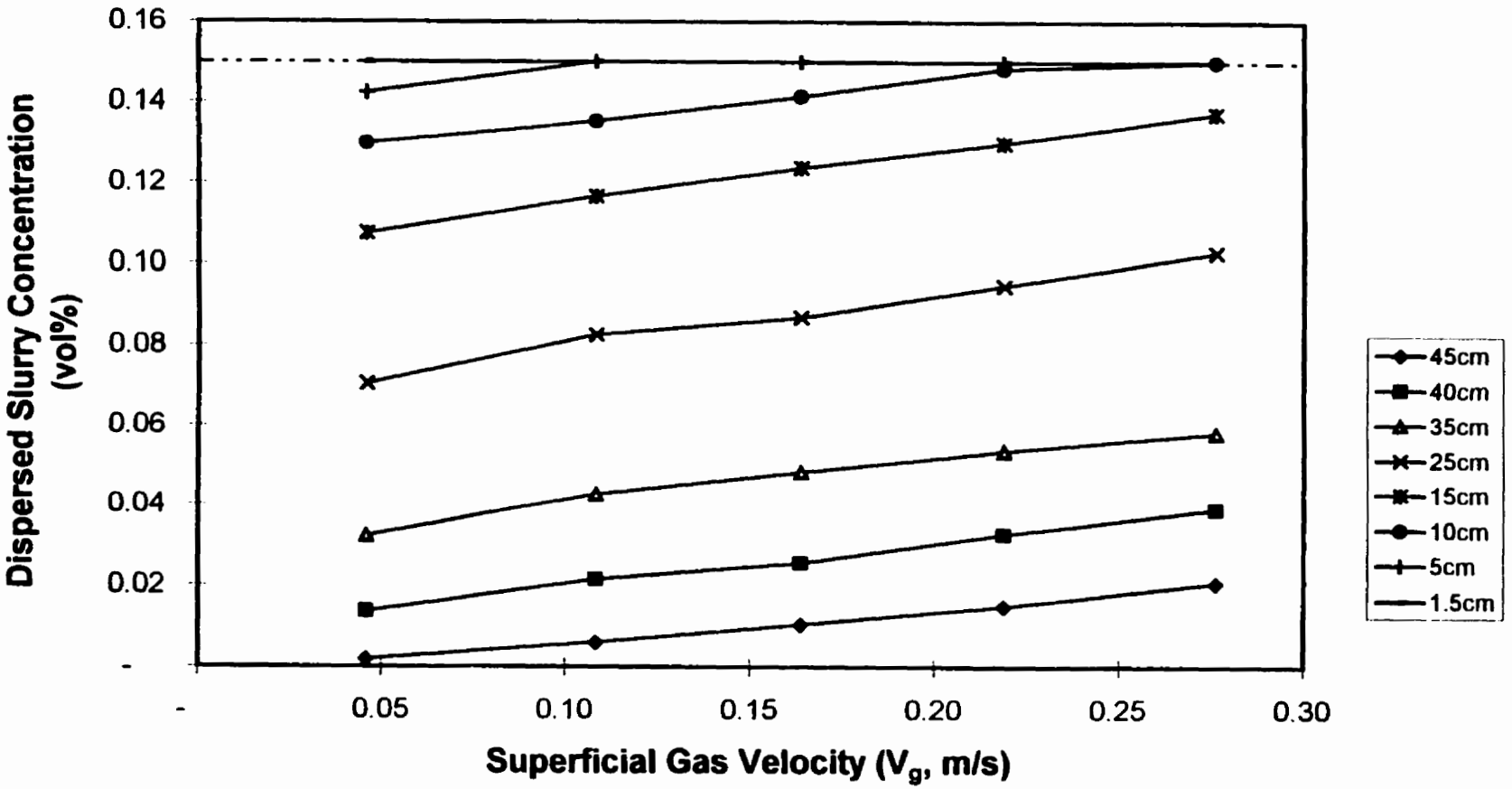

height for different superficial gas velocities is presented in Fig. 4.29. Two distinct regions can be identified - a region of uniform slurry concentration (no gradient) and one where the slurry concentration decreases continually. Uniform slurry concentration (which identifies full dispersion of solids) was achieved to higher sparger heights for higher gas velocities. For the highest gas velocity (0.28m/s), for example, this region was 10cm in length. For gas velocity of 0.16m/s, the region was 5cm in length. For the lowest gas velocity, no uniform slurry concentration region was observed for sparger heights above the minimum.

The dispersion of solids can be related to the gas jet length and circulation patterns within the column. Gas bubbles, which form from the penetrating jets, create an upward momentum of liquid. In turn, the liquid travels up the column center and back down at the column walls, creating circulation patterns. If there is enough kinetic energy in this recirculation, solids may also be entrained and dispersed. The jets are highly turbulent streams of gas which also contain enough energy to disperse the solids particles. Very little literature work has been done for gas jet lengths in gas-liquid or gas-liquid-solid systems. For gas-solid systems, Zenz (1968) proposed the following equation for vertical downward jets:

$$L_{jet} = \left(\frac{0.5 \log_{10}\left[\rho_g V_o^2\right] - 1.57}{0.044} \right) (d_o) \qquad (4.42)$$

According to this equation, for this study the gas jet lengths were calculated to range from 0.6cm to 2.0cm for corresponding column superficial gas velocities of 0.11m/s to 0.28m/s, respectively. For a superficial gas velocity of 0.05m/s, due to the low orifice Reynolds number, it was determined that only bubbles (and not jets) would form at the sparger orifices. Abramovich (1963) concluded that the principal jet zone extends about 18 nozzle diameters for air jets in water. This equates to a jet length of approximately 2.7cm for this study. The gas jets were

Fig. 4.29 Average Dispersed Slurry Concentration varying sparger heights with 15vol% average solids concentration in system

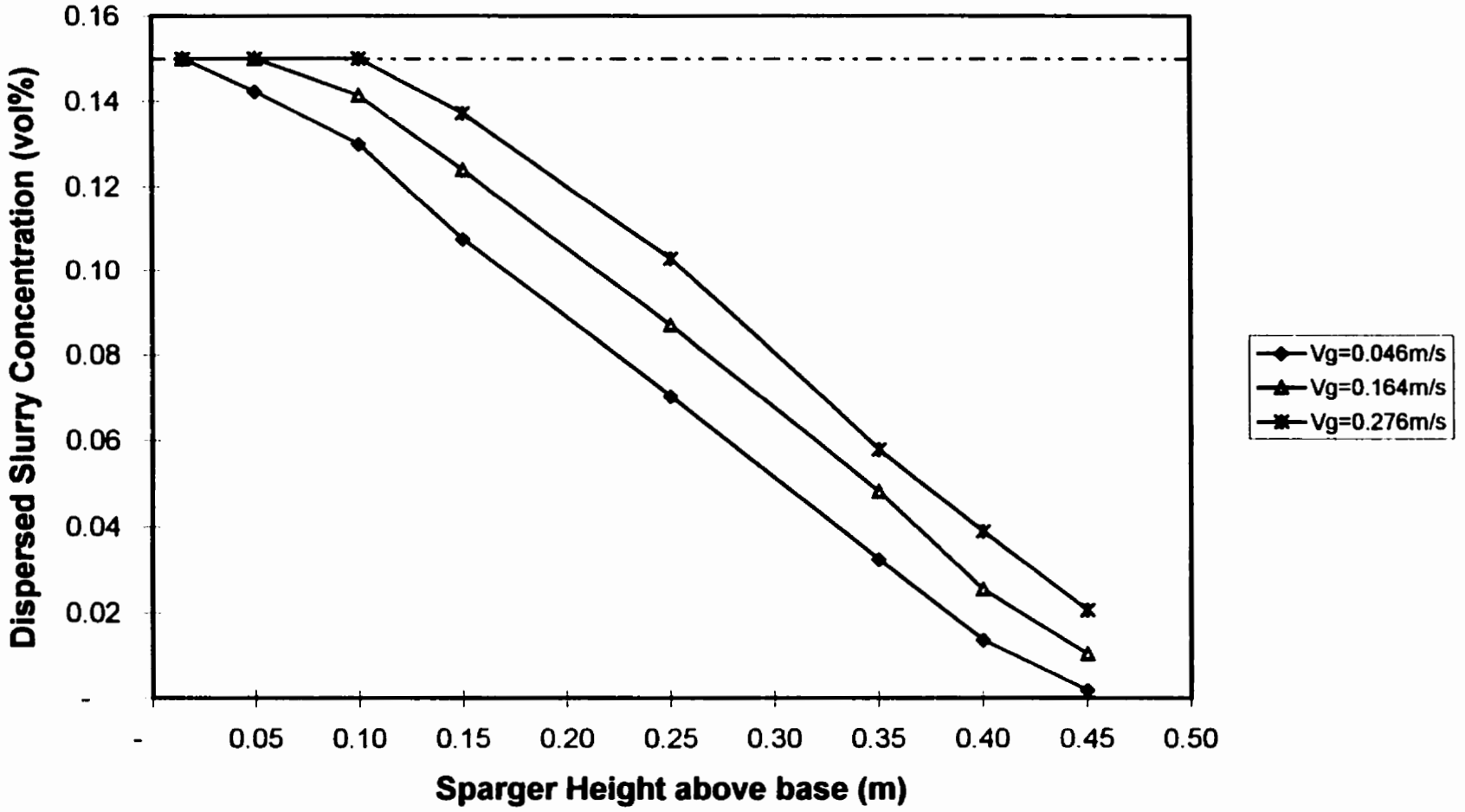

observed to be much longer than these calculated values during experimental runs. There are two possible reasons. First, plugging of sparger orifices was observed. This would lead to larger flowrates (and longer jets) through the remaining orifices. As many as half of the orifices were observed to have been plugged at any one time. Using the Zenz (1968) equation, this would increase the jet length by almost 33%. The second reason is that due to the spacing of orifices on sparger arms (see Appendix B) some jets were interacting and merging, creating one larger jet. This primarily occurred at the tips of the sparger arms where orifices were spaced close together.

For a velocity of 0.25m/s full dispersion was observed at a sparger height of 10cm or less. This dispersion was a result of the combined effect of gas jets and liquid recirculation in the column. However the individual contribution made by each effect is difficult to distinguish. In order to separate these effects, additional studies would be required with vertically upward facing orifices. The effect of liquid circulation alone could be determined from those experiments and, therefore (assuming liquid patterns remain constant), the net contribution of the gas jets could be determined.

The ratio of dispersed solids to initial settled solids height as a function of superficial gas velocity is presented in Fig 4.30. From this summary, it is possible to determine the sparger height setting to achieve 100% dispersion of solids while avoiding impingement of gas jets. For example, if a reactor system is to operate with 15vol% solids and a superficial gas velocity of 0.16m/s, then the sparger would have to be set 5cm above the base. For a gas velocity of 0.28m/s, the sparger needs only to be set at about 9cm for 100% dispersion. The summary is presented for a superficial gas velocity range of 0.05 to 0.28m/s and a slurry system containing 15vol% solids, but it may be possible to extend to other gas velocities and slurry concentrations.

Fig. 4.30 Fraction of Dispersed Solids for a 15vol% Solids Concentration System with varying Sparger Heights and Superficial Gas Velocities

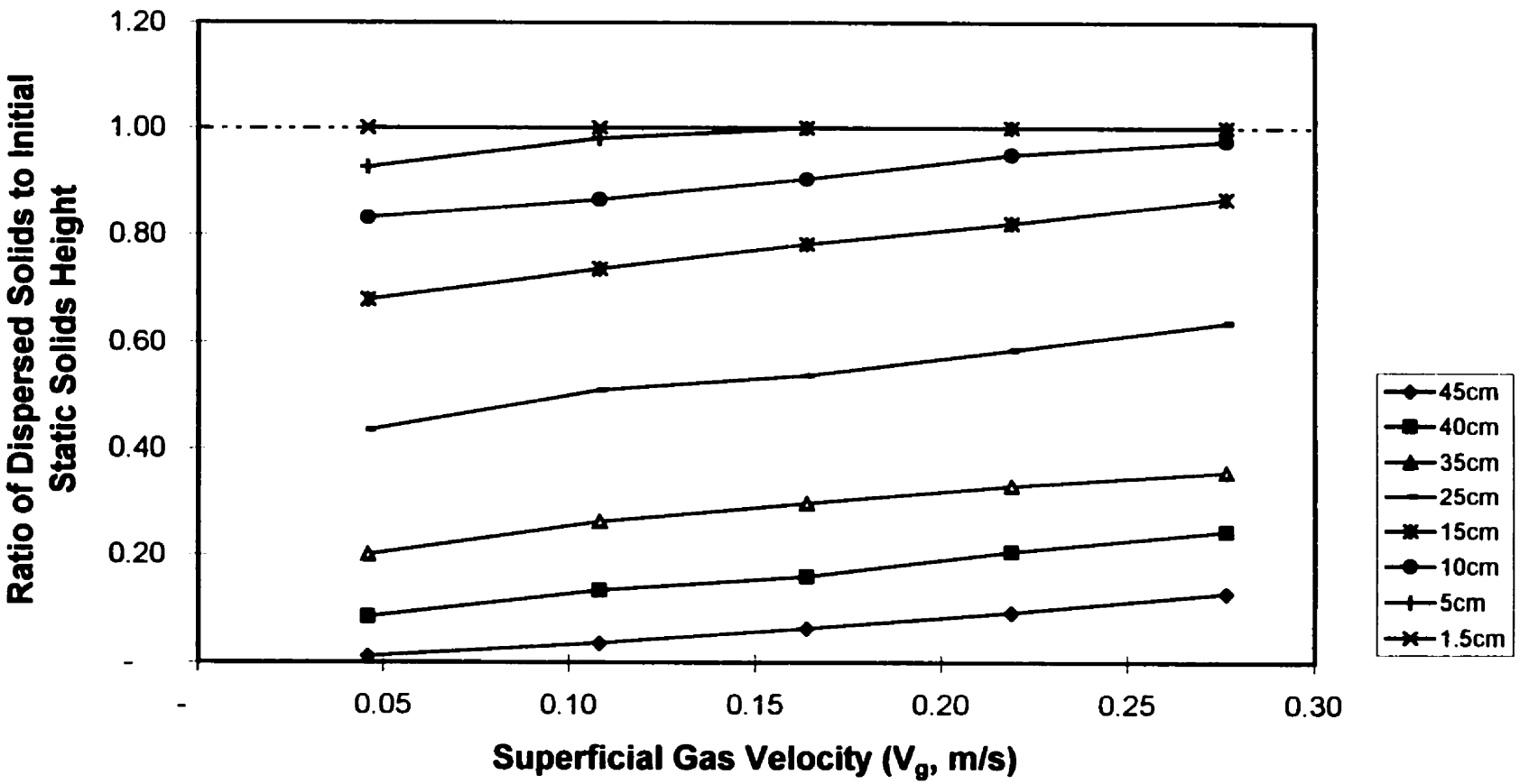

To achieve 100% solids dispersion without pitting and erosion on the base of the column, the sparger would be placed at a specific distance from this base. However, during system startup, the sparger must also be maintained at a certain distance from the top of the static solids bed to prevent plug formation. To accomplish these goals, a multi-level sparger (similar to that shown in Fig. 3.2a) can be designed. The parameters which would have to be known are the solids characteristics and concentration, the gas velocity range, and reactor diameter. A bottom sparger would be placed for normal system operation and, to avoid plug formation, an additional sparger(s) can be placed above it. However, the use of a multi-level sparger may not be practical in certain applications with large beds (where 3 or more spargers are required). Therefore, another approach would be to maintain a minimum bubbling rate (using an inert gas) during the shutdown period. This would eliminate the possibility of solids plugs forming during system startup. For this study, air was successfully used (with an approximate gas velocity of 2.5cm/s) to maintain minimum bubbling for slurry systems of 30vol% and greater during shutdown.

4.2.3 Plugging and Erosion of Sparger Orifices

During system shutdown, slurry would settle in the sparger arms and neck, resulting in plugging of orifices during system startup and operation. Most of the orifices could be unplugged by sending bursts (or pulses) of high pressure to the sparger. However, another problem of significance was observed during system shutdown - erosion of the orifice holes. Inspection revealed that the solids had eroded several of the orifice holes. Both of these problems would have to be addressed as they can lead to uneven flow patterns within the column. Visually, no such patterns could be observed.

4.2.4 Particle Entrainment

To capture any entrained solids in the exiting air flow, a cyclonic separator and bag filter system was employed (as shown in Fig. 3.1). To avoid release of these particles into the atmosphere, a cyclonic separator was attached to the exiting air from the system. A bag filter was also attached to the exit of the separator. Finally, as an additional precaution, the exiting air was directed out via a fumehood. Pressure drop was measured over the span of experiments and no significant changes were observed, indicating the filter had not plugged up. Only a negligible amount of solids were observed to have been collected in cyclone separator over the entire set of experiments.

5.0 Conclusions and Recommendations

5.1 Conclusions

1. A new method to measure the pressure profile along the column height was successfully developed and used in this project. It was demonstrated that the consistency of gas holdup measurements obtained using this new U-Tube technique with backflushing and the more commonly used liquid filled manometers was highly satisfactory.
2. Using the new backflushing technique, axial gas holdup profiles were obtained for slurry concentrations ranging from 0% (solids-free system) to 40vol% solids. The measured axial gas holdup profiles can generally be divided into three main regions. These are the distributor region (near column bottom), the bulk region and the foam region at the column top. The relative size and significance of each region varied depending on operating condition. In general, gas holdups were low in the distributor region, relatively constant in the bulk region and high in the foam region. The gas holdup gradient in the distributor region increased with increasing gas velocity, but was found to decrease with increasing slurry concentration.
3. Average gas holdups were found to increase with increasing superficial gas velocity for all slurry concentrations and generally decrease with increasing slurry concentrations (up to 30vol% solids). For a gas velocity of 0.05m/s, however, only a slight decrease in gas holdup was observed for increasing solids concentrations. Furthermore, the gradient of decrease of gas holdup with slurry concentration was much higher for increasing gas velocities. Iso-amyl alcohol (20vppm) was observed to inhibit bubble coalescence resulting in much higher gas holdups for low slurry concentration systems. For higher

slurry concentrations, due to reduced rates of bubble breakup, gas holdups for systems containing the coalescence inhibitor and for those systems without were very similar.

4. For slurry systems above 30vol%, the local and average gas holdups were found to increase with increasing slurry concentration. This was attributed to the significant changes in rheological properties of the slurry resulting from a sharp change in its pseudo-viscosity at the high concentrations.

5. Concerning the available models proposed to predict gas holdups for bubble columns, several correlations were in general agreement with that found in this study. The Hughmark correlation modified by Smith et al. (1984), which was developed over a similar velocity range, was found to give the best fit of experimental data. For slurry bubble columns, the correlation of Sada et al. (1986b) gave the best fit of experimental data for higher superficial gas velocities. This is due to the fact that the correlation does take into account the effect of particle size and slurry concentration and was developed using similar gas velocities and particle sizes. For gas velocity of 0.05m/s, due to only a slight decrease in gas holdup over the entire slurry concentration range, the correlation of Hughmark modified by Smith et al. (1984) was again found to give best fit.

6. Drift flux models were also developed to predict gas holdup for both coalescing and non-coalescing systems. The models were found to be able to predict the gas holdups quite satisfactorily. Comparison with other data from literature also indicates the models are adequate for gas velocities of 0.10m/s and higher.

7. A suitable solids sampling probe was also designed. Since radial sampling was also to be conducted, the sampling probe had to have an easy mechanism for withdrawal and insertion to various points of the column. The design also incorporated special features which prevented solids settling and gas bubble entrainment in the lines.

8. Decreasing gradients were observed for all solids concentrations along the column height due to settling effects. An increase in solids concentration also leads to an overall flatter axial solids concentration profile. This change was less significant at higher solids concentrations (30vol% to 40vol%) due to lower hindered settling velocities. The effect of gas velocity on the axial solids holdup profile, however, was found to be negligible, which can be related to the potential energy required to keep particles in suspension. Coalescence inhibitors were found to increase the solids concentration gradient for lower concentration slurry systems. For higher concentration systems, the effects of coalescence inhibition were negligible.

9. Sedimentation-dispersion models were found to give an excellent fit of experimental data for all solids systems, with correlations of Kato et al. (1972) and Smith and Ruether (1985) giving the best fits. The Axial Solids Holdup distribution model of Murray and Fan (1989) was found to deviate from experimental data at higher solids concentrations and higher axial locations, and therefore was not adequate.

10. Radial solids holdup profiles were found to vary with both slurry concentration and superficial gas velocity. For most cases, the radial solids holdup has a parabolic profile with a maximum concentration at the walls and a minimum at the center of the column. An increase in slurry concentration at lower gas velocities was found to flatten the radial solids concentration profile.

11. Several important issues of practical significance were also identified. These include formation of solids plugs for high concentration systems, pitting of the column base plate, and plugging of the sparger and erosion of its orifices. A solids dispersion analysis was performed to determine optimum sparger height settings to avoid such problems.

5.2 Recommendations

1. A more thorough investigation of gas holdups should be conducted for solids systems ranging from 20vol% to 50vol%. This should also help to quantify results observed in this study.
2. From a practical point of view, the effects of varying particle size and density and gas properties should also be studied, reflecting more industrial applications.
3. Since there was significant plugging and erosion of the sparger distributor, a new sparger should be developed. The new design should incorporate an orifice design that will minimize plugging and erosion. Further testing may also be done with a multi-level sparger to optimize design considerations.
4. A sparger with vertical upward facing orifices can also be designed to study the effects of solids dispersion due to liquid circulation alone.
5. The solids sampling probe design and technique, though adequate, could be improved to reduce sampling and measurement error. Some error was a result of splashing due to air trying to escape during sampling. A new container could be developed so that splashing is avoided. Furthermore, the sampling probe itself was not really suitable for local sampling. A new design is therefore required which allows for accurate local samples.
6. Since there exist radial profiles of gas and solids, more detailed models should be developed incorporating the radial distribution of gas and/or solids.

Appendix A - Design and Calibration of the Sonic Nozzles

Notation

A_t cross sectional area of throat (m^2)

F_g flowrate of air through the sonic nozzle (g/s)

M molecular mass of air (g/mol)

P_1 pressure upstream of the flow nozzle (Pa)

P_2 pressure downstream of the flow nozzle (Pa)

r_c critical pressure ratio

R gas law constant

T_1 temperature upstream of the flow nozzle (K)

V_g superficial gas velocity (m/s)

β ratio of throat area to pipe area

γ ratio of specific heats for air

ρ density of air (kg/m^3)

Flow nozzles are metering devices which are used to control inlet gas flowrates in numerous applications. They can be used over a wide range of flows and are fairly inexpensive to construct. For lower flowrates, these nozzles will operate in a subcritical region where the rate of discharge of a gas in the throat increases with a decrease in the absolute pressure ratio P_2/P_1. As this ratio is increased, a critical pressure ratio, r_c, is achieved at which the linear velocity of the gas in the throat reaches that of sound. This is important in that, at this point, the downstream pressure no longer has any effect on the rate of flow of gas through

the throat. Sonic nozzles are critical flow meters which operate above the critical pressure ratio (i.e. in which the linear velocity of the gas in the throat is higher than the speed of sound).

The critical pressure ratio, r_c, can be obtained from the following equation (Fluid Meters, 1959)

$$r_c^{(1-\gamma/\gamma)} + \left(\frac{\gamma - 1}{2}\right)\beta^4 r_c^{\gamma/\gamma} = \frac{2}{\gamma + 1} \qquad \text{(A.1)}$$

This equation assumes an ideal gas and frictionless nozzle. With $\beta < 0.2$, the second term becomes negligible. Furthermore, for air, $\gamma = 1.403$, therefore solving for the critical pressure ratio gives $r_c = 0.527$. This indicates that the downstream pressure cannot exceed more than half of the upstream pressure to maintain sonic conditions.

The equation for flow of gas through a sonic nozzle is defined in ES 496a Class Notes (Briens, 1993):

$$F_g = 1000\left[\gamma\rho P_1 A_t^2\left(\frac{2}{\gamma + 1}\right)^{\frac{\gamma+1}{\gamma-1}}\right]^{0.5} \qquad \text{(A.2)}$$

For air, this equation reduces to

$$F_g = 685.2 A_t\left[\rho P_1\right]^{0.5} \qquad \text{(A.3)}$$

An approximate superficial gas velocity can then be determined by dividing by the density of air and cross sectional area of the column. Due to the wide range of flows to be used ($0.05\text{m/s} < V_g < 0.25\text{m/s}$) and restrictions placed on the incoming compressed air flow (20 psig to 75 psig), two separate sonic nozzles were designed - with diameters of 1.5mm and 2.5mm, respectively.

The sonic nozzles were calibrated using an orifice meter. The standard setup of the orifice meter is shown in Fig. A.1. A program written by Dr. Cedric Briens (1994) was used to calculate the flow and is shown as Program A.1. The only variables that need to be measured are the upstream and downstream pressures (in mm H_2O) for given regulator pressure settings. A 5.1mm (0.2") orifice plate was used to calibrate the 1.5mm sonic nozzle and a 7.7mm (0.3") orifice plate was used to calibrate the 2.5mm sonic nozzle. A rough approximation of the critical pressure was also measured for each case by slowly shutting valve V_1 until an appreciable change in flow (via the manometers) was observed. The results of the calibration are shown in Figures A.2 and A.3, respectively. The workable range for the 1.5mm sonic nozzle is 1.0 g/s to 2.25 g/s which corresponds to superficial gas velocities of approximately 0.04m/s to 0.09m/s. The working range for the 2.5mm sonic nozzle is 3.0 g/s to 6.5 g/s which corresponds to gas velocities of 0.10m/s to 0.30m/s.

Comparisons between theoretical gas flowrates through the sonic nozzles and measured flowrates are presented in Table A.1. For the 2.5mm nozzle, we observe that the measured flowrate are approximately 8.5% less than theoretical values. For the 1.5mm nozzle, the error is approximately 14.5%. This was most probably due to the design of the nozzles themselves. As a further check, the flowrate through a calibrated Rotameter was measured with the orifice meter. Since the Rotameter is calibrated, the measured values from the two meters should be very close. The results are presented in Fig. A.4. The average difference between the measured and calibrated gas flowrates was calculated to be less than 5%. This indicates that the orifice meter is accurate and the error is more probably due to design of the sonic nozzles.

Figure A.1 - Orifice Plate Setup for Calibration of Sonic Nozzles

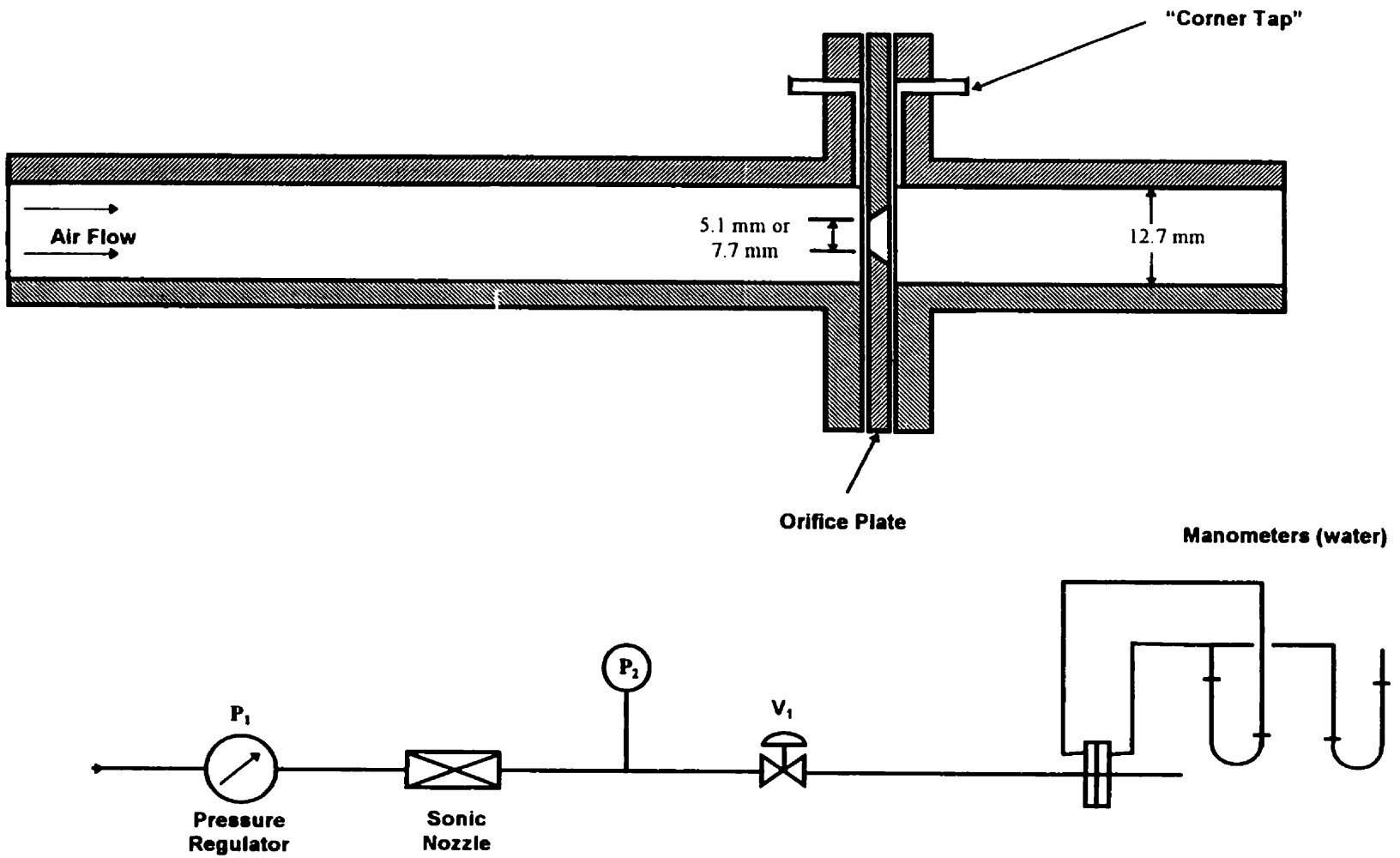

Fig. A.2 - Calibration Chart for 1.5mm Sonic Nozzle (using 5.1mm orifice plate and meter)

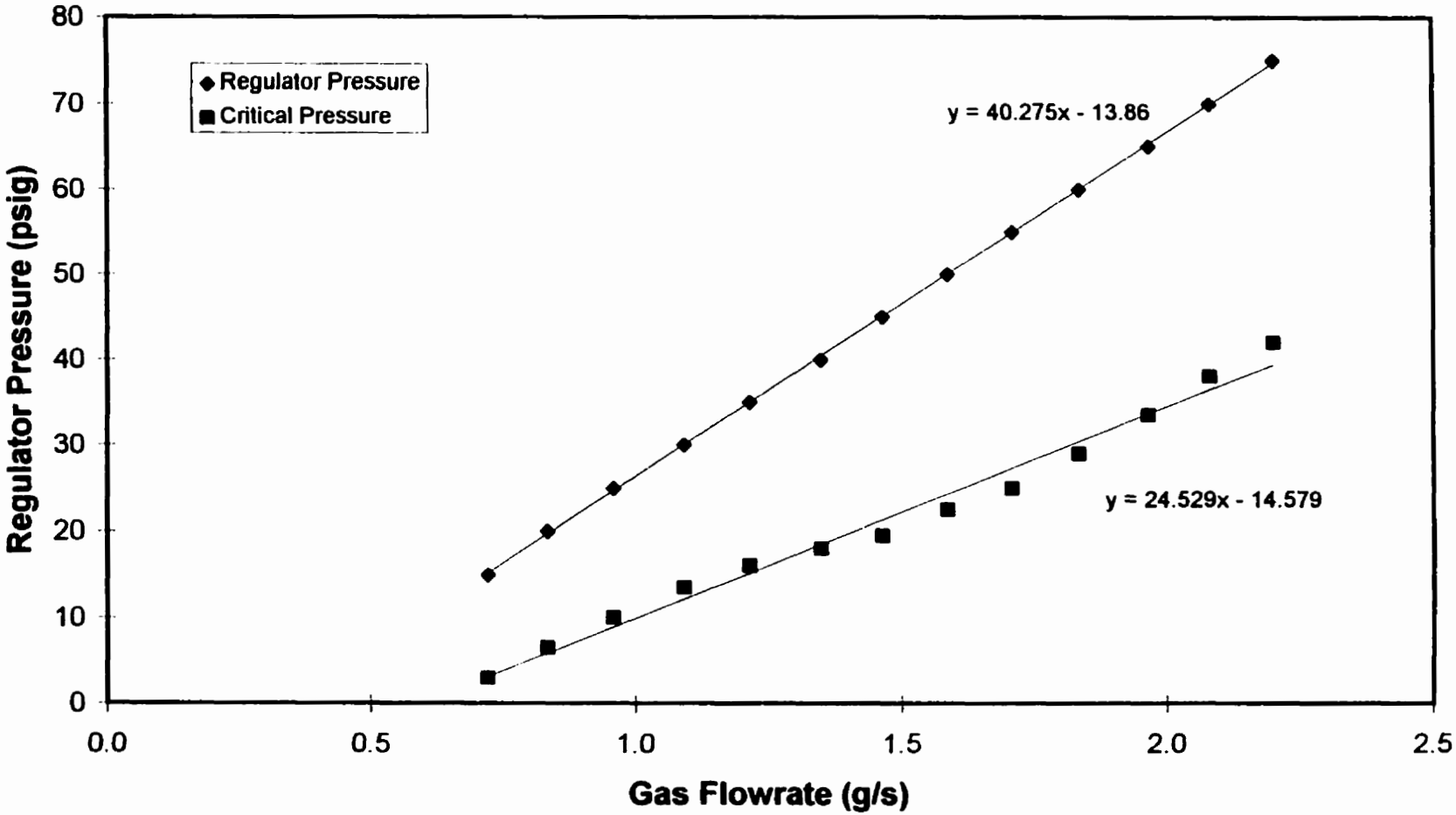

Fig. A.3 - Calibration Chart for 2.5mm Sonic Nozzle (using 7.7mm orifice plate and meter)

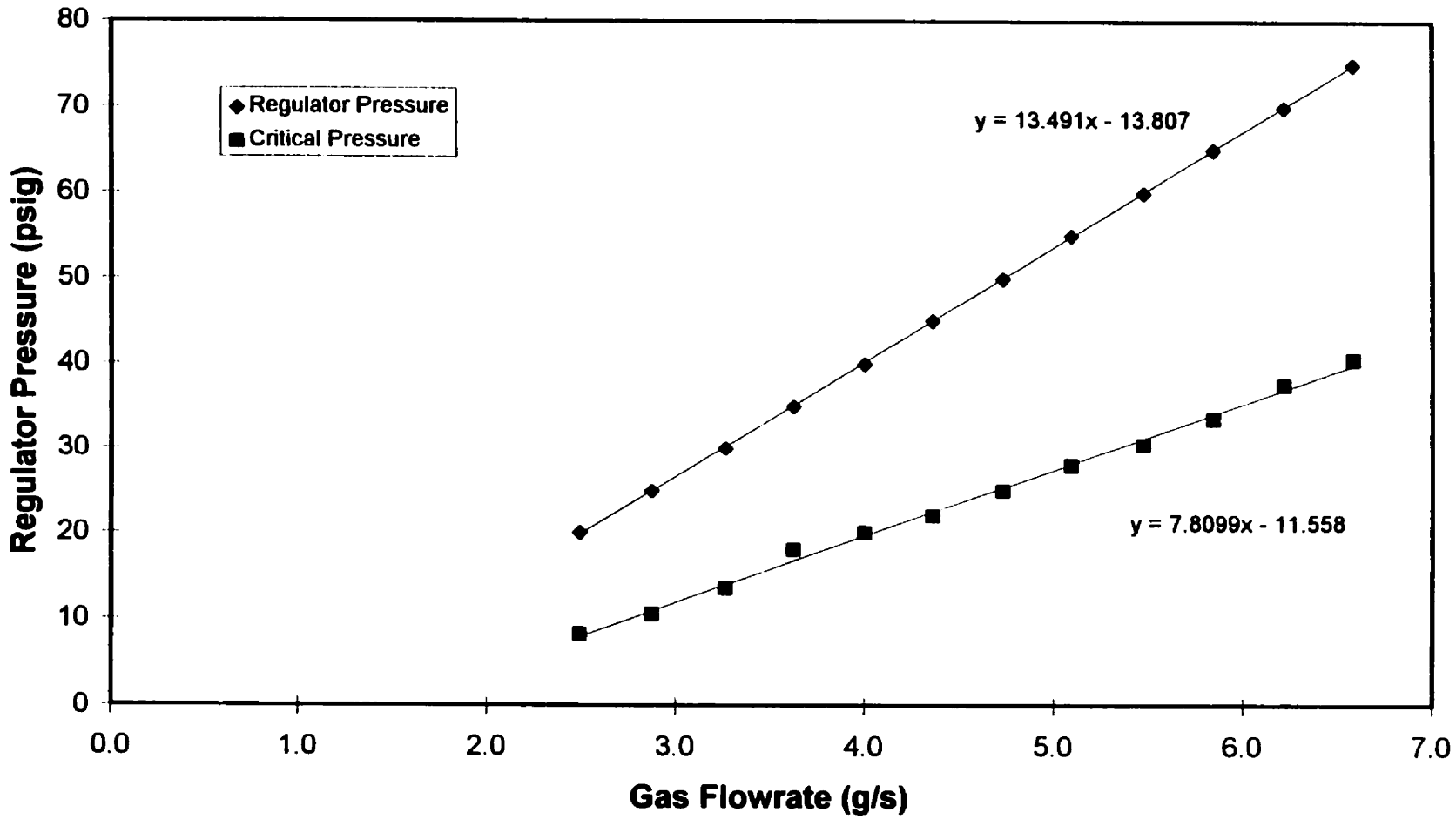

Table A.1 - Comparison of Sonic Nozzle Calibration with Theory

Diameter of Sonic Nozzle (m) 2.50E-03

P (psig)	Theory (g/s)	Measured (g/s)	%change	abs. change
20	2.75	2.51	-8.9%	-0.25
25	3.15	2.88	-8.6%	-0.27
30	3.54	3.25	-8.4%	-0.30
35	3.94	3.62	-8.2%	-0.32
40	4.34	3.99	-8.1%	-0.35
45	4.73	4.36	-7.9%	-0.38
50	5.13	4.73	-7.8%	-0.40
55	5.53	5.10	-7.7%	-0.43
60	5.92	5.47	-7.6%	-0.45
65	6.32	5.84	-7.6%	-0.48
70	6.72	6.21	-7.5%	-0.50

Diameter of Sonic Nozzle (m) 1.50E-03

P (psig)	Theory (g/s)	Measured (g/s)	%change	abs. change
20	0.99	0.84	-15.1%	-0.15
25	1.13	0.96	-14.9%	-0.17
30	1.28	1.09	-14.7%	-0.19
35	1.42	1.21	-14.5%	-0.21
40	1.56	1.34	-14.4%	-0.22
45	1.70	1.46	-14.3%	-0.24
50	1.85	1.59	-14.2%	-0.26
55	1.99	1.71	-14.1%	-0.28
60	2.13	1.83	-14.0%	-0.30
65	2.28	1.96	-13.9%	-0.32
70	2.42	2.08	-13.9%	-0.34

Fig. A.4 - Comparison of Rotameter and Orifice Meter Calibrations (with 10 psi backpressure)

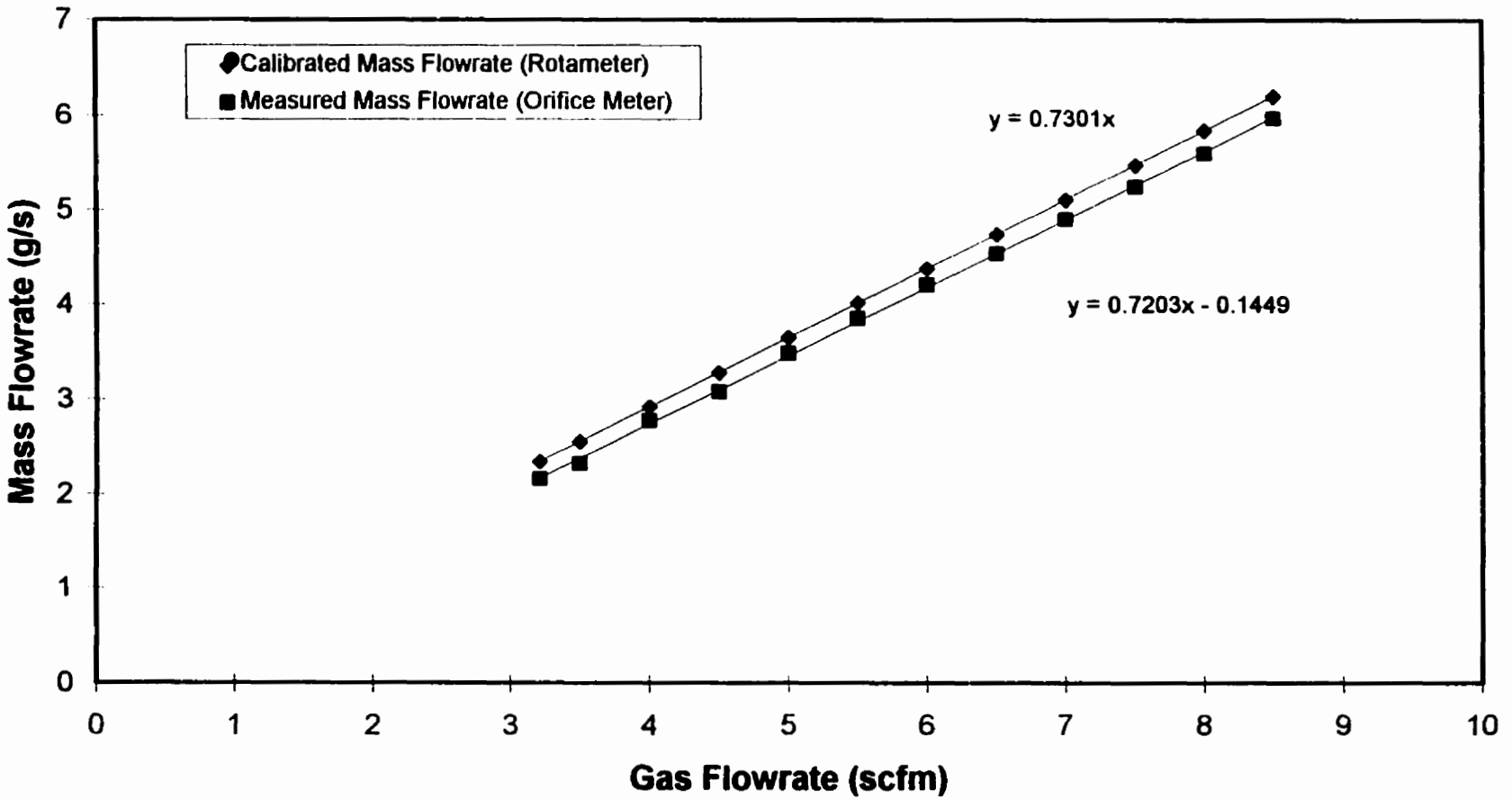

It should be noted that initially the error between theoretical flow through a sonic nozzle and that measured via the orifice plate meter was much greater. There was also a large difference between the flows measured through the Rotameter and the orifice. This indicated that there was a systematic problem with the design of the orifice meter and plate. An exhaustive effort was then undertaken to determine this problem. This work was done in conjunction with Yasser Ibrahim (1996). According to ASME standards (Fluid Meters, 1959), the orifice meter and plate design must meet the following design parameters:

1. The orifice should be preceded by 100 pipe diameters or more on the inlet side and 25 or more pipe diameters on the outlet side.
2. No rounding should be observed in the upstream edge of the orifice. The edge should be sharp enough so that, without magnification, the corner does not appear to reflect a beam of light.
3. The thickness (t) of the square edge part of the orifice plate should not exceed any of the following: 1/30 of the pipe diameter (d_p), 1/8 of the orifice diameter(d_o), or 1/4 of the dam height (d_p-d_o)/2.
4. If the orifice plate is thicker than (t), then the outlet corner of the orifice should be beveled at an angle of 45° or less to the face of the orifice plate.
5. The type and location of the pressure taps should be carefully selected and designed.

It was found that steps (1) and (3) were not met in the original plate designs. The square edge thickness (t) was found to be five to ten times thicker than it should have been. The effect of step (1) should be minimal compared to the square edge thickness, therefore, it was decided to design new plates which met all of these specifications. The results from the new orifice plates are shown above.

```
'PROGRAM A.1 - PROGRAM TO CALCULATE MASS FLOWRATE THROUGH AN ORIFICE PLATE
'=========================================================================


'generic s type module

' copyright Cedric Briens 1994/06/03

Option Base 1

Public XMIN

Function MASS_FLOW_FROM_ORIFICE_PLATE(SEL_TAP, DORIFICE, DPIPE, ROG1ATM, XMUG, GAMMA
, PUPSTREAM, DELTAP, PROOM)

 SEL_TAP = UCase(SEL_TAP)

W = MASS_FLOW_FROM_ORIFICE_PLATE_xl(SEL_TAP, DORIFICE, DPIPE, ROG1ATM, XMUG, GAMMA,
PUPSTREAM, DELTAP, PROOM)


MASS_FLOW_FROM_ORIFICE_PLATE = W

End Function



Private Function MASS_FLOW_FROM_ORIFICE_PLATE_xl(SEL_TAP, DORIFICE, DPIPE, ROG1ATM,
XMUG, GAMMA, PUPSTREAM, DELTAP, PROOM)

'^^^^^^^^^^^^^^^^^^^^^^^^^^^^^^^^^^^^^^
' calculates the flowrate through a sharp-edged orifice meter
'  from its pressure drop
'^^^^^^^^^^^^^^^^^^^^^^^^^^^^^^^^^^^^^^
' for more information to  consult "Fluid meters.  Their theory and application" ste
p
' publ. in 1959 by the American Society of Mechanical Engineers,
' 29 West 39th street, New York, N.Y..
'^^^^^^^^^^^^^^^^^^^^^^^^^^^^^^^^^^^^^^
' INPUT
' dorifice  orifice diameter
' dpipe     pipe diameter
' seltap    CORNER  corner taps
'       FLANGE  flange taps
'               PIPE    pipe taps
'       VENA    vena contracta taps
' roglatm   density of the gas at the same temperature and at 1 atm
' xmug      gas viscosity at the appropriate temperature
' gamma     ratio of specific heats (cp/cv)
' pupstream pressure upstream of the plate (RELATIVE TO 1 atm.)
' deltap    pressure drop through the plate
' proom     absolute pressure in the room
'^^^^^^^^^^^^^^^^^^^^^^^^^^^^^^^^^^^^^^
' OUTPUT
' w     mass flowrate
'^^^^^^^^^^^^^^^^^^^^^^^^^^^^^^^^^^^^^^

      Dim PAR(20), PARLAB(5)
```

```
      SELTAP = SEL_TAP

      BETA = DORIFICE / DPIPE

'     correct pupstream for room pressures different from 1 atm
      PUPSTREAM = PUPSTREAM + (PROOM - 101325#)
      ROG = ROG1ATM * (PUPSTREAM + 101325#) / 101325#

      AORIFICE = 3.14159 / 4# * DORIFICE ^ 2

'    get first approximation of mass flowrate
      CK = 0.61

      Y = YEXPANSION(SELTAP, PUPSTREAM, DELTAP, BETA, GAMMA)
      W = CK * Y * AORIFICE * Sqr(2# * ROG * DELTAP)

'     find the mass flowrate
      START = W
      STEP = START / 10#
      PREC = 0.000000000001
      NMAX = 500
      PARLAB(1) = SELTAP
      PAR(1) = PUPSTREAM
      PAR(2) = DELTAP
      PAR(3) = BETA
      PAR(4) = GAMMA
      PAR(5) = DPIPE
      PAR(6) = ROG
      PAR(7) = XMUG
      PAR(8) = AORIFICE

      Call EONOR4(START, STEP, EPS, NMAX, PAR, PARLAB)

      W = XMIN

      MASS_FLOW_FROM_ORIFICE_PLATE_x1 = W

End Function


      Private Function YEXPANSION(SELTAP, PUPSTREAM, DELTAP, BETA, GAMMA)
'^^^^^^^^^^^^^^^^^^^^^^^^^^^^^^^^^^^^
' calculates the expansion factor
'^^^^^^^^^^^^^^^^^^^^^^^^^^^^^^^^^^^^
' INPUT
' seltap    CORNER  corner taps
'       FLANGE  flange taps
'               PIPE    pipe taps
'       VENA    vena contracta taps
' pupstream pressure upstream of the plate (RELATIVE TO 1 atm.)
' deltap    pressure drop through the plate
' beta      ratio of orifice diameter to pipe diameter
' gamma     ratio of specific heats (cp/cv)
'^^^^^^^^^^^^^^^^^^^^^^^^^^^^^^^^^^^^^^^^^^^^
' OUTPUT
' yexpansion    expansion factor
'^^^^^^^^^^^^^^^^^^^^^^^^^^^^^^^^^^^^^^^^^^^^
```

```
      PUPABS = 101325# + PUPSTREAM
      PDOWNABS = PUPABS - DELTAP
      R = PDOWNABS / PUPABS

      If (SELTAP = "PIPE  ") Then
'       equation # 302 page 139
        XINT = 0.333 + 1.145 * (BETA ^ 2 + 0.7 * BETA ^ 5 + 12# * BETA ^ 13)
       Else
'       equation # 303
        XINT = 0.41 + 0.35 * BETA ^ 4
      End If
      Y = 1# - (1# - R) / GAMMA * XINT

      YEXPANSION = Y
      End Function


      Private Function CORIFICE(DPIPE, SELTAP, XMUG, BETA, W)
'^^^^^^^^^^^^^^^^^^^^^^^^^^^^^^^^^^^^^
' INPUT
' dpipe     pipe diameter
' seltap    CORNER  corner taps
'       FLANGE  flange taps
'               PIPE    pipe taps
'       VENA    vena contracta taps
' xmug      gas viscosity at the appropriate temperature
' beta      ratio of orifice diameter to pipe diameter
' w     mass flowrate
'^^^^^^^^^^^^^^^^^^^^^^^^^^^^^^^^^^^^^
' OUTPUT
' corifice  orifice coefficient
'^^^^^^^^^^^^^^^^^^^^^^^^^^^^^^^^^^^^^

'     pipe Reynolds number at upstream conditions
      REPIPE = 4# * W / (3.14159 * DPIPE * XMUG)
      XLAMBDA = 1000 / Sqr(REPIPE)

      If (SELTAP = "CORNER") Then
'       equation 299, 300, 301 page 139
        CKE = 0.6004 + 0.35 * (BETA ^ 4)
        XINT1 = 0.5 - BETA
        If (XINT1 > 0#) Then
          CKE = CKE - 0.052 * (XINT1 ^ 1.5)
        End If
        XINT2 = BETA - 0.7
        If (XINT2 > 0#) Then
          CKE = CKE + 0.62 * (XINT2 ^ (5# / 3#))
        End If
        B = CKE * (0.002 + 0.026 * (BETA ^ 4))
        CK = CKE * (1# + B * XLAMBDA)

       ElseIf (SELTAP = "FLANGE") Then
        DINCH = DPIPE / 0.3048 * 12#
        CKE = 0.5993 + 0.007 / DINCH
        CKE = CKE + (BETA ^ 4) * (0.364 + 0.076 / Sqr(DINCH))
        XINT = 0.07 + 0.5 / DINCH - BETA
        If (XINT > 0#) Then
          CKE = CKE + 0.4 * ((1.6 - 1# / DINCH) ^ 5#) * (XINT ^ 2.5)
        End If
        XINT = 0.5 - BETA
```

```
        If (XINT > 0#) Then
          CKE = CKE - (0.009 + 0.034 / DINCH) * (XINT ^ 1.5)
        End If
        XINT = BETA - 0.7
        If (XINT > 0#) Then
          CKE = CKE + (65# / (DINCH ^ 2#) + 3#) * (XINT ^ 2.5)
        End If
        DORINCH = BETA * DINCH
        A = DORINCH * (830# - 5000# * BETA + 9000# * BETA * BETA - 42000# * (BETA ^
3) + 530# / DINCH)
        CK0 = CKE * 1000000# * DORINCH / (1000000# * DORINCH + 15# * A)
        CK = CK0 * (1# + BETA * A / REPIPE)

       ElseIf (SELTAP = "PIPE") Then
        DINCH = DPIPE * 0.3048 / 12#
        CKE = 0.5925 + 0.0182 / DINCH
        XINT = 0.44 - 0.06 / DINCH
        CKE = CKE + XINT * BETA * BETA
        CKE = CKE + (0.935 + 0.225 / DINCH) * (BETA ^ 5)
        CKE = CKE + 1.35 * (BETA ^ 14)
        XINT = 0.25 - BETA
        If (XINT > 0#) Then
          CKE = CKE + 1.43 / Sqr(DINCH) * (XINT ^ 2.5)
        End If
        DORINCH = BETA * DINCH
        A = DORINCH * (905# - 5000# * BETA + 9000# * BETA * BETA - 4200# * (BETA ^ 3
) + 875# / DINCH)
        CK0 = CKE * 1000000# * DORINCH / (1000000# * DORINCH + 15# * A)
        CK = CK0 * (1# + BETA * A / REPIPE)
       ElseIf (SELTAP = "VENA  ") Then
        DINCH = DPIPE * 0.3048 / 12#
        XINT = 1.25 * (BETA ^ 16) + (BETA ^ 4)
        XINT = XINT + 0.0006 / ((DINCH * BETA) ^ 2 + 0.01 * DINCH)
        CKE = 0.5922 + 0.4252 * XINT
        XINT = BETA + 1.75 * (BETA ^ 4) + 10# * (BETA ^ 12)
        XINT = XINT + 2# * DINCH * (BETA ^ 16)
        B = 0.00025 + 0.002325 * XINT
        CK = XLAMBDA * B + CK0
      End If

      CORIFICE = CK
      End Function


      Private Sub EONOR4(START, STEP, EPS, NMAX, PAR, PARLAB)
      NFUNEV = 0
      A1 = 1.5
      A2 = -0.25
      BIG = 1E+25
      X = START

1     dummy = 0
      NFUNEV = NFUNEV + 1
      F = FUNCT(X, PAR, PARLAB)

2     dummy = 0
      F1 = F
      F0 = -BIG
      STEP1 = 0#
      XMIN = X
```

```
3       dummy = 0
        STEP2 = STEP1 + STEP
        X = XMIN + STEP2

4       dummy = 0
        If (Abs(STEP) <= EPS) Then
           FMIN = FUNCT(XMIN, PAR, PARLAB)
           Exit Sub
        End If
        If (NFUNEV > NMAX) Then
          ' warn ("MAXIMUM NUMBER OF private function EVALUATIONS REACHED")
           Exit Sub
        End If

5       dummy = 0
        NFUNEV = NFUNEV + 1
        F = FUNCT(X, PAR, PARLAB)

6       dummy = 0
        If (F < F1) Then GoTo 10

7       dummy = 0
        If (F0 >= F1) Then GoTo 11

8       dummy = 0
        F0 = F
        STEP0 = STEP2

9       dummy = 0
        STEP = A2 * STEP
        GoTo 3

10      dummy = 0
        STEP0 = STEP1
        F0 = F1
        STEP1 = STEP2
        F1 = F
        STEP = A1 * STEP
        GoTo 3

11      dummy = 0
        STEP0 = STEP0 - STEP1
        F0 = (F0 - F1) * STEP
        F = (F - F1) * STEP0

12      dummy = 0
        If (Abs(F - F0) < 1E-20) Then GoTo 18

13      dummy = 0
        STEP = 0.5 * (F * STEP0 - F0 * STEP) / (F - F0)

14      dummy = 0
        STEP2 = STEP1 + STEP
        X = XMIN + STEP2

15      dummy = 0
        If (Abs(XMIN + STEP1 - X) < 1E-25) Then GoTo 20

16      dummy = 0
```

```
      NFUNEV = NFUNEV + 1
      F = FUNCT(X, PAR, PARLAB)

17    dummy = 0
      If (F < F1) Then GoTo 19

18    dummy = 0
      X = XMIN + STEP1
      F = F1
      GoTo 20

19    dummy = 0
      STEP1 = STEP2

20    dummy = 0
      STEP = STEP * A2
      GoTo 2

      End Sub


      Private Function FUNCT(X, PAR, PARLAB)

      WSAVE = X
      W = WSAVE

      SELTAP = PARLAB(1)
      PUPSTREAM = PAR(1)
      DELTAP = PAR(2)
      BETA = PAR(3)
      GAMMA = PAR(4)
      DPIPE = PAR(5)
      ROG = PAR(6)
      XMUG = PAR(7)
      AORIFICE = PAR(8)

      Y = YEXPANSION(SELTAP, PUPSTREAM, DELTAP, BETA, GAMMA)

      CK = CORIFICE(DPIPE, SELTAP, XMUG, BETA, W)

      W = CK * Y * AORIFICE * Sqr(2# * ROG * DELTAP)

      XINT = (W - WSAVE) ^ 2

      If (W <= 0) Then
        FUNCT = (1 + Abs(W)) * 1000000000000#
      End If

      FUNCT = XINT

      End Function
```

Appendix B - Design and Testing of the Gas Distributor

Special consideration was given in designing the gas distributor. This was done due to the large range of gas flowrates (0 to 0.30m/s) and slurry concentrations (0% to 40vol%) which were to be used. To minimize the ratio of sparger pressure drop to bed pressure drop, a dual sparger had to be designed. Wherever possible, it was attempted to keep this ratio between 10% and 100%. The design procedure was adapted from ES 496a Class Notes (Briens, 1991) and is presented in Tables B.1 through B.3 for varying solids concentrations and gas velocities. A summary of sparger use is outlined in Table B.4.

A diagram of the sparger is shown in Figure 3.2a. There were two main sections to the sparger - a lower sparger which would handle the lower gas flowrates and an upper sparger which could handle higher gas flowrates. The lower sparger arms consisted four arms with an inside diameter of 6.35mm and five orifices per arm. The upper sparger consisted of four arms with an inside diameter of 9.53mm and seven orifices per arm. The upper sparger was located 25mm above the lower sparger and was rotated over 45° to ensure there was no erosion of the bottom sparger arms from the gas jets. The orifices were all 1.5mm in diameter and were located facing vertically downwards to help minimize plugging and settling of solids in the sparger itself. The spacing between orifices is shown in Fig. 3.2b. To ensure equal distribution of gas (to the cross sectional area of the column), several outer orifices were spaced closer together. To maintain a minimum spacing, a few were angled towards the column wall.

Table B.1 - Low Volume Sparger - four arms with five Orifices per arm

	Units	0% Solids with variable gas velocities					
(1) Calculate bed pressure drop							
assumed weight fraction solids	%	0%	0%	0%	0%	0%	0%
volume fraction solids	%	0%	0%	0%	0%	0%	0%
density of water	kg/m^3	1000	1000	1000	1000	1000	1000
density of solids	kg/m^3	2500	2500	2500	2500	2500	2500
density of mixture	kg/m^3	1000	1000	1000	1000	1000	1000
height of bed	m	1.5	1.5	1.5	1.5	1.5	1.5
pressure drop across bed	Pa	14715	14715	14715	14715	14715	14715
(2) Calculate mass flowrate in column							
superficial gas velocity	m/s	0.05	0.1	0.15	0.2	0.25	0.3
column inside diameter	m	0.1524	0.1524	0.1524	0.1524	0.1524	0.1524
density of air	kg/m^3	1.2928	1.2928	1.2928	1.2928	1.2928	1.2928
area of column	m^2	1.82E-02	1.82E-02	1.82E-02	1.82E-02	1.82E-02	1.82E-02
volumetric flowrate of air	m^3/s	9.12E-04	1.82E-03	2.74E-03	3.65E-03	4.56E-03	5.47E-03
mass flowrate of air	kg/s	1.18E-03	2.36E-03	3.54E-03	4.72E-03	5.90E-03	7.07E-03
(3) Calculate mass flowrate per orifice							
number of orifices per arm		5	5	5	5	5	5
number of arms		4	4	4	4	4	4
total number of orifices		20	20	20	20	20	20
mass flowrate per orifice	kg/s	5.90E-05	1.18E-04	1.77E-04	2.36E-04	2.95E-04	3.54E-04
(4) Calculate pressure drop per orifice							
selected orifice diameter	m	0.0015	0.0015	0.0015	0.0015	0.0015	0.0015
area of orifice	m^2	1.8E-06	1.8E-06	1.8E-06	1.8E-06	1.8E-06	1.8E-06
flowrate per square meter	kg/sm^2	33.4	66.7	100.1	133.5	166.8	200.2
pressure drop per orifice	Pa	1119	4477	10073	17908	27981	40293
(5) Calculate tube diameter							
number of orifices per arm		5	5	5	5	5	5
selected orifice diameter	mm	1.5	1.5	1.5	1.5	1.5	1.5
tube diameter must be >	mm	4.79	4.79	4.79	4.79	4.79	4.79
selected tube diamter	mm	6.35	6.35	6.35	6.35	6.35	6.35
(6) Calculate centre pipe (top section) diameter							
number of orifices		4	4	4	4	4	4
centre pipe orifice diameter	mm	6.35	6.35	6.35	6.35	6.35	6.35
tube diameter must be >	mm	18.14	18.14	18.14	18.14	18.14	18.14
selected pipe diameter	mm	25.4	25.4	25.4	25.4	25.4	25.4
(7) Calculate percentage pressure drop across sparger							
pressure drop across sparger	Pa	1119	4477	10073	17908	27981	40293
pressure drop across bed	Pa	14715	14715	14715	14715	14715	14715
percentage pressure drop	**%**	**7.6%**	**30.4%**	**68.5%**	**121.7%**	**190.2%**	**273.8%**

Table B.2 - Low Volume Sparger - four arms with five Orifices per arm

	Units	25vol% Solids with variable gas velocities					
(1) Calculate bed pressure drop							
assumed weight fraction solids	%	45%	45%	45%	45%	45%	45%
volume fraction solids	%	25%	25%	25%	25%	25%	25%
density of water	kg/m^3	1000	1000	1000	1000	1000	1000
density of solids	kg/m^3	2500	2500	2500	2500	2500	2500
density of mixture	kg/m^3	1675	1675	1675	1675	1675	1675
height of bed	m	1.5	1.5	1.5	1.5	1.5	1.5
pressure drop across bed	Pa	24648	24648	24648	24648	24648	24648
(2) Calculate mass flowrate in column							
superficial gas velocity	m/s	0.05	0.1	0.15	0.2	0.25	0.3
column inside diameter	m	0.1524	0.1524	0.1524	0.1524	0.1524	0.1524
density of air	kg/m^3	1.2928	1.2928	1.2928	1.2928	1.2928	1.2928
area of column	m^2	1.82E-02	1.82E-02	1.82E-02	1.82E-02	1.82E-02	1.82E-02
volumetric flowrate of air	m^3/s	9.12E-04	1.82E-03	2.74E-03	3.65E-03	4.56E-03	5.47E-03
mass flowrate of air	kg/s	1.18E-03	2.36E-03	3.54E-03	4.72E-03	5.90E-03	7.07E-03
(3) Calculate mass flowrate per orifice							
number of orifices per arm		5	5	5	5	5	5
number of arms		4	4	4	4	4	4
total number of orifices		20	20	20	20	20	20
mass flowrate per orifice	kg/s	5.90E-05	1.18E-04	1.77E-04	2.36E-04	2.95E-04	3.54E-04
(4) Calculate pressure drop per orifice							
selected orifice diameter	m	0.0015	0.0015	0.0015	0.0015	0.0015	0.0015
area of orifice	m^2	1.8E-06	1.8E-06	1.8E-06	1.8E-06	1.8E-06	1.8E-06
flowrate per square meter	kg/sm^2	33.4	66.7	100.1	133.5	166.8	200.2
pressure drop per orifice	Pa	1119	4477	10073	17908	27981	40293
(5) Calculate tube diameter							
number of orifices per arm		5	5	5	5	5	5
selected orifice diameter	mm	1.5	1.5	1.5	1.5	1.5	1.5
tube diameter must be >	mm	4.79	4.79	4.79	4.79	4.79	4.79
selected tube diamter	mm	6.35	6.35	6.35	6.35	6.35	6.35
(6) Calculate centre pipe (top section) diameter							
number of orifices		4	4	4	4	4	4
centre pipe orifice diameter	mm	6.35	6.35	6.35	6.35	6.35	6.35
tube diameter must be >	mm	18.14	18.14	18.14	18.14	18.14	18.14
selected pipe diameter	mm	25.4	25.4	25.4	25.4	25.4	25.4
(7) Calculate percentage pressure drop across sparger							
pressure drop across sparger	Pa	1119	4477	10073	17908	27981	40293
pressure drop across bed	Pa	24648	24648	24648	24648	24648	24648
percentage pressure drop	**%**	**4.5%**	**18.2%**	**40.9%**	**72.7%**	**113.5%**	**163.5%**

Table B.3 - Low Volume Sparger - four arms with five Orifices per arm

	Units	40vol% Solids with variable gas velocities					
(1) Calculate bed pressure drop							
assumed weight fraction solids	%	63%	63%	63%	63%	63%	63%
volume fraction solids	%	40%	40%	40%	40%	40%	40%
density of water	kg/m^3	1000	1000	1000	1000	1000	1000
density of solids	kg/m^3	2500	2500	2500	2500	2500	2500
density of mixture	kg/m^3	1937.5	1937.5	1937.5	1937.5	1937.5	1937.5
height of bed	m	1.5	1.5	1.5	1.5	1.5	1.5
pressure drop across bed	Pa	28510	28510	28510	28510	28510	28510
(2) Calculate mass flowrate in column							
superficial gas velocity	m/s	0.05	0.1	0.15	0.2	0.25	0.3
column inside diameter	m	0.1524	0.1524	0.1524	0.1524	0.1524	0.1524
density of air	kg/m^3	1.2928	1.2928	1.2928	1.2928	1.2928	1.2928
area of column	m^2	1.82E-02	1.82E-02	1.82E-02	1.82E-02	1.82E-02	1.82E-02
volumetric flowrate of air	m^3/s	9.12E-04	1.82E-03	2.74E-03	3.65E-03	4.56E-03	5.47E-03
mass flowrate of air	kg/s	1.18E-03	2.36E-03	3.54E-03	4.72E-03	5.90E-03	7.07E-03
(3) Calculate mass flowrate per orifice							
number of orifices per arm		5	5	5	5	5	5
number of arms		4	4	4	4	4	4
total number of orifices		20	20	20	20	20	20
mass flowrate per orifice	kg/s	5.90E-05	1.18E-04	1.77E-04	2.36E-04	2.95E-04	3.54E-04
(4) Calculate pressure drop per orifice							
selected orifice diameter	m	0.0015	0.0015	0.0015	0.0015	0.0015	0.0015
area of orifice	m^2	1.8E-06	1.8E-06	1.8E-06	1.8E-06	1.8E-06	1.8E-06
flowrate per square meter	kg/sm^2	33.4	66.7	100.1	133.5	166.8	200.2
pressure drop per orifice	Pa	1119	4477	10073	17908	27981	40293
(5) Calculate tube diameter							
number of orifices per arm		5	5	5	5	5	5
selected orifice diameter	mm	1.5	1.5	1.5	1.5	1.5	1.5
tube diameter must be >	mm	4.79	4.79	4.79	4.79	4.79	4.79
selected tube diamter	mm	6.35	6.35	6.35	6.35	6.35	6.35
(6) Calculate centre pipe (top section) diameter							
number of orifices		4	4	4	4	4	4
centre pipe orifice diameter	mm	6.35	6.35	6.35	6.35	6.35	6.35
tube diameter must be >	mm	18.14	18.14	18.14	18.14	18.14	18.14
selected pipe diameter	mm	25.4	25.4	25.4	25.4	25.4	25.4
(7) Calculate percentage pressure drop across sparger							
pressure drop across sparger	Pa	1119	4477	10073	17908	27981	40293
pressure drop across bed	Pa	28510	28510	28510	28510	28510	28510
percentage pressure drop	**%**	**3.9%**	**15.7%**	**35.3%**	**62.8%**	**98.1%**	**141.3%**

Table B.4 - Predicted Sparger Use Summary

Slurry solution	Superficial Gas Velocity in Column					
	5 cm/s	10 cm/s	15 cm/s	20 cm/s	25 cm/s	30 cm/s
0% Solids (% bed pressure drop)	Low (7.6%)	Low (30.4%)	High (34.9%)	High (62.1%)	High (97.0%)	High (139.7%)
10% Solids by Volume (% bed pressure drop)	Low (5.8%)	Low (23.1%)	High (26.6%)	High (47.2%)	High (73.8%)	High (106.2%)
25% Solids by Volume (% bed pressure drop)	Low (4.5%)	Low (18.2%)	Low (40.9%)	High (37.1%)	High (57.9%)	High (83.4%)
40% Solids by Volume (% bed pressure drop)	Low (3.9%)	Low (15.7%)	Low (35.3%)	High (32.0%)	High (50.1%)	High (72.1%)

Low Sparger = sparger designed to meet minimum pressure drop considerations
High Sparger = sparger designed to meet maximum pressure drop considerations

Several verification experiments were ran. Wet and dry pressure drop measurements were conducted and results were compared to theoretical values. Dry pressure drop measurements were initially run in an empty column (i.e. with atmospheric pressure downstream from the sparger). The results for the lower sparger are shown in Figures B.1 and B.2. For the higher gas flowrate system (using the 2.5mm sonic nozzle) shown in Fig. B.1, the measured pressure drop was found to be approximately 15% greater than theoretical values. This error was significantly larger for the lower gas flowrate (using the 1.5mm nozzle) system shown in Fig. B.2. For this case the measured values were found to be 50% greater than theoretical values. The errors were similar for the upper sparger, indicating that problem is more related to sonic nozzle design than sparger design. This increase in pressure drop was gladly received. The 1.5mm nozzle would only be required for low gas flowrates (0.05m/s), however, as seen in Table B.9, the ratio of sparger pressure drop to bed pressure drop for all systems with 0.05m/s superficial gas velocity was less than 10%, thus an increase in pressure drop would be welcomed. Wet pressure drop measurements were then conducted with a gas-liquid system for the lower sparger only and results were compared to the measured dry pressure drops. The results are shown in Figs. B.3 and B.4, representing low and high gas flowrate systems, respectively. The error for both systems was determined to be approximately 5%. This indicates that there is negligible effect of the sparger on the surface tension of the liquid.

The design procedure for the variable height sparger was similar to that of the dual sparger. A diagram is shown in Figure 3.3.

Fig. B.1 - Comparison of Measured Dry Pressure Drop to Theoretical Dry Pressure Drop across the Lower Sparger for higher gas flowrates

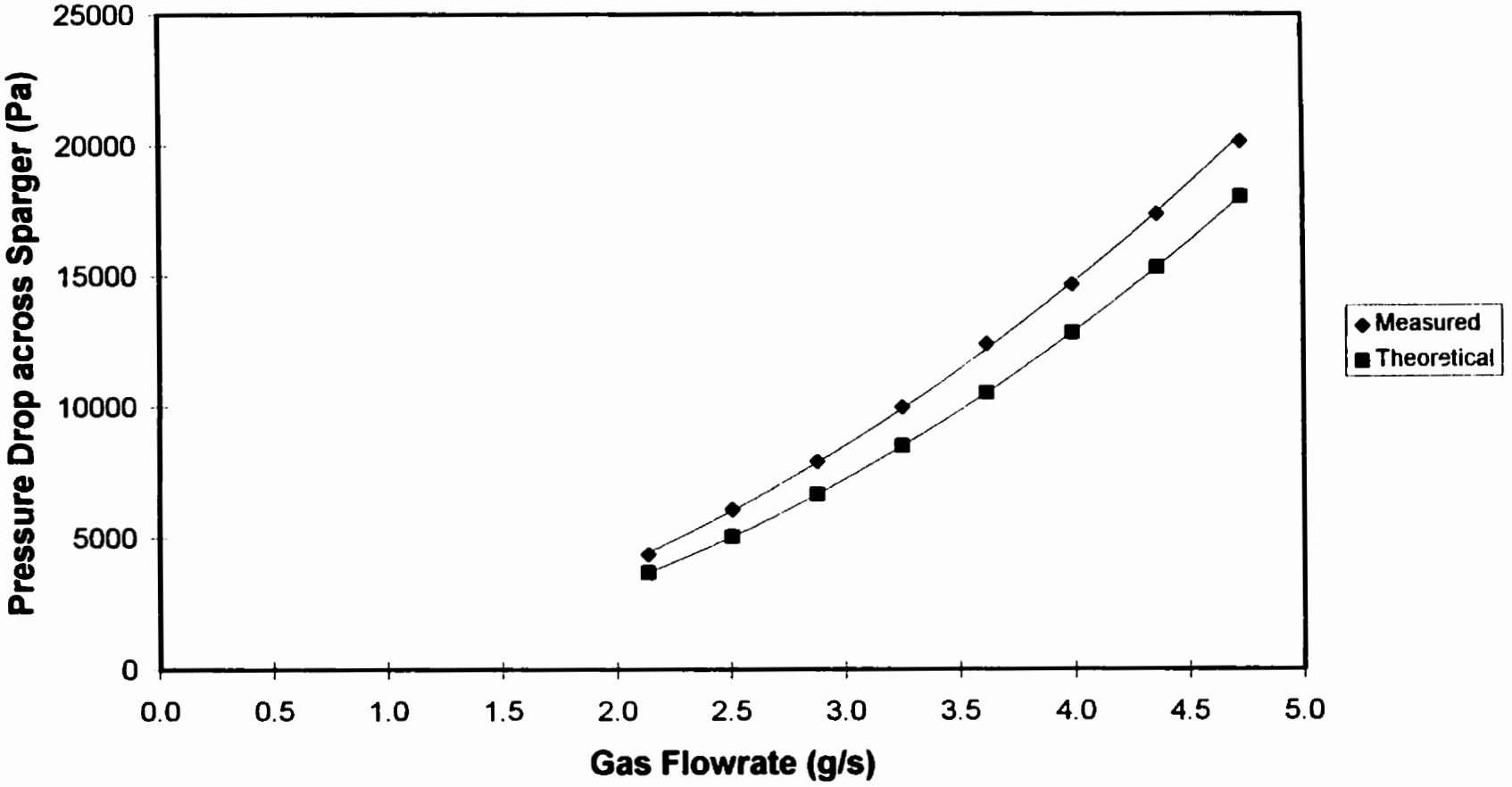

Fig. B.2 - Comparison of Measured Dry Pressure Drop to Theoretical Dry Pressure Drop across the Lower Sparger for lower gas flowrates

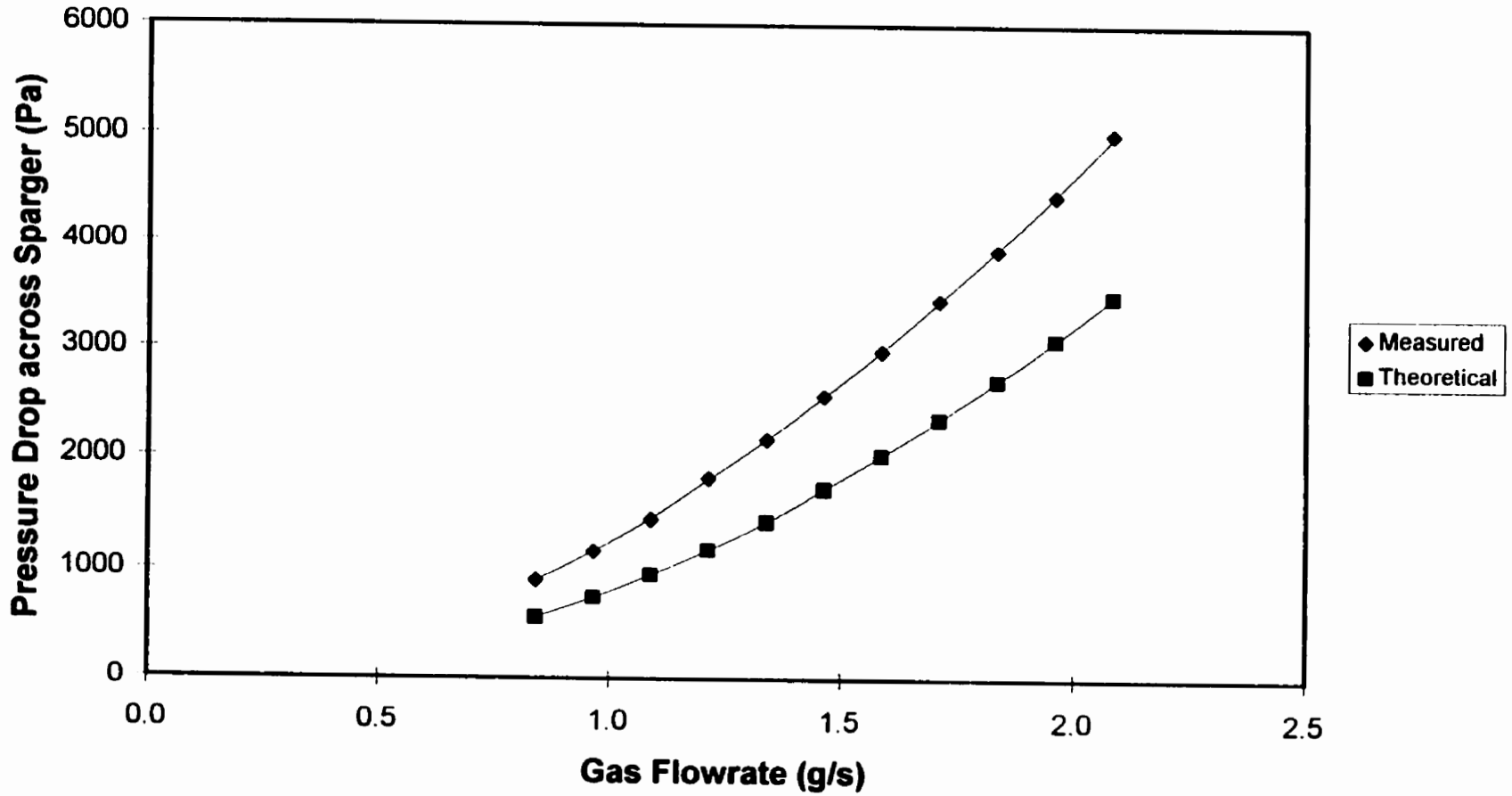

Fig. B.3 - Comparison of Wet and Dry Pressure Drops Measured across the Lower Sparger for lower gas flowrates

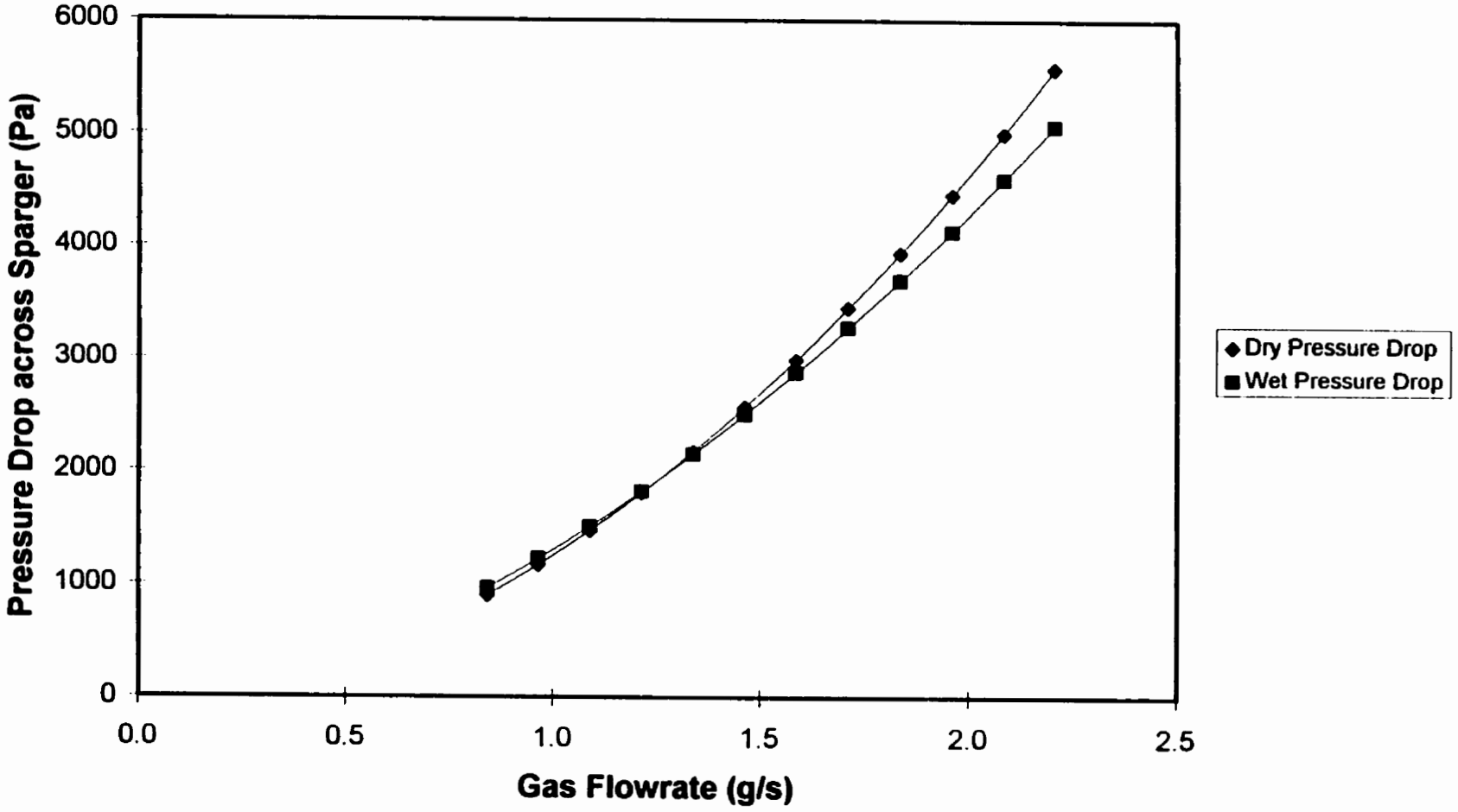

Fig. B.4 - Comparison of Wet and Dry Pressure Drops Measured across the Lower Sparger for higher gas flowrates

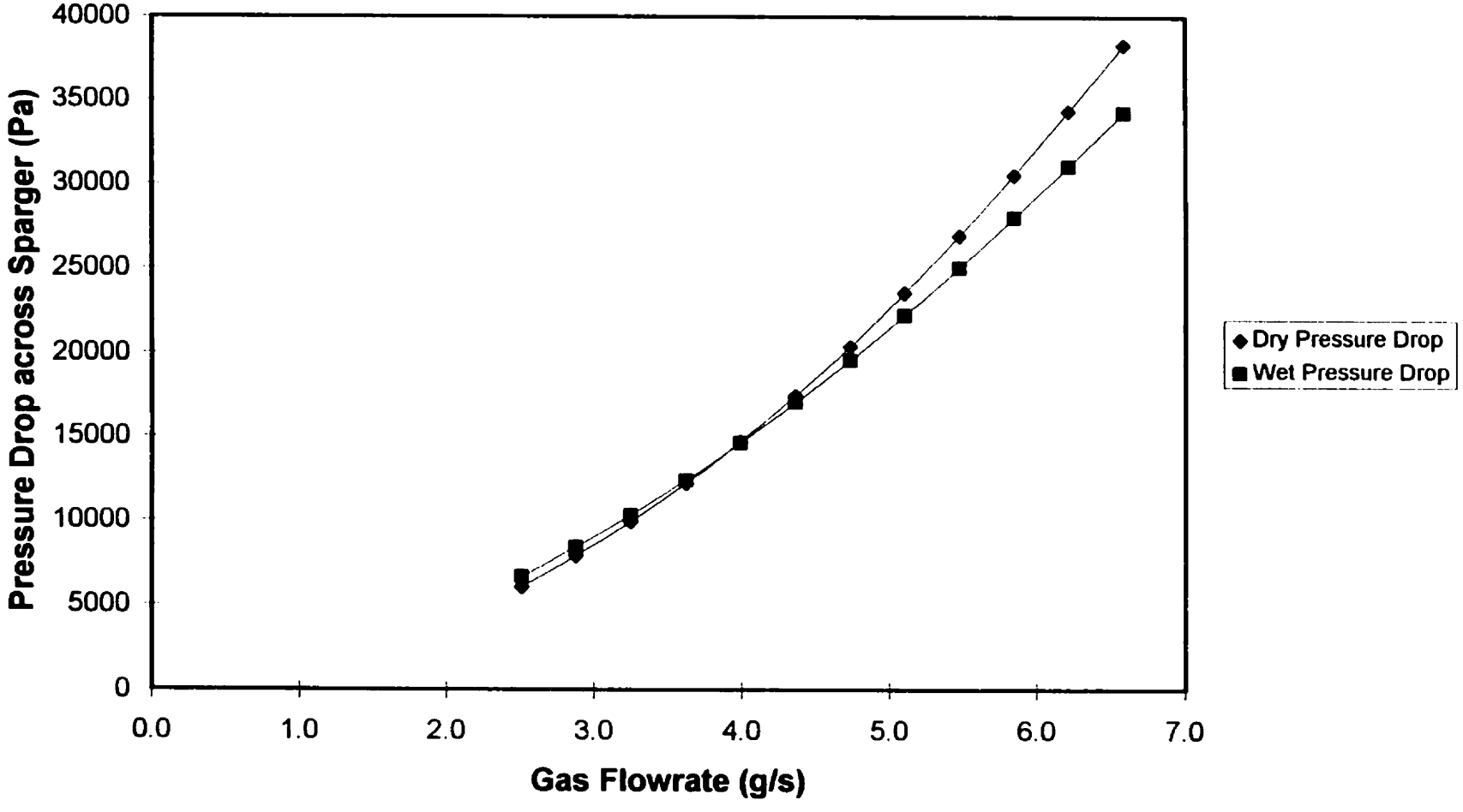

Appendix C - Solids Characteristics and Handling

The glass beads were purchased from Flex-O-Lite Ltd., St. Thomas, Ontario. Various properties were supplied by Flex-O-Lite and are listed in Table C.1. It should be noted that the properties listed are a generalization based on a number of different soda-lime glasses. Therefore, it was decided to re-measure density and particle diameter. The particle density was measured using the pycnometric technique. A known mass of solids was placed in a 1L volumetric cylinder. This was preceded by a small, known volume of water to prevent air pockets from forming. Additional water was then added, filling the cylinder to the 1L mark. By measuring the initial and final masses of the cylinder, it is possible to calculate the exact density of the solids. To measure particle size, special permission was obtained from Dr. Inculet to use the Brinkman Particle Size Analyzer in his laboratory. The Brinkman Particle size analyzer itself uses a laser to measure the particle size distribution. Several independent samples were taken and the results were compared. Typical particle size distribution tables and curves obtained from the Brinkman analyzer for the glass beads are presented in Tables C.2 to C.4 and Figures C.1 to C.3, respectively. The average particle diameter was found to be 35μm.

Since a large amount of solids (500+ lbs) were initially purchased, a proper procedure also had to be used to ensure that the bulk particles were divided into representative workable fractions. Coning and quartering was first used. This method of sample dividing consists of pouring the material into a conical heap and relying on its radial symmetry to give four identical samples when the heap is flattened and divided by a metal cutter. Using this method, we were able to divide the bulk particles into 100-150 lb fractions. A chute splitter was then

Table C.1 - Various Phyical and Chemical Properties of Soda-Lime Glass (from Flex-O-Lite)

Flex-O-Lite manufactures ground Glass from soda-lime glass produced by a number of companies. Since their formulations differ, properties of our ground glass exhibit slight variations. The following properties are a generalization based on a number of different soda-lime glasses:

COMPOSITION: 73% SiO_2; 15% Na_2O; 7% CaO; 4% MgO; 1%Al_2O_3

BULK DENSITY . . . . . 1.5 gcm^{-3}

DENSITY . . . . . 2.5 gcm^{-3}

SOFTENING TEMPERATURE . . . . . 700°C.

YOUNG'S MODULUS. . . . . 72 GPa

POISSON'S RATIO 0.25

THERMAL CONDUCTIVITY @ 0°C. . . . . $10Wcm^{-1}°C^{-1}$

THERMAL CONDUCTIVITY @ 100°C. . . . . $11.2Wcm^{-1}°C^{-1}$

MEAN HEAT CAPACITY (25-175°C.) . . . . . $0.87Jg^{-1}°C^{-1}$

COEFFICIENT OF EXPANSION (0-300°C.) . . . . . $92x10^{-7}$ ($°C^{-1}$)

DIELECTRIC PROPERTIES @ 25°C. & 10Hz
- DIELECTRIC CONSTANT 7.3
- LOSS FACTOR 5.1%
- POWER FACTOR 0.70%

CHEMICAL DURABILITY IN (N/50) H_2SO_4 . . 7.8 (relative units)

FREE SILICA . . . . . NONE

Above information is not to be taken as a warranty or representation for which we assume legal responsibility. It is offered solely for your consideration, investigation and verification.

NOTE: SiO_2 and other constituents CANNOT be separated from the glass by mechanical means.

Table C.2 - Particle Size Volume Distribution Table for Glass Beads (sample # 1)

B r i n k m a n n

Particle Size Analyzer

VOLUME DISTRIBUTION TABLE (RANGES)

SAMPLE NAME : EXP5
FILE NAME : Data Not Saved.

DATE	: 14/08/1996	ACQ. RANGE	: 0.5-150	COUNTS	: 22155
TIME	: 14:21	ACQ. MODE	: SAMPLE	S.N.F.	: 0.74
CONFIG.	: 1 (0.7 S1)	ACQ. TIME	: 110 SEC	S.D.U.	: 2282
CELL TYPE	: MAGNETIC (3)	SAMPLE SIZE	: 2	CONCENTR.	: 9.9E+05 #/ml
SAMPLE TYPE	: REGULAR	REQ. CONF.	: None	SOLIDS	: 2.0E-02 %

RANGE (microns)	LOCAL (%)	UNDER(%)-CUMULATIVE-OVER(%)
0.0 - 1.0	0.06	0.06 99.94
1.0 - 2.0	0.21	0.27 99.73
2.0 - 3.0	0.24	0.50 99.50
3.0 - 4.0	0.37	0.87 99.13
4.0 - 5.0	0.65	1.53 98.47
5.0 - 6.0	0.53	2.06 97.94
6.0 - 7.0	0.32	2.38 97.62
7.0 - 8.0	0.23	2.61 97.39
8.0 - 9.0	0.21	2.83 97.17
9.0 - 10.0	0.17	2.99 97.01
10.0 - 20.0	10.37	13.36 86.64
20.0 - 30.0	29.04	42.41 57.59
30.0 - 40.0	24.39	66.80 33.20
40.0 - 50.0	21.30	88.09 11.91
50.0 - 60.0	6.93	95.03 4.97
60.0 - 70.0	2.85	97.88 2.12
70.0 - 80.0	0.00	97.88 2.12
80.0 - 90.0	0.00	97.88 2.12
90.0 - 100.0	2.12	100.00 0.00
100.0 - 150.0	0.00	100.00 0.00

Fig. C.1 - Particle Volume Density Graph for Glass Beads (sample # 1)

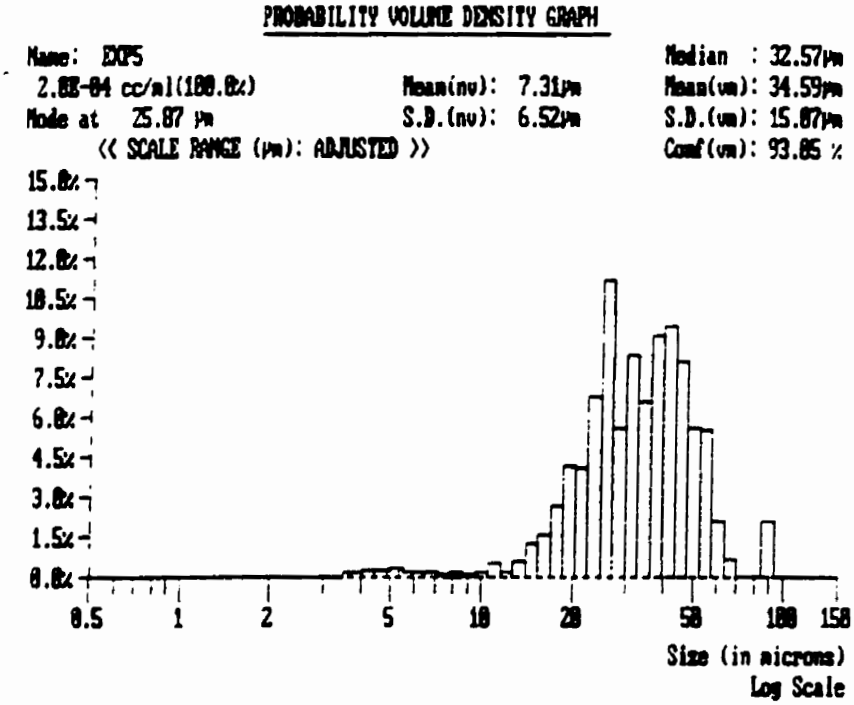

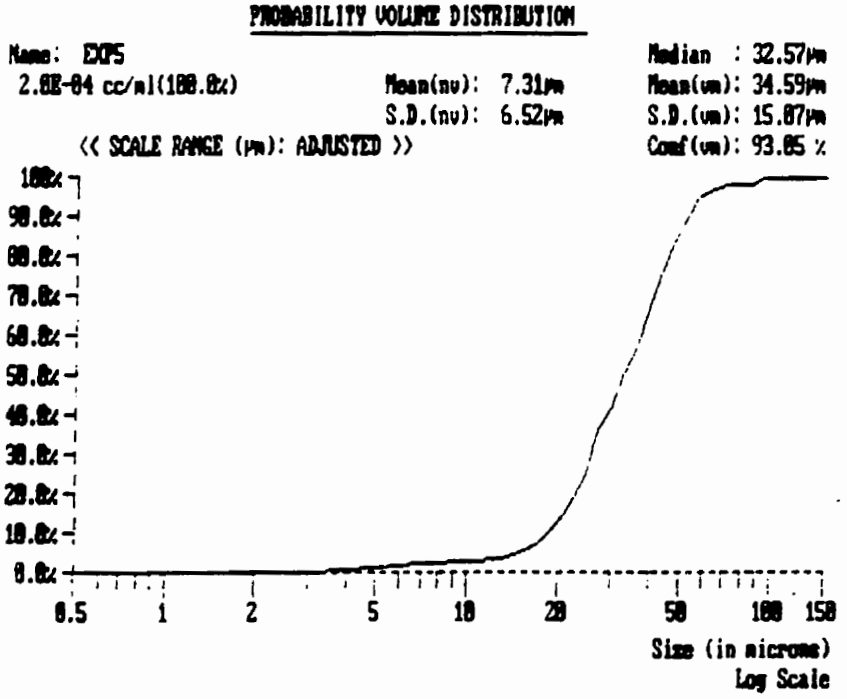

Table C.3 - Particle Size Volume Distribution Table for Glass Beads (sample # 2)

B r i n k m a n n

Particle Size Analyzer

VOLUME DISTRIBUTION TABLE (RANGES)

SAMPLE NAME : EXP10B
FILE NAME : Data Not Saved.

DATE	: 14/08/1996	ACQ. RANGE	: 0.5-150	COUNTS	: 36281
TIME	: 14:57	ACQ. MODE	: SAMPLE	S.N.F.	: 0.78
CONFIG.	: 1 (0.7 S1)	ACQ. TIME	: 353 SEC	S.D.U.	: 2223
CELL TYPE	: MAGNETIC (3)	SAMPLE SIZE	: 2	CONCENTR.	: 1.3E+05 #/ml
SAMPLE TYPE	: REGULAR	REQ. CONF.	: None	SOLIDS	: 1.4E-02 %

RANGE (microns)	LOCAL (%)	UNDER(%)	-CUMULATIVE-	OVER(%)
0.0 - 1.0	0.01	0.01		99.99
1.0 - 2.0	0.03	0.04		99.96
2.0 - 3.0	0.05	0.09		99.91
3.0 - 4.0	0.17	0.26		99.74
4.0 - 5.0	0.17	0.43		99.57
5.0 - 6.0	0.20	0.63		99.37
6.0 - 7.0	0.21	0.84		99.16
7.0 - 8.0	0.14	0.97		99.03
8.0 - 9.0	0.12	1.09		98.91
9.0 - 10.0	0.24	1.33		98.67
10.0 - 20.0	10.08	11.41		88.59
20.0 - 30.0	28.03	39.44		60.56
30.0 - 40.0	27.03	66.47		33.53
40.0 - 50.0	21.03	87.50		12.50
50.0 - 60.0	7.79	95.28		4.72
60.0 - 70.0	3.27	98.56		1.44
70.0 - 80.0	0.66	99.22		0.78
80.0 - 90.0	0.78	100.00		0.00
90.0 - 100.0	0.00	100.00		0.00
100.0 - 150.0	0.00	100.00		0.00

Fig. C.2 - Particle Volume Density Graph for Glass Beads (sample # 2)

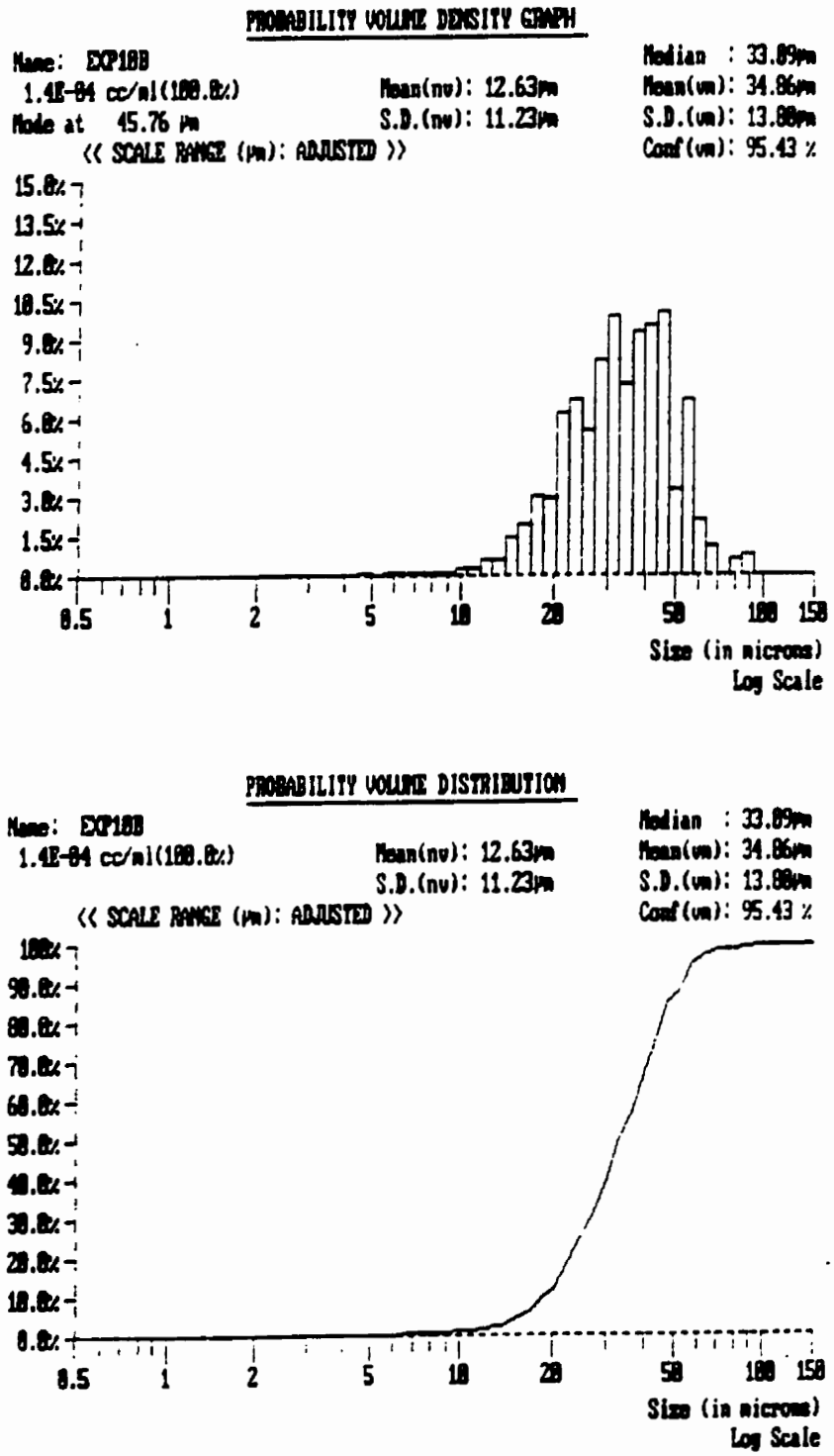

Table C.4 - Particle Size Volume Distribution Table for Glass Beads (sample # 3)

B r i n k m a n n

Particle Size Analyzer

VOLUME DISTRIBUTION TABLE (RANGES)

SAMPLE NAME : EXP5B
FILE NAME : Data Not Saved.

DATE	: 14/08/1996	ACQ. RANGE	: 0.5-150	COUNTS	: 32328
TIME	: 14:34	ACQ. MODE	: SAMPLE	S.N.F.	: 0.77
CONFIG.	: 1 (0.7 S1)	ACQ. TIME	: 141 SEC	S.D.U.	: 2436
CELL TYPE	: MAGNETIC (3)	SAMPLE SIZE	: 2	CONCENTR.	: 6.7E+05 #/ml
SAMPLE TYPE	: REGULAR	REQ. CONF.	: None	SOLIDS	: 2.3E-02 %

RANGE (microns)	LOCAL (%)	UNDER(%)	-CUMULATIVE-	OVER(%)
0.0 - 1.0	0.03	0.03		99.97
1.0 - 2.0	0.13	0.16		99.84
2.0 - 3.0	0.16	0.32		99.68
3.0 - 4.0	0.31	0.63		99.37
4.0 - 5.0	0.40	1.03		98.97
5.0 - 6.0	0.29	1.31		98.69
6.0 - 7.0	0.22	1.53		98.47
7.0 - 8.0	0.23	1.76		98.24
8.0 - 9.0	0.20	1.96		98.04
9.0 - 10.0	0.19	2.15		97.85
10.0 - 20.0	9.57	11.72		88.28
20.0 - 30.0	29.86	41.58		58.42
30.0 - 40.0	27.73	69.31		30.69
40.0 - 50.0	19.58	88.89		11.12
50.0 - 60.0	4.73	93.61		6.39
60.0 - 70.0	3.93	97.54		2.46
70.0 - 80.0	1.21	98.75		1.25
80.0 - 90.0	1.25	100.00		0.00
90.0 - 100.0	0.00	100.00		0.00
100.0 - 150.0	0.00	100.00		0.00

Fig. C.3 - Particle Volume Density Graph for Glass Beads (sample # 3)

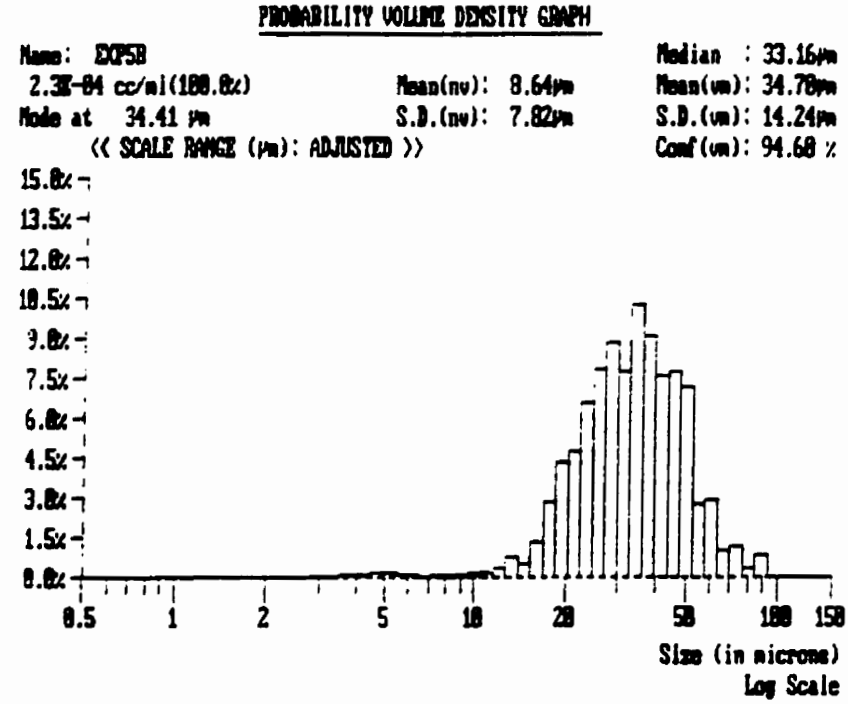

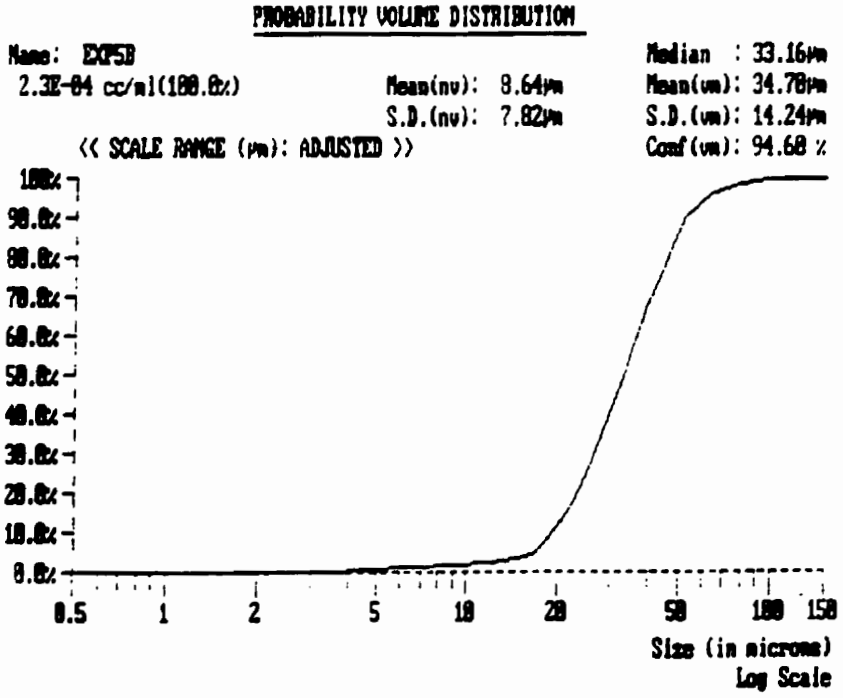

employed to further reduce the workable fractions to 35 lbs. The chute splitter consists of a V-shaped trough along the bottom of which is a series of chutes alternately feeding two trays placed on either side of the trough. Finally, a table sampler was used to reduce samples to 3-5 lbs each. For this method, the material is fed to the top of an inclined plane in which there are a series of holes. Prisms placed in the path of the stream break it into smaller fractions. Some powder falls through the holes while the remaining powder on the plane passes on to the next row of prisms and holes. When smaller samples were still required (like for the Brinkman Particle Size Analyzer), a particle riffling machine was used.

To study particle settling effects, a simple test was run with 15vol% solids in the system and an initial superficial gas velocity of 0.10m/s and sparger height of 10cm above the base. Once mixing was achieved, the gas flow was shut off and solids samples were taken from Probe # 3 every five minutes. After an hour the frequency of samples was reduced. The results are shown in Fig. C.4. Two distinct regions of settling are observed. It takes approximately one hour for 90% of the solids to settle to 2vol%, after which the settling is very slow. Another sample was taken after 1300 minutes (24 hours) which is not shown on the graph and the dispersed solids was still calculated to be 1.3vol%.

During experimental runs, initial static solids heights (or settled heights) were also recorded. A calibration curve of static solids height as a function of slurry concentration is presented in Fig. C.5. This was useful in determining dispersed solids concentrations for sparger height variation runs.

Fig. C.4 - Solids Settling Rate Characteristics with 15% average solids concentration and an initial superficial velocity of 0.10 m/s

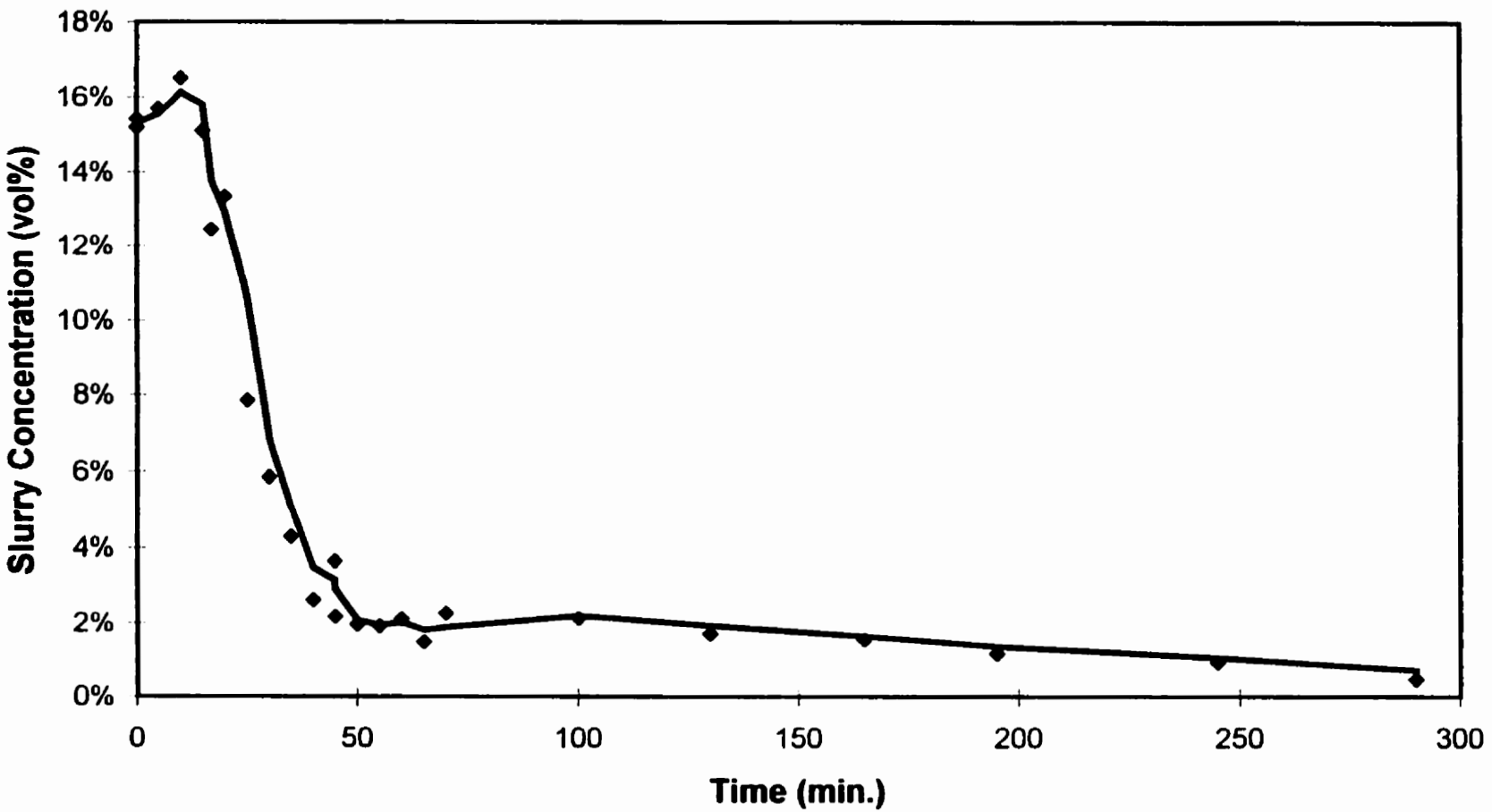

Fig. C.5 - Calibration curve for static solids height in column with a total bed height of 1.5m

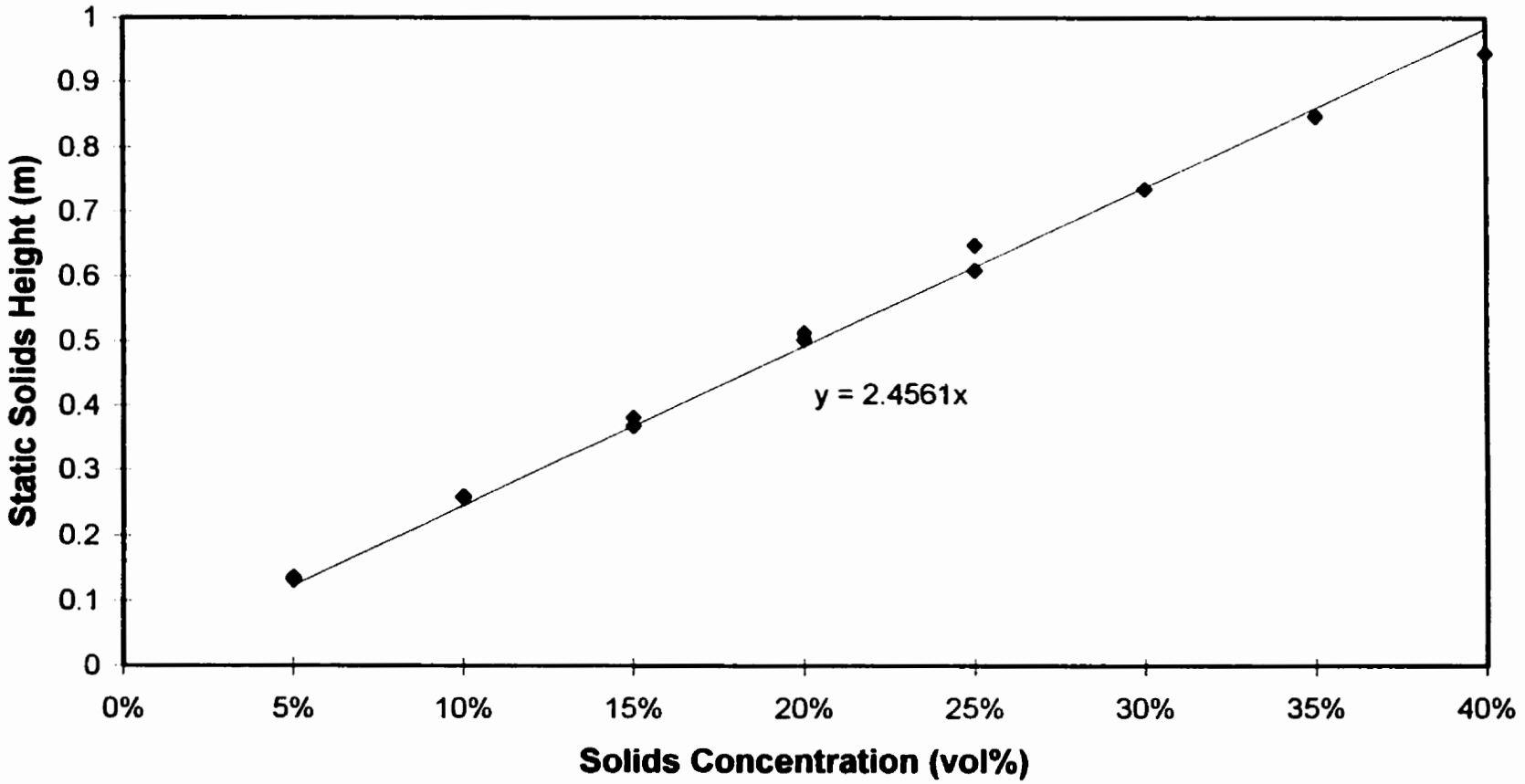

Appendix D - Gas Holdups Calculations

A schematic for liquid filled manometers and U-tube manometers are presented in Figures D.1 and D.2, respectively. We should also note that there is a constant backpressure (P*) being applied to each system.

Liquid filled manometers

let $\Delta z = (z_2 - z_1)$ and $\Delta y = (y_2 - y_1)$ and $\Delta P = (P_2 - P_1)$

$P_2' = P_2 + \rho_l g h = P^* + \rho_l y_2 g$

$P_1' = P_1 + \rho_l g (h - \Delta z) = P^* + \rho_l y_1 g$

therefore, we get

$P_2' = P_2 + \rho_l g h = P^* + \rho_l y_2 g$ (D.1)

$P_1' = P_1 + \rho_l g (h - \Delta z) = P^* + \rho_l y_1 g$ (D.2)

take (D.1) - (D.2) to get

$(P_2 - P_1) + \rho_l g \Delta z = \rho_l g (y_2 - y_1)$

$\therefore \Delta P + \rho_l g \Delta z = \rho_l g \Delta y$

rearranging, we get

$$\frac{\Delta P}{\Delta z} = \rho_l g\left(\frac{\Delta y}{\Delta z} - 1\right) \qquad \text{(D.3)}$$

Figure D.1 - Schematic for two adjacent liquid filled pressure taps

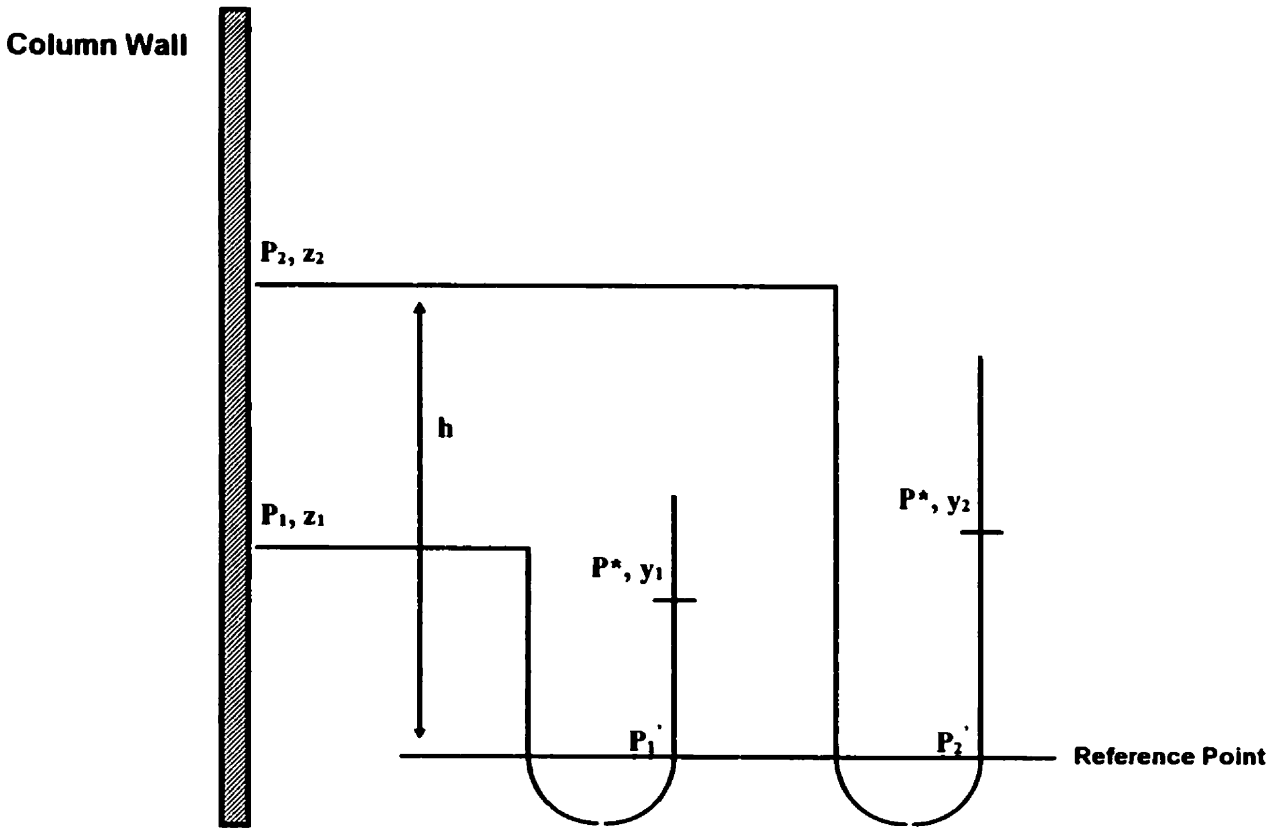

Figure D.2 - Schematic for two adjacent U-tube pressure taps

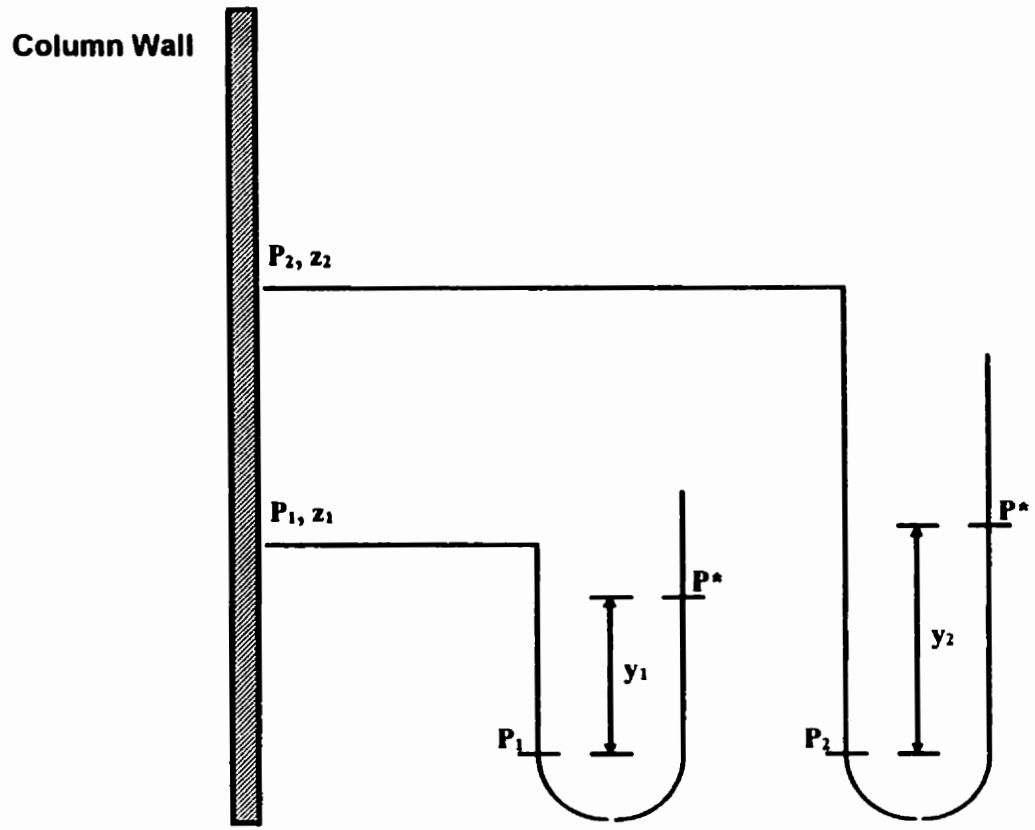

but

$$-\frac{\Delta P}{\Delta z} = g\left(\rho_l \varepsilon_l + \rho_g \varepsilon_g\right)$$

we can assume ($\rho_g \varepsilon_g$) to be negligible, therefore

$$-\frac{\Delta P}{\Delta z} = \rho_l \varepsilon_l g \qquad \text{(D.4)}$$

substituting (D.4) into (D.3), we get

$$-\rho_l \varepsilon_l g = \rho_l g \left(\Delta y/\Delta z - 1\right)$$

finally, by canceling like terms and substituting $\varepsilon_l = 1 - \varepsilon_g$ we get

$$\varepsilon_g = \left(\Delta y / \Delta z\right) \qquad \text{(D.5)}$$

Thus, the gas holdup can be calculated by taking a ratio of pressure differential (in mm H_2O) to the height difference of the pressure taps.

U-tube manometers

let $\Delta z = (z_2 - z_1)$ and $\Delta y = (y_2 - y_1)$ and $\Delta P = (P_2 - P_1)$

since the liquid in the manometers need not be the same as the liquid in the column, we will give this fluid a subscript 'f'.

$$P_2 = P^* + \rho_f y_2 g \qquad (D.6)$$

$$P_1 = P^* + \rho_f y_1 g \qquad (D.7)$$

take (D.6) - (D.7) to get

$$(P_2 - P_1) = \rho_f g (y_2 - y_1)$$

rearranging, we get

$$\frac{\Delta P}{\Delta z} = \rho_f g\left(\frac{\Delta y}{\Delta z}\right) \qquad (D.8)$$

but

$$-\frac{\Delta P}{\Delta z} = g\left(\rho_l \varepsilon_l + \rho_s \varepsilon_s + \rho_g \varepsilon_g\right)$$

let the dispersion density (ρ_d) in the column be

$$\rho_d = \left(\rho_l \varepsilon_l + \rho_s \varepsilon_s + \rho_g \varepsilon_g\right)$$

therefore, we get

$$-\frac{\Delta P}{\Delta z} = \rho_d g \qquad \text{(D.9)}$$

substituting (D.9) into (D.8), we get

$- \rho_d g = \rho_f g (\Delta y/\Delta z)$

finally, by simplifying we get

$$\left(\Delta y / \Delta z\right) = \left(-\rho_d / \rho_f\right) \qquad \text{(D.10)}$$

For a gas-liquid only system, $\varepsilon_s = 0$, therefore the dispersion density may be simplified to

$\rho_d = \rho_g \varepsilon_g + \rho_l \varepsilon_l$

also, we can assume $(\rho_g \varepsilon_g)$ to be negligible, therefore

$\rho_d = \rho_l \varepsilon_l$

substituting into (D.10) we get

$$\left(\Delta y / \Delta z\right) = \left(-\rho_l \varepsilon_l / \rho_f\right)$$

furthermore, assuming the fluid in the manometers is the same as the fluid in the column (i.e. $\rho_f = \rho_l$), we get

$$\varepsilon_l = \left(\Delta y / \Delta z\right)$$

finally, substituting $\varepsilon_l = 1 - \varepsilon_g$ we get

$$\varepsilon_g = 1 + \left(\Delta y / \Delta z\right) \qquad \text{(D.11)}$$

Thus for a gas-liquid only system, the gas holdup can also be calculated by taking the a ratio of pressure differential (in mm H_2O) to the height difference of the pressure taps.

For a gas-liquid-solid system, the derivation is more complicated. Let us define the dispersion density (ρ_d) as the density of the mixture including air and slurry density (ρ_{sl}) as the density of the mixture without air. Therefore, we have

$$\rho_d = \frac{m_s + m_l + m_g}{V_s + V_l + V_s} \qquad \text{(D.12)}$$

and $$\rho_{sl} = \frac{m_s + m_l}{V_s + V_l} \qquad \text{(D.13)}$$

multiply (D.12) by V_g to get

$$\rho_d = \left(\frac{V_g}{V_s + V_l + V_g}\right)\left(\frac{m_s + m_l + m_g}{V_g}\right)$$

but $\varepsilon_g = \left(\frac{V_g}{V_s + V_l + V_g}\right)$, therefore we have

$$\rho_d = \varepsilon_g\left(\frac{m_s + m_l + m_g}{V_g}\right)$$

$$\therefore\ \rho_d = \varepsilon_g\left(\frac{m_s + m_l}{V_g} + \rho_g\right)$$

multiply by ($V_s + V_l$) to get

$$\rho_d = \varepsilon_g\left(\left(\frac{m_s + m_l}{V_s + V_l}\right)\left(\frac{V_s + V_l}{V_g}\right) + \rho_g\right)$$

substituting (D.13) and multiply by V_T to get

$$\rho_d = \varepsilon_g\left(\rho_{sl}\left(\frac{V_s + V_l}{V_T}\right)\left(\frac{V_T}{V_g}\right) + \rho_g\right) \qquad \text{(D.14)}$$

now, we have $\varepsilon_l + \varepsilon_g + \varepsilon_s = 1$, therefore

$$\varepsilon_g + \frac{V_s}{V_T} + \frac{V_l}{V_T} = 1$$

$$\therefore \frac{V_s + V_l}{V_T} = 1 - \varepsilon_g$$

furthermore, $(V_g/V_T) = \varepsilon_g$, therefore substituting into (D.14) yields

$$\rho_d = \varepsilon_g\left(\rho_{sl}\left(\frac{1 - \varepsilon_g}{\varepsilon_g}\right) + \rho_g\right)$$

therefore, rearranging and simplifying yields the following

$$\varepsilon_g = \left(\frac{\rho_d - \rho_{sl}}{\rho_g - \rho_{sl}} \right)$$

and, finally, since $\rho_{sl} >> \rho_g$ we can simplify to

$$\varepsilon_g = \left(1 - \frac{\rho_d}{\rho_{sl}} \right) \qquad \text{(D.15)}$$

The dispersion density can be calculated using equation (D.10) by taking a ratio of pressure differential (in mm H_2O) to the height difference of the pressure taps and multiplying by the density of the fluid in the manometers. The slurry density would have to be calculated by taking axial slurry samples and plotting an axial slurry density (concentration) profile.

References

Abramovich, G.N., (1963), "Theory of Turbulent Jets", MIT Press, Cambridge

Achwal, S.K. and J.B. Stepanek, (1975), "An Alternative Method of Determining Holdup in Gas-Liquid Systems", Chem. Eng.Sci., **30,** 1443

Akita, K. and F. Yoshida, (1973), "Gas Holdup and Volumetric Mass Transfer Coefficient in Bubble Columns", Ind. Eng. Chem. Proc. Des. Dev., **12(1),** 76-80

Bach, H.F., and T. Pilhofer, (1978), "Variation of Gas Holdup in Bubble Columns with Physical Properties of Liquids and Operating Parameters", Ger. Chem. Eng., **1**, 270-275

Barnea, E. and J. Mizrahi, (1973), Chem. Eng. Journ., **5,** 171-189

Batchelor, G.K., (1953), "The Theory of Homogeneous Turbulence", Cambridge University Press, Cambridge

Begovich, M. and J.S. Watson, (1978), "An Electroconductivity Method for the Measurement of Axial Variation of Holdups in Three-Phase Fluidized Beds", AIChE Journ., **24,** 351-354

Bhatia, V.K. and N. Epstein, (1974), "In Fluidization and its Applications", Wiley, New York

Briens, C., (1991), "E.S. 496 Class Notes: Procedure #1 - Design of Sparger Distributor", The University of Western Ontario, London

Briens, C., (1993), "E.S. 496 Class Notes: Procedure #6 - Design and Calibration of Sonic Nozzle Flowmeters", The University of Western Ontario, London

Brown, D.M., (1984), "Modelling of Methanol Synthesis in the Liquid Phase", IChemE Symp. Ser., **87,** 699-708

Bukur, D.B. and J.G. Daly, (1987), "Gas Holdup in Bubble Columns for Fischer-Tropsch Synthesis", Chem. Eng. Sci., **42(12),** 2967-2969

Bukur, D.B., S.A. Patel and R. Matheo, (1987), "Hydrodynamic Studies in Fischer-Tropsch Derived Waxes in a Bubble Column", Chem. Eng. Comm., **60,** 63-78

Bukur, D.B. and S.A. Patel, (1989), "Hydrodynamic Studies with Foaming and Non-Newtonian Solutions in Bubble Columns", Can. Journ. Chem. Eng., **67,** 741-751

Bukur, D.B., S.A. Patel and J.G. Daly, (1990), "Gas Holdup and Solids Dispersion in a Three-Phase Slurry Bubble Column", AIChE Journ., **36(11),** 1731-1735

Catros, A., (1986), "Hydrodynamics and Mass Transfer in Bubble Columns and Three-Phase Fluidized Beds with and without Baffles", Ph.D Thesis, Univ. of Western Ont., London

Chabot, J., (1993), "Fluid Dynamics of High Temperature Bubble and Slurry Bubble Columns", Ph.D Thesis, Univ. of Western Ont., London

Chang, J.S. and G.D. Harvel, (1992), "Determination of Gas-Liquid Bubble Column Instantaneous interfacial Area and Void Fraction by a Real-Time Neutron Radiography Method", Chem. Eng. Sci., **47(13/14),** 3639-3646

Chen, R.C., and L.S. Fan, (1992), " Particle Image Velocimetry for Characterizing the Flow Structure in Three-Dimensional Gas-Liquid-Solid Fluidized Beds", Chem. Eng. Sci., **47(13/14),** 3615-3622

Chen, R.C., J. Reese and L.S. Fan, (1994), "Flow Structures in a Three-Dimensional Bubble Column and Three Phase Fluidized Bed", AIChE Journ., **40(7),** 1093-1104

Clark, K.N., (1990), "The Effect of High Pressure and Temperatures on Phase Distribution in a Bubble Column", Chem. Eng. Sci., **45,** 2301-2307

Cova, D.R., (1966), "Catalytic Suspension in Gas-Agitated Tubular Reactors", Ind. Eng. Chem. Proc. Des. Dev, **5,** 20

Darton, R.C. and D. Harrision, (1975), "Gas and Liquid Holdup in Three-Phase Fluidization", Chem. Eng. Sci., **30,** 581

Daly, J.G., S.A. Patel and D.B. Bukur, (1992), "Measurement of Gas Holdups and Sauter Mean Bubble Diameters in Bubble Column Reactors by Dynamic Gas Disengagement Method", Chem. Eng. Sci., **47(13/14),** 3647-3654

de Lasa, H.I., S.L.P. Lee and M.A. Bergougnou, (1984), "Bubble Measurement in Three Phase Fluidized Beds Using U-Shaped Optical Fiber Probe", Can. Journ. Chem. Eng., **62,** 165

Deckwer, W., Y. Louisi, A. Zaldi and M. Raiek, (1980), "Hydrodynamic Properties of the Fischer-Tropsch Slurry Process", Ind. Eng. Chem. Proc. Des. Dev., **19,** 699-708

Deckwer, W. and A. Schumpe, (1993), "Improved Tools for Bubble Column Reactor Design and Scale-up" Chem. Eng. Sci., **48(5),** 889-911

Del Pozo, M., C.L. Briens and G. Wild, (1992), "Effect of Column Inclination on the Performance of Three-Phase Fluidized Beds", AIChE Journ., **38(8),** 1206-1212

Dhanuka, V.R. and J.B. Stepanek, (1978), "Gas and Liquid Holdup and Pressure Drop Measurements in a Three-Phase Fluidized Bed", Fluidization, Cambridge University Press, 179-183

Dudukovic, M.P. and N. Devanathan, (1992), "Bubble Column Reactors: Some Recent Developments", Nato-ASI Symposium Series, Kluwer Publishing

El-Temtamy, S.A. and N. Epstein, (1978), "Bubble Wake Solids Content in Three-phase Fluidized Beds", Int. Journ. Multiphase Flow, **4,** 19

El-Temtamy, S.A. and N. Epstein, (1980), "Simultaneous Solids Entrainment and De-entrainment Above a Three Phase Fluidized Bed", In Fluidization, Pleanum Publishing, New York

Epstein, N., (1981), "Three-Phase Fluidization: Some Knowledge Gaps", Can. Journ. Chem. Eng., 59

Fan, L.S., A. Matsuura and S.H. Chern, (1985), "Hydrodynamic Characteristics of a Gas-Liquid-Solid Fluidized Bed Containing a Binary Mixture of Particles", AIChE Journ., **31,** 1801

Fan, L.S., S. Satija and K. Wisecarver, (1986a), "Pressure Fluctuation Measurements and Flow Regime Transitions in Gas-Liquid-Solid Fluidized Beds", AIChE Journ., **32,** 338

Fan, L.S., F. Bavarian, R. Gorawara, B. Kreischer, R.D. Buttke and L.E. Peck, (1986b), "Hydrodynamics of Gas-Liquid-Solid Fluidization Under High Gas Holdup Conditions", AIChE Mtg., Miami Beach

Fan, L.S., R.H. Jean and K. Kitano, (1987), "On the Operating Regimes of Cocurrent upward Gas-Liquid-Solid Systems with liquid as the Continuous Phase", Chem. Eng. Sci., **42,** 1853-1855

Fan, L.S., (1989), "Gas-Liquid-Solid Fluidization", Butterworths, Boston

Fischer, J., H. Kumazawa and E. Sada, (1994), "On the Local Gas Holdup and Flow Pattern in Standard-Type Bubble Columns", Chem. Eng. Proc., 33, 7-21

Godbole, S.P.. S. Joseph and Y.T. Shah, (1984), Can. Journ. Chem. Eng., **62,** 440-445

Grover, G.S., C.V. Rode and R.V. Chaudhari, (1986), "Effect of Temperature on Flow Regimes and Gas Holdup in a Bubble Column", Can. Journ. Chem. Eng., **64,** 501

Guy, C., P.J. Carreau and J. Paris, (1986), "Mixing Characteristics and Gas Hold-Up of a Bubble Column", Can. Journ. Chem. Eng., **64,** 23-35

Hardy, J.E. and J.O. Hylton, (1984), "Electrical Impedance String Probes for Two Phase Void and Velocity Measurements", Int. Journ. Multiphase Flow, **1,** 541-556

Harvel, G.D. and J.S. Chang, (1992), "Determination of Time Dependent Void Distributions Using a Real Time Neutron Radiography Method in Gas-Liquid Two Phase Flow", Proceeding of 6th Miami Int. Heat Trans. Conf., New York

Hatate, Y., H. Nomura, T. Fujita, S. Tajiri and A. Ikari, (1986), "Gas Holdup and Pressure Drop in Three-Phase Horizontal Flows of Gas-Liquid-Fine Solid Particles System", Journ. Chem. Eng. Japan, **19(4),** 330-335

Hewitt, G.F., (1978), "Measurement of Two Phase Flow Parameters", Academic Press, New York

Hewitt, G.F., (1982), "Handbook of Multiphase Systems", McGraw Hill Book Company

Hikita, H., S. Asai, K. Tanigawa, K. Segawa and M. Kitao, (1980), "Gas Hold-up in Bubble Columns", Chem. Eng. Journ., **20,** 59-67

Hills, J.H., (1974), "Radial Non-uniformity of Velocity and Voidage in a Bubble Column", Trans IChemE., **52,** 1-8

Hills, J.H., (1976), "The Operation of a bubble Column at High Throughputs: Gas Holdup Measurements", Chem. Eng. Journ., **12,** 89

Hinze, J.O., (1959), "Turbulence", McGraw Hill, New York

Hinze, J.O., (1972), "Turbulent Fluid and Particle Interaction", Prog. Heat Mass Trans., **6,** 433-452

Hu, T.T., B.T. Yu and Y.P. Wang, (1986), "Holdups and Models of Three Phase Fluidized Beds", Fluidization V, Engineering Foundation, New York, 338-360

Hudson, C.L., (1996), "Effect of Inclination on Hydrodynamics in Bubble Columns and Fluidized Beds", Ph.D Thesis, Univ. of Western Ont., London

Hughmark, G.A., (1967), "Holdup and Mass Transfer in Bubble Columns", Int. Eng.Chem. Proc. Des. Dev., **6(2),** 218-220

Idogawa, K., K. Ikeda, T. Fukuda and S. Morooka, (1986), "Behaviour of Bubbles of the Air-Water System in a Column Under High Pressure", Int. Chem. Eng., **26(3),** 468-474

Idogawa, K., K. Ikeda, T. Fukuda and S. Morooka, (1987), "Effect of Gas and Liquid Properties on the Behaviour of Bubbles in a Column Under High Pressure", Int. Chem. Eng., **27(1),** 93-99

Ishida, M. and H. Tanaka, (1982), "An Optical Probe to Detect Both Bubles and Suspended Particles in a Three Phase Fluidized Bed", Journ. Chem. Eng. Japan, **15,** 389

Jean, R.H., W.T. Tang and L.S. Fan, (1989), "The Sedimentation-Dispersion Model for Slurry Bubble Columns", AIChE Journ., **35(4),** 662-665

Kara, S., B.G. Kelkar, Y.T. Shah and N.L. Carr, (1982), "Hydrodynamics and Axial Mixing in a Three-Phase Bubble Column", Ind. Eng. Chem. Proc. Des. Dev., **21,** 584-594

Kato, Y., A. Nishiwaki, T. Fukuda and S. Tanaka, (1972), "The Behaviour of Suspended Solid Particles and Liquid in Bubble Columns", Journ. Chem. Eng. Japan, **5(2),** 112-118

Kato, Y., A. Nishiwaki, T. Kago, T. Fukuda and S. Tanaka (1973), "Gas Holdup and Overall Volumetric Absorption Coefficient in Bubble Columns with Suspended Solid Particles. Absorption Rate of Oxygen by an Aqueous Solution of Sodium Sulfite", Int. Chem. Eng., **13(3),** 562-567

Kato, Y., K. Uchida, T. Kago and S. Morooka, (1981), "Liquid Holdup and Heat Transfer Coefficient Between Bed and Wall in Liquid-Solid and Gas-Liquid-Solid Fluidized Beds", Powder Tech., **2,** 173-179

Kato, Y., S. Morooka, T. Kago, T. Saruwatari and S. Yang, (1985), "Axial Holdup Distributions of Gas and Solid Particles in Three-Phase Fluidized Bed for Gas-Liquid (Slurry)-Solid Systems", Journ. Chem. Eng. Japan, 18(4), 308-312

Kawagoe, K., T. Inoue, K. Nakao and T. Otake, (1976), "Flow Pattern and Gas Holdup Conditions in Gas Sparged Contactors", Journ. Chem. Eng. Japan, **8,** 254-256

Kelkar, B.G., S.P. Godbole, M.F. Honath, Y.T. Shah, N.L. Carr and W.D. Deckwer, (1983), "Effect of Addition of Alcohols on Gas Holdup and Backmixing in Bubble Columns", AIChE Journ., **29(3),** 361-369

Kelkar, B.G., Y.T. Shah and N.L. Carr, (1984), "Hydrodynamics and Axial Mixing in a Three-Phase Bubble Column. Effects of Slurry Properties", Ind. Eng. Chem. Proc. Des. Dev., **23,** 308-313

Khare, A.S. and J.B. Joshi, (1990), "Effect of Fine Particles on Gas Holdup in Three Phase Sparged Reactors", Chem. Eng. Journ., **44,** 11-25

Kim, S.D., C.G.J. Baker and M.A. Bergougnou, (1972), "Hold-up and Axial Mixing Characteristics of Two and Three-Phase Fluidized Beds", Can. Journ. Chem. Eng., **50,** 695

Kim, S.D. and C.H. Kim, (1983), "Axial Dispersion Characteristics of Three-Phase Fluidized Beds", Journ. Chem. Eng. Japan, **16(3),** 172-178

Kim, K.S. and P.K. Agarwal, (1992), " Bubble Velocity in Fluidized Beds: The Effect of Non-Vertical Bubble Rise on its Measurement using Submersible Probes and its Relationship with Bubble Size", Powder Tech., **69,** 239-248

Kleijntjens, R.H., R.G.J.M. van der Lans and K.C.A.M. Luyben, (1994), "Particle Suspension Hydrodynamics in a Tapered Gas Agitated Reactor", Can. Journ. Chem. Eng., **72,** 392-404

Klug, P. and A. Vogelpohl, (1986), "Bubble Formation at Sieve Plates - Effects on Gas Holdup in Bubble Columns", Ger. Chem. Eng., **9,** 93-101

Koide, K., A. Takazawa, M. Komura and H. Matsunaga, (1984), "Gas Holdup and Volumetric Liquid-Phase Mass Transfer Coefficient in Solid Suspended Bubble Columns", Journ. Chem. Eng. Japan, **17(5),** 459-466

Koide, K., (1996), "Design Parameters of Bubble Column Reactors With and Without Solid Suspensions", Journ. Chem. Eng. Japan, **29(5),** 745-759

Kojima, H. and K. Asano, (1981), "Hydrodynamic Characteristics of a Suspension-Bubble Column", Int. Chem. Eng., **21(3),** 473-481

Kojima, H., H. Anjyo and Y. Mochizuki, (1986), "Axial Mixing in Bubble Column with Suspended Solid Particles", Journ. Chem. Eng. Japan, **19(3),** 232-234

Kojima, H., B. Okumura and A. Nakamura, (1991), "Effect of Pressure on Gas Holdup ina Bubble Column and a Slurry Bubble Column", Journ. Chem. Eng. Japan, **24(1),** 115-117

Krishna, R., P.M. Wilkinson and L.L. van Dierendonck, (1991), "A model for Gas Holdup in Bubble Columns Incorporating the Influence of Gas Density on Flow Regime Transitions", Chem. Eng. Sci., **46,** 2491-2496

Kurten, H. and P. Zehner, (1979), "Slurry Reactors", Ger. Chem. Eng., **2,** 220-227

Lamont, A.G.W., (1985), "Air Agitation and Pachuca Tanks", Can. Journ. Chem. Eng., **36,** 153-160

Lee, S.L.P., H.I. de Lasa and M.A. Bergougnou, (1984), "Bubble Phenomenon in Three Phase Fluidized Beds as Viewed by a U-Shaped Fiber Optic Probe", AIChE Symp. Ser. 80, **241,** 110

Lee, Y.H., Y.J. Kim, B.G. Kelkar and C.B. Weinberger, (1985), "A Simple Digital Sensor for Dynamic Gas Holdup Measurements in Bubble Columns", Ind. Eng. Chem. Fundam., **24(1),** 105-107

Lee, S.L.P., (1986), "Bubble Dynamics in Three Phase Fluidized Beds", Ph.D Thesis, Univ. of Western Ont., London

Lee, S.L.P. and H.I. de Lasa, (1987), "Phase Holdups in Three Phase Fluidized Beds", AIChE Journ., **33,** 1359

Leibsan, I., E.G. Holcomb, A.G. Cacoso and J.J. Jacmic, (1956), "Rate of Flow and Mechanics of Bubble Formation from Single Submerged Orifices", AIChE Journ., **2(3),** 296-306

Leung, L.S., (1980), "Vertical Pneumatic Conveying: A Flow Regime Diagram and a Review of Choking versus Non-choking systems", Powder Tech., **25,** 185-190

Lewnard, J.J., T.H. Hsiung, J.F. White and D.M. Brown, (1990), "Single-step Synthesis of Dimethyl Ether in a Slurry Reactor", Chem. Eng. Sci., **45(8),** 2735-2741

Lin, T.L., J. Reese, T. Hong and L.S. Fan, (1996), "Quantitative Analysis and Computation of Two-Dimensional Bubble Columns", AIChE Journ., **42(2),** 301-318

Lockett, M.J. and R.D. Kirkpatrick, (1975), "Ideal Bubbly Flow and Actual Flow in Bubble Columns", Trans. Inst. Chem. Eng., **53,** 267-273

Maezawa, A, S. Muramatsu, S. Uchida and S. Okamura, (1993), "Measurement of Gas Holdup in Three Phase Systems by Ultrasonic Technique", Chem. Eng. Tech., **16,** 260-262

MacTaggart, R.S., H.A. Nasr-El-Din and J.H. Masliyah, (1993), "Sample Withdrawal from a Slurry Mixing Tank", Chem. Eng. Sci., 48(5), 921-931

Marchese, M.M., A. Uribe-Salas and J.A. Finch, (1992), "Measurement of Gas Holdup in a Three-Phase Concurrent Downflow Column", Chem. Eng. Sci., **47(13/14),** 3475-3482

Matsuura, A. and L.S. Fan, (1984), "Distribution of Bubble Properties in a Gas-Liquid-Solid Fluidized Bed", AIChE Journ., **30,** 894

Michelsen, M.L. and K. Ostergaard, (1970), "Hold-up and Fluid Mixing in Gas-Liquid Fluidized Beds", Chem. Eng. Journ., 1

Miller, D.N., (1980), "Gas Holdup and Pressure Drop in Bubble Column Reactors", Ind. Eng. Chem. Proc. Des. Dev., **19,** 371-377

Miyahara, T., Y. Matsuka and T. Takahashi, (1983), "The Size of Bubbles Generated from Perforated Plates", Int. Chem. Eng., **23(3),** 517-533

Morooka, S., T. Mizoguchi, T. Kago, Y. Kato and N. Hikada, (1986), "Effect of Fine Bubbles on Flow Properties in Bubble Column with Suspended Solids Particles", Journ. Chem. Eng. Japan, **19,** 507

Muroyama, K. and L.S. Fan, (1985), "Fundamentals of Gas-Liquid-Solid Fluidization", AIChE Journ., **31(1),** 1-34

Murray, P. and L.S. Fan, (1989), "Axial Solid Distribution in Slurry Bubble Columns", Ind. Eng. Chem. Res., **28,** 1697-1703

Nacef, C.G.J., G. Wild, A. Laurent and S.D. Kim, (1988), "Effects D'Echelle en Fluidization Gaz-Liquide-Solide", Entropie, **83,** 143-144

Nasr-El-Din, H., C.A. Shook and M.N. Esmail, (1985), "Wall Sampling in Slurry Systems", Can. Journ. Chem. Eng., **63,** 746-753

Nicklin, D.J., (1962), "Two Phase Bubble Flow", Chem. Eng. Sci., **17,** 693-702

Nigam, K.D.P. and A. Schumpe, (1987), "Gas-Liquid Mass Transfer in a Bubble Column with Suspended Solids", AIChE Journ., **33(2),** 328-330

Nottenkaemper, R., A. Steiff and P.M. Weinspach, (1983), "Experimental Investigation of Hydrodynamics of Bubble Columns", Ger. Chem. Eng., **6,** 147-155

O'Dowd, W., D.N. Smith, J.A. Ruether and S.C. Saxena, (1987), "Gas and Solids Behaviour in a Baffled and Unbaffled Slurry Bubble Column", AIChE Journ., **33(12),** 1959-1970

Oels, U., J. Lucke, R. Buchholz and K. Schugerl, (1978), "Influence of Gas Distributor Type and Composition of Liquid on the Behaviour of a Bubble Column Bioreactor", Ger. Chem. Eng., **1,** 115-129

Ostergaard, K., (1968), "Gas-Liquid-Particle Operation in Chemical Reaction Engineering", Adv. in Chem. Eng., **7,** Academic Press

Ostergaard, K., (1971), "Three-Phase Fluidization", Academic Press, New York

Ozturk, S.S., A. Schumpe and W.D. Deckwer, (1987), "Organic Liquids in a Bubble Column: Holdups and Mass Transfer Coefficients", AIChE Journ., **33(9),** 1473-1480

Pal, S.S., A.K. Mitra and A.N. Roy, (1980), "Pressure Drop and Holdup in Vertical Two-Phase Cocurrent Flow with Improved Gas-Liquid Mixing", Ind. Eng. Chem. Proc. Des. Dev., **19,** 67-75

Pandit, A.B. and J.B. Joshi, (1984), "Three Phase Sparged Reactors Some Design Aspects", Rev. Chem. Eng., 1-84

Parulekar, S.J. and Y.T. Shah, (1980), Chem. Eng. Journ., **20,** 21-23

Patel, S.A, J.G. Daly and D.B. Bukur, (1989), "Holdup and Interfacial Area Measurements using Dynamic Gas Disengagement", AIChE Journ., **35(6),** 931-942

Peterson, D.A, R.S. Tankin and S.G. Bankoff, (1984), "Holographic Measurements of Bubble Size and Velocity in Three-Phase Systems", IUTAM Symposium, Measuring Techniques in Gas-Liquid Two Phase Flows, Springer Verlag Berlin, 1-21

Pino, L.R.Z., M.M. Yepez and A.E. Saez, (1990a), "Hydrodynamics of a Semibatch Slurry Bubble Column with a Foaming Liquid", AIChE Journ., **36(11),** 1758-1762

Pino, L.Z., M.M. Yepez, A.E. Saez and G. De Drago, (1990b), "An Experimental Study of Gas Holdup in Two-Phase Bubble Columns with Foaming Liquids", Chem. Eng. Comm., **89,** 155-175

Pino, L.Z., R.B. Solari, S. Siquier, A. Estevez, M.M. Yepez and A.E. Saez, (1992), "Effect of Operating Conditions on Gas Holdup in Slurry Bubble Columns with a Foaming Liquid", Chem. Eng. Comm., **117,** 367-382

Prakash, A., (1991), "Enhancement of Gas-Liquid and Particle-Liquid Mass Transfer in Bubble Columns and Three Phase Fluidized Beds", Ph.D Thesis, Univ. of Western Ont., London

Prince, M.J. and N.W. Blanch, (1990), "Bubble Coalescence and Break-up in Air-Sparged Bubble Columns", AIChE Journ., **36,** 1485

Quicker, G. and W.D. Deckwer, (1981), "Gas Holdup and Interfacial Area in Aerated Hydrocarbons", Ger. Chem. Eng., **4,** 363-370

Razumov, I.M., V.V. Manshilin and L.L. Nemets, (1973), "The Structure of Three Phase Fluidization Beds", Int. Chem. Eng., **13,** 57

Reilly, I.G., D.S. Scott, T. de Bruijn, A. Jain and J. Piskorz, (1986), "A Correlation for Gas Holdup in Turbulent Coalescing Bubble Columns", Can. Journ. Chem. Eng., **64,** 705-717

Richardson, J.F. and W.N. Zaki, (1954), "Sedimentation and Fluidization: Part 1", Trans. Inst. Chem. Eng., **32,** 35

Rigby, G.R., G.P. Van Blockland, W.H. Park and Capes, (1970), "Properties of Bubbles in Three-Phase Bed as Measured by an Electroresistivity Probe", Chem. Eng. Sci., **25,** 1729

Rizk, F., (1983), "A comparison between Horizontal and Vertical Pneumatic conveying Systems considering Optimal Conditions", Journ. Powder & Bulk Solids Tech., **7(3),** 5-11

Roberts, G.W., D.M. Brown, T.H. Hsiung and J.J. Lewnard, (1990), "Catalyst Poisoning during the Synthesis of Methanol in a Slurry Reactor", Chem. Eng. Sci., **45(8),** 2713-2720

Sada, E., H. Kumazawa and C.H. Lee, (1986a), "Influences of Suspended Fine Particles on Gas Holdup and Mass Transfer Characteristics in a Slurry Bubble Column", AIChE Journ., **32(5),** 853-856

Sada, E., H. Kumazawa, C.H. Lee and T. Iguchi, (1986b), "Gas Holdup and Mass Transfer Characteristics in a Three-Phase Bubble Column", Ind. Eng. Chem. Proc. Des. Dev., **25,** 472-476

Sauer, T. and D.C. Hempel, (1987), "Fluid dynamics and Mass Transfer in Bubble Column with Suspended Particles", Chem. Eng. Tech, **10,** 180-189

Saxena, S.C., R. Vadivel and A.C. Saxena, (1989), "Gas Holdup and Heat Transfer from Immersed Surfaces in Two- and Three- Phase Systems in Bubble Columns", Chem. Eng. Comm., **85,** 63-83

Saxena, S.C., N.S. Rao and A.C. Saxena, (1990a), "Heat-Transfer and Gas Holdup Studies in a Bubble Column: Air-Water-Glass Bead System", Chem. Eng. Comm., **96,** 31-55

Saxena, S.C., N.S. Rao and A.C. Saxena, (1990b), "Heat Transfer from a Cylindrical Probe Immersed in a Three-Phase Slurry Bubble Column", Chem. Eng. Journ., **44,** 141-156

Saxena, S.C., N.S. Rao and P.R. Thimmapuram, (1992a), "Gas phase Holdup in Slurry Bubble Columns for two- and three-phase systems", Chem Eng. Journ., **49,** 151-159

Saxena, S.C., N.S. Rao and A.C. Saxena, (1992b), "Heat Transfer and Gas Holdup Studies in a Bubble Column: Air-Water-Sand System", Can. Journ. Chem Eng., **70,** 33-41

Saxena, S.C. and Z.D. Chen, (1994), "Hydrodynamics and Heat Transfer of Baffled and Unbaffled Slurry Bubble Columns", Rev. Chem. Eng., 193-400

Schumpe, A. and G. Grund, (1986), "The Gas Disengagment Technique for Studying Gas Holdup Structure in Bubble Columns", Can. Journ. Chem. Eng., **64,** 891-896

Shah, Y.T., G.J. Stiegel and M.M. Sharma, (1978), Backmixing in Gas-Liquid-Solid Reactors", AIChE Journ., **24,** 369

Shah, Y.T., B.G. Kelkar, S.P. Godpole and W.D. Deckwer, (1982), "Design Parameters Estimations for Bubble Column Reactors", AIChE Journ., **28(3),** 353-379

Sherwin, M.B. and M.E. Frank, (1976), "Make Methanol by Three-Phase Reaction", Hydrocarbon Processing, November, 122-126

Smith, D.N., W. Fuchs, R.J. Lynn, D.H. Smith and M. Hess, (1984), "Bubble Behavior in a Slurry Bubble Column Reactor Model", Chem. And Catalytic Reactor Modelling, ACS Symp. Ser., 237, 125

Smith, D.N. and J.A. Ruether, (1985), "Dispersed Solid Dynamics in a Slurry Bubble Column"" Chem. Eng. Sci., **40(5),** 741-754

Smith, D.N., J.A. Ruether, Y.T. Shah and M.N. Badgujar, (1986), "Modified Sedimentation-Dispersion Model for Solids in a Three-Phase Slurry Column", AIChE Journ., **32(3),** 426-436

Soong, Y., A.G. Blackwell, R.R. Schehl, M.F. Zarochak and J.A. Rayne, (1995a), "Ultrasonic Characterization of Three-Phase Slurries", Chem. Eng. Comm., **138,** 213-224

Soong, Y., I.K. Gamwo, A.G. Blackwell, R.R. Schehl and M.F. Zarochak, (1995b), "Measurements of Solids Concentration in a Three-Phase Reactor by an Ultrasonic Technique", Chem. Eng. Journ., **60,** 161-167

Soria-Lopez, A., (1991), " Kinematic Waves and Governing Equations in Bubble Column and Three-Phase Fluidized Beds", Ph.D Thesis, Univ. of Western Ont., London

Sriram, K. and R. Mann, (1977), " Dynamic Gas Disengagement: A New Technique for Assessing the Behavior of Bubble Columns", Chem. Eng. Sci., **32,** 571-580

Suganuma, T. and T. Yamanishi, (1966), "Behavior of Solid Particles in Bubble Columns", Kagaku Kogaku, **30,** 1136

Tang, W.T. and L.S. Fan, (1989), "Hydrodynamics of a Three Phase Fluidized Bed Containing Low Density Particles", AIChE Journ., **35(3),** 355-364

Trudell, Y., (1995), "Three-Phase Fluidization Conductivity - Holdup Modelling", MESc. Thesis, Univ. of Western Ont., London

Tsuchiya, K and O. Nakanishi, (1992), "Gas Holdup Behavior in a Tall Bubble Column with Perforated Plate Distributors", Chem. Eng. Sci., **47(13/14),** 3347-3354

Turner, J.C.R., (1976), "Two Phase Conductivity: The Electrical Conductance of Liquid Fluidized Beds of Spheres", Chem. Eng. Sci., **31,** 487-492

Uribe-Salas, A., C.O. Gomez and J.A. Finch, (1994), "A Conductivity Technique for Gas and Solids Holdup Determination in Three-Phase Fluidized Beds", Chem. Eng. Sci., **49(1),** 1-10

Vasalos, I.A., D.N. Rundell, K.E. Megiris and G.J. Tjatjopoulos, (1982), "Holdup Correlations in Slurry-Solid Fluidized Beds", AIChE Journ., **28(2),** 346-348

Wachi, S., H. Morikawa and K. Ueyama, (1987), "Gas Holdup and Axial Dispersion in Gas-Liquid Concurrent Bubble Column", Journ. Chem. Eng. Japan, **20(3),** 309-316

Wallis, G.B., (1969), "One Dimensional Two-Phase Flow", McGraw Hill, New York

Warsito, A. Maezawa, S. Uchida and S. Okamura, (1995), "A Model for Simultaneous Measurement of Gas and Solid Holdups in a Bubble Column Using Ultrasonic Method", Can. Journ. Chem. Eng., **73,** 734-743

Weimer, R.F., D.M. Terry and P. Stepanoff, (1987), "Laboratory Kinetics and Mass Transfer in the Liquid-Phase Methanol Process", AIChE Annual Meeting, New York, Paper 25d

Wenge, F., Y. Chisti and M. Moo-Young, (1995), "A New Method for the Measurement of Solids Holdup in Gas-Liquid-Solid Three-Phase Systems", Ind. Eng. Chem. Res., **34,** 928-935

Wild, G., M. Saberian, J.L. Schwartz and J.C. Charpentier, (1984), "Gas-Liquid-Solid Fluidized Bed Reactors. State of the Art and Industrial Possibilities", Int. Chem. Eng., **24(4),** 639-678

Wilkinson, P.M. and L.L. van Dierendonck, (1990), "Pressure and Gas Density Effects on Bubble Break-up and Gas Hold-up in Bubble Columns", Chem. Eng. Sci., **45(8),** 2309-2315

Wilkinson, P.M., A.P. Spek and L.L. van Dierendonck, (1992), "Design Parameters Estimation for Scale-up of High Pressure Bubble Columns", AIChE Journ., **38(4),** 544-554

Wolff, C., F.U. Briegleb, J. Bader, K. Hektor, and H. Hammer, (1990), "Measurements with Multi-Point Microprobes", Chem. Eng. Tech., **13,** 172-184

Yamashita, F. and H. Inoue, (1975), "Gas Holdup in Bubble Columns", Journ. Chem. Eng. Japan, **8(4),** 334-336

Yasunishi, A., M. Fukuma and K. Muroyama, (1986), "Measurement of Behaviour of Gas Bubbles and Gas Holdup in a Slurry Bubble by a Dual Electroresistivity Probe Method", Journ. Chem. Eng. Japan, **19(5),** 444-449

Ying, D.H., E.N. Givens and R.F. Weimer, (1990), "Gas Holdup in Gas-Liquid and Gas-Liquid-Solid Flow Reactors", Ind. Eng. Chem. Proc. Des. Dev., **19,** 635-638

Zenz, F.A., (1949), "Two-phase Fluid-Solid Flow", Ind. Eng. Chem., **11(12),** 2801-2806

Zenz, F.A. and D.F. Othmer, (1960), "Fluidization and Fluid-Particle Systems", Reinhold Publishing Corp., New York

Zenz, F.A., (1968), "Bubble Formation and Grid Design in Fluidization", Proceedings of a Symposium presented at the Tripartite Chemical Engineering Conference, Montreal, Sept. 1968

Zhou, P., R.D. Srivastava, A.C. Bose and G.J. Stiegel, (1992), "Applied Hydrodynamics in Three-phase Bubble-Column Reactors for Indirect Coal Liquefaction Processes", AIChE Annual Meeting, Miami Beach, Florida, Paper 55h

Zuber, N. and J.A. Findlay, (1965), "Average Volumetric Concentration in Two-Phase Flow Systems", Journ. Heat Transfer, Trans. ASME, **87,** 453-468

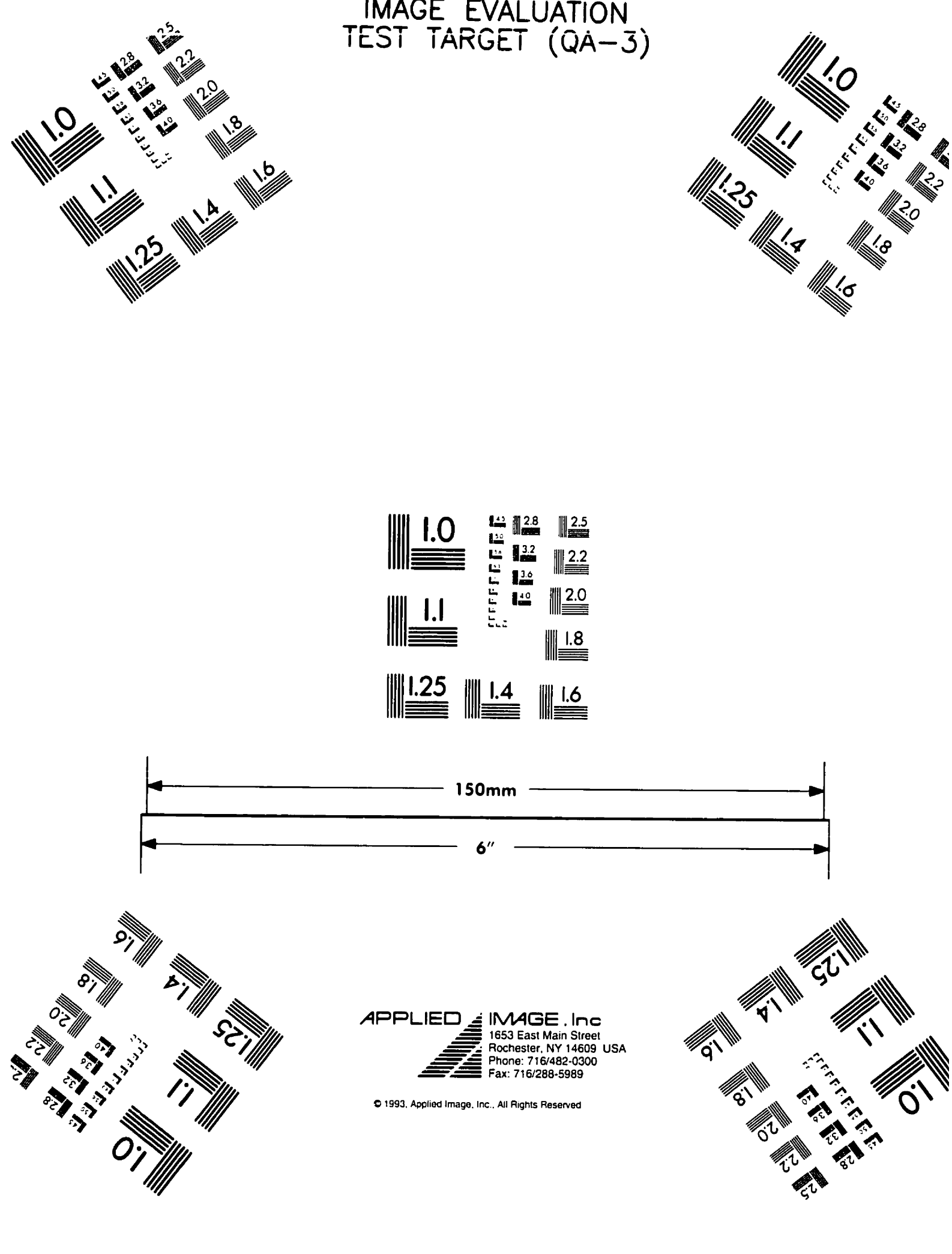
IMAGE EVALUATION
TEST TARGET (QA-3)
1.0
1.1
1.25
1.4
1.6
1.8
2.0
2.2
2.5
2.8
3.2
3.6
4.0
150mm
6"
APPLIED IMAGE, Inc
1653 East Main Street
Rochester, NY 14609 USA
Phone: 716/482-0300
Fax: 716/288-5989
© 1993, Applied Image, Inc., All Rights Reserved